Traffic eco-management in urban traffic networks

Giovanni de Nunzio

UNIVERSITÉ GRENOBLE ALPES

THÈSE

Pour obtenir le grade de

DOCTEUR DE L'UNIVERSITÉ GRENOBLE ALPES

Spécialité : **Automatique-Productique**

Arrêté ministériel : 7 août 2006

Présentée par

Giovanni DE NUNZIO

Thèse dirigée par **Carlos CANUDAS DE WIT**
et codirigée par **Philippe MOULIN**

Préparée au sein de l'**IFP Energies Nouvelles** et du laboratoire **GIPSA-lab**
dans l'école doctorale **EEATS**

Traffic Eco-Management in Urban Traffic Networks

Thèse soutenue publiquement le **2 octobre 2015**
devant le jury composé de :

M. Pierre ROUCHON, Président
Professeur - Mines ParisTech (Paris, France)

M. Per-Olof GUTMAN, Rapporteur
Professeur - Israel Institute of Technology (Haifa, Israel)

M. Saïd MAMMAR, Rapporteur
Professeur - Université d'Evry Val-d'Essonne (Evry, France)

M. Nadir FARHI, Examinateur
Chargé de recherche - IFSTTAR (Champs-sur-Marne, France)

M. Damien KOENIG, Examinateur
Maître de Conférences - GIPSA-lab (Saint-Martin d'Hères, France)

M. Markos PAPAGEORGIOU, Examinateur
Professeur - Technical University of Crete (Chania, Crete, Greece)

M. Philippe MOULIN, Co-directeur
Ingénieur de recherche - IFP Energies Nouvelles (Rueil-Malmaison, France)

To Mia and Aria

Résumé de la Thèse

Le problème de la gestion éco-responsable du trafic urbain est adressé. Ce type de gestion du trafic vise à réduire les arrêts des véhicules, les accélérations, la consommation énergétique, ainsi que la congestion. L'éco-management du trafic dans les réseaux urbains peut être catégorisé dans deux classes principales : contrôle du véhicule et contrôle de l'infrastructure. Les deux domaines de contrôle peuvent présenter des caractéristiques soit isolées soit coordonnées, en dépendant du type d'information utilisée dans l'optimisation.

La gestion du trafic côté véhicule influe sur chaque véhicule en fonction de ses propres caractéristiques et position. Le contrôle isolé du véhicule vise principalement à optimiser la transmission et/ou le profil de conduite des véhicules, en utilisant éventuellement des informations sur les caractéristiques de la route, mais sans communiquer avec les autres agents du réseau. Le contrôle coordonné du véhicule, d'autre part, fait usage de la communication entre les véhicules et avec l'infrastructure pour obtenir des bénéfices plus importants en termes de consommation d'énergie et de fluidité de la circulation.

En revanche, la gestion du côté infrastructure influe sur les feux et les panneaux de signalisation, afin d'améliorer les performances de l'ensemble du trafic. Le contrôle isolé de l'infrastructure régule essentiellement les feux de signalisation pour une seule intersection, ou bien les limites de vitesse dans un seul tronçon de route, sans prendre en compte les interactions avec les jonctions et/ou les sections voisines. Le contrôle coordonné de l'infrastructure surmonte cette limitation en utilisant des informations sur les conditions de circulation dans d'autres sections de la route, afin de réduire la congestion.

Les contributions de ce travail peuvent être résumées comme suit.

Tout d'abord, une solution pour le contrôle coordonné du véhicule a été proposée, dans laquelle la communication avec l'infrastructure est exploitée pour réduire la consommation d'énergie. En particulier, les plans des feux de signalisation sont supposés être communiqués au véhicule et connus, et une vitesse optimale est suggérée au véhicule afin de traverser une séquence de carrefours à feux sans s'arrêter, tout en suivant une trajectoire d'énergie minimale. La stratégie proposée, appliquée indépendamment à chaque véhicule, a été testée dans un

simulateur de trafic microscopique afin d'évaluer l'impact sur les performances du trafic. L'analyse a montré que la consommation d'énergie et le nombre d'arrêts peuvent être considérablement réduits sans affecter le temps de parcours.

Ensuite, une solution pour le contrôle isolé de l'infrastructure a été proposée. L'évolution du trafic sur un tronçon de route urbaine a été étudiée à l'aide d'un modèle macroscopique, et la vitesse a été utilisée comme variable de contrôle pour améliorer les performances de la circulation. L'optimisation vise à trouver un compromis entre la réduction de consommation énergétique et le temps de parcours moyen des véhicules sur le tronçon de route considéré. Des expériences ont démontré qu'il existe une limite de vitesse optimale qui améliore les performances du trafic, et qui réduit la longueur de la file d'attente au feu de signalisation.

Enfin, une solution pour le contrôle coordonné de l'infrastructure a été proposée. La synchronisation des feux de signalisation sur les grands axes de circulation a été prouvée efficace pour réduire le temps de parcours. Notre analyse a démontré qu'un problème d'optimisation peut être formalisé pour prendre en compte également les aspects énergétiques. Des expériences approfondies dans un simulateur de trafic microscopique ont montré qu'il existe une corrélation entre la progression du trafic et ses performances. La stratégie de contrôle proposée a montré qu'une réduction significative de la consommation d'énergie peut être atteinte, en éliminant presque complètement les arrêts et le temps d'arrêt, sans affecter le temps de parcours.

Preface

Abstract

The problem of energy-aware traffic management in urban environment is addressed. Such traffic management aims at reducing vehicle stops, accelerations, energy consumption, and ultimately congestion. The eco-management in urban traffic networks may be divided in two broad categories: vehicle-side control and infrastructure-side control. Both control domains can feature isolated or coordinated characteristics, depending on the type of information used in the optimization.

The vehicle-side traffic management influences each single vehicle according to its own characteristics and position. Isolated vehicle control aims primarily at optimizing the powertrain and/or the driving profile of the vehicles, possibly using information about the road characteristics, but without communicating with the other agents of the traffic network. Coordinated vehicle control makes use of communication among vehicles and with the infrastructure in order to achieve larger benefits in terms of energy consumption and traffic fluidity.

The infrastructure-side management, on the other hand, influences traffic lights and road side panels in order to improve the performance of the traffic as a whole. Isolated infrastructure control regulates essentially the traffic lights at a single signalized intersection, or the speed limits in a single stretch of road, without taking into account the interactions with the neighboring junctions and/or road sections. Coordinated infrastructure control overcomes this limitation by using information about traffic conditions in other road sections to alleviate congestion.

The contributions of this work to the energy-aware traffic management may be summarized as follows.

Firstly, a solution for the coordinated vehicle control has been proposed, in which communication with the infrastructure is exploited to reduce energy consumption. In particular, the traffic lights timings are assumed to be communicated to the vehicle and known, and the vehicle is suggested an optimal speed to drive through a sequence of signalized intersections without stopping, while following a minimum-energy trajectory. The proposed strategy, independently applied to each

vehicle, has been tested in a microscopic traffic simulator in order to assess the impact on the traffic performance. The analysis has demonstrated that the energy consumption and the number of stops can be drastically reduced without affecting the travel time.

Then, a solution for the isolated infrastructure control has been proposed. A macroscopic urban traffic model has been introduced, and the variable speed limits have been used as actuation to improve traffic performance. In particular, the analysis has been carried out at saturated traffic conditions, with given and fixed traffic lights scheduling. The optimization aims at reducing the energy consumption in trade-off with the average travel time of the vehicles in the considered road section. Experiments have demonstrated that there exists an optimal speed limit that improves traffic performance and reduces the length of the queue at the traffic light.

Lastly, a solution for the coordinated infrastructure control has been proposed. Traffic lights coordination on arterials has been proved to be effective in terms of traffic delay reduction. Our analysis has demonstrated that an optimization problem can be cast to take into account also energetic aspects. Extensive experiments in a microscopic traffic simulator have shown that a correlation exists between traffic progression and traffic performance indexes, such as energy consumption, travel time, idling time, and number of stops. The proposed control strategy has showed that a significant reduction of energy consumption can be achieved, almost completely eliminating number of stops and idling time, without affecting the travel time.

Dissertation Outline

1. Introduction

After a quick overview of the impact of traffic on economy and environment, this chapter mainly deals with a comprehensive state-of-the-art of the traffic eco-management. The literary review has been divided into the two broad categories of vehicle management and infrastructure management. A further classification aims to distinguish in each category the isolated and the coordinated strategies, depending on the amount of traffic information used in the analysis. The chapter is concluded by a summary of the main contributions of this dissertation with respect to the reviewed scientific literature.

2. Energy-Optimal Vehicle Trajectory in a Signalized Urban Corridor

In this chapter we introduce the first contribution of the dissertation to the problem of coordinated vehicle control. Here the concept of coordination lies in the global utilization of information about the traffic lights timings. This information is used to find the energy-optimal trajectory through a sequence of signalized intersections for each vehicle. We start by introducing the vehicle model and the fixed law governing the traffic lights timings. Then we formulate the optimization problem, and we propose a simplification of the non-convex problem to reach a sub-optimal solution. The proposed strategy is described in all its steps: a preliminary phase of reducing the search space of the optimal trajectories, an approximation of the driving profiles by means of a graph, and finally a simplified optimization problem. Experiments aim at validating the sub-optimal approach against a benchmark, proving the robustness capabilities of the algorithm, and finally analyzing the performance in a microscopic traffic simulator.

3. Single-Section Control via Variable Speed Limits

The second contribution of this work concerns an isolated infrastructure management strategy. One road section under saturated traffic conditions is to be controlled via variable speed limits, in order to optimize energy consumption, travel time, and infrastructure utilization. After a quick review of the foundations of macroscopic traffic models, we introduce the macroscopic model proposed for the analysis of traffic behavior in the considered road section. The model is then adapted to the urban framework and simplified for control purposes. An analysis of the properties of the model is carried out both at steady-state, when the system converges to an equilibrium, and in transient regime. A set of macroscopic traffic performance metrics is defined for the considered system. A comprehensive evaluation of the cost of the equilibrium points of the system aims at showing the best traffic conditions and the best speed limit. A controller is then designed in order to speed up the convergence of the system to the desired operation conditions. The entire macroscopic analysis is finally validated in a microscopic traffic simulator.

4. Arterial Control via Signal Offsets and Variable Speed Limits

The last contribution of the dissertation concerns the coordinated infrastructure control. An urban arterial with several signalized intersections is controlled via variable speed limits and traffic lights offsets, in order to generate green waves and increase the traffic progression. We first formulate the problem as a simple integer linear program that explicitly takes into account energetic aspects. Then

a set of experiments aims at demonstrating the correlation between traffic progression and standard traffic performance metrics, such as energy consumption, travel time, idling time and number of stops. The problem is formulated under the assumption of existence of a traffic progression, therefore the traffic demand should be sustainable by the infrastructure in order to generate green waves. However, we demonstrate that the proposed strategy is effective also in the case of over-saturated traffic conditions. A microscopic traffic simulator was employed to validate the results.

5. Conclusions

In this final chapter we summarize the main contributions of the dissertation, and give an insight into the possible future extensions of our work.

List of Publications

Journals

   # G. De Nunzio, C. Canudas de Wit, P. Moulin, D. Di Domenico, "Eco-Driving in Urban Traffic Networks Using Traffic Signals Information", *International Journal of Robust and Nonlinear Control* (accepted).

   # G. De Nunzio, G. Gomes, C. Canudas de Wit, R. Horowitz, P. Moulin, "Arterial Bandwidth and Energy Consumption Optimization via Signal Offsets Control and Variable Speed Limits", *IEEE Transactions on Control Systems Technology* (under review).

Proceedings of Peer-Reviewed International Conferences

   # G. De Nunzio, C. Canudas de Wit, P. Moulin, D. Di Domenico, "Eco-Driving in Urban Traffic Networks Using Traffic Signal Information", *52nd IEEE Conference on Decision and Control*, pp. 892-898, 2013.

   # G. De Nunzio, C. Canudas de Wit, P. Moulin, "Urban Traffic Eco-driving: A Macroscopic Steady-State Analysis", *2014 European Control Conference*, pp. 2581-2587, 2014.

   # G. De Nunzio, C. Canudas de Wit, P. Moulin, "Urban Traffic Eco-Driving: Speed Advisory Tracking", *53rd IEEE Conference on Decision and Control*, pp. 1747-1752, 2014.

   # G. De Nunzio, G. Gomes, C. Canudas de Wit, R. Horowitz, P. Moulin, "Arterial Bandwidth Maximization via Signal Offsets and Variable Speed

Limits Control", *54th IEEE Conference on Decision and Control* (accepted).

Magazines

A. Sciarretta, G. De Nunzio, L. Leon Ojeda, "Optimal Ecodriving Control: Energy-Efficient Driving of Road Vehicles as an Optimal Control Problem", *IEEE Control Systems Magazine*, vol. 35, no. 5, pp. 71-90, 2015.

Contents

List of Figures

List of Tables

List of Acronyms

Chapter 1

Introduction

1.1 The Cost of Traffic

The International Energy Agency (IEA) affirms that the current trends in energy use and supply are unsustainable economically, environmentally and socially. Without decisive action, energy-related emissions of carbon dioxide (CO_2) will more than double by 2050, and increased oil demand will heighten concerns over the security of supplies. The IEA also estimated that over 50% of oil use around the world is for transportation, and three-quarters of the energy used in the transportation sector is consumed on the roads. Therefore, it is crucial that governments around the world tackle the problem of poor vehicle fuel economy [124].

The growth of transportation activity raises concerns for its environmental sustainability. According to data from the European Environment Agency [125], transportation accounted for close to a quarter (23.8%) of total greenhouse gas emissions and slightly more than a quarter (27.9%) of total CO_2 emissions in the EU-27 in 2006. No other sector has the growth rate of greenhouse gas emissions as high as in transportation.

Europe is the most urbanized continent in the world: at present over 80% of its population lives in towns and cities [108]. Vehicular traffic is a direct consequence of cities development and expansion. The same forces attracting people to congregate in large urban areas also lead to often unbearable levels of traffic congestion on urban roads. Congestion is a phenomenon that may be defined as the situation in which a certain demand of a roadway infrastructure exceeds the available supply. From a different perspective, congestion may be also defined as the obstruction that vehicles impose to each other when the operational conditions of the infrastructure are close to maximum capacity.

Over the last few decades, the number of circulating vehicles has increased exponentially, and traffic congestion has become a major problem, not only from

a safety point of view, but also from an economic and environmental perspective. Congestion involves queuing, lower speeds, and increased travel times, which impose costs on the economy and generate multiple impacts on urban regions and their inhabitants [68]. However, transportation is an essential component of the European economy accounting for about 7% of GDP and for over 5% of total employment in the European Union (EU) [125].

Eliminating urban congestion is neither an affordable, nor feasible goal in economically dynamic urban areas. Nevertheless, much can be done to reduce its occurrence and its impact on road users. The traditional approach of continuously expanding the existing infrastructure to increase capacity, although helpful, results to be too costly, besides being ecologically intrusive and space demanding. Most cities have taken or plan to take actions to address these problems in order to achieve their short and long-term objectives, which include changing the modal split in favor of public transport, reducing emissions, decreasing road accidents, etc. These measures comply also with the EU climate and energy package, a set of binding legislation which aims to ensure the achievement of three key objectives for 2020: a 20% reduction in EU's greenhouse gas emissions with respect to 1990 levels; raising the share of EU energy consumption produced from renewable resources to 20%; a 20% improvement in the EU's energy efficiency [1]. The targets were set by EU leaders in 2007, when they committed Europe to become a highly energy-efficient, low carbon economy, and were enacted through the climate and energy package in 2009. The EU is also offering to increase its emissions reduction to 30% by 2020, if other major economies in the developed and developing worlds commit to undertake their fair share of a global emissions reduction effort.

Therefore, the motivation for the traffic engineers and researchers to tackle the problem of a better traffic management is quite strong. A broad scenario of strategies may be adopted to address these problems, and for the last few decades we have been witnessing different techniques and new technologies. The scientific literature on energy-aware and/or congestion-relief traffic management strategies can be divided into two broad categories: vehicle-oriented control, and traffic-oriented control. For many years the available technology made the practitioners rely exclusively on physical sensors or local information in order to devise and deploy the control measures. However, without innovative thinking, integration of information, and flow control systems, severe congestion will be more and more a major concern for mobility. In the automotive sector, Intelligent Transportation Systems (ITS) are being developed to provide innovative services relating to different modes of transportation and traffic management. A trend that is enabling Intelligent Transportation Systems is a fundamental change in vehicle control systems. A typical vehicle in the early 2000s had between 20 and 100 individual networked micro-controllers using non real-time operating systems. The current trend is towards fewer, more capable microprocessor modules with

hardware memory management and real time operating systems. This increased capability allows potential for more sophisticated software applications to be implemented based on model-based control and artificial intelligence. Intelligent Transportation Systems will enable various users to be better informed and make safer, more coordinated, and "smarter" use of transportation networks.

In the following, a brief survey of the existing technologies in the field of traffic management will be presented.

1.2   Vehicle Eco-Management

At least three energy conversion steps are relevant for a comprehensive analysis of energy efficiency of passenger cars. In a first step ("grid-to-tank"), energy carriers that are available at stationary distribution networks are converted to an energy carrier that is suitable for on-board storage, such as gasoline, electricity, etc. This energy is then converted by the propulsion system to mechanical energy aimed at propelling the vehicle ("tank-to-wheels"). In the third energy conversion step ("wheel-to-meters"), this mechanical energy is ultimately converted into the kinetic and potential energy required by the displacement. Unfortunately, all of these conversion processes cause substantial energy losses.

In particular, Intelligent Transportation Systems are more interested in wheel-to-meters efficiency, which is influenced by vehicle parameters, such as weight, aerodynamic drag, rolling friction, and the driving behavior. The approach of improving wheel-to-meters efficiency by "controlling" the driving profile is particularly appealing when considering that it does not require structural changes to the system.

The adoption of an energy-aware driving style is the goal of "eco-driving". The driving behavior can have a big impact on emissions, as demonstrated by several studies [133]. Typically a few heuristic guidelines are generally known, such as anticipate traffic flow, avoid braking, shift up early, switch off the engine at short stops. In addition, software tools and systems that help the driver (or replace him) in performing eco-driving have also emerged. A possible classification of existing eco-driving systems is [117]:

1. *Pre-trip* systems, besides giving generic advice on eco-driving, are integrated within navigation systems. For any given start and destination points, and for defined time windows for departure or arrival, the system calculates optimal start time and route, based on car and driver's characteristics, so as to minimize environmental impact of the journey. Pre-trip advising devices include in-vehicle equipment, the internet, phone services, mobile devices, television, and radio. These communication devices may be also consulted by a potential road user to make decisions about the time

when to start the trip, the choice of means of transportation, the choice of the route, etc.

2. *In-trip* systems are part of the broader category of Advanced Driver Assistance Systems (ADAS) and are further classified as *online assessment* systems, which provide feedback advice based on current performance, *online advice* systems, which give a predictive, feedforward advice, based on upcoming events, and *predictive cruise controllers*, where automatic drive is performed. In-trip advice is accomplished through radio service, road side variable messages and in-vehicle equipment, which assist and inform the drivers so as to make appropriate routing decisions. While radio services have been operating for many years now, the concept of in-vehicle technology, intelligent vehicles and the notion of ADAS are relatively new and of great interest for scientific community and enterprises. As a main interface, the majority of systems use visual displays, while audible alerts and haptic gas pedal are applied in only a few solutions. In-trip advice can be provided either as an information-only message or as an explicit route recommendation. According to different surveys [130], the majority of the drivers seem to prefer the less intrusive information-only message and be able to make their own decisions. However this type of advice has several drawbacks. The translation of the information into a proper routing decision requires a good knowledge of the traffic network and a very quick response of the driver. Dissemination of the information is bounded by the capability of the employed means. The real limit is imposed anyways by the amount of information that drivers are able to process quickly enough to make a decision. Finally the influence on traffic conditions is not ensured because the decision is left to the drivers, and compliance plays a major role. On the other hand, although capable of influencing traffic conditions, explicit route recommendations are constrained by the ideal requirement of not suggesting routes disadvantageous for complying drivers.

3. *Post-trip* systems attempt to increase the driver's motivation for eco-driving by displaying encouraging results, and generating summaries and statistics that can be compared to other drivers.

Most approaches are based on heuristic rules of thumb or good practices that are associated with an energy-efficient drive. Moreover, only a few are predictive, that is, based on estimates of future external conditions, while the rest is solely based on current driving information, typically extracted from vehicle network data. Even more rudimentary concepts, essentially consisting of alerts based on the acceleration sensor of smartphones, are typically found among mobile application software labeled "eco-drive". However, several concepts are emerging

that attempt at implementing eco-driving in a more rigorous framework. In these concepts, eco-driving is regarded as an optimal control problem where the drive commands minimize the energy consumption for a given trip.

In the following, a brief literary review of the vehicle eco-management problem is presented. The categorization will be based on the level of communication that the different approaches rely on. In particular we distinguish between isolated strategies, which do not utilize information received from the surrounding environment, and strategies that make use of the road communication networks in order to fuse different pieces of information coming from the nearby traffic agents.

1.2.1 Isolated Control

Works on energy optimal control are found in several application areas. Pre-trip and post-trip systems have been proposed for electric vehicles (EVs) [34, 35, 36, 37, 105], where the analytical and numerical solutions of the energy-optimal control problem aim at finding motor torque and/or brake force. Metrics for the evaluation of the actual driving profile with respect to the theoretical optimal one are provided to the driver for an eco-driving education. Similar works have been carried out for hybrid electric vehicles (HEVs) where an analytical solution of the eco-driving problem has been proposed [43, 71] by finding the optimal gear, or the on/off switching policy of the internal combustion engine, the quantity of injected fuel, or the engine speed and torque. Also, online sub-optimal optimization strategies suitable for online adoption without a previous knowledge of the driving horizon have been presented [115]. As for internal combustion engines (ICEs), the eco-driving solutions involve trajectory optimization [93], and/or gear selection optimization [55], in order to reduce fuel consumption.

Other works qualify as in-trip eco-driving systems. There have been instances of visual ADAS with the objective of minimizing fuel consumption and emissions by providing suggestions on speed profiles and gear selection to the driver [11]. Also, it is possible to find in literature some attempts to provide an online eco-management of HEVs, with an action transparent to the driver that minimizes the fuel consumption [97, 72].

All the aforementioned works address the eco-driving problem from the vehicle perspective, without exploiting information coming from the other agents of the traffic network (e.g. other vehicles, traffic lights, etc.). With the rise of communication technologies, interest in "communication cooperation" is growing: vehicle-to-vehicle (V2V), vehicle-to-infrastructure (V2I), and infrastructure-to-vehicle (I2V). This can be used for warning drivers of upcoming hazards, to provide recommendations to avoid traffic, or to suggest an optimal (in some sense) driving profile.

The European Commission defines communication cooperation as [125]:

"Road operators, infrastructure, vehicles, their drivers and other road users will cooperate to deliver the most efficient, safe, secure and comfortable journey. The vehicle-vehicle and vehicle-infrastructure cooperative systems will contribute to these objectives beyond the improvements achievable with standalone systems."

1.2.2 Coordinated Control

The concept of leveraging wireless communication in vehicles has fascinated researchers since the end of the 80s. In the last few years, there has been a large boost in research and development in the area of road communication networks for a coordinated vehicle control. Several factors have contributed to this trend: the wide adoption and subsequent drop in cost of Wi-Fi technologies; the embrace of information technology to address the safety, environmental, and comfort issues of their vehicles; and the commitment of governments to allocate wireless spectrum for vehicular wireless communication. Although cellular networks enable convenient voice communication and simple infotainment services to drivers and passengers, they are not well-suited for certain direct V2V or V2I communications. Vehicular ad-hoc networks (VANETs), which offer direct communication between vehicles and to road-side units (RSUs), can send and receive hazard warnings or information on the current traffic situation with minimal latency.

The major goal of these activities is to increase road safety and transportation efficiency, as well as to reduce the impact of transportation on the environment. These three classes of applications of VANETs are not completely orthogonal: for instance, reducing the number of accidents can in turn reduce the number of traffic jams, which could reduce the level of environmental impact. Due to the importance of these goals for both the individual and the collectivity, various projects are underway, or recently completed, and several consortia were set up to explore the potential of VANETs, with the participation of different members such as the automotive industry, the road operators, tolling agencies, and other service providers (SPEEDD 2014 [121], CVIS 2006-2010, C2C-CC 2001 [18], COMeSafety2 2011-2013 [26], Drive C2X 2011-2013 [41], iTETRIS 2008-2010 [66]).

Extensive lists of potential applications have been compiled and assessed by the various projects and consortia. Typically, applications are categorized as safety, transport efficiency, and information/entertainment applications. Examples for each category are [60]: cooperative forward collision warning, traffic light optimal speed advisory, remote wireless diagnosis, to make the state of the vehicle accessible for remote diagnosis.

To evaluate the chances of success, applications were analyzed as to whether their requirements can be satisfied and whether (and to what degree) they will provide a beneficial impact. On the requirements side, a prominent factor is the
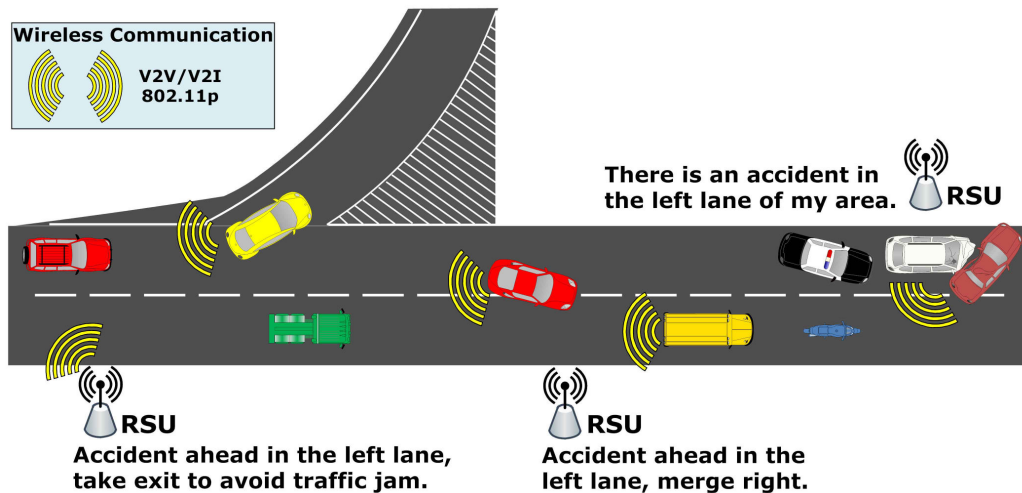
Figure 1.1 – Example of VANETs application to rerouting and lane changing for safety and traffic efficiency purposes (source: Google).

required penetration rate (i.e., the percentage of vehicles equipped with VANETs technology as compared to the vehicles population) to enable acceptable operation of the application. Technical requirements define packet sizes, required frequency or accuracy of updated information, communication ranges, latency constraints, security levels, and required infrastructure. On the added-value side, applications are assessed with respect to the level they increase safety or transportation efficiency, or serve desirable information requirements. Quantitative evaluations of added value are tricky because human factors come into play: for instance, accurate prognoses of road traffic proved to be an extremely hard task because those prognoses must take into account the *feedback loop* (i.e. how humans react).

For safety-related applications, the Vehicle Safety Communications (VSC) consortium identified eight potential uses [136]: traffic signal violation warning, curve speed warning, emergency electronic brake light, pre-crash sensing, cooperative forward collision warning, left turn assistant, lane-change warning, and stop sign movement assistant. Note that four of these applications require V2V communication, whereas the other four require communication with roadside infrastructure. For transportation efficiency applications, the Car-to-Car Communication Consortium analyzed enhanced route guidance and navigation, green light optimal speed advisory, and lane merging assistants. While for the first two applications roadside infrastructure is considered a prerequisite, the lane merging assistant is assumed to be based on V2V communication. Ideas for information and entertainment applications consist of quite a diverse set: tolling (one of the initial motivators for V2I communications), point-of-interest notifications, fuel consumption management, pod-casting, and multi-hop wireless Internet access,

to name a few.

A central challenge of VANETs is that no communication coordinator can be assumed, and several applications will be expected to function reliably using decentralized communications. Because no central coordination or handshaking protocol can be assumed, and given that many applications will be broadcasting information of interest to many surrounding vehicles, the necessity of a single shared control channel is paramount. To respond to this problem, IEEE 1609 WAVE standard was proposed as a stack of protocols of the Wi-Fi family to represent the network infrastructure for wireless access in vehicular environment. The IEEE 802.11p wireless access in vehicular environments (WAVE) provides a protocol suite solution to support vehicular communications in the licensed frequency band at 5.9 GHz (5.85-5.925 GHz). A WAVE system consists of road-side units (RSUs) and on-board units (OBUs), and can enhance road safety and driving efficiency, complementing other communication protocols by providing high data transfer rates (3-54 Mbps).

V2I and V2V communications promise revolutionary improvements in transportation, greater energy efficiency, reduced collisions, and safety of vehicle occupants as well as pedestrians and bicyclists. Control is a key contributing discipline for both topics.

In V2I, the infrastructure plays a coordination role by gathering global or local information on traffic and road conditions, and then suggesting or imposing certain behaviors to groups of vehicles. One example is ramp metering, already widely used, which requires limited sensors and actuators (measurements of traffic density on a highway and traffic lights on ramps). In a more sophisticated scenario, the velocities and accelerations of vehicles and inter-vehicle distances would be suggested by the infrastructure on the basis of traffic conditions, with the goal of optimizing overall emissions, fuel consumption, and traffic velocities. Suggestions to vehicles could be broadcast to drivers via road displays, or directly to vehicles via wireless connections. Looking further ahead, in some cases suggestions could be integrated into the vehicle controls and implemented semi-automatically (always taking into account the restrictions on automatic vehicle driving imposed by the Vienna Convention on Road Traffic [1]). Some experts predict that the first V2I systems may be developed and deployed in the 2015-2020 time frame.

---

1. This international treaty, designed to facilitate international road traffic and increase road safety, was agreed upon at the United Nations Economic and Social Council's Conference on Road Traffic in 1968 and came into force in 1977. The convention states that "Every driver shall at all times be able to control his vehicle", which conflicts somewhat with the automatic control concept. Systems such as anti-lock braking systems or electronic stability programs are acceptable because they do not take full control of the vehicle but wider use of technology will require amendment of the convention.

It is well known that approximately half of fuel consumption in urban traffic is caused by starting and stopping, therefore the role of traffic lights is crucial. Although traffic lights are very important for flow regulation at intersections, especially at peak hours, they cause an energy consumption increase of about 10-20% on main arterials with respect to the case of an ideal road without intersections. Situation becomes even worse if we consider also cross traffic, which has lower priority and is more likely to stop at traffic lights. Therefore, presence of traffic lights in the total urban area can lead to a 20-40% higher consumption [14]. Severe consequences on health and air quality are also to be considered. Average particles concentration in the air at traffic lights during delay conditions can be up to twenty-nine times higher as compared to free-flow conditions due to changes in driving (deceleration, idling and acceleration) conditions. It has also been found that the typical 2% of journey time exposure under delay conditions at traffic lights contributes up to about 25% of total commuting exposure doses of pollutants [54].

Research in this sub-category of traffic communication has shown how V2I communication can benefit fuel consumption and emissions at a signalized intersection. In other words it is possible to follow an optimal speed and acceleration profile to avoid idling time at traffic lights and to reduce energy consumption. The Green Light Optimized Speed Advisory (GLOSA) application provides the advantage of timely and accurate information about traffic lights cycles and traffic lights position information. It provides drivers with speed advice, guiding them with a more constant speed and with less stopping time through traffic lights. A 7% reduction in average fuel consumption and up to 89% in average stop time has been proved in preliminary studies [69].

Several works propose an advanced driving assistance system that provides traffic signal status information to help drivers avoid hard braking at the intersections, defines a method for evaluating vehicle energy consumption and emissions, and investigates the potential benefits of such system. This analysis can be carried out at different levels of complexity, considering a single-segment GLOSA or a multi-segment GLOSA. When the scenario involves a single traffic light, the goal is to optimize the velocity and acceleration profiles for the approach to the intersection in order to reduce energy consumption [78, 80, 107]. This eco-driving strategy could also be improved by taking into account the probabilistic evolution of the queue at the traffic light, in order to refine the speed advisory for the "smart" vehicles that approach the intersection and avoid stops [114, 113].

However, it has been demonstrated that a GLOSA involving multiple signalized intersections yields a better performance than the single-segment scenario, both in terms of energy consumption and of travel time [119]. In the multi-segment GLOSA, the optimization aims at improving traffic performance through a sequence of signalized intersections. The objectives of the optimization and the analysis approach can be various. Some works address the energy consumption in

an indirect way, that is by minimizing acceleration [91, 90] or by avoiding the use of brakes in order not to waste kinetic energy [10]. Some of these approaches can also have predictive features, either on the signal timings [90], or on the driving receding horizon [10]. However, there exist also several studies where the energy consumption minimization is explicitly considered in the optimization process, by defining energy consumption models. The multi-intersection eco-driving problem has been treated in sub-urban environment where the length of the segments is rather long [101], but also in a strictly urban environment. Instances with few traffic lights and offline-oriented optimization showed already promising improvements in terms of energy consumption [95]. More extensive studies demonstrated the benefits of the eco-driving assistance through an arbitrarily long sequence of traffic lights, also providing online applicability of the strategy in a receding horizon framework [45, 44, 30]. The optimal speed advisory problem could also be solved at higher levels of abstraction. For instance, vehicles could be seen as processes, and each intersection acts as a machine that should schedule the "arrival times" of its own processes [140]. However, these approaches do not explicitly consider the energy minimization objective, and the problem boils down to a mere synchronization between vehicles and green phases at the traffic lights. An interesting insight into the difference between the synchronization speed advisory and the eco-driving speed advisory has been provided in [98]. In particular, the eco-driving vehicle velocity trajectory is generally smoother than that of the green-wave vehicle, and the average compliance rate with the eco-driving assistance is higher than the green-wave one. This results in lower energy consumption and emissions. Finally, other works address the problem of fuel consumption while idling at traffic lights; an automatic shut off and start of the engine could be commanded, based on information about the duration of the red signal provided to the vehicles via I2V communication [112].

Another application of V2I communication is represented by the Adaptive Route Change (ARC) in which communication between vehicles and infrastructure is bidirectional, and is used to gather information about the length of the queues at traffic lights. When the queue grows larger than a certain threshold, a routing advice is broadcast to the vehicles in order for them to find alternative and faster routes to the destination [142].

V2V, more difficult to realize because of its decentralized structure, aims at organizing the interaction among vehicles, and possibly developing collaborations among them. Information is interchanged, and decisions are made on a "local" basis. In the V2V concept, when two or more vehicles or roadside stations are in radio communication range, they connect automatically and establish an ad-hoc network enabling the sharing of position, speed, and direction data. Every vehicle is also a router, and allows sending messages over multi-hop to more distant vehicles and roadside stations. The routing algorithm is based on the position of

the vehicles, and is able to handle fast changes of the network topology. Control technology comes into play at local and higher layers of the architecture. Uncertainties, delays, partial measurements, safety and performance objectives, and other aspects must be considered, and the system must be capable of making automatic or semi-automatic decisions, providing warnings/information and potentially effective actions. Research on the advantages of using V2V communication has brought up several interesting applications of this technology to improve general traffic performance. Vehicles equipped with cameras on the windshields may be able to identify the switching signals of traffic lights and, by communicating with other vehicles in the neighborhood of the intersection, may also construct a timings map of the junction. This would enable services like GLOSA and ARC, since a vehicle approaching an about-to-turn-green light would adjust its speed for a smoother passage through the intersection, whilst a vehicle approaching a red light might decide to reroute [73]. Another application of V2V is the Self-Organising Traffic Information System (SOTIS), which uses vehicular communication to collect information on the local traffic situation. In SOTIS, vehicles gather information, such as average velocity for all driven road segments, and exchange it by wireless ad-hoc communication. Cars heading to a traffic jam are informed by the opposing traffic, and may avoid it by rerouting. In urban environment vehicles could generate intelligent maps (with information about travel time and road conditions) on their own by using a Global Positioning System (GPS) receiver, and a global reference grid may be known to all vehicles [42]. V2V communication may be also employed to infer information about the intentions of the preceding vehicles by communicating inter-distances. This may be seen as the cooperative extension of the standard Adaptive Cruise Control (ACC), and allows to improve the energy consumption of vehicles constrained by safety distances from the preceding ones [77, 76, 67, 24, 141, 132].

1.3   Traffic Eco-Management

Congestion arises every time traffic demand approaches or exceeds the road and/or junction capacity. All the measures to manage congestion aim at reducing the demand/supply ratio [106].

On the supply side, strategies can be designed to increase the physical road capacity (building additional pieces of infrastructure, such as lanes or roads, or altering the already existing ones), or maximize the use of existing facilities (improved traffic signals control).

On the demand side, measures have as objective a substantial change in mode, route, and/or destination of trips. These measures might be restrictive, and are typically enforced via regulatory procedures. Practically, at microscopic level,

demand control is executed through physical restrictions (e.g. closing a street), delay based restrictions (e.g. access points metering), or tolls and usage fees.

On the supply side, traffic lights at road intersections represent the major control measure in urban traffic networks [103]. Traffic lights were originally installed in order to simply guarantee the safe crossing of antagonistic streams of vehicles and pedestrians. However with the increase of traffic demand, it was soon realized that they may be exploited to improve the efficiency of network operations.

In traffic control it is often the case to encounter technical terms, which is advisable to get familiar with to better understand all the components of the traffic network architecture. An *intersection* consists of a number of approaches and the crossing area. An *approach* may have one or more lanes but has a unique, independent queue. Approaches are used by corresponding traffic streams, that are typically measured in vehicles per hour. A *saturation flow* is the average flow crossing the stop line of an approach when the corresponding stream has right of way, the upstream demand (or the waiting queue) is sufficiently large, and the downstream links are not blocked by queues. Two compatible streams can safely cross the intersection simultaneously, otherwise they are called antagonistic.

When dealing with traffic lights as control inputs for the traffic control problem, traffic engineers have the possibility to act on four variables, which fully describe the operational modes of the lights [103]:

- *Cycle time*: one repetition of the basic series of signal combinations at a junction; longer cycle times typically increase the intersection capacity because the proportion of the constant lost times becomes accordingly smaller; on the other hand, longer cycle times may increase vehicle delays in under-saturated intersections due to longer waiting times during the red phase.
- *Stage* or *phase*: is a part of the signal cycle, during which one set of streams has the right of way; it may have a major impact on intersection capacity and efficiency.
- *Split*: relative green duration of each stage that should be optimized according to the demand.
- *Offset*: phase difference between cycles for successive intersections that may give rise to a "green wave".

Traffic signal setting strategies can be either *fixed-time* or *traffic-responsive*. Fixed-time (also called pre-timed) strategies use historical traffic data, and yield one traffic signal setting for the considered time of day. The optimization problem is solved offline. On the other hand, traffic-responsive (also called real-time) methods use real-time data to define timings for immediate implementation that are used over a short time horizon. Furthermore, signal timings can be derived by considering either a single (isolated methods) or a set (coordinated methods)

of intersections [103]. Methods that handle individual intersections are based on models that capture the local dynamics of the network. They describe in detail the dynamics at an intersection, but at the expense of capturing less well the interactions between intersections.

Locally traffic lights can be also used as metering devices, in fact the green phases of adjacent signalized intersections can be appropriately scheduled in order to regulate the number of vehicles released from the upstream signal so that the downstream link can always be cleared. This protects the storage area between nodes and allows a full employment of green stages. Capacity can be also protected by installing signals on the approaches, upstream of the stop lines; as a consequence traffic is metered and the "gaps" created in this way facilitate downstream clearance.

Metering, as demand regulator, can be also extended to cover larger areas of the urban traffic network. It can be classified into internal metering, which comprises all the strategies aiming at managing the traffic approaching critical intersections and arterials to avoid congestion to build up and saturate the infrastructure, and external metering, which basically consists of the control at the periphery of an area to limit the inflow of traffic to improve the overall quality of traffic flow within the controlled area [50].

The main criticism against implementing metering control schemes is that such measures could be ineffective and, in some cases, the net effect of metering could simply be a transfer of congestion from inside to outside the control area without any change in overall travel time, ambient air quality or other effects of traffic congestion. Finally, it should be kept in mind that, while traffic metering can be applied to protect a busy area from the sudden inflow of morning peak traffic, it is less easy to achieve during the evening peak when much of the traffic originates from within the control area [106].

An arguably more intelligent way of exerting demand regulation is represented by the routing advice system provided to the drivers of a traffic network. Freeway or urban traffic networks can always be imagined as a graph with a large number of origins and destinations with multiple paths connecting each origin-destination pair. Fixed direction signs at bifurcation nodes of the network typically indicate the direction that gives the shortest travel time in absence of congestion. However, during rush hours, the travel time on many routes changes drastically due to traffic congestion, and alternative routes may become faster than the original ones. Drivers who are familiar with the traffic conditions in a network naturally optimize their individual routes based on their past experience, thus leading to a sort of user-equilibrium conditions. However daily varying demands, changing weather conditions, exceptional aggregation events (sport events, fairs, concerts, etc.) and, most importantly, incidents may change the traffic conditions in an unpredictable way. This may lead to an under-utilization of the overall network

capacity, with some links heavily congested and capacity reserves available on alternative routes. Route guidance and driver information systems (RGDIS) may be employed to improve the network efficiency via direct or indirect recommendation of alternative routes.

A type of driver information system that is gaining popularity for its simplicity is the display on variable message signs of travel times on particular stretches of road downstream the signal. This information is easily understandable by the drivers and it can provide help with route decision making. For instance, about 350 variable message signs are installed on the *Boulevard Périphérique* of Paris and on its on-ramps. The displayed information is the instantaneous travel time from the location of the signal to two significant points far downstream (e.g. an exit, an important junction, etc.). The instantaneous travel time on a freeway stretch is defined to be the travel time of a virtual vehicle that travels the stretch under the assumption that the currently prevailing traffic conditions will not change during the trip. The calculation of this important traffic measure is rather simple in case inductive loop detectors are available: mean speed is collected or indirectly computed from other measurements at each sensor location, and then the travel time is easily calculated knowing the distance between two successive sensors. Intuitively enough, instantaneous travel time information, although working quite well in practice, is not very reliable in case of rapidly changing traffic conditions and unexpected drops of velocity within the segment between two successive sensors. Methodologies based on historical data and/or traffic conditions forecast are known as improvements of this measure.

Besides the tentative travel time information provided via radio broadcast or roadside panels, speed advisory has been proposed in the 80s as a driving assistance service, and has become more popular nowadays for its impact on energy consumption and idling time reduction. One of the drawbacks of information-only driving assistance is the efficacy strictly dependent on the rate of compliance with the advisory system. However information based on speed advisory in urban environment can rely on the innate aversion of the drivers to stop at traffic lights, and this may assure a high compliance.

The key idea is rather simple: a certain speed is suggested to the drivers in order to catch a green light at the forthcoming signalized intersection. The simplest way of doing so is to place a sign, displaying electronically controlled digits, at the side of the road about a hundred meters past the previous traffic light. The sign is connected to the lights ahead and, from the knowledge of how many seconds will elapse before these turn green, the electronic controls compute and display an appropriate speed to be maintained. The complying driver is rewarded with a green light; non-conformists will most likely meet with a red. That set of circumstances becomes a very powerful teacher, as experience with such a system has shown in Düsseldorf, Germany, where practically all the drivers comply with the

Figure 1.2 – The pioneering example of advisory speed signs in Düsseldorf, Germany (source: [14]).

posted speed [14]. Obviously, the posted speed increases as time elapses, until a speed greater than the legal maximum would be necessary to catch the end of the present green cycle. At this point the screen goes blank, to be soon followed with the speed that will get the driver to the first seconds of the next green phase. So the sign will advance from, say, 30 km/h through progressively higher speeds to an appropriate maximum. Its effect will be to aggregate cars together into "platoons" that will pass through series of green lights without stopping.

This strategy considerably increases traffic flow, and it may be seen as an improvement of the traffic-responsive signal timings control which favor higher-density vehicles streams. The weakness of the latter approach is traffic dispersion, resulting in some traffic always being forced to stop. Advisory speed signs work well against this dispersal phenomenon, and therefore produce an increase in the infrastructure carrying-capacity. Smoother traffic flow, more relaxed and less competitive drivers, increased safety, and reduced energy consumption and pollution are among the benefits of this strategy.

Düsseldorf, Germany, has been most likely one of the pioneers of this strategy, dating back more than 30 years ago, with road sign variable signs indicating the speed to follow in order to catch the green light at the downstream intersection. No detailed evaluation of its impact and performance was documented, but it was able to smoothen flows and avoid stops. A few more experimental setups have been installed in America, England, Holland, but a real assessment of costs and

benefits was lacking. One of the main drawbacks of this measure is that the installation costs have to be accepted and met by government institutions, while the advantages will be mainly enjoyed by the drivers; as a general rule, projects with public cost and private gain are difficult to be appreciated and realized. On the other hand, cost of fuel keeps on increasing and pollution abatement has become a critical concern, plus computational efficiency has increased enormously. All this surely gives a more favorable ratio between costs and advantages, and has helped with an easier acceptance of this type of traffic control strategy.

Obviously, the more drivers comply with the advisory system, the better the strategy works, and consequently its implementation appears more meaningful. Some people may not be willing to drive slowly, according to the sign, when they see an open road ahead. It becomes a bit easier when the vehicle is not a platoon leader and it would be restrained by the maybe complying drivers ahead. It would be pointless to change lane and speed up because one would find an inevitable red light at the intersection. The practical problem that may arise is that, when the advisory panel goes temporarily blank (before giving the next suggestion to catch the next green phase), drivers may be tempted to speed up to reach the preceding platoon and try to pass through the signalized intersection at an amber light or, even worse, a red light. On the other hand, a number of drivers can always be expected to be willing to drive slower than the signs indicate. Moreover, buses or pedestrians can easily interfere with the system, especially when changing lane is not easy (heavy traffic). Introducing additional signs at different distances from the intersection could help refine the system to be more robust to unpredictable perturbations, and to keep the platoons compact. The degree of compliance is clearly a critical variable in achieving desired results, and it affects both travel time and co-ordination speeds of the traffic lights. Below a certain minimum suggested speed, compliance is likely to fall drastically and safety issues may emerge if the speed difference between compliant and non-compliant drivers is too high. To conclude advisory speed signs make the driver feel part of an intelligent, co-operative network. Recent works have attempted to evaluate the impact of lowering speed limits in urban areas, and demonstrated benefits in terms of safety and energy consumption [8].

In the following a brief literary review of the traffic management strategies will be presented. There exist very comprehensive and exhaustive surveys on road traffic control strategies [103, 100]. In the following, the classification will be made according to the level and the complexity of communication and information that the different strategies rely on. In particular we will distinguish among isolated management strategies, which use only local information, and coordinated strategies, which make use of information coming from the network in order to devise either a centralized or a distributed control measure.

1.3.1 Isolated Control

Isolated fixed-time strategies are only applicable to under-saturated traffic conditions. Stage-based strategies under this class determine the optimal splits and cycle time so as to minimize the total delay (i.e. the time wasted due to congestion) or maximize the intersection capacity. Phase-based strategies determine not only optimal splits and cycle time, but also the optimal sequence of phases, which may be an important feature for complex intersections.

Well-known examples of stage-based strategies are SIGSET and SIGCAP [6, 7], which are able to determine the splits and the cycle time at one intersection given some predefined stages. Also, these strategies feature some capacity constraints in order to avoid queue building, as well as constraints on maximum cycle and minimum green duration. SIGSET solves a nonlinear programming problem to minimize the total intersection delay for given traffic demands. On the other hand, SIGCAP solves a linear programming problem and may be used to maximize the intersection capacity.

Phase-based approaches [64] solve a similar problem, suitably extended to consider different staging combinations. Phase-based approaches consider the compatibility relations of involved streams as pre-specified, and deliver the optimal staging, splits, and cycle time, so as to minimize total delay or maximize the intersection capacity. The resulting optimization problem is of the binary-mixed-integer-linear-programming type, which calls for branch-and-bound methods for an exact solution. The related computation time is naturally much higher than for stage-based approaches, but this is of minor importance, as calculations are performed offline.

Isolated traffic-responsive strategies make use of real-time measurements provided by inductive loop detectors, which are usually located some meters upstream from the stop line. One of the simplest strategies under this class is the vehicle-interval method that is applicable to two-stage intersections. Minimum-green duration is assigned to both stages. If no vehicle passes the related detectors during the minimum green of a stage, the strategy proceeds to the next stage. If a vehicle is detected, a critical interval is created, during which any detected vehicle leads to a green prolongation that allows the vehicle to cross the intersection. If no vehicle is detected during the critical interval, the strategy proceeds to the next stage, else a new critical interval is created, and so forth, until a pre-specified maximum-green value is reached. An extension of the method also considers the traffic demand on the antagonistic approaches to decide whether to proceed to the next stage or not. A more sophisticated version of this kind of strategies was proposed by Miller [94], and is included in the control tool MOVA [137].

In the early 1960s Gazis studied over-saturated conditions and delay minimization at a single intersection, and wrote among the earliest papers available

in literature about this problem [49]. For fixed-time scheduling of the traffic lights, it has been shown that, in presence of saturation arising in both directions, the minimum delay objective is achieved by exhausting both queues at the same time. Gazis also suggests that during off-peak hours the minimum-delay algorithm should be employed, replaced by a maximum-capacity algorithm as soon as congestion starts to build up on one or more of the incoming streams. The maximum-capacity algorithm will allow the creation of queues at the traffic light; additional green time is provided for the directions having more saturation flows. However, once the peak of the demand is reached, a third phase of synchronized queue clearance is triggered. After queue depletion, the minimum-delay algorithm is reintroduced. Note that, only recently Gazis' solution to the minimum-delay problem has been found inexact and non-optimal, and new optimal control strategies for the isolated intersection have been proposed [58, 65].

Furthermore, the optimal phase ordering of a signalized intersection to reduce stopped delay has been proved effective in [13], in that up to one hundred gallons of fuel could be saved per day at each intersection. Studies on platoon accommodation at signalized intersections by adjusting the green phase duration have been also conducted in [23], and lately have found practical implementation in few instances [99]. For complex isolated intersections with multiple incoming roads, an optimization of the right-of-way priority parameters has been presented in [27]. An interesting solution of the isolated intersections management is represented by the self-organizing methods for traffic lights control [51, 52, 74]. These methods are fully decentralized, no communication between traffic lights is required, and the traffic lights are affected by their neighbors only stigmergically, by using vehicles and platoons as traveling information. The methods are very simple: they give preference to cars that have been waiting longer, and to larger groups of cars. These methods have been proved to be more effective than fixed-time strategies, in that they show some traffic-responsive characteristics. Some instability issues may occur in the case of saturation of the traffic conditions since the traffic lights are not coordinated. An extension with a supervisory control level has been proposed in order to increase the robustness of the strategy for higher traffic flows [75]. In literature there exist also some model-based isolated-intersection control strategies. A cause-effect model has been proposed [88], and the optimization concerns the hypothesized vehicles departure curve, which is a sole function of the signal timing plan. Then the optimized departure flow (the effect) is converted to corresponding signal control parameters (the cause). A more standard approach involves simple queue models at the junction, based on the vehicles conservation law, and aims at minimizing the total length of the queues by controlling the green split times [31].

Isolated control strategies have been proposed not only for traffic lights, but also for speed advisory when approaching a traffic light. The Australian research

lab CSIRO, in the 80s, substantially contributed to the evaluation of pros and cons of this technique, by means of extensive simulations and experimental campaigns in real traffic conditions in Melbourne, Australia [128, 127]. Their claim was that at least two billion dollars per year were spent on petrol consumed in driving on traffic-light-controlled arterial roads in Australian cities (one third of the total petrol consumption). If petrol economy could be improved by 10%, that would be worth two hundred million dollars. To implement an advisory speed system, an illuminated speed sign would be needed near each traffic light that regulates arterial traffic flow. Computer simulations and on-road experiments by the CSIRO team have shown substantial fuel savings, which suggest that the system could pay back its cost in less than a year.

A simulation of actual traffic conditions on Military Road, North Sydney, using data collected during studies on the relationship between flow and fuel consumption, showed that with full compliance fuel consumption is reduced by 7%, the number of stops is reduced by 48%, and travel time is reduced by 10%. This improvement has to be seen in addition to the benefits introduced by a traffic lights coordinating strategy, that can by itself improve fuel consumption by 20-35%. Intuitively, once drivers catch the "green wave", travel time can be further reduced by increasing the co-ordination speed of the traffic lights.

1.3.2 Coordinated Control

In presence of a sequence of signalized intersections on an urban arterial, coordination of traffic lights is very important and the notion of offset comes into play. If properly coordinated and shifted in time, traffic lights may give rise to a "green wave", so that catching a green light at an intersection ensures catching a green also at downstream ones. This is true under free flow conditions; when congestion arises and perturbs the system, this time coordination becomes ineffective and queues spill back into upstream intersections. Other measures are thus required in order to alleviate the congestion.

In general, the fixed-time coordinated strategies are applicable to under-saturated traffic conditions. All fixed-time control methodologies fall under the general category of static strategies. In other words the queue management strategy is applied on the roadway network at pre-set times, suggested by empirical observations and historical statistical data about peak and off-peak hours. In the following we briefly summarize the most popular and adopted control algorithms.

MAXBAND [86, 87] considers a two-way arterial with n signals (intersections), and specifies the corresponding offsets so as to maximize the number of vehicles that can travel within a given speed range without stopping at any signal (i.e. bandwidth), in the two directions of travel. The problem could be also formulated with the speeds in each segment as additional decision variables.

For such problem formulation, having the arrival times at the intersections variable, it is necessary to introduce some binary decision variables, which leads to a binary-mixed-integer-linear-programming problem. The employed branch-and-bound solution method benefits from a number of nice properties to reduce the required computational effort. Attempts to further reduce the computational effort required by the method are reported in [22]. Little extended the basic MAXBAND method via incorporation of some cycle constraints to render it applicable also to networks of arterials. MAXBAND has been applied to several road networks in North America. A number of significant extensions have been introduced in the original method in order to consider a variety of new aspects such as: time of clearance of existing queue, left-turn movements, and different bandwidths for each link of the arterial (MULTIBAND) [47, 122].

TRANSYT [111] is probably the most famous "offline" traffic signals control algorithm and is based on a traffic model that is used to estimate evolution in time of queue sizes. The objective function to be minimized is the sum of the average queues in the area by acting on the control inputs. First field implementations of TRANSYT-produced signal plans indicated savings of about 16% of the average travel time through the network. The method proceeds in an iterative way: for given values of the decision variables (i.e. splits, offsets, and cycle time) the dynamic network model calculates the corresponding performance index (e.g. the total number of vehicle stops). A heuristic "hill-climb" optimization algorithm introduces small changes to the decision variables and orders a new model run, and so forth, until a (local) minimum is found. The key knowledge for this algorithm to work properly is the data on average flows, maximum flows, cruise times and so on that have to be provided as inputs to the program. The main limitation of this strategy is that these data are collected most of the time physically by workers on the roadside, and the task is tedious as well as time consuming. Moreover, this information is stored and not systematically updated, hence the "offline" nature of this strategy. Its inventor used to say 25 years ago: "I find it difficult to believe that, as we approach the end of this century, traffic engineers and drivers will continue to tolerate signals with green and red times that were decided by the flows and queues that happened to be observed on one day many years earlier, rather than in the last five minutes." [110].

The main drawback of fixed-time strategies is that their settings are based on historical rather than real-time data. Traffic patterns and demands are not constant within the same day, and may vary in the long term or occasionally due to special events. Turning movements may also vary affecting the demands; furthermore the turning movements could vary in response to the optimized signal settings, since the drivers might try to optimize their individual travel times. Aging of the optimized settings may also lead to high inefficiency. For instance, if the capacity-maximizing phase of the algorithms is applied too late (e.g. high traffic demand

42
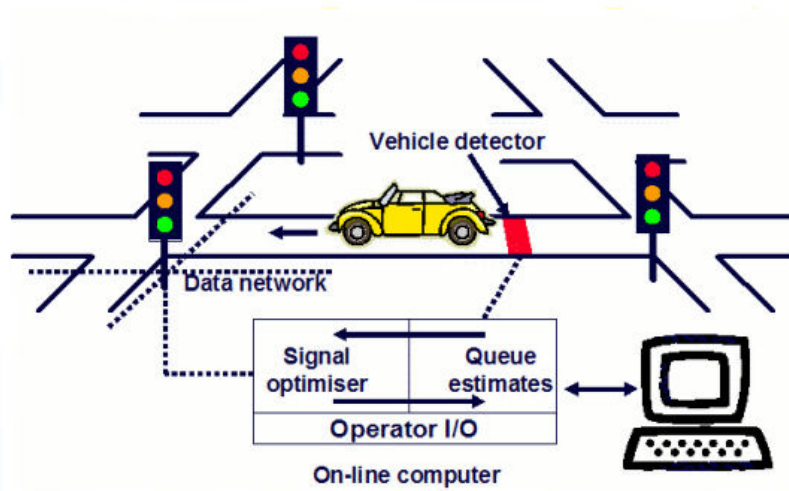
Figure 1.3 – The functioning principle of SCOOT (source: SCOOT website).

earlier than expected), queues quickly grow leading to a collapse of the network. In order to avoid this situation, traditionally the "peak-hours" phase of the algorithm is moved up in time, causing sometimes undesirable and unnecessary traffic delays.

Static strategies result to be a "blind" approach to the traffic control problem for several reasons, therefore a better solution is definitely provided by the so-called traffic-responsive algorithms, which are designed to trigger appropriate measures in response to the actual traffic conditions. In order to be able to respond to real-time varying traffic conditions, these strategies need sensors to retrieve traffic data, usually represented by magnetic loops embedded in the asphalt, and central control rooms for the processing of the data, besides higher installation and maintenance costs. In other words dynamic strategies are more reliable and efficient, but also more costly [103].

SCOOT [63] is probably nowadays the most famous and adopted traffic-responsive control measure. It is a hierarchical control strategy, it runs in a central computer, but it is functionally decentralized. It was designed to be the dynamic version of TRANSYT, and it found practical implementation in more than 150 cities in the United Kingdom, Santiago of Chile, Beijing, Sao Paulo, etc. In SCOOT (Split Cycle Offset Optimization Technique), the average one-way flow of vehicles past an intersection during each cycle time is collected in real-time, rather than calculated offline. This is accomplished by looking at the output of vehicle sensors located well upstream from stop lines at junctions, and ideally right after the previous intersection. In this position, sensors allow to have a very early information about arrivals in the monitored section, and also detect if the queue fills up completely

the section. In the case of gridlock, SCOOT optimizer can take specific measures. SCOOT has a traffic model running in real-time which, based on the readings of the flow profiles, is used to calculate the length of the queues in the whole controlled area. The algorithm tries incremental optimization to deal with variations in traffic demand. A few seconds before every phase change, the split optimizer computes whether it is beneficial to advance or delay the scheduled change or to leave it unchanged. Then, once per cycle, the offset optimizer calculates whether the objective (the sum of the average queues in an area, as in TRANSYT) can be reduced around each junction by changing the offset. Splits and offsets are adapted immediately, cycle times of a group of intersections are varied similarly every few minutes. SCOOT makes a large number of decisions, approximately ten thousand per hour on a network comprising one hundred intersections. However, this system is not robust in case of over-saturated traffic conditions. If the queue reaches the upstream detector, SCOOT is not able to understand the presence of stationary vehicles, and it may mistake the situation for a lower demand, decrease the duration of green time at the downstream intersection and cause in turn an increase in congestion.

SCATS [89] was developed almost at the same time in Australia. In order to better describe the functioning principles of this alternative traffic control strategy, which is used in some cities in Europe, Australia, USA and Hong Kong, the main differences between SCATS and SCOOT will be briefly described [116]. SCATS (Sydney Coordinated Adaptive Traffic System) relies upon offline pre-calculated plans with few local adaptations. In SCOOT the whole network is modeled, no plans are required, and the cyclic flow profiles are computed online and updated every four seconds. In SCATS the system is made up of several regional sub-systems, which contain different junctions. A junction in each sub-network is set to be the critical one, and cycle times and splits are optimized for this particular intersection. Plans are then selected for the other intersections based on the specific choice made for the critical one. In SCOOT the system consists of many regions with many intersections all controlled by a central computer. In SCATS the cycle time optimization is run once each cycle, whereas in SCOOT it is run once every two to five minutes. The split optimization in SCATS takes place once per cycle, whereas in SCOOT once per stage. In SCATS the offset is not optimized and is simply selected from the plans pre-computed offline; in SCOOT it is calculated once per cycle. SCATS calculates green splits based on the flow information collected in the previous cycle, therefore it may be unresponsive to abrupt changes in the demand. SCOOT bases its optimization on the data collected by the sensors in real-time and on the current queue at the traffic light, therefore it is more responsive to unpredictable arrival flows. SCATS utilizes two types of detectors, one near the stop line at the intersection to measure flow and occupancy, one (optional) upstream to measure queues. SCOOT needs only the detectors upstream

the intersections to measure flows, occupancy and queues. SCATS needs the specification of the critical node in each subsystem, which normally comprises up to five intersections. Plans to be used at the "secondary" nodes need to be defined, and the task to derive them may be quite time consuming. SCOOT needs some model parameters, such as travel times between detectors and stop lines, and they do not need to be further updated. An investigation conducted by the Australian research board showed no advantage of SCATS in terms of travel time with respect to TRANSYT. There was however a reduction of the number of stops by about 9% in the central area, and 25% on main arterials. As for SCOOT, results show a total delay reduction of about 12% as compared to TRANSYT, and this is expected to increase with time as fixed-time plans become outdated.

After these first, and yet largely employed, dynamic queue management strategies, a number of model-based more rigorous traffic-responsive algorithms have been developed: OPAC [46], RHODES [118], PRODYN [61], CRONOS [15], UTOPIA [92]. These algorithms do not treat explicitly cycles, splits ad offsets; based on pre-specified plans for the traffic lights phases, they calculate online the optimal switching schedule over a future rolling time horizon [103]. These methods solve an online dynamic optimization subject to realistic traffic models with a sample time of the order of few seconds and fed with traffic measurements. Discrete variables are employed to describe traffic lights behavior, and several constraints are imposed on the inputs, such as minimum and maximum green signals duration, etc. The performance index to be minimized, in these newer strategies, is the total time spent by the vehicles in the network. The rolling horizon adopted in the online optimization is rather long (i.e. about sixty seconds), but the results of the optimization are applied on a much shorter time window (i.e. about four seconds), before the algorithm is run again using new data information. The longer horizon optimization allows to avoid shortsighted control actions in a traffic-responsive framework.

One of the main problems of these strategies is the presence of discrete variables to model the alternating nature of the traffic lights, which requires exponential-complexity algorithms for a global optimization. OPAC utilizes an online optimizer based on complete enumeration to generate integer switching sequences. PRODYN and RHODES use dynamic programming and, due to the computational load of this mathematical tool, they are not suitable for an online implementation for more than one intersection. Therefore these two strategies are decentralized and split into multiple optimization subsystems, whose results are coordinated by a supervisory control layer. In particular in RHODES, the upper level of the control strategy also performs a prediction of future traffic conditions to allow a proactive behavior of the controllers at the lower level. CRONOS employs a heuristic global optimization method with polynomial complexity which allows for simultaneous management of several junctions, although specifying a local

minimum. Its performance has not been tested for networks with more than six-eight junctions. UTOPIA, currently operational at many intersections in Turin, Italy, is based on the concept of a fully variable cycle on a rolling horizon. The local controller performs a branch-and-bound optimization over a horizon of two minutes. The local cost function takes into account the queue length integrals and exceeding link storage capacity at all incoming roads of the junction. Each local controller receives from the neighboring junctions traffic lights timing plans, and information about queues, capacity, saturation flows and a reference nominal cycle for the specific area. Using this information, the local controller is able to assess how its signal timings affect downstream intersections and how neighboring nodes influence its released traffic. Queues at downstream intersections are monitored, and this allows to calculate the optimal offset between cycles to generate green waves in the main stream, along with reduction of the green stage of the cycle when downstream sections are close to saturation. By calibrating the parameters of the control algorithm, it is possible to balance the requirement of capacity maximization for low traffic conditions and spill-backs management for saturated and over-saturated traffic conditions.

To summarize, renowned traffic control strategies like SCOOT and SCATS have been often criticized for their incremental optimization approach and for their consequent lack of a real traffic-responsive behavior during rapidly changing conditions. Moreover these strategies are known to be not very robust to over-saturated conditions. In other already described strategies, the control decisions are taken in a decentralized way at junction level while the network coordination is carried out at higher supervisory levels. However the superior levels are heuristic and may fail to ensure a real effective network coordination, while lower levels rely on computationally heavy optimization algorithms which allow local application only to a reduced number of nodes. As a consequence, none of the aforementioned queue management strategies is truly centralized and applicable to large-scale networks. Simplifications introduced in some strategies (e.g. PRO-DYN considers a two-stage cycle at each junction with an equal amount of lost time between each phase, etc.) to facilitate real-time execution of the algorithm may affect the generality of the strategy and limit their suitability to real situations. Finally, despite maintenance activity on vehicle detectors installed in the roads, failures and communications faults may occur, and the described strategies do not address the problem of robustness to sensor failure, resulting in a collapse of the queue management algorithm.

The aforementioned traffic-responsive strategies represent industrial solutions that found large practical implementations. However, their complex hierarchical and layered architecture, as well as the lack of detailed scientific references, make it difficult to fully understand their functioning principles, and to compare them against other strategies. On the contrary, the control strategies described hereafter

are well documented in the literature.

The next traffic-responsive control strategy here to be presented was developed in order to overcome the limitations of sensor failure robustness and large-scale applicability. TUC [32] is based on the store-and-forward modeling approach [49], and it consists of four distinct control modules for split times, cycle times, offsets and priorities for public transportation. All control modules are based on feedback concepts which ensure a certain implementation simplicity, without compromising its efficiency [104, 39, 33]. The split control is a network-wide centralized module which, using all the available measurements, computes the duration of green phases of all the traffic lights in the monitored area. This calculation is run once per cycle. The cycle control computes one single cycle for all nodes in the network in order to enable offset coordination. The offset control module is decentralized and operates on pairs of junctions in order to generate green waves on successive links, also taking into account the presence of queues in the respective sections. The public transportation priority module is implemented locally at the junction level in order to enable fast communication with the detectors. Therefore traffic data measurements are needed only once per cycle, and only occupancy data are required, since the algorithm embeds a mathematical relation to convert occupancy to average number of vehicles. Splits and cycles control are truly centralized and network-wide applied; this makes the strategy more robust to failures of some sensors in the road network. TUC found practical implementation and employment in Glasgow and Southampton, UK, and Chania, Greece, often outperforming the resident traffic control strategies (e.g. SCOOT in the UK). The problem of the large-scale network control in the case of saturated traffic conditions has been further treated in future works, always making use of the store-and-forward modeling approach [2, 3, 4].

Other model-based coordinated strategies have been recently proposed in the literature. In general, centralized strategies need to deal with the issue of scalability and computational complexity, since the control algorithm is typically run in a central machine for the entire monitored network. Therefore, the main challenge for this type of management strategies is to model the traffic network in a simple but representative way, in order to devise an effective control with a relatively low computational cost. In [17], a cellular-automaton model has been used to describe an urban network, and to devise different traffic lights controllers that increase the vehicular flow. Cellular automaton models have the distinction of being able to capture micro-level dynamics and relate these to macro-level traffic flow behavior. This is in contrast with other existing models, which are either aggregate in their treatment of traffic flow (macroscopic models) or too detailed and limited in scope (microscopic models). A possible macroscopic traffic model for real-time optimization of signalized urban areas has been proposed in [12], and then extended in [40] to take into account some more realistic elements of a traffic net-

work, such as different types of vehicles, pedestrians movements, amber phases for the traffic lights, etc. The optimization problem in [40] tries to minimize the number of vehicles in the road network by acting on splits and offsets of the traffic lights. Other modeling and control solutions for the network-wide control of traffic lights have been proposed in [84, 83, 85]. Here the optimization makes use of model-based predictive control techniques to minimize the total time spent by the vehicles in the traffic network.

In order to solve the issues of scalability and real-time applicability of the control measures, only in recent times few interesting distributed control strategies have been presented. An application of the distributed model-based predictive control has been proposed in [19, 120]. The traffic network has been linearly modeled, and the control objective is to discharge vehicle queues while penalizing deviation from a nominal control plan, by acting on the stage times of the traffic lights. The network is conceptually modeled as a graph with links carrying the information. The influence of the other agents is captured through the saturation flows and the turning rates from the agent-corresponding upstream links.

A recent distributed approach that inspired several further research investigations is the max-pressure algorithm, defined for arbitrary networks of signalized intersections [135, 134, 138], and inspired by the scheduling of packet transmission in wireless networks. The calculations in the max-pressure strategy are local: the evaluation at each intersection at any time requires knowledge only of the queues at adjacent links at that time. The max-pressure control represents an alternative to the signal control systems that attempt to minimize the cost over an infinite or finite rolling horizon. Calculation of this future cost requires prediction of future demands and turn ratios, and if the prediction is biased, the control strategy will not be optimal. By contrast, the max-pressure requires no knowledge of the demand, although it does require knowledge of turn ratios, which could also be estimated in the adaptive version of the algorithm. Lastly, other traffic control systems do not come with a guarantee that the resulting closed loop system will be stable. The max-pressure control is claimed to be a stabilizing control, if there exists any stabilizing control, and it maximizes throughput.

1.4   Main Contributions of the Dissertation

A visual summary of the literary review is given in Figure 1.4. The contributions of this work to the energy-aware traffic management lie in both vehicle-side management and infrastructure-side management, and may be summarized as follows.

Firstly, a solution for the coordinated vehicle management has been proposed, in which communication with the infrastructure is exploited to reduce the vehicle
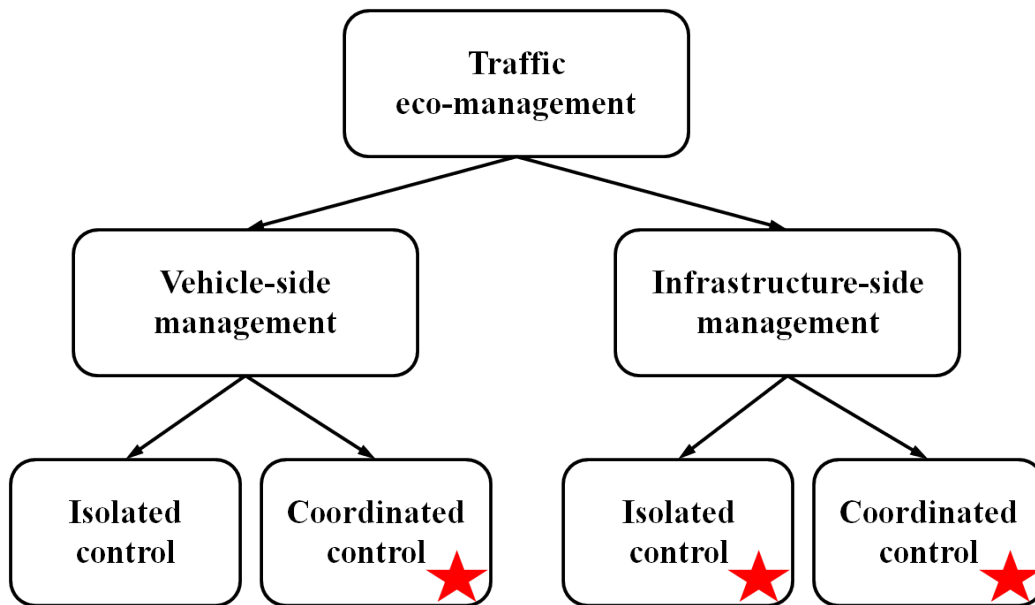
Figure 1.4 – Traffic management strategies categorization. The red stars indicate where the contributions of this dissertation lie with respect to the existing scientific literature.

energy consumption. In particular, the traffic lights timings are assumed to be communicated to the vehicle and known, and the vehicle is suggested an optimal speed to drive through a sequence of signalized intersections without stopping, and following a minimum-energy trajectory. As compared to the existing literature, the proposed solution addresses the energy consumption problem by explicitly considering it in the optimization, takes into account multiple traffic lights in an urban corridor, and presents an energy consumption model that depicts also accelerations induced by the variable speed advisory. The proposed algorithm, independently applied to each vehicle, has been tested in a microscopic traffic simulator in order to assess the impact on the traffic performance. The analysis has demonstrated that the energy consumption and the number of stops can be drastically reduced without affecting the travel time.

Secondly, a solution for the isolated infrastructure management has been proposed. A novel macroscopic urban traffic model has been introduced to describe the traffic evolution, and the variable speed limits have been used as actuation to improve traffic performance. A macroscopic energy consumption model has been tailored to the introduced traffic model. The analysis has been carried out at saturated traffic conditions, with given and fixed traffic lights scheduling. The optimization aims at reducing the energy consumption in trade-off with the average travel time of the vehicles in the considered road section. Experiments have

demonstrated that there exists an optimal speed limit that improves traffic performance by reducing the length of the queue at the traffic light, and by redistributing the traffic density more efficiently.

Lastly, a solution for the coordinated infrastructure management has been proposed. Traffic lights coordination on arterials has been proved to be effective in terms of traffic delay reduction. Our analysis has demonstrated that an optimization problem can be cast to take into account also energetic aspects. In particular the control action is exerted both on the traffic lights coordination and on the variable speed limits in each road section of the considered topology. Extensive experiments in a microscopic traffic simulator have shown that a correlation exists between traffic progression and traffic performance metrics, such as energy consumption and travel time. The proposed control strategy is able to achieve a significant reduction of energy consumption, almost completely eliminating number of stops and idling time, without affecting the travel time.

Chapter 2

Energy-Optimal Vehicle Trajectory in a Signalized Urban Corridor

2.1 Introduction

Traffic congestion and idling time at signalized intersections are among the main causes of energy consumption. In [54], experiments showed that the concentration of fine particles in the air at traffic lights during stops is twenty-nine times higher as compared to free-flow conditions. Also, even though the delay time at intersections represents only a minor portion of the entire commuting time, it may contribute up to about 25% of the total trip emissions.

The state-of-the-art in wireless communication, the deployment of dedicated communication protocols for Vehicular Ad-hoc Networks (VANETs), and the decreasing price of GPS receivers, allow more and more to rely on communication between the different agents of an urban traffic network for the design of robust and efficient traffic control strategies [60]. Specifically, infrastructure-to-vehicle (I2V) and vehicle-to-vehicle (V2V) communications attracted the attention of many due to their potential to enable fast and cheap Advanced Driver Assistance Systems (ADAS).

Knowledge of the traffic lights signal timings has been proved to be significantly beneficial in terms of energy efficiency in urban traffic. Green Light Optimized Speed Advisory (GLOSA), with different penetration rate of the technology, has shown promising advantages in terms of fuel consumption and average idling time [69]. Vehicles energy consumption is strictly related to the accelerations in driving profiles. Soft decelerations to traffic lights on red, using advanced wireless-transmitted information, have been proved to be more energy efficient than sudden stops, allowing a reduction of both fuel consumption and emissions [80]. In general, it is possible to reduce energy consumption by preventing a

vehicle from coming to a full stop at the intersections and by advising cruising velocities in order to catch as many green lights as possible. This goal can be achieved in different ways. In [91], authors developed an algorithm to minimize the acceleration profile while driving through a sequence of signalized intersections, simulating scenarios with stochastically varied parameters and showing a systematic reduction of fuel consumption, emissions and travel time. Interesting results on eco-driving with probabilistic Signal phase and timing (SPAT) information are shown in [90], where a comparison between an uninformed driver and a driver with different information levels (full horizon and short-term) is conducted using Dynamic Programming (DP). An innovative solution to the velocity advisory problem, in proximity to a traffic light, was proposed in [73], where smartphones make use of their cameras to build a SPAT map of every intersection by relying only on V2V communication, without directly interacting with the infrastructure. This approach may enable GLOSA service and adaptive route change (ARC). Predictive Cruise Control (PCC) in traffic networks with signalized intersections was extensively treated in [10]. The objective is to penalize the braking action to indirectly reduce energy consumption and travel time, and to discourage deviations from a suggested speed that allows to cross intersections without stopping. Somewhat similar approach was used in [101]. A preliminary algorithm determines the arrival times at each traffic light, by assuming that the closest trajectory to the one of the unconstrained case (i.e. no traffic lights) is the most energy-efficient. Then an analytical and numerical solution to the fuel consumption minimization problem is proposed, for a scenario with three traffic lights over a driving horizon of nine kilometers. In [107] only one traffic light is considered and accelerations upstream and downstream from the intersection are varied to find sub-optimal values for the fuel consumption minimization problem. In [95] DP is used to find the minimum energy solution, for a driving horizon enclosing up to two traffic lights. An approach to the multi-segment speed advisory is presented in [119]. The fuel consumption is indirectly minimized by penalizing speed variations between adjacent road sections. The strategy accounts for multiple intersections and shows how such optimization yields better results with respect to the single-segment approach. However nothing is stated about the computation time and online applicability of the algorithm.

Assuming I2V communication, and therefore full knowledge of the traffic lights timings, the goal of this work is to analyze the driving horizon and compute an energy-efficient speed advisory for the driver. As in previous works, stops at a red traffic light are to be avoided. The novelty of this work is summarized as follows. Given a set of green traffic light phases, there exist different driving profiles to reach a given destination at a given final time in compliance with traffic lights constraints (i.e. always catching the green light) and city speed limits. The presented strategy is capable of an a priori identification of the most energy-efficient

velocity trajectory, by approximating the available trajectories and their energy cost with an oriented weighted graph. The computational complexity of the graph creation could be also reduced from exponential [30] to polynomial, thanks to the introduction of the line graph. The computation time is consequently significantly reduced. Only after this preliminary stage of trajectory selection, a formal optimization problem is solved in order to calculate the optimal arrival times at each intersection, by explicitly minimizing the energy consumption of the vehicle. This approach qualifies as a pre-trip eco-driving ADAS, since the speed advisory is provided to the driver at the beginning of the driver horizon. However, given the very little computation time required by the algorithm, it may be employed online thus enabling in-trip assistance features. This allows to respond dynamically to traffic perturbations and/or deviations from the speed advisory, and to increase the robustness and the applicability of the strategy in a realistic environment. Simulations in a microscopic traffic simulator demonstrate that the proposed strategy is able to deal online with perturbations coming from traffic and to reduce the overall energy consumption without affecting travel time.

In the following we will first introduce the vehicle model and formulate the optimization problem. Then, we will present in detail the methodology that we followed for the sub-optimal solution of the problem. We will show some validation results of the proposed algorithm with respect to the true energy consumption calculated offline via DP. Finally, we will demonstrate the robustness capabilities of the algorithm through experiments in a microscopic traffic simulator.

2.2 Problem Formulation

This work has as objective the minimization of the energy consumed by vehicles in a traffic network to travel from an initial to a final point, in presence of signalized intersections in the driving horizon. Clearly this problem is not trivial because the travel time, and more importantly the acceleration and velocity profiles of a vehicle, are affected by other agents of the traffic network (i.e. traffic lights), whose actions and priorities may conflict with the time constraints of the vehicles.

The analysis is carried out for a simplified urban traffic network with vehicles in free flow, with no constraints coming from other users of the infrastructure. However, we will show that the algorithm may be employed also in more realistic scenarios where the presence of multiple vehicles requires the speed advisories to be updated dynamically.

I2V communication is assumed, and the vehicles have full knowledge of the n traffic lights timings in the driving horizon.

From a mathematical point of view, a constrained optimization problem can

be cast. Energy consumption over the trip horizon is to be minimized, subject to the vehicle dynamical model, and time constraints to impose arrivals at the intersections during a green phase.

2.2.1 Vehicle Model

Vehicles equipped with electric motors will be considered in this work. The equivalent circuit model of a DC motor gives [105]:

$$
\begin{aligned}
V_a &= i_a R_a + e \\
e &= \kappa \omega_m \\
T_m &= \kappa i_a
\end{aligned}
\tag{2.1}
$$

where V_a is the armature voltage, i_a is the armature current, R_a is the armature resistance, e is the back electromotive force, κ is the speed constant, ω_m is the rotational speed of the motor, T_m is the electromagnetic motor torque. The motor power supply is converted into mechanical power and electric power loss due to heating of the armature coil, as follows:

$$
P = V_a i_a = \omega_m T_m + \frac{R_a}{\kappa^2} T_m^2
\tag{2.2}
$$

where $V_a i_a$ is the electric power supplied to the armature, $\omega_m T_m$ is the actual mechanical power developed by the armature, and $\frac{R_a}{\kappa 2} T_m^2$ is the electric power wasted in the armature. The control input u is represented by the motor torque:

$$
u = T_m
\tag{2.3}
$$

The vehicle longitudinal dynamical model may be generally written as:

$$
m \frac{\mathrm{d}v}{\mathrm{d}t} = F_t - F_{\text{aero}} - F_{\text{friction}} - F_{\text{slope}}
\tag{2.4}
$$

where F_t is the traction force at the wheels, F_{aero} the aerodynamic force, F_{friction} the rolling resistance force, F_{slope} the gravity force, v the vehicle speed, and m its mass.

In the following we assume that there are no losses in the transmission, no slip at the wheels, and that the road slope does not vary in space. In particular, the road slope could be approximated by an average value. Therefore, from (2.4) the vehicle model shall be written as:

$$
\begin{cases}
\dot{x} = v \\
m\dot{v} = \frac{u R_t}{r} - \frac{1}{2} \rho_a A_f c_d v^2 - mg c_r - mg \sin(\alpha)
\end{cases}
\tag{2.5}
$$

where x is the vehicle displacement, R_t is the transmission ratio, r is the wheel radius, ρ_a is the external air density, A_f is the vehicle frontal area, c_d is the aerodynamic drag coefficient, c_r is the rolling resistance coefficient, α is the road slope, and g is the gravity.

The sum of the aerodynamic and rolling frictions can be approximated as a second order polynomial in the velocity v:

$$F_{\text{res}} = F_{\text{aero}} + F_{\text{friction}} = a_0 + a_1 v + a_2 v^2 \tag{2.6}$$

where a_0, a_1 and a_2 are parameters identified in previous works [34, 36].

Under these assumptions the vehicle model can be simplified as follows:

$$\begin{cases} \dot{x} = v \\ \dot{v} = h_1 u - h_2 v^2 - h_3 v - h_0 \end{cases} \tag{2.7}$$

with

$$h_1 = \frac{R_t}{mr}, \quad h_2 = \frac{a_2}{m}, \quad h_3 = \frac{a_1}{m}, \quad h_0 = \frac{a_0}{m} + g\sin(\alpha) \tag{2.8}$$

Therefore, the power demand can be expressed as:

$$P = b_1 u v + b_2 u^2 \tag{2.9}$$

where

$$b_1 = \frac{R_t}{r}, \quad b_2 = \frac{R_a}{\kappa^2} \tag{2.10}$$

2.2.2 Traffic Lights Timings

In this study the traffic lights are not actuated, therefore cycle time, phase time and offset are deterministic and given. It is possible to formulate mathematically the state evolution of the traffic lights as follows:

$$s_i(\tau) = \begin{cases} 1, & kT < \tau - \theta_i \leqslant kT + T_{\text{gr}} \\ 0, & kT + T_{\text{gr}} < \tau - \theta_i \leqslant (k+1)T \end{cases} \tag{2.11}$$

where s_i is the state of the i-th traffic light, $k \in \mathbb{Z}$ is the number of cycles, T is the cycle time, T_{gr} is the duration of the green phase, and $\theta_i \in [0, T)$ is the traffic light offset at intersection i, for $i \in \{1, \ldots, n\}$.

2.2.3 Optimal Control Problem

Finally, the optimization problem may be stated as follows:

$$
\begin{cases}
\min_{u} \quad J = \int_{t_0}^{t_f} b_1 uv + b_2 u^2 \, \mathrm{d}t \\[2mm]
\text{s.t.} \quad \dot{x} = v \\[1mm]
\qquad \dot{v} = h_1 u - h_2 v^2 - h_3 v - h_0 \\[1mm]
\qquad x(t_0) = d_0, \quad x(t_f) = D \\[1mm]
\qquad x(t_i) = d_i \wedge s_i(t_i) = 1 \\[1mm]
\qquad v(t_0) = v_0, \quad v(t_f) = v_f \\[1mm]
\qquad v_{\min} \leq v \leq v_{\max} \\[1mm]
\qquad u_{\min} \leq u \leq u_{\max}
\end{cases}
\tag{2.12}
$$

where (t_0, d_0) are the vehicle coordinates at the origin of the driving horizon, (t_f, D) are the coordinates of the destination of the driving horizon, t_i is the crossing time at the i-th intersection, d_i is the position of the i-th intersection, for $i \in \{1, \ldots, n\}$, v_0 and v_f are the desired initial and final velocities.

A solution to a simpler problem, with no traffic lights and a simplified vehicle model, was found analytically in [105]. In the case under analysis, the traffic lights introduce an additional complexity to the problem, expressed mathematically by the constraint:

$$
x(t_i) = d_i \wedge s_i(t_i) = 1
\tag{2.13}
$$

Equation (2.13) imposes a non-stop requirement at the signalized intersection, by specifying that the vehicle has to be at the intersection d_i at time t_i, when the traffic light s_i is green. This constraint may result in disjoint sets due to the presence of multiple available green phases at each intersection, and may affect the convexity of the problem. In other words the constraint (2.13) defines a non-convex set, and the nonlinear objective function, because of such discontinuity in the constraints, assumes multiple local minima. Therefore, the solution to this optimal control problem has to be sought in a sub-optimal way, by use of algorithms that simplify the control envelope, recover the convexity of the constraints set and solve the optimization advising the driver on the velocity to track.

The problem can be solved in a local optimal way by the DP, provided that the selection of the green phases to be traversed is made a priori. In order to obtain a global optimum, DP should be run extensively on all the possible trajectories to find the one with minimum cost. However its high computational load is clearly not suitable for online uses. In the following, the results obtained via DP will be

used as a benchmark for validation and evaluation of the employed sub-optimal strategy.

2.3 Optimization Algorithm

The original optimal control problem (2.12) will be now divided into sub-problems for the simplification of constraint (2.13) and the formulation of a convex optimization problem. The idea is to identify the best green phase at each intersection, in order to finally optimize over a single trajectory from origin to destination.

The methodology may be summarized as in Figure 2.1, and described as follows:

1. Pruning algorithm to identify the set of feasible portions of green phases at each intersection. The notion of feasibility refers to the time intervals that allow not to stop and to drive in compliance with the speed limits ($v \in [v_{\min}, v_{\max}]$). The pruning algorithm will reduce the search space of the best non-stop trajectory in the driving horizon.

2. Construction of a weighted directed acyclic graph in the feasibility region to approximate the energy cost of all the possible trajectories in the driving horizon. Dijkstra's algorithm [38] is then run on the approximating graph in order to identify the "best" trajectory (i.e. most energy efficient). With the selection of a single trajectory in the driving horizon, the optimization problem will become convex.

3. Solution of a simple convex optimization problem to obtain the optimal crossing times at each intersection through the previously selected feasible green phases.
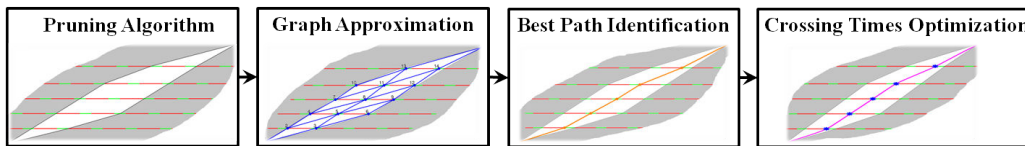
Figure 2.1 – Block diagram representation of the proposed strategy.

2.3.1 Pruning Algorithm

The velocity pruning algorithm reduces the search space of available green phases by identifying only the feasible ones that allow to reach the destination
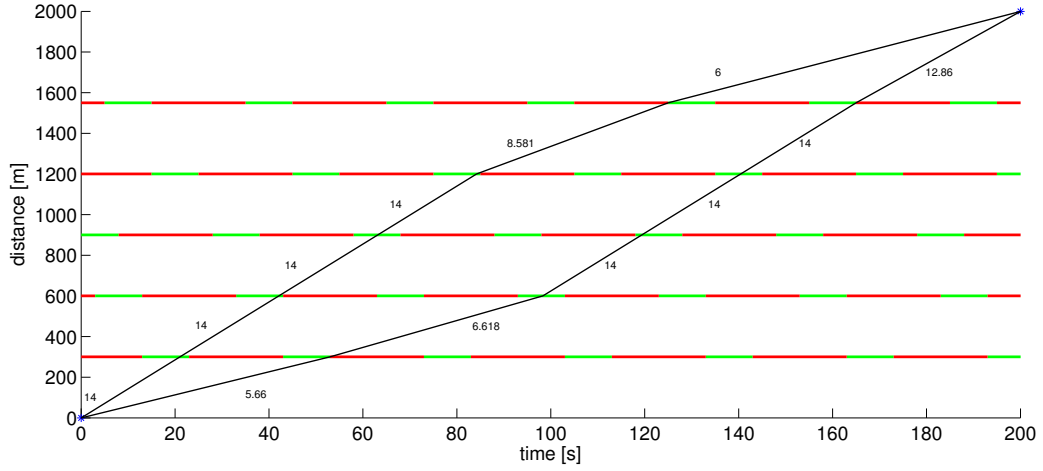
Figure 2.2 – Feasibility region obtained via the pruning algorithm. The labels indicate the speed of the region boundaries, calculated from $t_{i,\min}$ and $t_{i,\max}$. The speed limits were set to $\{v_{\min}, v_{\max}\} = \{5, 14\}$ m/s.

at the specified final time without stopping, and in compliance with the imposed speed limits.

The algorithm will output $\{t_{i,\min}, t_{i,\max}\}, \forall i \in \{1, \ldots, n\}$, which represent respectively the minimum and the maximum feasible crossing time at the i-th intersection. The algorithm may be described as follows:

At each intersection $i \in \{1, \ldots, n\}$, the minimum and the maximum feasible crossing times $t_{i,\min}$ and $t_{i,\max}$ are calculated, as indicated in step 2-3 of Algorithm 1. A check on the feasibility of $t_{i,\max}$ is performed in step 4, by checking whether it is possible to reach the destination in compliance with $v_{\max}$. If not feasible, $t_{i,\max}$ is anticipated to the last feasible time instant. The two crossing times $t_{i,\min}$ and $t_{i,\max}$ are verified to belong to a green phase in steps 5-10. If not, they are set to the first instant of the next green phase (line 6) or the last instant of the previous green phase (line 9), respectively. Finally a backward check is performed at each intersection in steps 12-19. If there is any $t_{i,\max} \le t_{i-1,\max}$ or any $t_{i,\max}$ that induces higher speeds than $v_{\max}$, then $t_{i-1,\max}$ is anticipated to the last feasible time instant (step 14). The new $t_{i-1,\max}$ is verified to belong to a green phase in steps 15-17. If not, it is set to the last instant of the previous green phase.

In case no feasible region is found (i.e. $t_{i,\min} > t_{i,\max}$ for any $i \in \{1, \ldots, n\}$), a non-stop trajectory does not exist. However the pruning algorithm is not computationally demanding and may be quickly run again at the beginning of the next green phase or in the case of a triggering event (e.g. a sudden stop, an unexpected deceleration, a deviation from the advised velocity, etc.).

In Figure 2.2 an example of feasible region found by the pruning algorithm

---

Algorithm 1 Pruning algorithm

1: **for** $i \leftarrow 1$ to n **do**
2: $\quad t_{i,\min} = \frac{d_i - d_{i-1}}{v_{\max}} + t_{i-1,\min}$;
3: $\quad t_{i,\max} = \frac{d_i - d_{i-1}}{v_{\min}} + t_{i-1,\max}$;
4: $\quad t_{i,\max} = \min \left\{ t_{i,\max}, t_f - \frac{D - d_i}{v_{\max}} \right\}$;
5: $\quad$ **if** $s_i(t_{i,\min}) \neq 1$ **then**
6: $\quad\quad t_{i,\min} = \left(\left\lfloor \frac{t_{i,\min}}{T} \right\rfloor + 1 \right) T + \theta_i$;
7: $\quad$ **end if**
8: $\quad$ **if** $s_i(t_{i,\max}) \neq 1$ **then**
9: $\quad\quad t_{i,\max} = \left\lfloor \frac{t_{i,\max}}{T} \right\rfloor T + T_{\text{gr}} + \theta_i$;
10: $\quad$ **end if**
11: **end for**
12: **for** $i \leftarrow n$ to 1 **do**
13: $\quad$ **if** $t_{i,\max} \leq t_{i-1,\max} \; || \; \frac{d_i - d_{i-1}}{t_{i,\max} - t_{i-1,\max}} > v_{\max}$ **then**
14: $\quad\quad t_{i-1,\max} = t_{i,\max} - \frac{d_i - d_{i-1}}{v_{\max}}$;
15: $\quad\quad$ **if** $s_{i-1}(t_{i-1,\max}) \neq 1$ **then**
16: $\quad\quad\quad t_{i-1,\max} = \left\lfloor \frac{t_{i-1,\max}}{T} \right\rfloor T + T_{\text{gr}} + \theta_{i-1}$;
17: $\quad\quad$ **end if**
18: $\quad$ **end if**
19: **end for**

---

is shown. It is easy to observe how the algorithm was capable of shrinking the feasible driving domain to the region bounded by the black lines. The algorithm ensures that inside the feasible region a trajectory compliant with the speed limits exists. All the green phases outside the feasible region will be no longer considered because they would induce driving profiles in violation of the speed limits.

2.3.2   Optimal Trajectory

After running Algorithm 1, the set of feasible green phases is significantly reduced. However many possible trajectories from origin to destination are still present, and constraint (2.13) still defines a disjoint set, due to the presence of multiple available green phases at each intersection.

The idea is to approximate, by means of a weighted directed acyclic graph, the energy cost of all the possible trajectories from the initial to the final point within the feasibility region, as shown in Figure 2.3. The approximation consists in placing the nodes of the graph at specified crossing times in the feasible green phases. The number of nodes per feasible green phase depends on the fineness
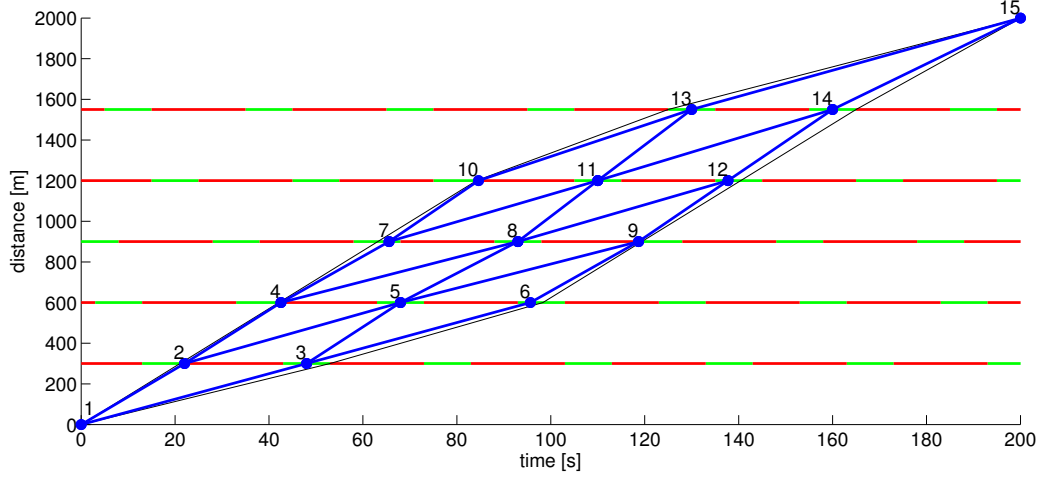
Figure 2.3 – Graph of the possible trajectories within the feasibility region, with one node per green phase (nodes = 15, edges = 22). The labels indicate the ID of the node.

of the approximation. In the case of one node per green phase, the node will be placed at the midpoint of the feasible green interval. In the case of three nodes per green phase, the nodes will be placed at the midpoint and at the two ends of the feasible green interval. In the case of a finer approximation, the nodes will be equally spaced, always keeping one node at the phase and two nodes at the two ends of the feasible green interval.

Therefore, let $\mathcal{G} = (N, M)$ be such a graph, where N is the set of vertices (or nodes) p_i, for $i = 1, \ldots, |N|$, representing the crossing times at each feasible green phase, and M is the set of feasible edges (or links) connecting the vertices of the graph. Let us also define a weighting function $w : M \to W$, which associates each edge of the graph with a weight. In this application the weight W is the energy cost to travel along the trajectory, and it may be seen as the sum of two contributions:

$$W = E_{\text{total}} = E_{\text{link}} + E_{\text{jump}} \tag{2.14}$$

The energy consumed by the vehicle on a link is due to a constant-speed trip, which is completed in ΔT seconds, with no acceleration and time-invariant power demand:

$$E_{\text{link}} = \Delta T \left(b_1 \bar{u} \bar{v} + b_2 \bar{u}^2 \right) \tag{2.15}$$

where $\bar{v} = \frac{d_i - d_{i-1}}{\Delta T}$ is the constant velocity on the edge, and $\bar{u} = \frac{1}{h_1} \left(h_2 \bar{v}^2 + h_3 \bar{v} + h_0 \right)$ from (2.7). The link travel time is defined as $\Delta T = \tau_{p_j} - \tau_{p_i}$, for every edge $(p_i, p_j) \in M$, and $p_i, p_j \in N$, with τ being the crossing time associated with the relative vertex.

The energy associated with the change of velocity at a node between two edges, is defined as:

$$E_{\text{jump}} = \int_0^{t_{\text{jump}}} b_1 u(t)v(t) + b_2 u(t)^2 \, dt \tag{2.16}$$

where $u(t) = \frac{1}{h_1}\left(\dot{v}(t) + h_2 v(t)^2 + h_3 v(t) + h_0\right)$ from (2.7), and $v(t)$ is the time-varying velocity in every transient linearly modeled as $v(t) = \bar{v}_{\text{in}} \pm a \cdot t$, with a being a constant fixed acceleration, $\bar{v}_{\text{in}}$ the constant velocity on the incoming edge to the node. The speed change is assumed to be performed in $t_{\text{jump}} = \frac{|\bar{v}_{\text{out}} - \bar{v}_{\text{in}}|}{a}$, with $\bar{v}_{\text{out}}$ being the constant velocity on the outgoing edge from the node. Note that regenerative braking is not considered in this analysis, therefore E_{jump} is lower-bounded by 0.

The main challenge of such graph approximation is represented by the weight assignment to the edges. Every node of the graph with two or more incoming edges is critical because $\bar{v}_{\text{in}}$ is not unique, and this generates multiple and ambiguous contributions E_{jump} for the outgoing edge. Therefore, the critical nodes need to be "decoupled" in order to have a correct weight assignment.

Tree Expansion

One option to deal with this problem is to transform the directed acyclic graph into a tree [30]. The decoupling of the graph into the tree of all the possible trajectories is shown in Figure 2.4. It was necessary to create duplicates of the critical nodes in order to have independent trajectories, and in the case under analysis the initial setting with 15 nodes (Figure 2.3) results in a bigger network (Figure 2.4) with 55 nodes.

Well known theorems in graph theory allow to analyze a priori the complexity of this procedure [53]. Specifically, being A the adjacency matrix of a graph $\mathcal{G} = (N, M)$, the number of paths of length r from a node a to a node b is given by $(A^r)_{a,b}$, that is the matrix entry (a, b) of the adjacency matrix to the power r.

The number of nodes of the expanded decoupled tree is given by the sum of the entries of the first row of the geometric series of the adjacency matrix up to the length of the trip r. The geometric series generated by the matrix A, if $|\lambda_i| \leq 1$ for each eigenvalue $|\lambda_i|$ of A, is known to converge to

$$\sum_{k=0}^r A^k = (I - A)^{-1}(I - A^{r+1}) \tag{2.17}$$

The problem has evidently an exponential complexity and its computational load might increase significantly.
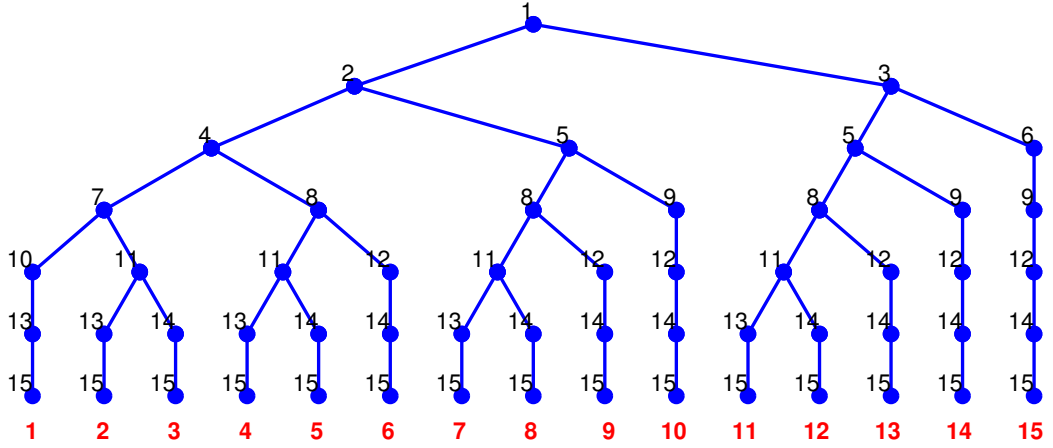
Figure 2.4 – Tree expansion of the possible trajectories from the root to the destination (nodes = 55, edges = 54). The black labels indicate the ID of the node as in Figure 2.3. The red labels indicate the trajectory ID.

To transform the decoupled tree back into a graph, a fictitious destination node is added and connected to all the leaves, resulting in 56 nodes and 69 edges.

Once the weighted directed acyclic graph structure is recovered, Dijkstra's algorithm is run on the expanded graph in order to find the minimum energy trip from the origin to the destination.

Line Digraph

A more efficient solution, in terms of memory allocation and computational load, is proposed in this work, and it is represented by the extension of the original graph into a line digraph [59].

The line graph, $\mathcal{L}(G)$ of a graph $\mathcal{G}$ has as vertices the edges of $\mathcal{G}$, and two vertices of $\mathcal{L}(G)$ are adjacent whenever the corresponding edges of $\mathcal{G}$ are adjacent. In other words each link of the line digraph represents a turning movement of the original graph. The in-degree $\text{id}(p_i)$ of a vertex p_i is the number of edges incident to p_i (the inlines at p_i), while its out-degree $\text{od}(p_i)$ is the number of edges leaving p_i (the outlines at p_i). A point with no inlines is a source, one with no outlines is a sink.

Let $\mathcal{G} = (N, M)$ be the graph with N nodes and M edges as before. Then in $\mathcal{L}(G) = (N^*, M^*)$, the number of nodes is $|N^*| = |M|$ and the number of edges is:

$$|M^*| = \sum_{i=1}^{|N|} \text{id}(p_i) \cdot \text{od}(p_i)$$
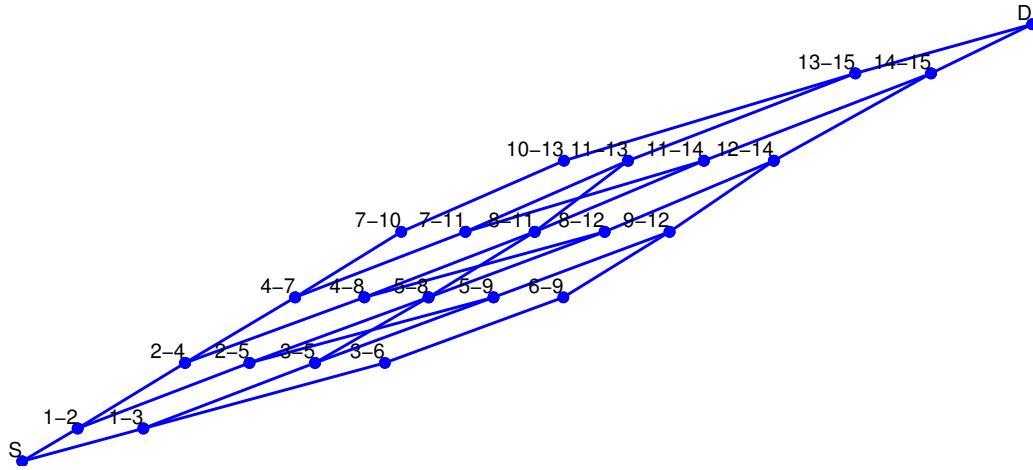
Figure 2.5 – Line graph of the original graph in Figure 2.3 (nodes = 24, edges = 34). The labels indicate the node identifier in the line graph, that is the corresponding link in the original graph.
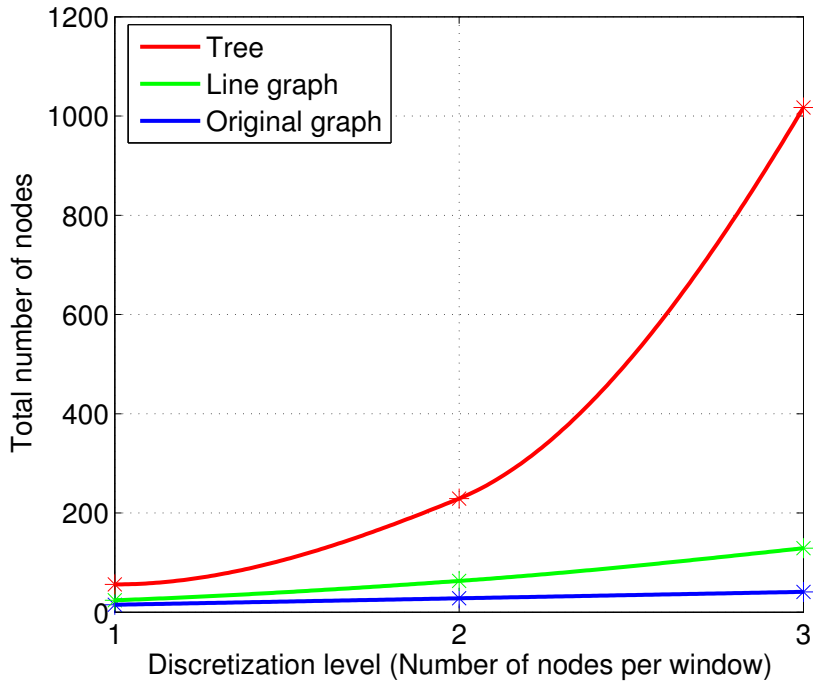
Figure 2.6 – Comparison of the computation time for the creation of the expanded tree as an adjacency matrix and the line digraph as an edge list. In abscissa the number of nodes of the original graph.

The adoption of the line graph allows to solve the criticality of the original graph by intrinsically decoupling the nodes with multiple incoming edges. The problem boils down to assigning to each edge of the line graph a weight corresponding to the sum of E_{link} relative to the edge indicated in the identifier of the destination node, and the E_{jump} relative to the speed change when coming from the link indicated in the origin node (see Figure 2.5). Furthermore, the size of $\mathcal{L}(G)$ is smaller than the size of the tree of all the possible trajectories [30]. As shown in Figure 2.6, the number of nodes in the expanded tree grows with an exponential law, whereas the number of nodes of the line graph grows with a polynomial law (namely quadratic).

Having as objective the online adoption of the algorithm, further improvements can be achieved by exploiting the specific structure of the graph. The adjacency matrix of a directed acyclic graph is highly sparse, in fact all the diagonal and lower-diagonal terms are zero. The high sparsity of the adjacency matrix leads to very inefficient memory management and matrix operations, therefore it is highly beneficial to define the directed graph as a list of edges.

By adding the two fictitious nodes S and D in the line graph, the structure of a directed graph with one source and one destination is recovered. At this point, Dijkstra's algorithm can be run on the line graph in order to obtain the most energy efficient trajectory from origin to destination on the approximating graph. Dijkstra's algorithm will return the optimal nodes to be traversed, which will be mapped back into the optimal trajectory on the original graph. In Table 2.1, the possible paths and their identifiers are reported.

Table 2.1 – Possible trajectories in the original graph

Path	Path Identifier	Path	Path Identifier
1-2-4-7-10-13-15	1	1-2-5-8-12-14-15	9
1-2-4-7-11-13-15	2	1-2-5-9-12-14-15	10
1-2-4-7-11-14-15	3	1-3-5-8-11-13-15	11
1-2-4-8-11-13-15	4	1-3-5-8-11-14-15	12
1-2-4-8-11-14-15	5	1-3-5-8-12-14-15	13
1-2-4-8-12-14-15	6	1-3-5-9-12-14-15	14
1-2-5-8-11-13-15	7	1-3-6-9-12-14-15	15
1-2-5-8-11-14-15	8		

2.3.3 Simplified Optimization Problem

Once Dijkstra's algorithm has provided the most energy-efficient trajectory on the approximating graph, the problem can be finally formulated as a convex optimization. The disjoint sets given by constraint (2.13) are resolved, and only one time interval per intersection represents now the optimization domain. The mathematical formulation may be carried out in multiple ways.

Velocities as Variables

In order to formulate the optimization problem using velocity as variable, let us define the vector of optimization variables (velocities to track in each segment), assuming n to be the number of intersections:

$$\mathbf{x} = [v_1, v_2, \ldots, v_n, v_{n+1}]^T \in \mathbb{R}^{n+1} \tag{2.18}$$

Then a vector of time intervals for each segment is defined:

$$\begin{aligned} \mathbf{t} = \mathbf{t}(\mathbf{x}) &= [t_1 - t_0, t_2 - t_1, \ldots, t_n - t_{n-1}, t_f - t_n]^T \\ &= \left[\frac{d_1 - d_0}{v_1}, \frac{d_2 - d_1}{v_2}, \ldots, \frac{d_n - d_{n-1}}{v_n}, \frac{D - d_n}{v_{n+1}} \right]^T \end{aligned} \tag{2.19}$$

where d_i is the known position of the i-th traffic light, D is the destination/horizon, and $\mathbf{t} \in \mathbb{R}^{n+1}$.

The objective function is the same as the one in the original optimization problem (2.12):

$$J = \int_{t_0}^{t_f} P \, \mathrm{d}t = \int_{t_0}^{t_f} b_1 uv + b_2 u^2 \, \mathrm{d}t \tag{2.20}$$

By using the same procedure as in the graph weights assignment, we may split the objective function in an energy term related to the contributions of the segments traveled at constant velocity, and energy terms related to the velocity variations between subsequent segments.
Therefore, the objective function may be rewritten as:

$$J(\mathbf{x}) = \mathbf{t}^T \bar{P}(\mathbf{x}) + \sum_{i=0}^{n+1} E_{\text{jump}} \tag{2.21}$$

where $\bar{P}(\mathbf{x})$ is the power required by the vehicle when traveling at constant velocity (no velocity variation in time):

$$\bar{P}(\mathbf{x}) = b_1 \bar{u}(\mathbf{x})\mathbf{x} + b_2 \bar{u}(\mathbf{x})^2 \tag{2.22}$$
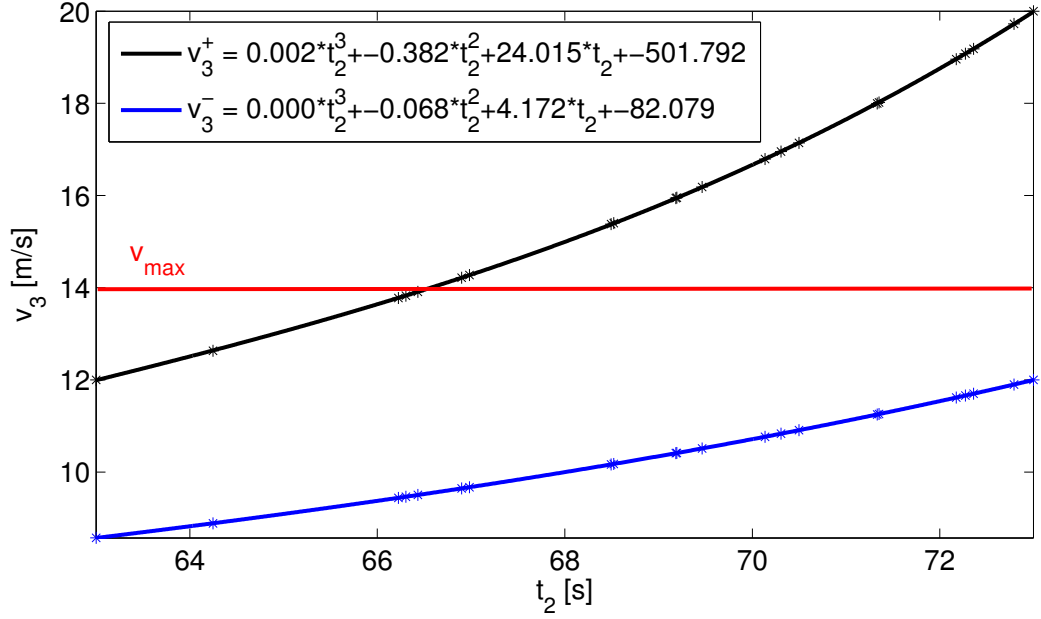
Figure 2.7 – Example of the polynomial variation of the upper and lower bound for the decision variable v_3. In red the maximum speed limit v_{max}.

with

$$\bar{u}(\mathbf{x}) = \frac{1}{h_1}\left(h_2\mathbf{x}^2 + h_3\mathbf{x} + h_0\right) \tag{2.23}$$

Finally the optimization problem may be formulated as:

$$\begin{cases} \min_{\mathbf{x}} \ J(\mathbf{x}) \\ \max\left\{v_i^-, v_{\min}\right\} \leq v_i \leq \min\left\{v_i^+, v_{\max}\right\} \end{cases} \tag{2.24}$$

Note that in this case, the constraints are nonlinear. Specifically the bounds of the constant velocity to be tracked in each segment (v_i) depend on the crossing time at the previous intersection (t_{i-1}) and experimentally they are found to be approximated by cubic functions, as shown in Figure 2.7.

Crossing Times as Variables

A more efficient formalization makes use of the crossing times at each intersection as decision variables of the optimization problem. Thus the constraints become constant.

Let us first define a vector of optimization variables (crossing times at intersections), supposing n to be the number of intersections:

$$\mathbf{x} = [t_1, t_2, \ldots, t_n]^T \in \mathbb{R}^n \tag{2.25}$$

Then a vector of travel times for each segment is defined:

$$\mathbf{t} = \mathbf{t}(\mathbf{x}) = [t_1 - t_0, t_2 - t_1, \ldots, t_n - t_{n-1}, t_f - t_n]^T \tag{2.26}$$

Knowing the position of the traffic lights, let us then define the vector of the constant velocities in each segment:

$$\begin{aligned}
\mathbf{v} = \mathbf{v}(\mathbf{x}) &= [v_1, v_2, \ldots, v_n, v_{n+1}]^T \\
&= \left[\frac{d_1 - d_0}{t_1 - t_0}, \frac{d_2 - d_1}{t_2 - t_1}, \ldots, \frac{d_n - d_{n-1}}{t_n - t_{n-1}}, \frac{D - d_n}{t_f - t_n} \right]^T
\end{aligned} \tag{2.27}$$

where d_i is the position of the i-th traffic light with respect to the origin, D is the destination, t_f is the horizon time, and $\mathbf{t} \in \mathbb{R}^{n+1}$, $\mathbf{v} \in \mathbb{R}^{n+1}$.

The objective function is the same as the one in the original optimization problem (2.12):

$$J = \int_{t_0}^{t_f} P \, \mathrm{d}t = \int_{t_0}^{t_f} b_1 u v + b_2 u^2 \, \mathrm{d}t \tag{2.28}$$

By using the same procedure as in the graph weights assignment, we may split the objective function into an energy term related to the segments traveled at constant velocity, and an energy term related to the velocity variations between subsequent segments. Therefore, it may be rewritten as:

$$J(\mathbf{x}) = \mathbf{t}^T \bar{P}(\mathbf{v}) + \sum_{i=0}^{n+1} E_{\mathrm{jump}} \tag{2.29}$$

where $\bar{P}(\mathbf{V})$ is the power required by the vehicle when traveling at constant velocity (no velocity variation in time):

$$\bar{P}(\mathbf{v}) = b_1 \bar{u}(\mathbf{v})\mathbf{v} + b_2 \bar{u}(\mathbf{v})^2 \tag{2.30}$$

with

$$\bar{u}(\mathbf{v}) = \frac{1}{h_1} \left(h_2 \mathbf{v}^2 + h_3 \mathbf{v} + h_0 \right) \tag{2.31}$$

Finally the optimization problem may be formulated as:

$$\begin{cases} \min_{\mathbf{x}} \ J(\mathbf{x}) \\ \max\left\{ t_i^-, t_{i,\mathrm{min}} \right\} \leq t_i \leq \min\left\{ t_i^+, t_{i,\mathrm{max}} \right\} \end{cases} \tag{2.32}$$

where t_i^- and t_i^+ are constants and represent the end times of the selected green phase at each intersection, and $t_{i,\mathrm{min}}$ and $t_{i,\mathrm{max}}$ are the minimum and the maximum feasible crossing times returned by the pruning algorithm.

2.4 Experiments

In the following, the performance of the proposed sub-optimal algorithm is compared to the optimal solution provided by DP [123].

Table 2.2 – Simulation parameters

(a) Vehicle parameters

Parameter	Value
m	1190 kg
r	0.2848 m
R_t	6.066
a	1.5 m/s^2
α	0 rad
a_0	113.5 N
a_1	0.774 N/(m/s)
a_2	0.4212 N/(m/s)^2
b_2	0.1515 Ω

(b) Scenario parameters

Parameter	Value
T	30 s
T_{gr}	10 s
n	5
$\theta_{1,\ldots,n}$	[13, 3, 28, 15, 5] s
t_f	200 s
D	2000 m
t_0	0 s
d_0	0 m
$d_{1,\ldots,n}$	[300, 600, 900, 1200, 1550] m
v_f	10 m/s
$v_{\min}$	5 m/s
$v_{\max}$	14 m/s

2.4.1 Control Scenario

The case under study presents a scenario with only one vehicle in the traffic network. However it can be conceptually extended to the case of multiple vehicles in free flow, each equipped with the presented algorithm. Traffic effects, such as inter-distance constraints and pedestrians cross-walks, are taken care of by new runs of the algorithm.

The vehicle is supposed to be traveling through $n = 5$ signalized intersections, along a road stretch of 2000 m on a total time horizon of 200 s. The distance between the intersections is about 300 m. The choice of the final time and distance of the driving horizon is made in such a way to keep a realistic overall average speed of about $v = 10$ m/s. The vehicle objective is to follow an energy optimal velocity profile which allows to find all the traffic lights on green. No assumption is made on the existence of a "green wave". Clearly its existence would enable an easier solution, which the presented algorithm is able to find. The problem is made more challenging and interesting by the random disposition of the green phases, and consequently by the presence of more trip options. The green phase duration is 10 s, the total cycle time is set to 30 s. Note that, although some traffic lights might be phased so to give rise to a "green wave", the distribution of the green phases may be such that the velocity of the wave is not energy optimal.

The initial velocity of the vehicle (i.e. the initial kinetic energy) is varied throughout the simulations to assess its impact on the energy consumption and on the optimal trajectory. Traffic lights timings, final velocity, horizon are fixed for consistency in results comparison. The objective of the performed simulations is to prove the importance of a methodology which allows to achieve a fast sub-optimal solution suitable for online implementation and eco-driving assistance.

The employed simulation parameters are provided in Table 2.2.

2.4.2 Optimal Trajectory Validation

The first part of the presented simulation results aims at validating the pruning algorithm and the optimal trajectory identification by means of the approximating graph and Dijkstra's algorithm. DP, used in the following as a benchmark, provides the optimal solution to the problem, and it was used to compute the energy cost of all the possible non-stop trajectories in the feasible region. The Dynamic Programming was set with the following parameters: vehicle displacement as first state discretized at $\Delta x = 1$ m, vehicle velocity as second state discretized at $\Delta v = 0.5$ m/s, vehicle traction force as input discretized at $\Delta u = 1$ N, simulation time discretized at $\Delta T = 0.2$ s.

Simulations have been run varying the initial velocity of the trip, which has an impact on the optimal trajectory. In the scenario under study the vehicle does not
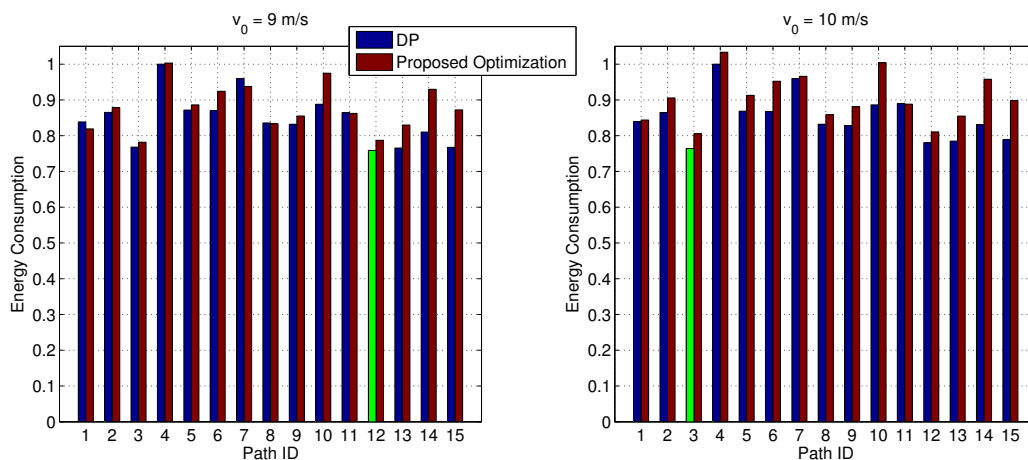
Figure 2.8 – Comparison of DP and proposed strategy energy consumption calculation on all the feasible trajectories. Two cases with different initial speeds are reported. In green the most energy-efficient trajectory.

stop at any intersection in the feasibility region shown in Figure 2.3.

In Figure 2.8 the energy consumption of each trajectory computed via DP is compared with the energy consumption approximation computed via the proposed strategy (i.e. numerical evaluation of the objective function of problem (2.32)). The results for two different choices of initial velocity are reported after normalization with respect to the maximum DP-cost trajectory in each configuration. The minimum cost trajectory, for each case, is highlighted in green. The path ID in abscissa refers to Table 2.1.

The energy cost approximation obtained with the proposed strategy is very close to the true energy cost computed with DP. The Root Mean Square Error (RMSE) of our approximation with respect to the true cost was calculated for the two experiments shown in Figure 2.8. It has been then normalized with respect to the mean value of the energy costs calculated via DP for each case. In the case of initial velocity $v_0 = 9$ m/s, the normalized RMSE is 6.3%. In the case of $v_0 = 10$ m/s, the normalized RMSE is 7.7%.

The energy consumption varies depending on the path choice; in the worst case, the choice of a trajectory rather than the optimal one, results to be up to 25% more expensive in terms of energy. In Figure 2.8 the DP and the proposed strategy results for only $v_0 = 9$ m/s and $v_0 = 10$ m/s are reported. For speeds $v_0 \geq 10$ m/s, the energy-optimal trajectory is always the number 3; for speeds $v_0 \leq 9$ m/s the optimal trajectory is always the number 12. Note that, the simpler algorithm proposed in [101], which chooses the non-stop trajectory by first analyzing the unconstrained problem in absence of traffic lights and then minimally adjusting

Table 2.3 – Optimal trajectory identification (Graph vs. DP)

v_0 [m/s] Graph	5	6	7	8	9	10	11	12	13	14
1 node/green phase	15	15	15	15	3	3	3	3	3	3
3 nodes/green phase	12	12	12	12	12	3	3	3	3	3
DP (optimal trajectory)	12	12	12	12	12	3	3	3	3	3

the path to fit into the green intervals, would return as solution the path number 8 in this scenario, which is by 8% less efficient than the true optimal trajectory.

The accuracy of the graph approximation, as well as the computational load, increases with the number of nodes per green phase. A graph with one node per green phase, as shown in Figure 2.3, and a graph with three nodes per green phase (one at the mid-point and two at the ends) have been tested, and the optimal path identification obtained with Dijkstra's algorithm is validated against the true minimum-energy trajectory, found via DP.

As summarized in Table 2.3, the graph with three nodes per green phase approximates better the whole energy cost, never failing, whereas the smaller graph fails in five cases. Clearly there exist other graph configurations where the approximation with three nodes per green phase does not always provide the right identification of the energy-optimal trajectory. One can increase the discretization level (i.e. use more nodes per green phase), increasing consequentially also the computational load. Thanks to the newly introduced line graph expansion, the computational time does not grow as dramatically as with the tree expansion, so this becomes more affordable. Nevertheless this is a sub-optimal solution, the path identification is not flawless, and a trade-off between fineness of discretization and computational effort is required. However, it is possible to note that even a graph with a less fine discretization is able to provide a path identification that is not far from the true optimal one. For instance, as reported in Table 2.3, the graph with one node per green phase fails for $v_0 = 9$ m/s, suggesting path number 3, which is only 2% more costly than the true optimal one, as shown in Figure 2.8.

2.4.3 Optimal Crossing Times

Finally, once Dijkstra's algorithm provides the optimal green phases, the optimal crossing times at each intersection are to be calculated, in order to provide the eco-driving assistance by suggesting a velocity profile to the driver. The solver employed to solve the optimization problem (2.32) in MATLAB® is fmincon, using the interior-point method algorithm.

In Figure 2.9, the optimal solution provided by DP through the optimal green
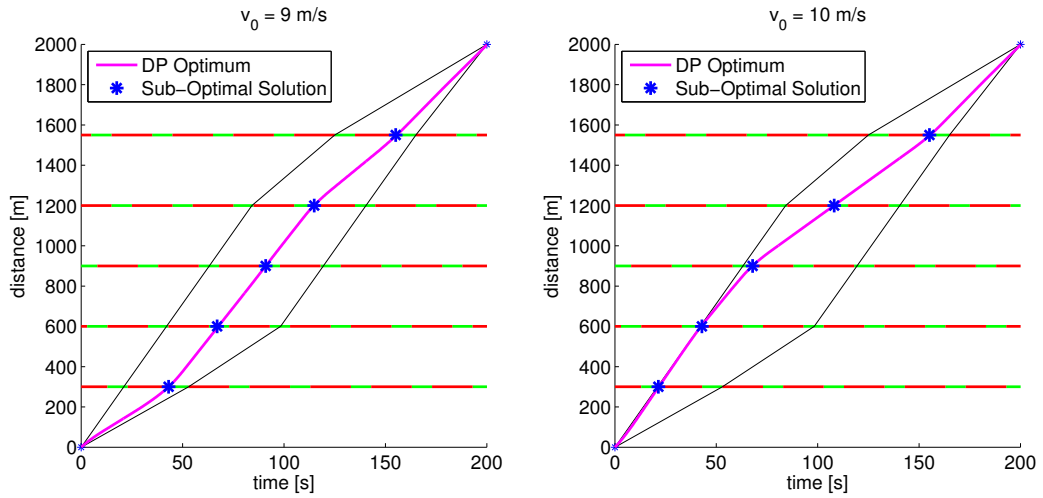
Figure 2.9 – Sub-optimal crossing times compared to the optimal solution provided by DP, for two different initial speeds.

Table 2.4 – Time deviation from the optimal crossing times for the five intersections

	Int. #1	**Int. #2**	**Int. #3**	**Int. #4**	**Int. #5**
$v_0 = 9$ m/s	0.03 s	0.62 s	0.03 s	0.07 s	0.5 s
$v_0 = 10$ m/s	0.22 s	0.36 s	0.05 s	0.08 s	0.4 s
Overall average deviation: 0.23 s					

phases (path 12 for $v_0 = 9$ m/s and path 3 for $v_0 = 10$ m/s) is compared to the sub-optimal proposed solution. In Table 2.4 the time deviations of the sub-optimal solution from the DP solution at the five intersections are summarized, for the two different initial velocities.

The simulations were run with a laptop equipped with an Intel(R) Core(TM) i7-2760QM at 2.40GHz and 8GB of RAM. DP takes about 2.5 hours per path to provide the optimal solution. In order to have an assessment of the cost of all trajectories and find the minimum-energy one, DP has to be run as many times as the number of possible paths. The proposed methodology takes 1.2 seconds (graph three-nodes/green phase) or 0.85 seconds (graph one-node/green phase) to run all the steps presented in Figure 2.1 and provide the sub-optimal crossing times at each intersection.
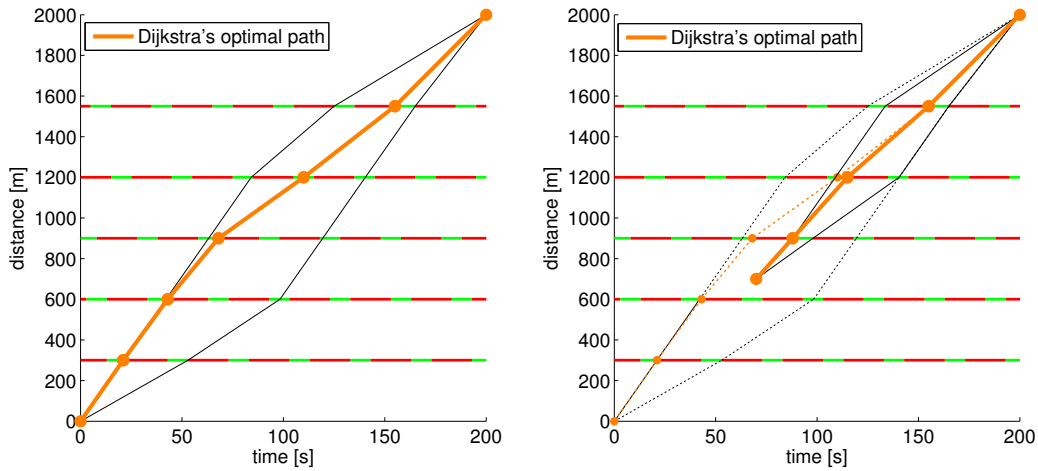
Figure 2.10 – The graph on the left shows the trajectory suggested by Dijkstra's algorithm for $v_0 = 10$ m/s, when going from the origin $(0, 0)$ to the horizon $(200, 2000)$. The graph on the right shows the suggested trajectory when the origin is moved to the point of coordinates $(70, 700)$.

2.4.4 Robustness of the Algorithm

As already mentioned, the algorithm is capable of coping with unexpected deviations from the suggested trajectory and handling new information coming from the traffic network in a receding-horizon fashion. The horizon can be thought of as the range of the wireless I2V communication.

The following simulation results show how new runs of the algorithm can provide new speed advisory in the case of triggering events.

Let us recall once again, on the left-hand side of Figure 2.10, Dijkstra's optimal trajectory relative to the simulation scenario described so far, and for an initial velocity $v_0 = 10$ m/s. Let us suppose now that an unexpected event occurs at time $t = 70$ seconds, and the equipped vehicle has to slow down or stop, thus deviating from the suggested trajectory. A new run of the algorithm shows that it is still possible to recover from the perturbation and reach the desired horizon at the desired final time. Evidently, the new feasibility region is smaller, the approximating graph also will be smaller, leading to a smaller set of available paths and a faster solution of the algorithm. On the right-hand side of Figure 2.10, the new Dijkstra's optimal trajectory is shown, while the old one is left dotted in the background for the sake of comparison.

Let us show now an example of the receding-horizon capabilities of the algorithm. The coordinates of the horizon are assumed to change as new information from the traffic network is collected. Let the point of coordinates $(70, 700)$ be the new origin of the driving horizon, that is the point of the occurred perturbation
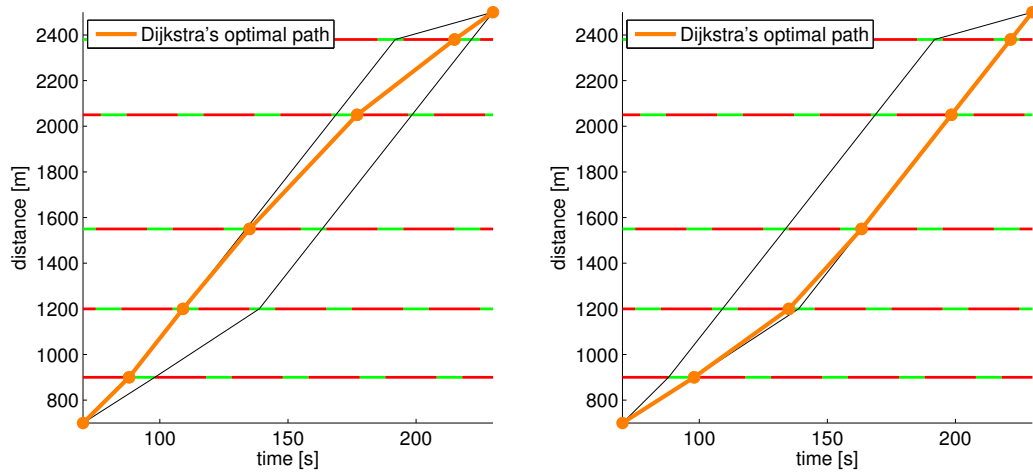
Figure 2.11 – The graph on the left shows the trajectory suggested by Dijkstra's algorithm for $v_0 \geq 9$ m/s, when going from the new origin $(70, 700)$ to the new horizon $(230, 2500)$. The graph on the right shows the suggested trajectory when the initial velocity is $v_0 < 9$ m/s.

as discussed above. New timings information are received from the traffic lights and two new intersections appear in the driving horizon, which now has as destination the point of coordinates $(230, 2500)$. The algorithm is run on the new horizon, defining a new feasibility region, a new approximating graph, and providing again the optimal crossing times at each intersection in order to reach the new destination without stopping. On the left-hand side of Figure 2.11, Dijkstra's optimal trajectory is shown, in case the vehicle is able to recover quickly from the perturbation and be at the new origin with an initial velocity $v_0 \geq 9$ m/s. However, if the vehicles is forced to stop or slow down considerably ($v_0 < 9$ m/s), the optimal trajectory to reach the desired destination at the desired time is reported on the right-hand side of Figure 2.11.

2.4.5 Microscopic Traffic Simulator

As mentioned, the whole analysis of the energy-optimal trajectory in this work was carried out under the assumption of a vehicle on the road network in free flow conditions (i.e. unperturbed by the presence of other vehicles). The assumption was made for the purpose of a simpler and more abstract analysis of the optimization problem. However, the discussion about the robustness properties of the algorithm demonstrated that the algorithm is capable of dealing with perturbations coming from other agents of the traffic network. The optimal trajectory is quickly recalculated in the event of deviation from the original speed advisory.
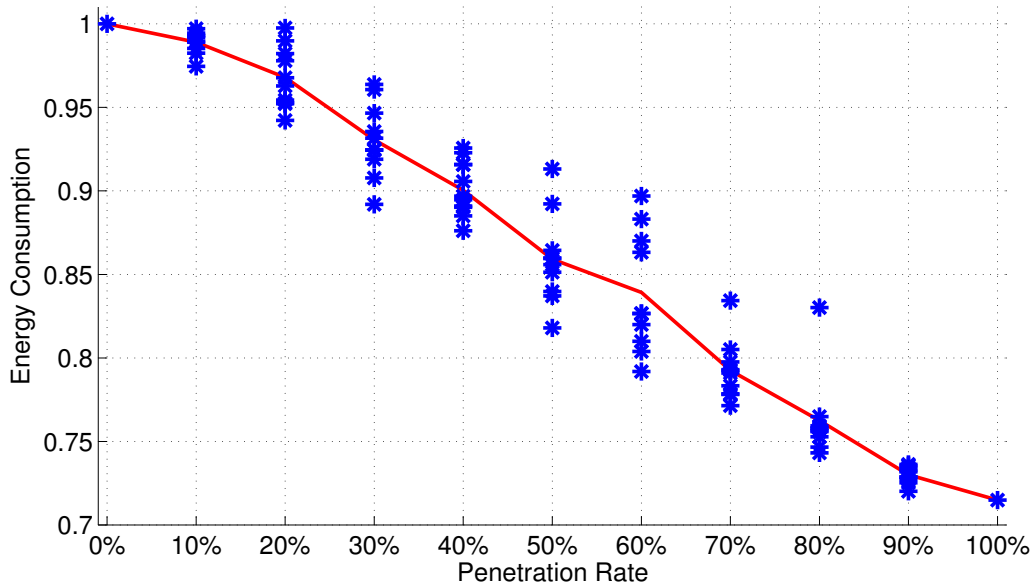
Figure 2.12 – Variation of traffic energy consumption with respect to the technology penetration rate. The red line describes the average energy consumption at the different penetration rates.

In order to prove the actual capabilities of the proposed strategy in a more realistic scenario, the traffic microscopic simulator Aimsun has been used [1]. The road topology treated in this work and shown in Figure 2.2 has been faithfully replicated in Aimsun, as well as the traffic lights positions and signal timings. A flow of 400 vehicles per hour has been set to enter the road network at the initial velocity $v_0 = 50$ km/h. The vehicles have been equipped with the algorithm here presented, and, evidently, the assumption of unperturbed vehicles in such realistic scenario does not hold anymore. In particular, being each vehicle independently equipped with the algorithm and entering the network at different time instants, the speed advisories may conflict with one another causing deviations from the optimal speed advisory.

The experiment has been set up in such a way that only one lane is available and no pass is allowed, in order to generate as many perturbations as possible to the speed advisories. Note that the space coordinate of the origin d_0 is the same for all vehicles, whereas the time coordinate of the origin t_0 is different for every vehicle. This evidently affects the time coordinate of the destination of the driving horizon, but not its time span, which is the same for all vehicles. The online adaptation of the proposed strategy in the multi-vehicle scenario is

---

1. For details about the software interface between Aimsun and MATLAB used in this dissertation, the reader is invited to refer to Appendix A.

Table 2.5 – Traffic performance metrics values

	Penetration Rate 0%	Penetration Rate 100%
Energy Consumption	$2*10^8$ J	$1.43*10^8$ J
Mean Travel Time	213.9 s	205.7 s
Mean Number of Stops	2.7	0
Mean Idling Time	37.9 s	0 s

quite simple and intuitive. When a new vehicle enters the network, the algorithm is run and the optimal crossing times at each intersection are calculated. The optimal crossing times are then converted in speed advisory, which is continuously updated according to the current position of the vehicle. When the suggested speed grows larger than the maximum speed limit, meaning that a perturbation has occurred, the algorithm is run again. The time horizon is not extended if a new optimal trajectory can be found, otherwise small successive extensions of the time horizon are recursively tried until an optimum is found.

Several experiments were conducted at different levels of penetration rate of the proposed technology (i.e. percentage of equipped vehicles), in order to assess the impact of the proposed algorithm on the traffic energy consumption. For the sake of results consistency and comparison, the vehicle average travel time is set to be the same independently of the penetration rate. In other words, the time horizon of the proposed algorithm was set up in order to achieve the same travel time as in the uncontrolled case (i.e. all vehicles traveling at the maximum speed limit). A statistical analysis on the travel time conducted at the different levels of technology penetration rate demonstrated that the average travel time can be considered as constant: mean value of 208.5 seconds, and standard deviation of 3.8 seconds (i.e. 1.8% of the mean value).

In Figure 2.12, the variation of traffic energy consumption with respect to the technology penetration rate is shown. The proposed strategy has been applied to a gradually increasing number of vehicles in the road network. At penetration rate equal to 0%, the experiment has been conducted with no vehicle equipped with the algorithm, and all the vehicles were allowed to drive up to the maximum speed limit. For penetration rates greater than 0%, a total of 10 simulations per each tested value has been run. The equipped vehicles were chosen randomly, and it is possible to observe that the order of "smart" vehicles in traffic can affect significantly the energy consumption. As expected, a penetration rate of 100% results to be highly beneficial with respect to the uncontrolled case in terms of several traffic performance metrics (see Table 2.5). A reduction of 28.5% in traffic energy consumption has been observed, without negative impact on the average travel
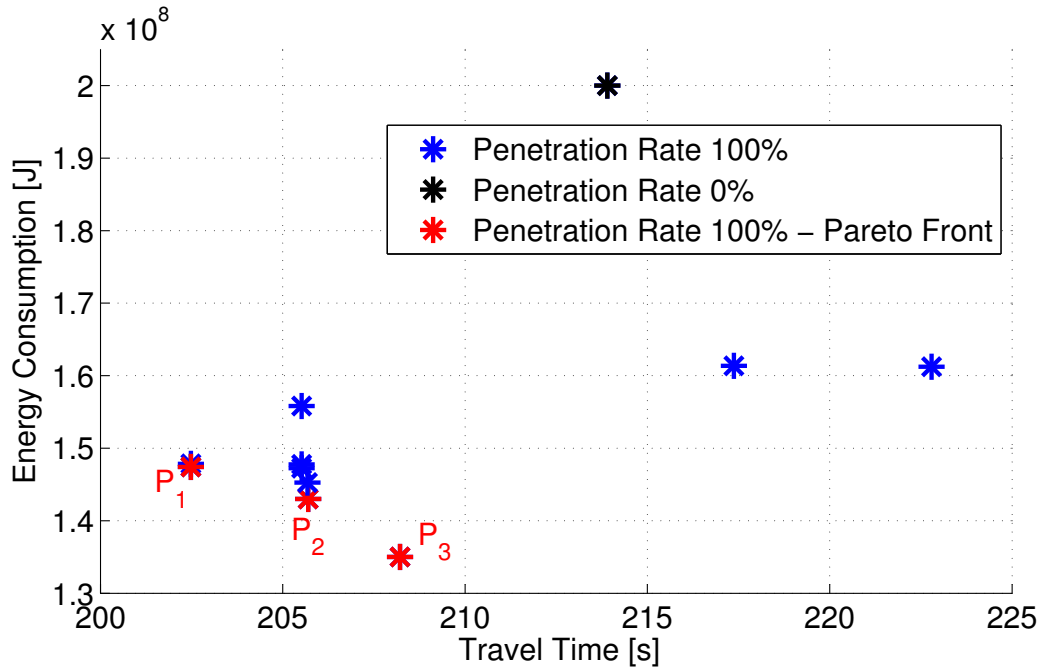
Figure 2.13 – Different selections of the time horizon parameter give different performance at 100% penetration rate of the algorithm. In black the traffic performance in the uncontrolled case. In red the set of experiments with the best performance in the sense of Pareto.

time. More specifically, the average travel time results to be even smaller than the uncontrolled case by 4%. The stops and the idling time are completely eliminated. One may argue that a global deployment of the proposed strategy would be difficult to achieve in a close future. A penetration rate of 40% is more realistic and results to be already appealing in terms of energy consumption, yielding an average reduction of about 10%.

In the results reported in Table 2.5, it appears that a total deployment of the technology leads not only to a reduction of the traffic energy consumption, but also to a reduction of the average travel time. Therefore, the following last experiment will treat the time horizon of the proposed algorithm as a tunable parameter. In other words, the time coordinate of the destination point used in the graph construction will be varied. The goal is to demonstrate that there exist some Pareto-efficient choices of the time horizon that will yield the best traffic performance in terms of both travel time and energy consumption.

As shown in Figure 2.13, such set of Pareto-optimal time horizons exists, and in particular the result P_1 is achieved for a time horizon of 160 s, P_2 is achieved for a time horizon of 190 s, and P_3 is achieved for a time horizon of 195 s.

2.5 Conclusions

The exchange of information between the infrastructure and the vehicles (I2V) has been proved in literature to be beneficial in terms of traffic energy consumption. This work focuses on the possibility of further improvements when information about many successive signalized intersections is available. The presented algorithm is capable of finding the energy-efficient trajectory among all the available ones, and returning the speed advisory to the drivers, in a sub-optimal way. The length of the optimization horizon can be arbitrarily long. The only limitations come from the I2V communication range and/or online execution constraints. However, for the already complex scenario analyzed in this study, the computation time required by the algorithm is very appealing for online implementation purposes. The robustness capabilities of the algorithm have been also presented, by showing how perturbations and deviations from the suggested trajectory are handled. In particular, experiments in a microscopic traffic simulator demonstrated that, even in presence of multiple vehicles, the proposed algorithms is able to cope with perturbations and to drastically reduce the traffic energy consumption without affecting travel time.

The experiments in the microscopic traffic simulator highlighted the fact that a performance improvement is achievable even though the vehicles are independently equipped with the proposed algorithm and do not exchange information among them. Further improvements could be achieved by exploiting V2V communication and by sharing information among the vehicles about their own optimal trajectory. Moreover, if the traffic flow grows larger, congestion and queues become inevitable. More sophisticated methods would be required, such as macroscopic models for the estimation of the queue length. In such a situation the problem of eco-driving changes its nature, and a different analysis would be necessary. Lastly, an energy consumption model for electric vehicles was considered in this work. Different energy and/or emissions models could be introduced into the problem, without any loss of generality for the proposed strategy.

Chapter 3

Single-Section Control via Variable Speed Limits

3.1 Traffic Flow Models

Managing traffic in congested networks requires a clear understanding of traffic flow operations. In particular, insights into what causes congestion, what determines the time and location of traffic breakdown, how the congestion propagates through the network, etc., are essential [62]. Traffic operations on roadways can be improved by field research and field experiments of real-life traffic flow. However, apart from the scientific problem of reproducing such experiments, costs and safety play a role of dominant importance as well. Traffic flow modeling and simulation represent extremely valuable tools to describe and replicate congestion phenomena in road networks, and to support and improve the design, testing and validation of the queue management strategies.

Traffic flow theory and modeling started in the 1930s, with the pioneering work by Greenshields [57]. In the 50s, Lighthill and Whitham [81] presented a model based on the analogy of vehicles in traffic flow and particles in a fluid. Since then, mathematical description of traffic flow has been a lively subject of research and debate for traffic engineers. However, since the 1990s, the field has gained considerable attraction as overall traffic demand has increased, and more data as well as easy access to computing power has become available.

Papageorgiou argued that it is unlikely that traffic flow theory will reach the descriptive accuracy attained in other domains of science (e.g. Newtonian physics or thermodynamics) [102]. The only accurate physical law in traffic flow theory is the conservation of vehicles equation. Consequently, the challenge of traffic flow researchers is to pursue useful theories of traffic flow that have sufficient descriptive power, where sufficiency depends on the application purpose of their
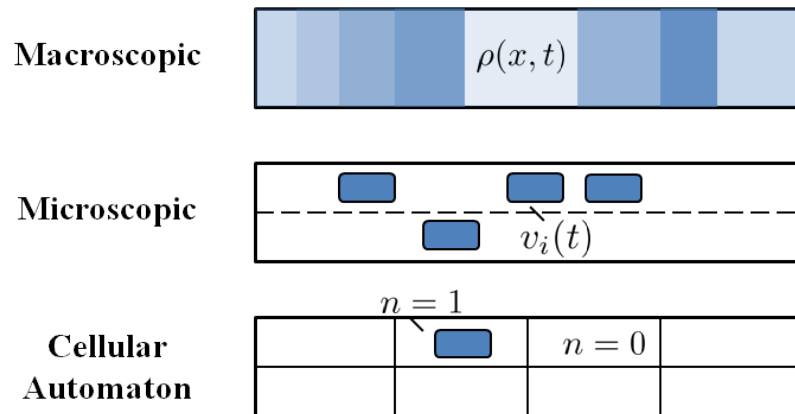
Figure 3.1 – Comparison of different traffic model categories with respect to their aggregation level.

theories.

Traffic flow models can be categorized with respect to a number of aspects: aggregation level (the way reality is represented), mathematical structure, and conceptual aspects [129].

3.1.1 Aggregation Level

Macroscopic models describe traffic flow analogously to liquids or gases in motion. Hence they are sometimes called hydrodynamic models. The dynamical variables are locally aggregated quantities such as the traffic density $\rho(x,t)$, flow $\varphi(x,t)$, mean speed $v(x,t)$. Because the aggregation is local, these quantities generally vary across space and time. Thus, macroscopic models are able to describe collective phenomena such as the evolution of congested regions or the propagation velocity of traffic waves. Furthermore, macroscopic models are useful when specific aspects of the traffic, such as lane change, different classes of vehicles, etc., do not need to be considered, and when computation time is critical.

Microscopic models, including car-following models and most cellular automata, describe individual "driver-vehicle particles" i, which collectively form the traffic flow. These models describe the reaction of every driver (accelerating, braking, lane-changing) depending on the surrounding traffic. In a broader context, microscopic traffic flow models are examples of driven multi-particle models. The dynamical variables are vehicle positions $x_i(t)$, speeds $v_i(t)$, and accelerations $\dot{v}_i(t)$. Microscopic models are particularly suited for the following applications:

- Modeling how single vehicles affect traffic: this is becoming more and more important as Advanced Driver Assistance Systems (ADAS) such

as adaptive cruise control (ACC) or infrastructure-to-vehicle (I2V) and vehicle-to-vehicle (V2V), as well as other applications of Intelligent Transportation Systems (ITS), see widespread use.
- Situations in which the heterogeneity of the traffic plays an important role.
- Describing human driving behavior, including estimation errors, reaction times, inattentiveness, and anticipation: microscopic models allow us to assess how different driving styles affect traffic capacity and stability.
- Generating the surrounding traffic for scientific driving simulators used for physio-psychological studies of human drivers, or even for game simulators.

Mesoscopic models combine microscopic and macroscopic approaches to a hybrid model and do not distinguish nor trace individual vehicles, but specify the behavior of individuals, for instance in probabilistic terms. To this end, traffic is represented by groups of traffic entities, whose activities and interactions are described at a low-detail level. For instance, a lane-change maneuver might be represented for an individual vehicle as an instantaneous event, where the decision to perform a lane-change is based on relative lane densities, and speed differentials. Some mesoscopic models are derived in analogy to gas-kinetic theory, which describe the dynamics of velocity distributions.

3.1.2 Mathematical Structure

Traffic flow models can be also classified by their mathematical structure.

Partial differential equations (PDEs). In models of this class both location x and time t are continuous and serve as the independent variables of continuous fields, such as the local speed $v(x, t)$ or density $\rho(x, t)$. The model equations contain these fields and their derivatives with respect to either of the two variables. This is the distinctive feature of PDEs. This mathematical form is suited to express macroscopic models or gas-kinetic based mesoscopic models. PDE traffic flow models generally allow for analytical steady-state solutions (fundamental diagram), and analytical expressions for propagation velocities of traffic waves and stability properties. Furthermore, in spite of their inherent mathematical complexity, most PDE traffic flow models allow for a fast numerical solution.

Coupled ordinary differential equations. In this mathematical class, the continuous state variables (e.g., location or speed) depend on only one variable, the time t. The model equations contain the state variables and their time derivatives and are coupled with the equations of the leading vehicle. This is the most natural form to describe time-continuous microscopic models (car-following models).

Cellular Automata. In models of this class, all variables are discrete. Space is divided into fixed cells and time is updated in fixed intervals. The state of each cell is either 0 ("no vehicle") or 1 ("vehicle" or "part of vehicle"). The occupation

of the cells is determined at every time step and depends on the occupation at the previous time step. In the traffic context, Cellular Automata (CA) are mainly used for microscopic models. However, macroscopic traffic flow models in the form of a CA are conceivable as well.

Static models. This class of models, also known as traffic stream models, describe pairwise relations between the macroscopic state variables (density, flow, speed or occupation). The speed-density relation $v(\rho)$ and the fundamental diagram $\phi(\rho)$ are examples of these models. The classical route-choice step of transportation planning uses the speed-flow relation, transformed into a travel time versus flow relation, for each link. This so-called capacity restraint function is an increasing function of the traffic demand. Notice that steady-state solutions of dynamic microscopic or macroscopic models can be considered as traffic-stream models as well.

3.2 Cell Transmission Model

Macroscopic models are a very reliable and versatile tool to represent traffic conditions on road networks, simply by treating vehicular flow as a fluid in a tube. The conventional macroscopic approach to simulate traffic behavior over networks keeps track of the number of vehicles in discrete sections of the network as time passes. The vehicle occupancy in each section is increased by the number of vehicles allowed to enter the section in each time interval, and is decreased by the number of vehicles allowed to leave it.

The first instance of a macroscopic traffic model, intended to solve the kinematic wave equation, was the Lighthill-Whitham-Richards (LWR) model introduced in [81, 109], which is a continuous first order model of the form:

$$\frac{\partial}{\partial t}\rho + \frac{\partial}{\partial x}\phi(\rho) = 0$$

where ρ indicates the density of vehicles, $\phi(\rho) = \rho v(\rho)$ is the flux of vehicles, and v is their average velocity.

When simulating the LWR model, the outflow is typically specified to be a function of the occupancy of the section emitting the flow, and not to be an explicit function of the downstream occupancy. Such approaches do not converge to the desired solution and cannot produce reasonable results, because traffic could be sent into a section even after it reaches its maximum occupancy.

In recognition of this problem, Daganzo introduced the Cell Transmission Model (CTM), which is one of the main and most famous traffic flow models to date [28, 29]. It belongs to the category of the macroscopic models, and it is a first order Godunov approximation of the LWR. If the relationship between traffic
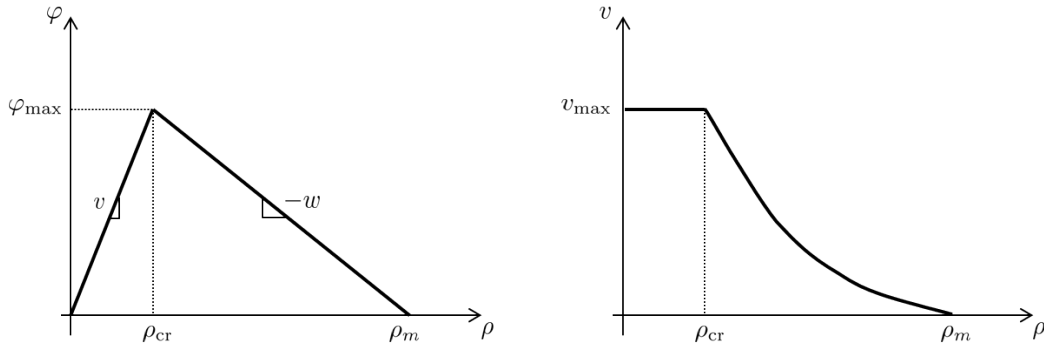
Figure 3.2 – Daganzo's macroscopic fundamental diagram.

flow φ and density ρ is of the form depicted in Figure 3.2:

$$\varphi = \min \{v\rho, \varphi_{\text{max}}, w(\rho_m - \rho)\} \tag{3.1}$$

then the LWR equations for a single road link can be approximated by a set of difference equations where current conditions (the state of the system) are updated with the tick of a clock. In the above expression v, φ_{max}, w and ρ_m are constants denoting respectively: the free-flow speed, the maximum flow (or capacity), the speed with which disturbances propagate backward when traffic is congested (the backward wave speed), and the maximum (or jam) density. The critical density ρ_{cr} is the transition density between free and congested state, and it can be defined as the ration between maximum flow and free-flow speed.

The method assumes that each road section k is divided into n homogeneous cells, whose minimum length must equal the distance traveled by free-flowing traffic in one clock interval. Although a closer approximation to the LWR results is obtained with short cell lengths (e.g. one hundred meters), the procedure can be applied with cells of any length. The state of the system at time t is then given by the density of vehicles $\rho_i(t)$ contained in each cell i, with $i = 1, \ldots, n$.

The density of the cells is updated based on the conservation of inflow and outflow. The evolution of the number of vehicles within any spatial section $(0, L)$ is given by the following car conservation law in terms of the number of vehicles N in the cell:

$$\frac{\mathrm{d}}{\mathrm{d}t}N = \varphi_{\text{in}} - \varphi_{\text{out}} \tag{3.2}$$

$$N = \int_0^L \rho(x, t)\mathrm{d}x \tag{3.3}$$

where φ_{in} and φ_{out} are the input (at $x = 0$) and output (at $x = L$) flows at the boundaries of the road section.

A simplification of equation (3.1) could be achieved by defining a demand and a supply function as the maximum flows that can be sent and received by cell i:

$$
\begin{aligned}
D_i(t) &= \min\left\{v_i\rho_i, \varphi_{\max}\right\} \\
S_i(t) &= \min\left\{w(\rho_m - \rho_i), \varphi_{\max}\right\}
\end{aligned}
\tag{3.4}
$$

Thus, in general the flow of vehicles on link k is the maximum that can be sent by its upstream cell unless prevented to do so by its downstream cell:

$$
\varphi_k(t) = \min\left\{D_1(t), S_n(t)\right\}
\tag{3.5}
$$

Therefore, it is possible to derive a continuous-time formulation of the density evolution in a generic cell i of length l_i:

$$
\dot{\rho}_i = \left(\min\left\{D_{i-1}, S_i\right\} - \min\left\{D_i, S_{i+1}\right\}\right)/l_i
\tag{3.6}
$$

As a consequence of the fundamental diagram, Daganzo defined also the average velocity of traffic as a function of the density:

$$
v_i(\rho) =
\begin{cases}
v_{\max} & \text{if } \rho_i \in [0, \rho_{\mathrm{cr}}] \\
-w\left(1 - \dfrac{\rho_m}{\rho_i}\right) & \text{if } \rho_i \in (\rho_{\mathrm{cr}}, \rho_m]
\end{cases}
\tag{3.7}
$$

3.3 Variable Length Model

Despite its notoriety and simplicity in modeling highway traffic, the CTM presents some critical drawbacks in realistically depicting density evolution and distribution when the discretization is not fine enough (i.e. small number of cells), or when congestion arises.

An alternative to the CTM, able to address more effectively the aforementioned problems, is given by the Variable Length Model (VLM), originally proposed in [20] and further modified in [21]. One of the main advantages of this model is the reduction of the dimension of the state space; in fact, the number of cells per section, independently of its length, is reduced to only two. Another appealing feature is the better representation of the congestion, which in urban networks is very likely to arise due to the presence of traffic lights, and needs to be properly treated. As shown in Figure 3.3, every road section is divided in only two cells and modeled with only three state variables: density in the upstream free cell ρ_f, density in the downstream congested cell ρ_c, position of the congestion front l. Consider a road section of length L, then the length of the free cell will be $(L - l)$, and the length of the congested cell will be l. The vehicles density in
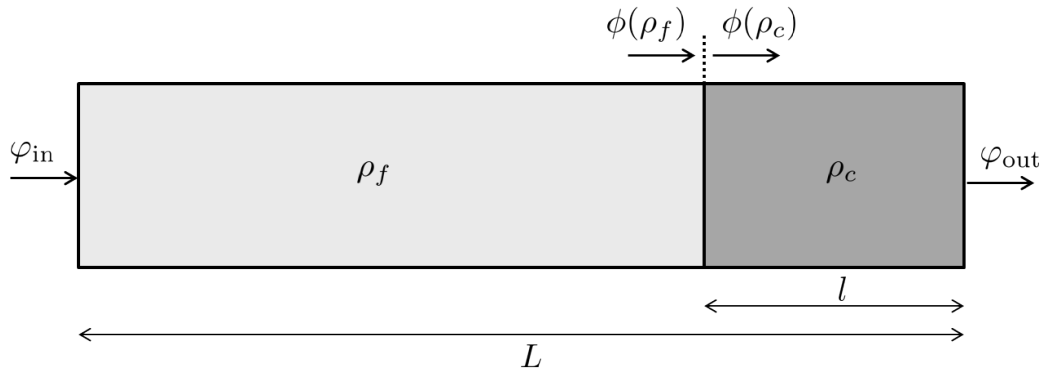
Figure 3.3 – Notation of the Variable Length Model.
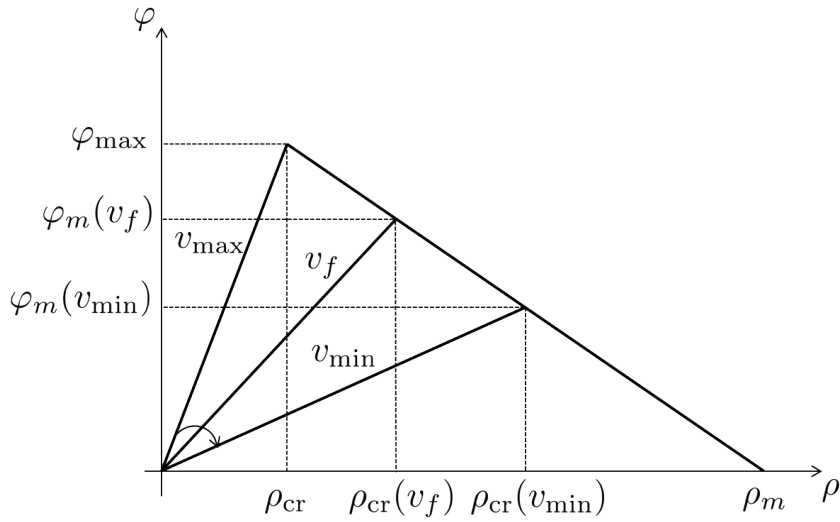
Figure 3.4 – Fundamental diagram with variable speed limits.

the two lumped cells is averaged, which means notion of single-vehicle behavior is lost, as it is typical for macroscopic models.

The domain of existence of the densities in the two cells is:

$$\rho_f \in [0, \rho_{cr}(v_f)]$$
$$\rho_c \in (\rho_{cr}(v_f), \rho_m]$$

$$(3.8)$$

where $\rho_{cr}(v_f)$ is the critical density relative to the current maximum allowed speed in the free cell,

$$\rho_{cr}(v_f) = \frac{w\rho_m}{v_f + w}$$

$$(3.9)$$

v_f may be thought of as the current speed limit in the free cell and would be utilized as the control input in a variable speed limits (VSL) traffic controller, and ρ_m is the jam density of the road section (see Figure 3.4).

The dynamic equations of the VLM are derived from the vehicles conservation principle in equations (3.2) and (3.3). In the VLM setting, the number of vehicles is defined as:

$$N_f = \rho_f(L - l)$$
$$N_c = \rho_c l$$

(3.10)

Thus, for a single road section, the model may be formalized as follows:

$$\begin{cases} \dot{\rho}_f = [\varphi_{\text{in}} - \phi(\rho_f)] \dfrac{1}{L - l} \\ \dot{\rho}_c = [\phi(\rho_c) - \varphi_{\text{out}}] \dfrac{1}{l} \\ \dot{l} = \dfrac{\phi(\rho_f) - \phi(\rho_c)}{\rho_c - \rho_f} \end{cases}$$

(3.11)

where the congestion front l represents the division line between the free and the congested cell, and its evolution in time is described by the Rankine-Hugoniot jump condition [79].

The interface flows $\phi(\rho_f)$ and $\phi(\rho_c)$ correspond to demand of the free cell and supply of the congested cell, respectively:

$$\phi(\rho_f) = D_f = \min\{\rho_f v_f, \varphi_m(v_f)\}$$
$$\phi(\rho_c) = S_c = \min\{w(\rho_m - \rho_c), \varphi_m(v_f)\}$$

(3.12)

Assuming that the two cells share the same fundamental diagram, interface flows are always theoretically saturated by the maximum value of the demand and supply functions:

$$\varphi_m(v_f) = \rho_{\text{cr}}(v_f)v_f = \frac{w\rho_m}{v_f + w}v_f$$

(3.13)

The system (3.11) has invariance properties with respect to the state variables ρ_f and ρ_c. In particular, the two state variables ρ_f and ρ_c remain in their domain of existence (3.8), assuming that initial conditions are taken in the domain of existence. Thanks to this property, the interface flows may be simply written as:

$$\phi(\rho_f) = D_f = \rho_f v_f$$
$$\phi(\rho_c) = S_c = w(\rho_m - \rho_c)$$

(3.14)

The boundary flows are defined as:

$$\varphi_{\text{in}} = \min\{D_{\text{in}}, S_f\}$$
$$\varphi_{\text{out}} = \min\{D_c, S_{\text{out}}\}$$

(3.15)

where D_c and S_f are:

$$D_c = \min\left\{\rho_c v_f, \varphi_m(v_f)\right\}$$
$$S_f = \min\left\{w(\rho_m - \rho_f), \varphi_m(v_f)\right\} \tag{3.16}$$

being $D_{\text{in}} \leq \varphi_{\max}$ the input demand and $S_{\text{out}} \leq \varphi_{\max}$ the output supply. The maximum capacity of the road section $\varphi_{\max}$, once fixed the maximum speed limit $v_{\max}$, the back-propagation speed of the congestion w, and the jam density ρ_m, is uniquely defined after the nominal critical density as:

$$\rho_{\text{cr}} = \frac{w\rho_m}{v_{\max} + w} \tag{3.17}$$

$$\varphi_{\max} = \rho_{\text{cr}} v_{\max} \tag{3.18}$$

3.3.1 Urban Variable Length Model

Let us now consider an urban road section with two traffic lights at its two ends. The same switching variable $\alpha(t)$ is supposed to model both traffic lights, and regulates the boundary flows of each section, as shown in Figure 3.5. The modeling variable takes on binary values according to the current phase of the traffic light. It is cycle-time (T_{cycle}) periodic and is simply defined as:

$$\alpha(t) = \alpha(t + T_{\text{cycle}}) = \begin{cases} 1, & \text{if } t \leq \tau < t + T_{\text{gr}} \\ 0, & \text{if } t + T_{\text{gr}} \leq \tau < t + T_{\text{cycle}} \end{cases}$$

where T_{gr} and T_{cycle} represent the green phase time and the cycle time of the traffic light, respectively.

The boundary flows, applying the known demand-supply formalism for merging traffic, vary depending on the traffic lights state and on the current speed limit.

The inflow is now defined as:

$$\varphi_{\text{in}}(t) = \alpha(t) \cdot \min\left\{D_{\text{in}}, S_f\right\} \tag{3.19}$$

and the outflow is:

$$\varphi_{\text{out}}(t) = \alpha(t) \cdot \min\left\{D_c, S_{\text{out}}\right\} \tag{3.20}$$

The system in (3.11) can be now rewritten for the urban setup in the following general form:

$$\begin{cases} \dot{\rho}_f = \left[\varphi_{\text{in}}(t) - \rho_f v_f\right] \dfrac{1}{L - l} \\[2mm] \dot{\rho}_c = \left[w(\rho_m - \rho_c) - \varphi_{\text{out}}(t)\right] \dfrac{1}{l} \\[2mm] \dot{l} = \dfrac{\rho_f v_f - w(\rho_m - \rho_c)}{\rho_c - \rho_f} \end{cases} \tag{3.21}$$

where the boundary flows are now functions of the time-variant variable $\alpha(t)$.
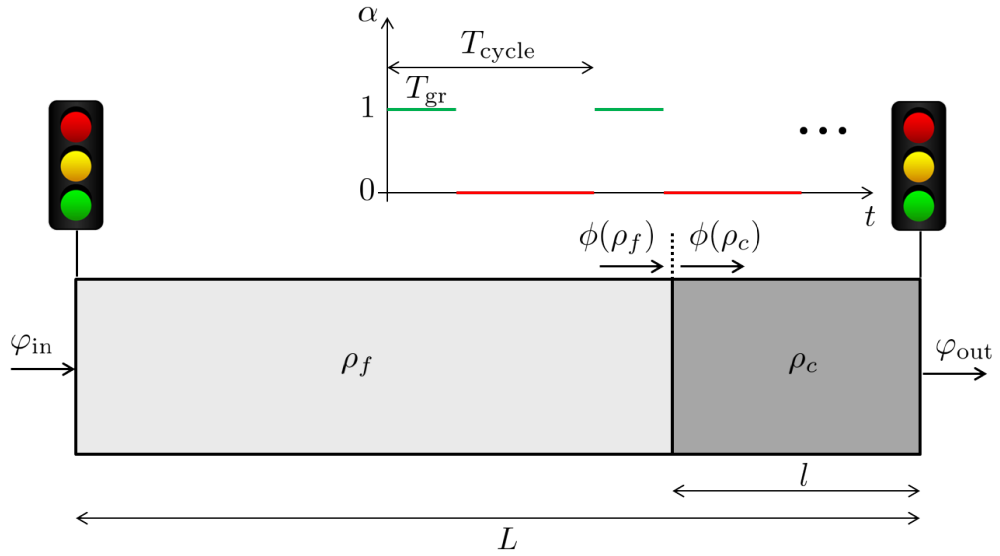
Figure 3.5 – Scheme of the Urban Variable Length Model.

3.3.2 Averaged Urban VLM

An interesting simplification of this model, in order to avoid the binary behavior of the switching variable modeling the traffic light, is obtained and formally justified with the perturbation and averaging theory [70]. Let us consider a system of the form

$$\dot{x} = \epsilon f(t, x, \epsilon) \tag{3.22}$$

where f is differentiable with respect to (x, ϵ) up to the second order and it is ΔT-periodic in t, then we associate with (3.22) an autonomous average system

$$\dot{x} = \epsilon f_{av}(x) \tag{3.23}$$

where

$$f_{av}(x) = \frac{1}{\Delta T} \int_{t}^{t+\Delta T} f(\tau, x, 0) \, \mathrm{d}\tau \tag{3.24}$$

In system (3.21), only the boundary flows depend on the purely time-dependent variable $\alpha(t)$, which can be averaged over the period (i.e. the cycle time of the traffic light):

$$\bar{\alpha} = \frac{1}{T_{\text{cycle}}} \int_{t}^{t+T_{\text{cycle}}} \alpha(\tau) \, \mathrm{d}\tau = \frac{1}{T_{\text{cycle}}} \int_{t}^{t+T_{\text{gr}}} \mathrm{d}\tau = \frac{T_{\text{gr}}}{T_{\text{cycle}}} \tag{3.25}$$

Hence, by applying the averaging method to the system in (3.21), the boundary
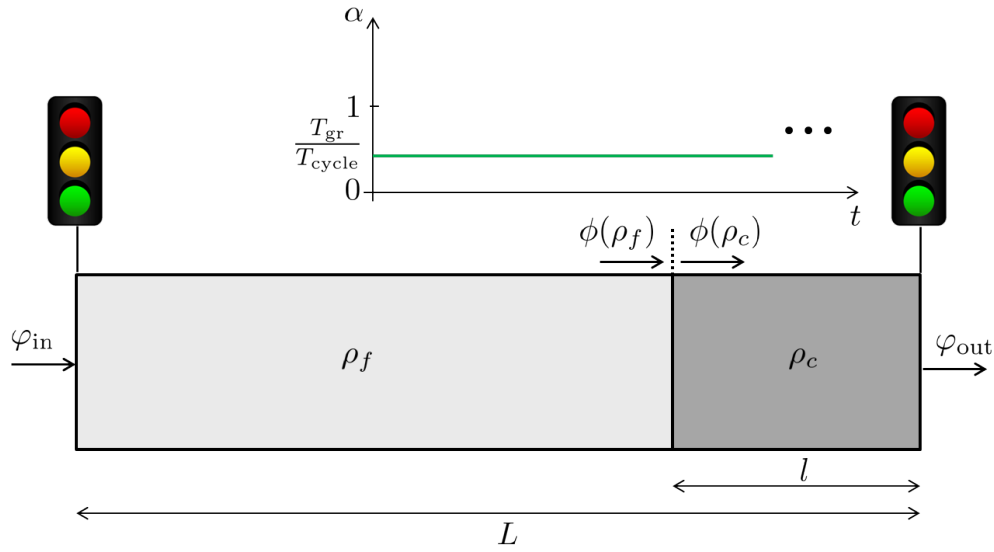
Figure 3.6 – Averaged Urban Variable Length Model.

flows may be defined as:

$$\begin{aligned} \bar{\varphi}_{\text{in}} &= \bar{\alpha} \cdot \min\left\{D_{\text{in}}, S_f\right\} \\ \bar{\varphi}_{\text{out}} &= \bar{\alpha} \cdot \min\left\{D_c, S_{\text{out}}\right\} \end{aligned} \tag{3.26}$$

and the new average system formulation, which will be the reference model in the following analysis, is:

$$\begin{cases} \dot{\rho}_f = \left[\bar{\varphi}_{\text{in}} - \rho_f v_f\right] \dfrac{1}{L - l} \\[2mm] \dot{\rho}_c = \left[w(\rho_m - \rho_c) - \bar{\varphi}_{\text{out}}\right] \dfrac{1}{l} \\[2mm] \dot{l} = \dfrac{\rho_f v_f - w(\rho_m - \rho_c)}{\rho_c - \rho_f} \end{cases} \tag{3.27}$$

This simplification is also consistent with the store-and-forward modeling approach. The discrete behavior of the system, induced by the traffic lights, is thus eliminated. The traffic light is modeled as an open valve, as shown in Figure 3.6, and the vehicles entering or leaving the section may be seen as a restricted continuous flow passing through a bottleneck. As a natural consequence of this approximation, oscillations of the queues at the traffic lights and notions cycle time and offset for the traffic lights are not represented by the averaged model, as shown in Figure 3.7.
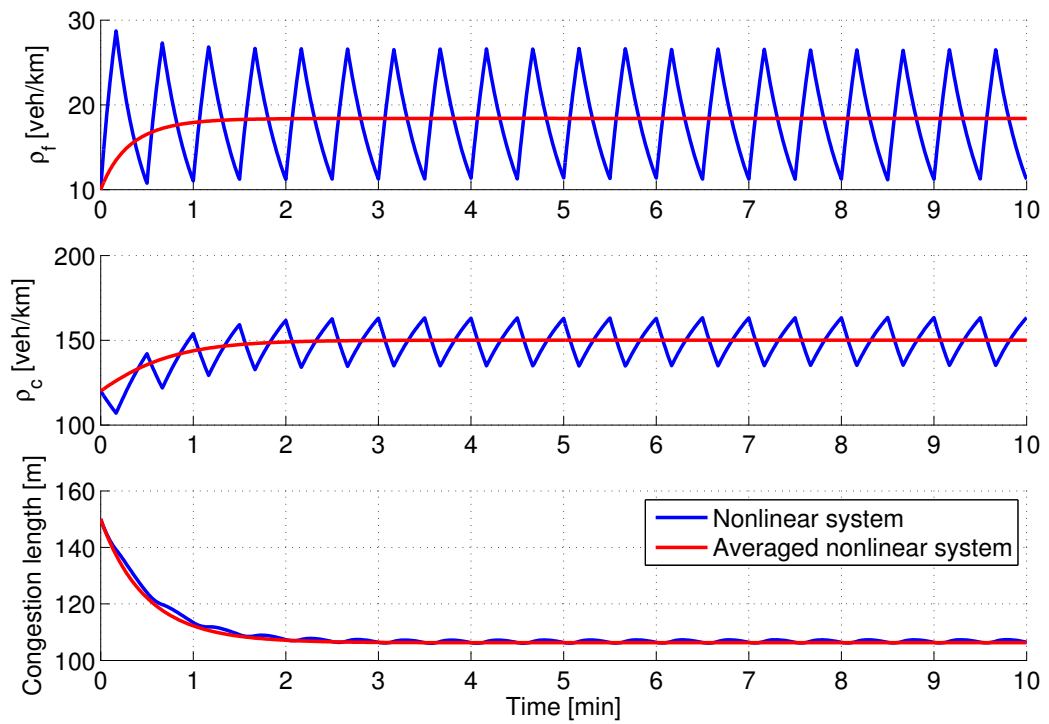
Figure 3.7 – Comparison example between the nonlinear system in (3.21) and the averaged nonlinear system in (3.27). Initial condition: $(\rho_f^0, \rho_c^0, l^0) = (10, 120, 150)$ [veh/km,veh/km,m], $v_f = 30$ km/h.

3.3.3 Model Singularities

One of the singularities of the system in (3.27) may be quite restrictive in an urban traffic context. If the congestion in the section is completely exhausted ($l = 0$) or the section is completely packed with vehicles ($l = L$), the first two dynamic equations of the system lose significance, and such a traffic condition cannot be represented by the model. The capability of representing spill-backs and propagation of vehicles through adjacent sections is of key importance in urban traffic networks, therefore the mentioned singularity was solved by fixing a minimum and maximum value for l, in compliance with numerical discretization constraints [21, 79]:

$$l \in [v\,\Delta k,\, L - v\,\Delta k] \tag{3.28}$$

with Δk being the time discretization step. Therefore there are two cases to be addressed, and the equations of the model, while respecting the vehicles conservation law, are modified as follows.

1. $l < v\,\Delta k$ and $v\rho_f \leq (\rho_m - \rho_c)w$
    The first condition states that the congested cell would become too small, and the second condition means that the congestion front is still retreating downstream. The model can be rewritten as:

$$
\begin{aligned}
\dot{\rho}_f &= [\bar{\varphi}_{\text{in}} - \phi(\rho_f)]\,\frac{1}{L - l} \\
\dot{\rho}_c &= [\phi(\rho_f) - (\rho_c - \rho_f)(v\,\Delta k - l) - \bar{\varphi}_{\text{out}}]\,\frac{1}{l} \\
\dot{l} &= v\,\Delta k - l
\end{aligned}
\tag{3.29}
$$

2. $l > L - v\,\Delta k$ and $v\rho_f \geq (\rho_m - \rho_c)w$
    The first condition states that the free cell would become too small, and the second condition means that the congestion front is still propagating upstream. The model can be rewritten as:

$$
\begin{aligned}
\dot{\rho}_f &= [\bar{\varphi}_{\text{in}} - (\rho_c - \rho_f)(L - v\,\Delta k - l) - \phi(\rho_c)]\,\frac{1}{L - l} \\
\dot{\rho}_c &= [\phi(\rho_c) - \bar{\varphi}_{\text{out}}]\,\frac{1}{l} \\
\dot{l} &= L - v\,\Delta k - l
\end{aligned}
\tag{3.30}
$$

At this operation conditions, assumption (3.8) does not hold anymore. The two cells do not necessarily represent the free one upstream and the congested one downstream, and are treated as fixed-length cells as in the CTM.
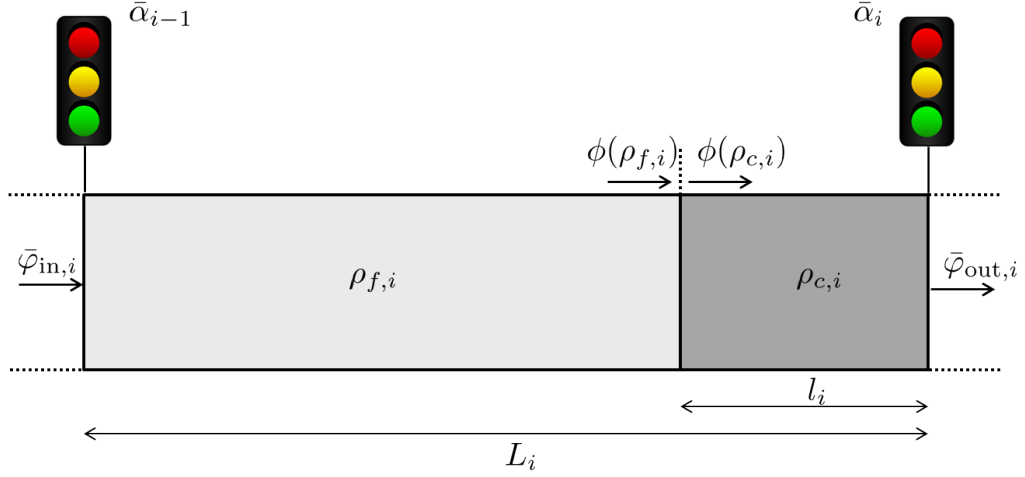
Figure 3.8 – Multi-section extension of the Urban Variable Length Model. Scheme of the i-th road section.

3.3.4 Extension to the Multi-Section Framework

Let us now consider an urban road network divided into n sections separated by traffic lights, all sharing the same macroscopic fundamental diagram. The now continuous variable $\bar{\alpha}_i$ models the downstream traffic light in section i, for $i = 1, \ldots, n$.

The boundary flows for the section i now vary depending also on the position of the considered section in the network, and potentially each section has its own speed limit $v_{f,i}$.

The inflow for the section i is now defined as:

$$\bar{\varphi}_{\text{in},i} = \bar{\alpha}_{i-1} \cdot \min\left\{D_{c,i-1}, S_{f,i}\right\} \tag{3.31}$$

where the variable $\bar{\alpha}_{i-1}$ models the upstream traffic light. The upstream demand at section input is:

$$D_{c,i-1} = \begin{cases} \min\left\{D_{\text{in}}, \varphi_{\max}\right\}, & \text{if } i = 1 \\ \min\left\{\rho_{c,i-1} v_{f,i-1}, \varphi_m(v_{f,i-1})\right\}, & \text{otherwise} \end{cases} \tag{3.32}$$

and the supply of the free cell of section i is:

$$S_{f,i} = \min\left\{w(\rho_m - \rho_{f,i}), \varphi_m(v_{f,i})\right\} \tag{3.33}$$

with the saturation function $\varphi_m(v_f)$ being defined as in (3.13).

The outflow is defined as:

$$\bar{\varphi}_{\text{out},i}(t) = \bar{\alpha}_i \cdot \min\left\{D_{c,i}, S_{f,i+1}\right\} \tag{3.34}$$

The downstream demand at section output is:

$$S_{f,i+1} = \begin{cases} \min\left\{S_{\text{out}}, \varphi_{\max}\right\}, & \text{if } i = n \\ \min\left\{w(\rho_m - \rho_{f,i+1}), \varphi_m(v_{f,i+1})\right\}, & \text{otherwise} \end{cases} \tag{3.35}$$

and the demand of the congested cell of section i is:

$$D_{c,i} = \min\left\{\rho_{c,i} v_{f,i}, \varphi_m(v_{f,i})\right\} \tag{3.36}$$

The model can be finally written as follows:

$$\begin{cases} \dot{\rho}_{f,i} = \left[\bar{\varphi}_{\text{in},i} - \rho_{f,i} v_{f,i}\right] \dfrac{1}{L_i - l_i} \\[2mm] \dot{\rho}_{c,i} = \left[w(\rho_m - \rho_{c,i}) - \bar{\varphi}_{\text{out},i}\right] \dfrac{1}{l_i} \\[2mm] \dot{l}_i = \dfrac{\rho_{f,i} v_{f,i} - w(\rho_m - \rho_{c,i})}{\rho_{c,i} - \rho_{f,i}} \end{cases} \tag{3.37}$$

Note that, due to concatenation effects, the boundary flows obey the following equalities:

$$\begin{aligned} \bar{\varphi}_{\text{in},i} &= \bar{\varphi}_{\text{out},i-1} \\ \bar{\varphi}_{\text{out},i} &= \bar{\varphi}_{\text{in},i+1} \end{aligned} \tag{3.38}$$

3.4 Model Properties Analysis

In the case of inequality of the boundary flows, the system converges naturally to a fully free or a fully congested state. These cases represent a criticality of the model and the eco-driving analysis. If the section is fully congested the control authority is drastically reduced and almost completely lost. The vehicles could not follow the control input v_f while heading towards the congestion front, and the advised speed limit would have an impact only on the outflow (i.e. the speed at which the vehicles are allowed to leave the section). A fully free section, on the contrary, has complete controllability and simply represents a particular case of the equal-boundary-flows analysis. Therefore, the existence of an equilibrium level of congestion within the section limits represents an interesting context of investigation for the eco-driving purposes.

3.4.1 Equal Boundary Flows

Let us consider one road section and let us assume that the traffic lights at the two ends are equally timed, that there is enough demand upstream and enough

supply downstream, and that the speed limit v_f is the same both upstream and downstream. Then the boundary flows are only determined by the maximum value of the demand/supply function:

$$\bar{\varphi}_{\text{in}}(v_f) = \bar{\varphi}_{\text{out}}(v_f) = \varphi_m(v_f) = \bar{\alpha}\frac{w\rho_m}{v_f + w}v_f \tag{3.39}$$

Thus, the system may be rewritten as:

$$\begin{cases} \dot{\rho}_f = \left[\bar{\alpha}\dfrac{w\rho_m}{v_f + w}v_f - \rho_f v_f\right]\dfrac{1}{L - l} \\[2mm] \dot{\rho}_c = \left[w(\rho_m - \rho_c) - \bar{\alpha}\dfrac{w\rho_m}{v_f + w}v_f\right]\dfrac{1}{l} \\[2mm] \dot{l} = \dfrac{\rho_f v_f - w(\rho_m - \rho_c)}{\rho_c - \rho_f} \end{cases} \tag{3.40}$$

Given a set of initial conditions $(\rho_f^0, \rho_c^0, l^0)$, the system (3.40) converges to the equilibrium:

$$\begin{aligned} \rho_f^* &= \frac{\varphi_m(v_f)}{v_f} \\[2mm] \rho_c^* &= \rho_m - \frac{\varphi_m(v_f)}{w} \\[2mm] l^* &= \frac{N_0 - \rho_f^* L}{\rho_c^* - \rho_f^*} \end{aligned} \tag{3.41}$$

which can be more conveniently written as an explicit function of the control input v_f:

$$\begin{aligned} \rho_f^* &= \bar{\alpha}\frac{w\rho_m}{v_f + w} \\[2mm] \rho_c^* &= \rho_m - \bar{\alpha}\frac{v_f \rho_m}{v_f + w} \\[2mm] l^* &= \frac{N_0(v_f + w) - \bar{\alpha}\rho_m wL}{\rho_m(v_f + w)(1 - \bar{\alpha})} \end{aligned} \tag{3.42}$$

where N_0, the initial and time-invariant number of vehicles, is given by:

$$N_0 = N = \rho_f^0(L - l^0) + \rho_c^0 l^0 \tag{3.43}$$

In the following, the stability properties of the system will be discussed.

Stability of the System

In order to study the stability of a nonlinerar system at the equilibrium, one possible approach is to study its Jacobian linearization around such equilibrium. Consider a nonlinear differential equation

$$\dot{x}(t) = f\left(x(t), u(t)\right) \tag{3.44}$$

where $f \colon \mathbb{R}^n \times \mathbb{R}^m \to \mathbb{R}^n$. A point $x^* \in \mathbb{R}^n$ is an equilibrium point if there is a specific equilibrium input $\bar{u} \in \mathbb{R}^m$ such that

$$f\left(x^*, \bar{u}\right) = 0 \tag{3.45}$$

If we start the system at $x(t_0) = x^*$, and apply the constant input $u(t) \equiv \bar{u}$, then the state of the system will remain fixed at $x(t) = x^*$ for all t. For the general case of initial conditions different from the equilibrium, deviation variables are introduced to measure:

$$\begin{aligned} \hat{x}(t) &= x(t) - x^* \\ \hat{u}(t) &= u(t) - \bar{u} \end{aligned} \tag{3.46}$$

Now the system in (3.44) can be rewritten as:

$$\dot{\hat{x}}(t) = f\left(x^* + \hat{x}(t), \bar{u} + \hat{u}(t)\right) \tag{3.47}$$

If we compute a Taylor expansion of the right-hand side, and neglect all the higher order terms, we obtain:

$$\dot{\hat{x}}(t) \approx f\left(x^*, \bar{u}\right) + \left.\frac{\partial f}{\partial x}\right|_{\substack{x = x^* \\ u = \bar{u}}} \hat{x}(t) + \left.\frac{\partial f}{\partial u}\right|_{\substack{x = x^* \\ u = \bar{u}}} \hat{u}(t) \tag{3.48}$$

but $f\left(x^*, \bar{u}\right) = 0$ leaving:

$$\dot{\hat{x}}(t) \approx \left.\frac{\partial f}{\partial x}\right|_{\substack{x = x^* \\ u = \bar{u}}} \hat{x}(t) + \left.\frac{\partial f}{\partial u}\right|_{\substack{x = x^* \\ u = \bar{u}}} \hat{u}(t) \tag{3.49}$$

This differential equation approximately governs (second order and higher terms are neglected) the deviation variables $\hat{x}(t)$ and $\hat{u}(t)$, as long as they remain small. It is a linear, time-invariant, differential equation, since the derivatives of $\hat{x}(t)$ are linear combinations of the $\hat{x}(t)$ variables and the deviation inputs, $\hat{u}(t)$. The matrices:

$$\begin{aligned} A &= \left.\frac{\partial f}{\partial x}\right|_{\substack{x = x^* \\ u = \bar{u}}} \in \mathbb{R}^{n \times n} \\[1em] B &= \left.\frac{\partial f}{\partial u}\right|_{\substack{x = x^* \\ u = \bar{u}}} \in \mathbb{R}^{n \times m} \end{aligned} \tag{3.50}$$

are constant matrices. With the matrices A and B as defined in (3.50), the linear system

$$\dot{\hat{x}}(t) = A\hat{x}(t) + B\hat{u}(t) \tag{3.51}$$

is called the Jacobian linearization of the original nonlinear system (3.44).

In the particular case of the model under analysis, with $x^* = (\rho_f^*, \rho_c^*, l^*)$ and $\bar{u} = v_f$, the Jacobian linearization of system (3.40) yields the following matrices:

$$A = \begin{bmatrix} -\frac{v_f}{L-l^*} & 0 & 0 \\ 0 & -\frac{w}{l^*} & 0 \\ -\frac{v_f}{(\bar{\alpha}-1)\rho_m} & -\frac{w}{(\bar{\alpha}-1)\rho_m} & 0 \end{bmatrix}$$

$$B = \begin{bmatrix} -\frac{\bar{\alpha}\rho_m v_f w}{(L-l^*)(v_f+w)} \\ -\frac{\bar{\alpha}\rho_m w^2}{l^*(v_f+w)^2} \\ -\frac{\bar{\alpha}w}{(\bar{\alpha}-1)(v_f+w)} \end{bmatrix} \tag{3.52}$$

where the equilibrium densities ρ_f^* and ρ_c^* have been replaced here by their equilibrium value defined in (3.42), for clarity of presentation.

Evidently, linearization fails to prove the stability of the original nonlinear system (3.40) at the equilibrium, since an eigenvalue lies on the imaginary axis. However the system does not diverge because the boundary flows are equal.

In the case of critical linearization of a nonlinear system (i.e. some eigenvalues equal to zero), the center manifold theorem could be applied to study the stability and controllability of the original system by looking at the qualitative behavior of the critical subspace. The center manifold theory, originally presented for autonomous systems [70], has been extended to non-autonomous and input-affine systems [5, 25]. The nonlinear system here under analysis is not affine in the input, therefore the calculation of the coefficients of the partial series expansion of the center manifold equation results more involved. Eventually, also the center manifold approach fails to provide a qualitative insight into the behavior of the unstable mode of the nonlinear system.

However, some further characteristics of the system will be hereafter discussed, which will help to shed some light on the behavior of the system.

Stability of the Equilibrium Points

Interestingly, the well known definition of stability of an equilibrium point does not hold for the system in (3.40). The classical definition of stable equilibrium point is:

Definition 1. *The equilibrium point $x^* = 0$ is stable at $t = t_0$ if for any $\epsilon > 0$ there exists a $\delta(t_0, \epsilon) > 0$ such that*

$$||x(t_0)|| < \delta \quad \Longrightarrow \quad ||x(t)|| < \epsilon, \quad \forall t \geq t_0$$

Our system seems to verify this definition. If there exists an equilibrium point of the system, and the initial conditions coincide with the equilibrium itself, the system remains at the equilibrium. If the initial conditions are slightly different from the equilibrium, then the system converges to the equilibrium with a small error, but it remains bounded within $\pm\epsilon$.

However this is where the conceptual difference arises. The value to which the system converges is an equilibrium point itself. In particular, for every choice of initial conditions and velocity in the free cell, the system evolves and converges naturally to a different equilibrium point. As a consequence of the equilibrium definition in (3.42), we may state the following properties:

Property 1. *For any choice of N_0 and v_f, the system converges to a new equilibrium $(\rho_f^*, \rho_c^*, l^*)$.*

Property 2. *The system always converges to the same equilibrium $(\rho_f^*, \rho_c^*, l^*)$ while conserving the input speed v_f if and only if:*

1. *the system starts from any combination of initial conditions resulting in the same N_0 associated with the equilibrium given in equation (3.42);*

2. *the system starts from the equilibrium itself.*

Therefore, the trajectories of the dynamical system that start near an equilibrium point $(\rho_f^*, \rho_c^*, l^*)$ converge to an always different equilibrium, depending on the initial conditions $(\rho_f^0, \rho_c^0, l^0)$. An invariance property of the system can be stated as:

Property 3. *For a choice of v_f and initial state $(\rho_f^0, \rho_c^0, l^0)$, the system will converge to the equilibrium point $(\rho_f^*, \rho_c^*, l^*)$ defined in (3.42).*

As a consequence of this property, starting from arbitrary initial conditions will make impossible to reach an equilibrium $(\rho_f^*, \rho_c^*, l^*)$ associated to different initial conditions while conserving also the speed v_f associated with it. In other words, given a certain initial traffic condition and calculated an optimal speed limit v_f^*, it is possible to track only the equilibrium (3.42) while conserving the optimal speed.

Reduced State Model

This dependence on the initial conditions, which affects the canonical definition of stability of the equilibrium, may be overcome by observing that N_0 appears only in the expression of l^*. The length of the congestion can be written as a function of the two densities ρ_f and ρ_c as follows:

$$l = \frac{N - \rho_f L}{\rho_c - \rho_f} \tag{3.53}$$

and a state transformation from l to N will allow the system in (3.27) to be equivalently written as:

$$
\begin{cases}
\dot{\rho}_f = [\bar{\varphi}_{\text{in}} - \rho_f v_f] \dfrac{\rho_c - \rho_f}{\rho_c L - N} \\[2ex]
\dot{\rho}_c = [w(\rho_m - \rho_c) - \bar{\varphi}_{\text{out}}] \dfrac{\rho_c - \rho_f}{N - \rho_f L} \\[2ex]
\dot{N} = \bar{\varphi}_{\text{in}} - \bar{\varphi}_{\text{out}}
\end{cases}
\tag{3.54}
$$

Being the number of vehicles time-invariant, the system (3.40) is then described by only two dynamic equations:

$$
\begin{cases}
\dot{\rho}_f = \left[\bar{\alpha} \dfrac{w\rho_m}{v_f + w} v_f - \rho_f v_f\right] \dfrac{\rho_c - \rho_f}{\rho_c L - N} \\[2ex]
\dot{\rho}_c = \left[w(\rho_m - \rho_c) - \bar{\alpha} \dfrac{w\rho_m}{v_f + w} v_f\right] \dfrac{\rho_c - \rho_f}{N - \rho_f L}
\end{cases}
\tag{3.55}
$$

given $N(t) = N_0$ for all $t > 0$, which now may be seen as a system parameter.

The parameter N has a well defined domain of existence, in order to ensure that the length of the congested cell l at steady-state does not exceed the boundaries of the section ($0 < l < L$). Therefore, by imposing $l^* \in (0, L)$, it follows from (3.42) that:

$$
\rho_m L \frac{\bar{\alpha} w}{v_f + w} < N < \rho_m L \left[(1 - \bar{\alpha}) + \frac{\bar{\alpha} w}{v_f + w}\right]
\tag{3.56}
$$

which can be also written as:

$$
\rho_f^* L < N < \rho_c^* L
\tag{3.57}
$$

Then, a condition has to be respected also by the initial conditions for the densities in the two cells:

$$
\rho_f^0 L < N < \rho_c^0 L
\tag{3.58}
$$

Intuitively, if the initial densities are too low (or too high), the condition in (3.43) would cause the initial length of the congested cell l^0 to be out of bounds.

After this simplification, a theorem for stability of system (3.55) can be given:

Theorem 1. *The equilibrium point (ρ_f^*, ρ_c^*) is asymptotically stable if and only if:*
   — *N satisfies (3.57);*

   — *the initial conditions (ρ_f^0, ρ_c^0) satisfy (3.58).*
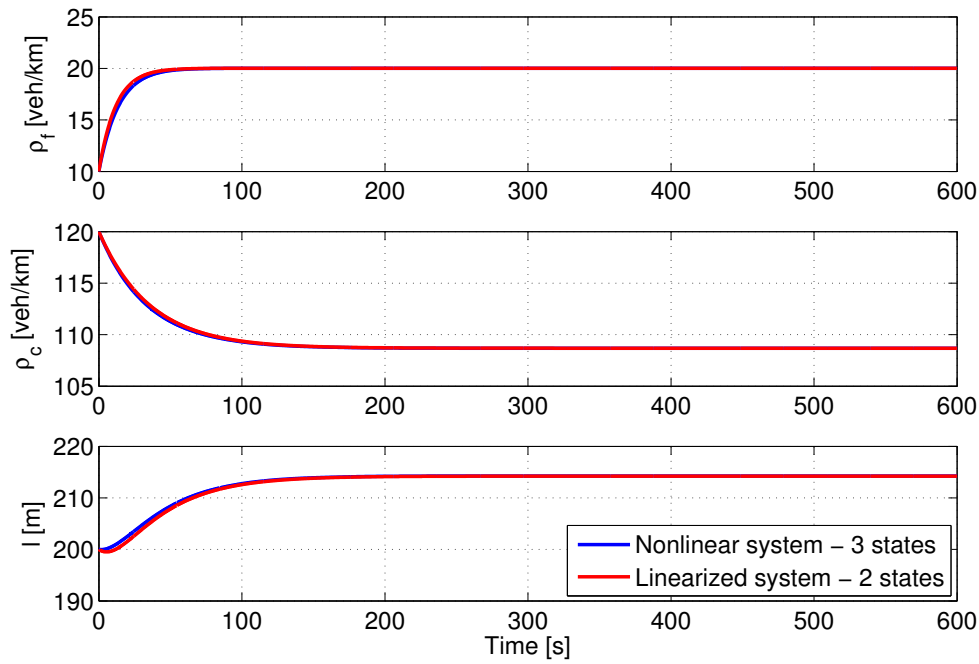
Figure 3.9 – Comparison between the nonlinear system in (3.27) and the reduced linearized system in (3.55). Initial condition: $(\rho_f^0, \rho_c^0) = (10, 120)$ veh/km, $v_f = 25$ km/h, $N = 25$.
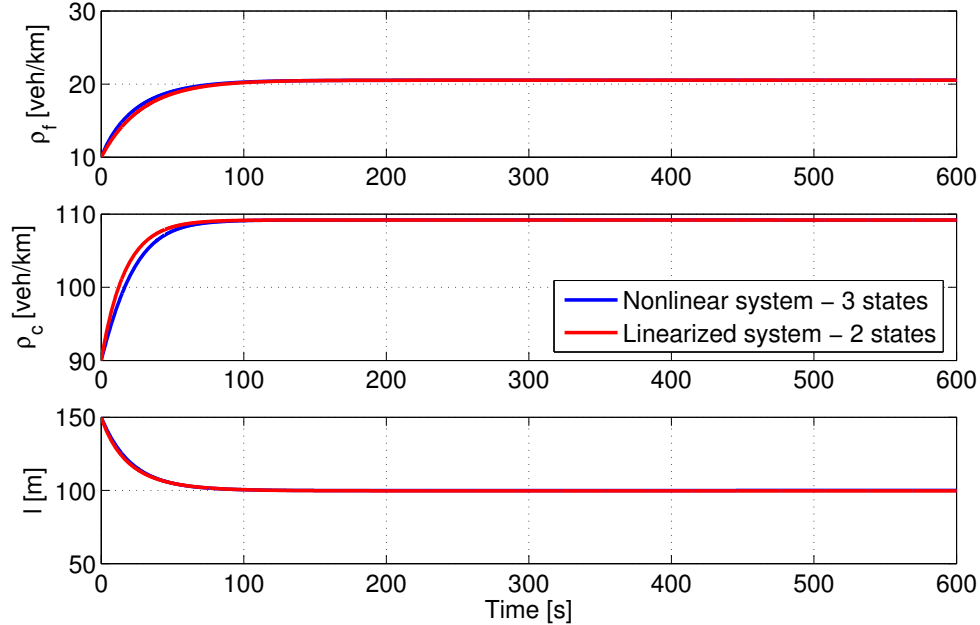
Figure 3.10 – Comparison example between the nonlinear system in (3.27) and the reduced linearized system in (3.55). Initial condition: $(\rho_f^0, \rho_c^0) = (10, 90)$ veh/km, $v_f = 25$ km/h $N = 15$.

Proof. Let the equilibrium state of system (3.55) be $x^* = [\rho_f^*, \rho_c^*]$ and the input be $\bar{u} = v_f$. The error system evaluated at the equilibrium is of the form:

$$\dot{x} = A|_{(x^*, \bar{u})}\, \hat{x} + B|_{(x^*, \bar{u})}\, \hat{u} \tag{3.59}$$

with $\hat{x} = x - x^*$ and $\hat{u} = u - \bar{u}$. For the reduced system in analysis the matrices A and B are:

$$A = \begin{bmatrix} -\dfrac{v_f(\rho_c^* - \rho_f^*)}{\rho_c^* L - N} & 0 \\[2em] 0 & -\dfrac{w(\rho_c^* - \rho_f^*)}{N - \rho_f^* L} \end{bmatrix}$$

$$\tag{3.60}$$

$$B = \begin{bmatrix} \dfrac{(\rho_c^* - \rho_f^*)(-\bar{\alpha}\rho_m w^2 + \rho_f^*(v_f + w)^2)}{(N - \rho_c^* L)(v_f + w)^2} \\[2em] \dfrac{-\bar{\alpha}(\rho_c^* - \rho_f^*)\rho_m w^2}{(N - \rho_f^* L)(v_f + w)^2} \end{bmatrix}$$

The eigenvalues of A are proved to be negative, for every choice of the equilibrium respecting the condition of the Theorem.

The Variable Length Model, by construction, ensures that $\rho_c > \rho_f$ [20]. The control variable is positive and is subject to the constraints $v_{\min} \leq v_f \leq v_{\max}$. Thus, the first eigenvalue, calculated at the equilibrium, is negative if:

$$N < \rho_c^* L$$

This is ensured by (3.57). The negativity of the second eigenvalue is proved analogously by the condition:

$$N > \rho_f^* L$$

$\square$

Asymptotic stability of the linearized system proves the asymptotic stability of the reduced nonlinear system (3.55) at any feasible equilibrium point. Feasibility of the equilibria is ensured by condition (3.57) on N together with condition (3.58) on the initial conditions, while respecting also the speed limits.

3.4.2 Unequal Boundary Flows

In the case of unequal boundary flows, the assumption on the time invariance of the number of vehicles in the section does not hold anymore, and system (3.55) is not sufficient to describe the state dynamics. Furthermore, the notion of convergence to a three-states equilibrium lose significance because the unbalance of the

boundary flows will lead eventually the system to converge to a fully-congested or a fully-free state, saturating the steady-state value of l.

The previous analysis on the stability of the equilibrium points cannot be applied directly to this case, due to the lack of analytic expressions fully describing the equilibrium $(\rho_f^*, \rho_c^*, l^*)$. However, although an analytical expression of the convergence value of l cannot be found, the densities preserve a well defined equilibrium unaffected by the varying number of vehicles:

$$
\begin{aligned}
\rho_f^* &= \bar{\alpha}_1 \frac{w \rho_m}{v_f + w} \\
\rho_c^* &= \rho_m - \bar{\alpha}_2 \frac{v_f \rho_m}{v_f + w}
\end{aligned}
\tag{3.61}
$$

where $\bar{\alpha}_1$ and $\bar{\alpha}_2$ are the variables modeling the upstream and the downstream traffic lights, respectively.

3.5 Traffic Performance Metrics

Traffic conditions described by the state of the variable length model $\mathbf{x} = (\rho_f, \rho_c, l)$ need to be evaluated and assessed with respect to traffic performance metrics properly defined and adapted to the model in (3.27). In the particular case of equal boundary flows, as already mentioned, the system would converge at a steady-state. Therefore, the traffic performance metrics could be rewritten for the steady-state regime, by evaluating them over the period of the traffic lights T_{cycle}.

Instantaneous Travel Time

The instantaneous travel time (ITT) may be defined as the travel time that would result if traffic conditions remained unchanged over the time span under analysis. It is computed at every time step, and it may be seen as the time a single vehicle entering the section at a certain time instant would take to travel along the section, while traffic conditions remain as they were at the initial time instant. It could be simply defined, for a single vehicle, as:

$$
\text{ITT}(\mathbf{x}) = \frac{L - l}{v_f} + \frac{l}{v_c}
\tag{3.62}
$$

where velocity in a cell is a function of the density in that cell, and it is given by the general relationship in (3.7).

In the case of equal boundary flows, the ITT shall be rewritten as a function of the control input (i.e. the speed limit) v_f, as follows:

$$
\text{ITT}(v_f) = \frac{N(v_f + w)}{\bar{\alpha} \rho_m v_f w}
\tag{3.63}
$$

where the speed in the congested cell is obtained from (3.7) and evaluated for the equilibrium density ρ_c^* in (3.42):

$$v_c = \frac{\bar{\alpha} v_f w}{(1 - \bar{\alpha}) v_f + w} \tag{3.64}$$

Total Time Spent

The total time spent (TTS) by the vehicles in the network is one of the most used and informative global traffic metrics to assess nature of traffic and vehicles behavior. If ITT gives a step-by-step quantification of the time a single vehicle would spend in the section, TTS is global and is only influenced by the number of vehicles evolution inside the section over the time horizon T. It is defined as:

$$\text{TTS}(\mathbf{x}) = \int_0^T \int_0^L \rho(x,t) \, \mathrm{d}x \, \mathrm{d}t \tag{3.65}$$

Knowing that the cells in the VLM are lumped and the density is space-invariant within the cells, the inner integral, representing the number of vehicles present in the whole section, may be written as:

$$\begin{aligned} N &= \int_0^L \rho(x) \, \mathrm{d}x = \int_0^{L-l} \rho_f \, \mathrm{d}x + \int_{L-l}^L \rho_c \, \mathrm{d}x \\ &= \rho_f (L - l) + \rho_c l \end{aligned} \tag{3.66}$$

Hence, TTS for the VLM may be written as:

$$\text{TTS}(\mathbf{x}) = \int_0^T \left[\rho_f L + (\rho_c - \rho_f) l \right] \, \mathrm{d}\tau \tag{3.67}$$

Minimization of total time spent in a traffic network is equivalent to maximization of flow. In other words, the earlier the vehicles are able to exit the network (by appropriate use of the available control measures) the smaller TTS will be [3].

It is important to notice that if a reduction of v_f does not induce a reduction of the inflow, the only effect would be a redistribution of the vehicles inside the road section; the average number of vehicles would not change and the TTS would not be affected. In other words, in the case of equal boundary flows, at steady-state TTS remains constant.

Total Travel Distance

The total travel distance (TTD) is a measure of how efficiently the infrastructure is used in terms of occupancy and traveling velocity. The infrastructure

manager would like to maximize this metric in order to have as many vehicles as possible traveling at the maximum allowed velocity. In other words, the purpose is to have a high utilization of the infrastructure with no congestion. It is defined and adapted to VLM in this framework as:

$$
\begin{aligned}
\text{TTD}(\mathbf{x}) &= \int_0^T \int_0^L \phi(\rho(x), t)\, \mathrm{d}x \mathrm{d}t \\
&= \int_0^T \int_0^{L-l} \phi(\rho_f, t)\, \mathrm{d}x \mathrm{d}t + \int_0^T \int_{L-l}^L \phi(\rho_c, t)\, \mathrm{d}x \mathrm{d}t \\
&= \int_0^T \int_0^{L-l} v_f \rho_f\, \mathrm{d}x \mathrm{d}t + \int_0^T \int_{L-l}^L w(\rho_m - \rho_c)\, \mathrm{d}x \mathrm{d}t \\
&= \int_0^T \left\{ v_f \rho_f L + \left[w(\rho_m - \rho_c) - v_f \rho_f \right] l \right\}\, \mathrm{d}t
\end{aligned}
\tag{3.68}
$$

In the case of equal boundary flows, the TTD is calculated at the equilibrium and over one traffic light cycle. Therefore, it can be written as a sole function of the control input as follows:

$$
\text{TTD}(v_f) = v_f \bar{\alpha} \frac{w \rho_m}{v_f + w} L \cdot T_{\text{cycle}}
\tag{3.69}
$$

Energy Consumption

Another important metric, usually not considered at macroscopic level, is the energy consumption of the vehicles. The energy consumption functional here is obtained as a macroscopic adaptation of the one introduced in Chapter 2, assuming that the vehicles in the traffic network are all equipped with an electric motor (analogous metrics could be used in the case of vehicles with combustion engines). It is recalled from (2.7) that for a single vehicle the model is written as:

$$
\begin{cases}
\dot{x} = v \\
\dot{v} = h_1 u - h_2 v^2 - h_3 v - h_0
\end{cases}
\tag{3.70}
$$

where parameters h are estimated for the electric motor under analysis [37], and the single vehicle control input (i.e. motor torque) is:

$$
u = \frac{1}{h_1} \left(h_2 v^2 + h_3 v + h_0 \right)
\tag{3.71}
$$

Then the power demand for an electric motor is given by:

$$P = b_1 uv + b_2 u^2 = f(v, \dot{v}) \tag{3.72}$$

where b_1 and b_2 are motor parameters.

Hence the energy functional may be generally written as:

$$E = \int_0^T P \, dt \tag{3.73}$$

At macroscopic level, the energy consumption is affected by the number of vehicles traveling in the road section under analysis, along with velocity and acceleration of the vehicles embedded in traffic flow. Therefore, by tailoring the energy cost functional to the VLM, energy consumption may be approximated as the sum of different contributions: energy consumption in the free cell, energy consumption in the congested cell, energy consumption at the interface points between two adjacent cells. The vehicles velocity in the cells is given by (3.7), and the acceleration at the jump points (i.e. interfaces between different cells) can be simply modeled as a constant $a = a_{\max}$. The parameter $a_{\max}$ indicates the maximum acceleration a driver is going to apply, and it can be fixed according to safety and/or comfort policies.

Finally, the energy cost functional for the VLM can be formulated as follows:

$$E = E_f + E_c + E_{f \to c} + E_{c \to f} \tag{3.74}$$

where the energy consumption in the free cell is:

$$E_f = \int_0^T P_f \cdot \rho_f \cdot (L - l) \, dt \tag{3.75}$$

with P_f being calculated as in (3.72) using v_f as velocity. The energy consumption in the congested cell is:

$$E_c = \int_0^T P_c \cdot \rho_c \cdot l \, dt \tag{3.76}$$

with P_c being calculated as in (3.72) using v_c as velocity. The energy consumption due to the velocity change between the free and the congested cell is:

$$E_{f \to c} = \int_0^{\frac{|v_c - v_f|}{a}} P \, dt \cdot \int_0^T w(\rho_m - \rho_c) \, dt \tag{3.77}$$

where the first integral computes the energy consumption of a single vehicle making the transition from the free cell to the congested cell. The time horizon of the integral is simply the time required to complete the transition, given the speed difference $|v_c - v_f|$ and the acceleration a. The second integral computes the number of vehicles that actually make the transition from the free to the congested cell over the time horizon T.

Analogously, the energy consumption due to the velocity change between the congested cell and the virtual free cell after the downstream traffic light is:

$$E_{c \to f} = \int_0^{\frac{|v_f - v_c|}{a}} P \, \mathrm{d}t \cdot \int_0^T \bar{\varphi}_{\text{out}} \, \mathrm{d}t \qquad (3.78)$$

Note that in the power demand expressions used to approximate energy consumption at the interfaces, $\dot{v}$ is assumed to be equal to a, and v can be linearly modeled as:

$$v(t) = v_0 + a \cdot t \qquad (3.79)$$

where v_0 will be either v_f or v_c depending on the considered transition. Note also that the temporal acceleration in the free and congested cell is neglected.

3.6 Optimal Speed Limit

Once the model is defined and simplified for control purposes, and after defining traffic performance metrics to assess the behavior of the system, the goal is to select an optimal control action (i.e. the velocity in the free cell) that minimizes an objective function of energy consumption, ITT, TTS and TTD.

As working hypotheses, the scenario under analysis takes into account one road section with a traffic light downstream regulating the outflow, and a traffic light upstream regulating the inflow.

The problem can be stated as follows:

Problem 1. *Given system* (3.27)*, and feasible initial conditions* $(\rho_f^0, \rho_c^0, l^0)$*, find the optimal speed limit*

$$v_f^* = \underset{v_f}{\mathrm{argmin}} \left\{ \sigma_1 E + \sigma_2 ITT - \sigma_3 TTD + \sigma_4 TTS \right\}$$

subject to

$$v_{min} \le v_f \le v_{max}$$
$$l_{min} \le l \le l_{max}$$

The maximum speed limit is set to the standard for an urban environment, the minimum speed limit may be fixed arbitrarily. Bounds for the congestion length are set in compliance with the model singularities and the discretization constraints, as in Section 3.3.3:

$$l_{\min} = v_f \Delta k, \quad l_{\max} = L - v_f \Delta k \tag{3.80}$$

As the model is defined, if there is a difference in the boundary flows the system converges naturally to either fully-free or fully-congested state. If the system is in fully-free state, Problem 1 is still well posed and would be simpler to solve since the energy consumption would be given only by the E_f contribution. On the contrary, if the system is in fully-congested state, no control action can be applied in the free cell to prevent section saturation.

If the boundary flows induced by the traffic lights are set to be equal (i.e. traffic lights split ratios are equal), the optimization problem results more interesting due to the presence of many possible steady-state equilibria, given by equation (3.42). Varying the speed limit in the free cell will cause the system to reach a different steady-state value without modifying the number of vehicles, hence complying with the hypothesis of equal boundary flows. This corresponds to a redistribution of vehicles inside the section, while moving the front of the congestion l.

Note that, in the case of equal boundary flows, TTS is constant because by hypothesis the number of vehicles does not change over time. Therefore, since TTS is not impacted by the regulation via variable speed limits, Problem 1 can be simplified and rewritten as follows:

Problem 2. *Given system* (3.27), *feasible initial conditions* $(\rho_f^0, \rho_c^0, l^0)$, *and a constant* $\bar{\alpha}$ *for the traffic lights, find the optimal speed limit*

$$v_f^* = \operatorname*{argmin}_{v_f} \left\{ \sigma_1 E + \sigma_2 ITT - \sigma_3 TTD \right\}$$

subject to

$$v_{min} \leq v_f \leq v_{max}$$
$$l_{min} \leq l \leq l_{max}$$

Note that the objective function in Problem 2, formulated for the case of equal boundary flows, can be written as a sole function of the input v_f.

The cost function in Problem 2 has been evaluated at the equilibrium for every feasible combination of speed limit and number of vehicles in the section. The feasibility of the equilibrium points is ensured by conditions (3.57) and (3.58) on the number of vehicles and on the initial conditions. A comprehensive cost map of
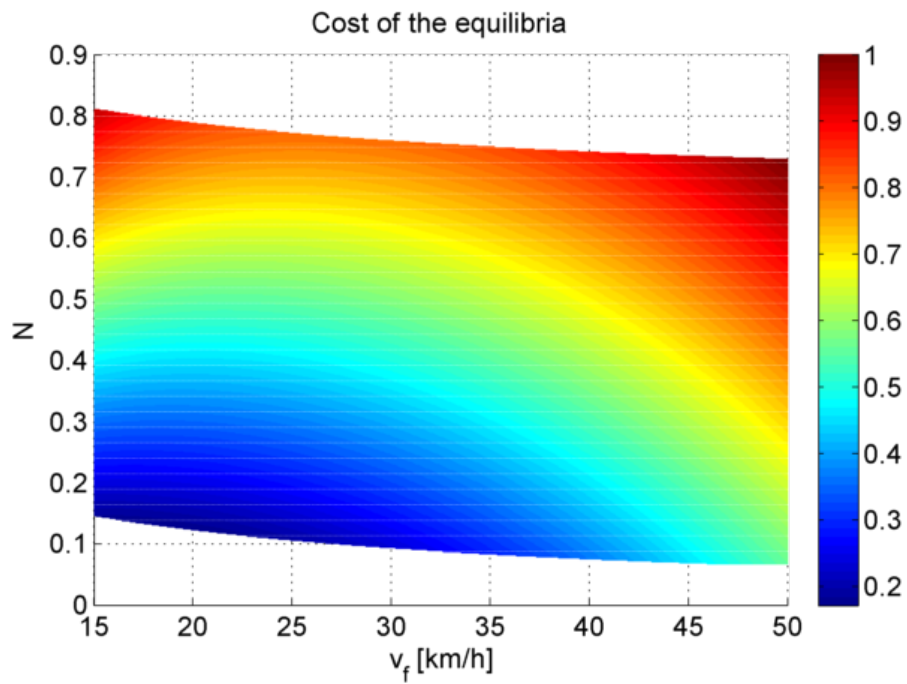
Figure 3.11 – Normalized cost of all the feasible equilibrium points as a function of the control input v_f and the normalized number of vehicles N.
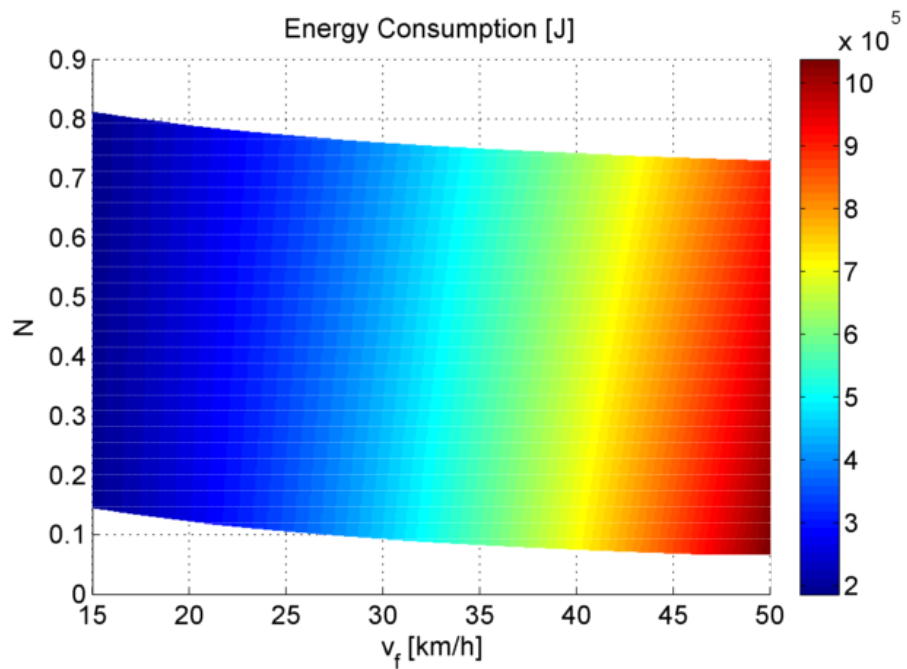
Figure 3.12 – Energy consumption variation as a function of the control input v_f and the normalized number of vehicles N.
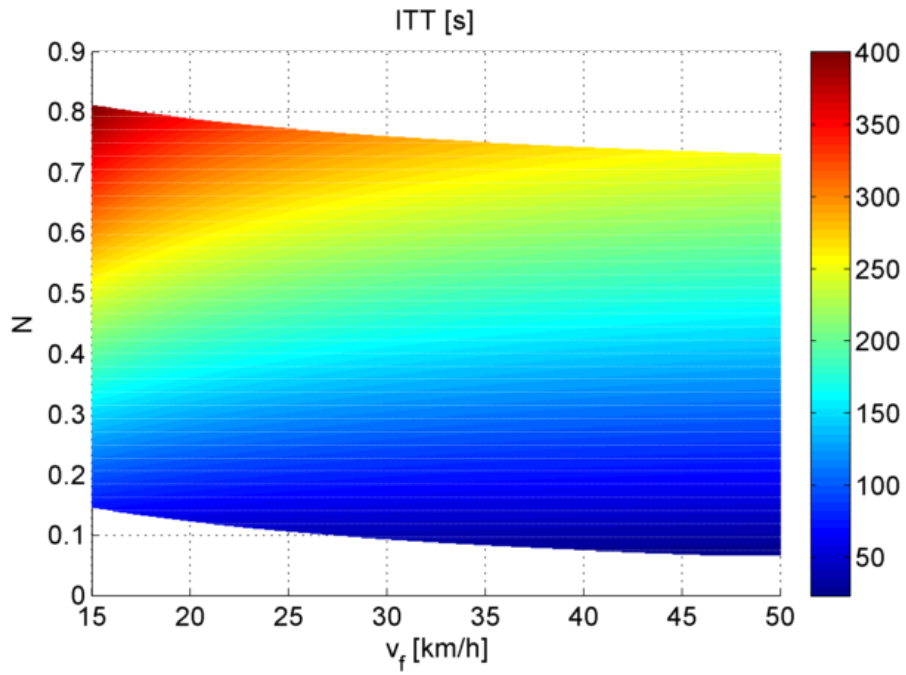
Figure 3.13 – ITT variation as a function of the control input v_f and the normalized number of vehicles N.
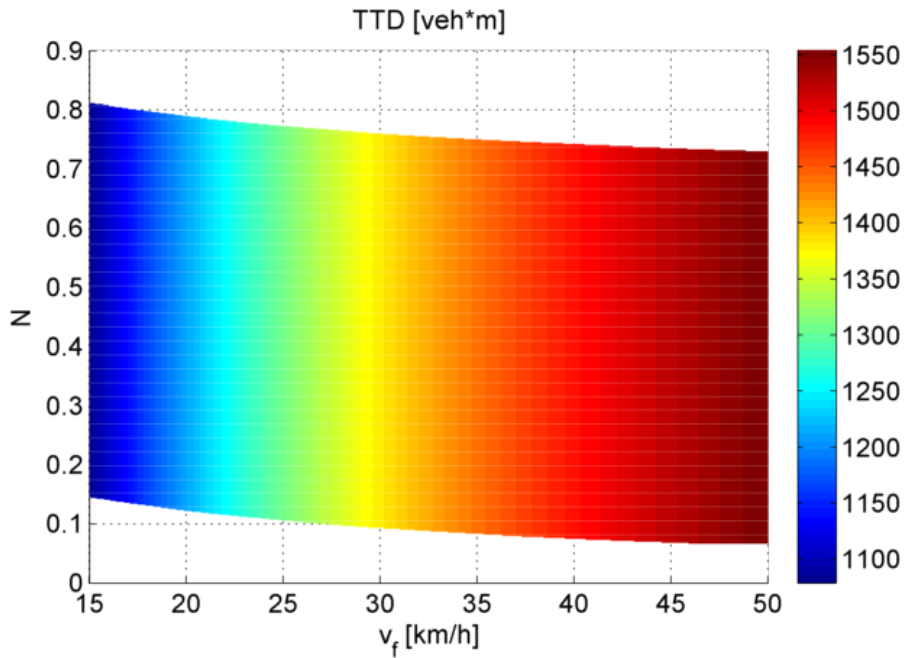
Figure 3.14 – TTD variation as a function of the control input v_f and the normalized number of vehicles N.
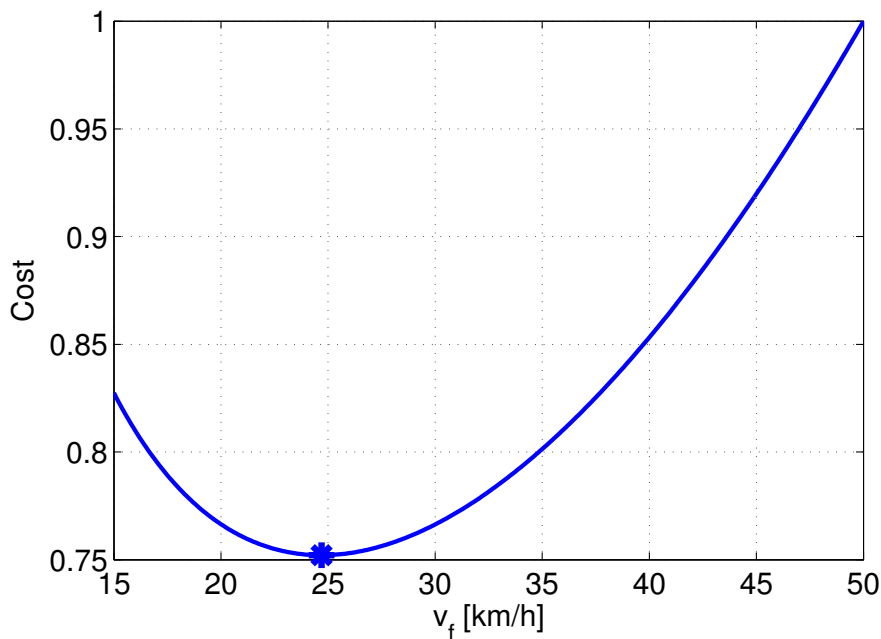
Figure 3.15 – Normalized cost variation as a function of the control input v_f for a given normalized number of vehicles $N = 0.7$ (i.e. 70% of the jam density).

the equilibria is given in Figure 3.11, which gives an insight into the expensiveness in terms of traffic performance of the possible traffic conditions. It is possible to observe that the lowest overall cost is given by traffic conditions in the section with low number of vehicles and low speed limit. A low speed limit in the presence of few vehicles reduces the traffic energy consumption also by reducing and almost eliminating the queue at the downstream traffic light, without deteriorating much the travel time. On the contrary, the worst performance is intuitively obtained for very saturated traffic conditions, almost regardless of the applied speed limit.

A separate analysis of the traffic performance metrics used in the cost function is shown in Figure 3.12, Figure 3.13, and Figure 3.14. The energy consumption decreases monotonically as the speed limit in the cell decreases, and it decreases at a faster rate for a higher number of vehicles. The ITT intuitively is highest for a low speed limit and a high number of vehicles, and it results more sensitive to a reduction of the number of vehicles than to an increase of the speed limit. The TTD, being a measure of the effective utilization of the infrastructure, is maximized for a high speed limit, and at steady-state is independent from the number of vehicles. All these experiments were run using the macroscopic parameters reported in Table 3.1, and the number of vehicles normalized with respect to the maximum number of vehicles that can be stored in the section at jam density can be seen as a rate of congestion.

Let us consider now a specific example, in which the number of vehicles in the section was selected to be 70% of the full occupancy. Given this number of vehicles, which remains constant due to the equality of the boundary flows, it is possible to solve Problem 2 and find an optimal v_f^* that minimizes the cost function. As shown in Figure 3.15, the optimal velocity for the choice of $N = 0.7$ is $v_f^* = 24.7$ km/h. The experiment demonstrates that by imposing the optimal speed limit in the section the overall performance is improved by about 25% with respect to the case of the standard speed limit of 50 km/h, and by about 10% with respect to the speed limit of 15 km/h.

Note that the choice of the weighting factors reported in Table 3.1 was made in order to achieve a substantial reduction in the traffic energy consumption. However the weighting factor assigned to the ITT is the highest, because trivial solutions of minimum energy consumption with too low speed limits are not desirable. A Pareto analysis of the multi-objective optimization could be conducted at this point to assist in the choice of the weighting factors.

Table 3.1 – Macroscopic parameters

Parameter	Description	Value	Unit
L	section length	300	m
w	congestion propagation speed	21.6	km/h
ρ_m	jam density	133	veh/km
$v_{\max}$	maximum velocity	50	km/h
$v_{\min}$	minimum velocity	15	km/h
$\bar{\alpha}$	traffic light split ratio	1/3	
$a_{\max}$	max acceleration	3	m/s^2
Δk	discretization step	1	s
σ_1	energy consumption weighting factor	1	
σ_2	ITT weighting factor	1.2	
σ_3	TTD weighting factor	0.2	

3.7 Control Design

The control system has been designed for the case of equal boundary flows. Since the system is asymptotically stable, a controller would not serve stabilization purposes, but, in absence of external disturbances, it would speed up the convergence of the system to the calculated optimal equilibrium point. The con-

trol action may be seen as the compliant drivers' response to the optimal speed advisory.

Given the linear system described by the matrices (3.60), a Linear Quadratic Regulator (LQR) is designed to track the optimal equilibrium $(x^*, u^*) = (\rho_f^*, \rho_c^*, v_f^*)$. The control law is of the form:

$$u = u^* - K(x - x^*) \tag{3.81}$$

where $\tilde{u} = -K\hat{x} = -K(x - x^*)$, and the gain K is obtained through the Linear Quadratic (LQ) design.

For the choice of the weighting matrices Q and R in the objective function of the LQR design, a specific characteristic of the eigenvalues of the reduced linear system was utilized. The real part of the eigenvalues of the linearized system becomes more or less negative depending on the initial conditions and the choice of the parameter N. In particular, roughly speaking, if N is high, the mode associated to ρ_f is more stable than the one of ρ_c, and viceversa.

Therefore, in the design of the weighting matrices Q and R of the LQ tracker, a sort of gain scheduling approach has been put in place, in order to weight more the less stable mode:

$$Q = \begin{bmatrix} 2000(1 - \frac{N}{\rho_m L}) & 0 \\ 0 & 2000\frac{N}{\rho_m L} \end{bmatrix} \tag{3.82}$$
$$R = 0.00005$$

3.8 Experiments

The simulation scenario under analysis presents one road section of length L with two traffic lights at the two ends regulating the inflow and outflow. The traffic lights are modeled by the continuous variable $\bar{\alpha}$. The section is divided into two cells according to the model dynamics, and one macroscopic fundamental diagram is defined by the parameters w, ρ_m and the control input v_f. Two sets of simulations, with the controller applied to the general system (3.27), aim at showing the effectiveness of the feedback control both in the case of equal boundary flows and in the case of varying upstream demand.

3.8.1 Equal Boundary Flows

The first simulation set is conducted with the traffic lights at the two ends of the section being equally timed. Under this assumptions, model (3.55) holds. The optimal velocity v_f^* is calculated based on the initial conditions, corresponding to an initial number of vehicles $N_0 = N = 25$. Here the feedback controller is
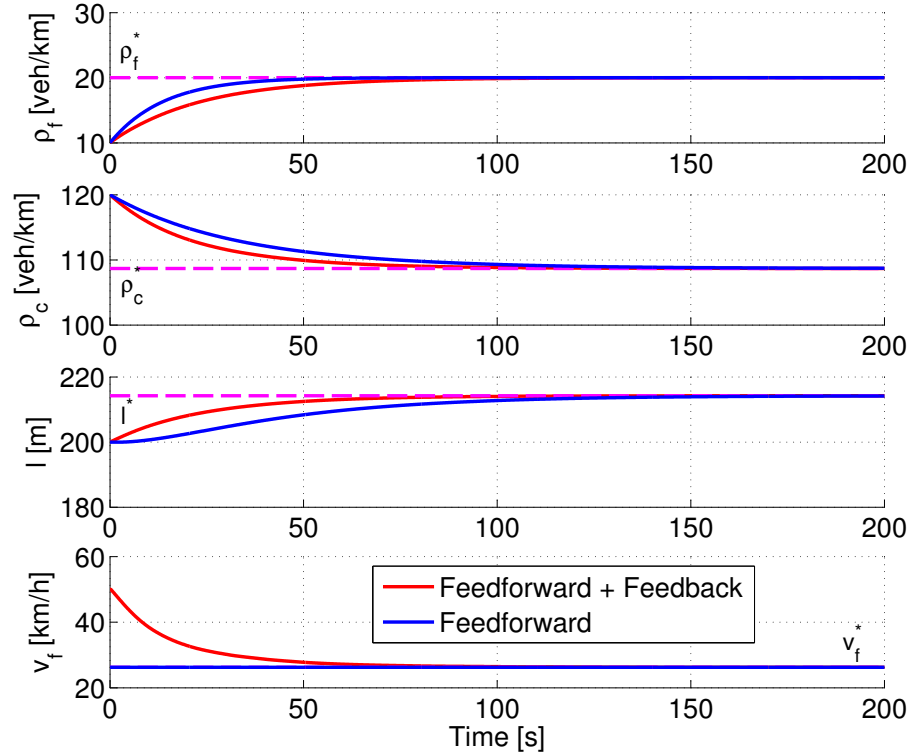
Figure 3.16 – Equal boundary flows - State dynamics of the nonlinear system and control input with and without LQ feedback control action.

able to drive faster the system to the optimal equilibrium $(\rho_f^*, \rho_c^*, l^*, v_f^*)$, as shown in Figure 3.16. In particular the length of the congestion settles at the equilibrium in a much shorter time: the rise time (i.e. 10-90% of the rising front) with the feedback control is 51.4 seconds, as opposed to 85.8 seconds with the only feedforward action, meaning a reduction of 40%. At steady-state there are no differences between the two responses of the system and, evidently, the performance metrics on a cycle time of the traffic lights at the equilibrium would give the same value. The transient of the system, however, has been improved and the feedback action helps to give an insight into the desired response of the compliant drivers to the speed advisory.

3.8.2 Varying Upstream Demand

In the case of a varying demand, the assumption on the time invariance of the number of vehicles does not hold, and system (3.55) is not sufficient anymore to

describe the state dynamics. Unbalance of the boundary flows will lead eventually the system to converge to a fully-congested or a fully-free state. The LQ feedback controller will still be tested on system (3.27).

The previous analysis on the optimality of the feasible and stable equilibrium points cannot be applied directly to this case, due to the lack of analytic expressions fully describing the equilibrium $(\rho_f^*, \rho_c^*, l^*)$. However, although nothing can be stated about the convergence value of l^*, the densities preserve a well defined equilibrium, as reported in (3.61), and can hence be used for feedback.

The split ratios $\bar{\alpha}_{1,2}$ modeling the two traffic lights still represent the time average of the flow enabled over a cycle, but this average value can slowly vary over time, simulating a variation in the traffic lights timing. Provided that no optimality is guaranteed in this scenario, the control strategy could be adapted to the case of time varying boundary flows by Algorithm 2.

Algorithm 2 Control strategy

1: v_f^* is computed based on N_0;
2: ρ_f^* and ρ_c^* are computed based on v_f^* and $\bar{\alpha}_{1,2}(0)$;
3: the system is linearized at the equilibrium and the gain K is obtained through the LQ design;
4: $v_f = v_f^* - K[(\rho_f - \rho_f^*), (\rho_c - \rho_c^*)]^T$
5: **while** $t \leq T_{\text{final}}$ **do**
6:     **if** $\text{rem}(t, T_{\text{cs}}) = 0$ **then**
7:         v_f^* is updated, based on $N(t)$;
8:         ρ_f^* and ρ_c^* are updated based on v_f^* and $\bar{\alpha}_{1,2}(t)$;
9:         $v_f = v_f^* - K[(\rho_f - \rho_f^*), (\rho_c - \rho_c^*)]^T$;
10:     **end if**
11: **end while**

At time $t = 0$, the reference velocity v_f^* and the associated equilibrium densities (ρ_f^*, ρ_c^*) are computed as in the case of equal boundary flows, assuming that there will be no variation of N. This will be the initial reference to be tracked by the controller, and an update will occur every T_{cs} seconds. The parameter T_{cs} represents the update rate for the speed advisory; in the following the speed advisory will be provided every 10 seconds.

As shown in Figure 3.17, simulations proved that this control strategy is beneficial in the case of varying upstream demand and the feedback action is able to provide performance improvement as compared to both the simpler feedforward controller $v_f = v_f^*$, and the case of a standard city speed limit of 50 km/h. The
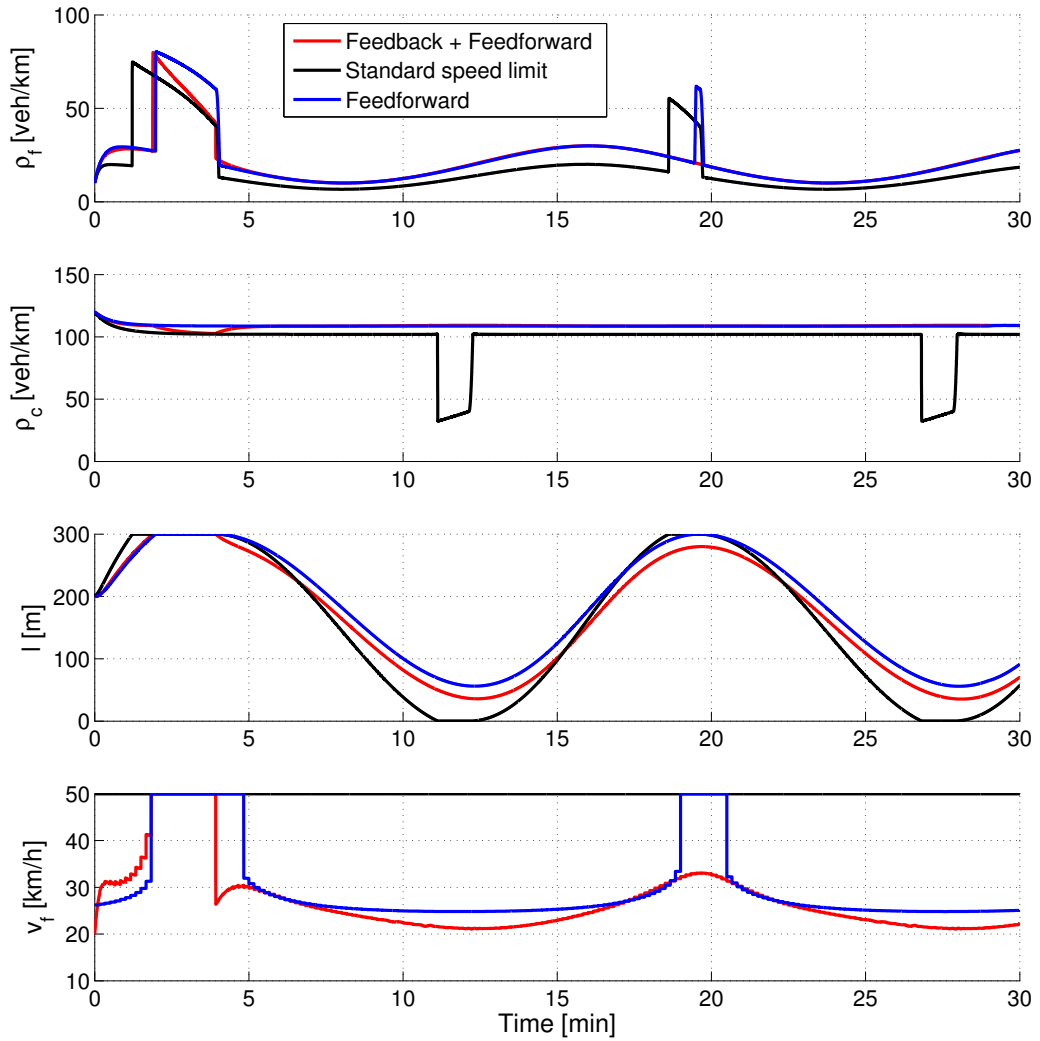
Figure 3.17 – Varying upstream demand - The proposed control strategy (in red) is compared to the simpler feedforward controller $v_f = v_f^*$ (in blue), and to the standard case with the maximum speed limit $v_f = 50$ km/h (in black).

test was conducted with the following values of $\bar{\alpha}_{1,2}$:

$$\bar{\alpha}_1 = \bar{\alpha}_2 + \frac{1}{6}\cos(t/150)$$
$$\bar{\alpha}_2 = \frac{1}{3}$$

(3.83)

Starting from the chosen initial conditions, with $\bar{\alpha}_1$ initially higher than $\bar{\alpha}_2$, the section quickly saturates in all scenarios. Saturation occurs earlier in the standard-speed-limit case, due to the constant higher speed $v_f = 50$ km/h. However at saturation, the feedback controller tries to reduce the density in the whole section and to approach the reference equilibrium by increasing the speed and letting vehicles out of the section at the maximum allowed flow. When the inflow becomes smaller than the outflow ($\bar{\alpha}_1 < \bar{\alpha}_2$), the proposed feedback control strategy manages to leave the fully-congested state before the other scenarios, and the reference v_f^* varies with N. Throughout the simulation, it is evident that the feedback controller is able to relieve the congestion much more effectively than the other two speed-limit policies, in particular at $t \simeq 20$ minutes saturation is completely avoided.

The performance evaluation here is carried out over the entire simulation time and by calculating the value of the following cost functional:

$$J = \sigma_1 E + \sigma_2 \text{ITT} - \sigma_3 \text{TTD} + \sigma_4 \text{TTS}$$

(3.84)

The cost function has been slightly modified with respect to the one previously introduced, because in this scenario the number of vehicles is time-varying, and the TTS is an important metric to be taken into account. The detailed results for each performance metric are reported in the following:

Table 3.2 – Metrics evaluation

	E	ITT	TTD	TTS
Proposed control strategy vs. Standard speed limit	-40%	+44%	-23%	+14%
Proposed control strategy vs. Feedforward	-3%	-8%	-2%	-7%

The proposed control strategy outperforms the standard speed limit in the energy consumption but loses performance in the other three metrics. As compared to the feedforward control $v_f = v_f^*$, the proposed strategy improves the performance in all the metrics, except a small loss in the TTD.

In order to evaluate the overall cost, the choice of the new weights is $(\sigma_1, \sigma_2, \sigma_3, \sigma_4) = (1, 0.6, 0.2, 0.6)$, after normalization of the terms of the cost functional.

Clearly the choice of the weighting factors influences the trade-off and the overall performance gain. However, even with the current choice of weights which gives more importance to the travel time metrics together than to the energy consumption, the proposed control strategy enables remarkable improvements. The details of the individual performance metrics comparison is reported in Table 3.2. The proposed control strategy achieves an overall cost improvement of 14% with respect to the standard speed limit case, and an improvement of 6% with respect to the feedforward control.

3.9   Microscopic Analysis and Validation

In order to evaluate the reliability of the proposed macroscopic model and the macroscopic traffic performance metrics, a microscopic traffic simulator was employed for validation purposes. In particular, the traffic simulator Aimsun has been calibrated to reproduce the macroscopic fundamental diagram used in the urban VLM. Once the calibration is completed, the proposed macroscopic model is expected to exhibit a behavior equivalent to the microscopic simulator. The process of setting up the microscopic simulator involves the following steps:

- calibration of the parameters in Aimsun to reproduce the macroscopic fundamental diagram used in the VLM;
- comparison of the state evolution of the macroscopic and the microscopic model;
- comparison of the macroscopic and microscopic traffic performance metrics.

3.9.1   Aimsun Calibration

The objective of Aimsun calibration is to replicate the same parameters of the fundamental diagram used for the macroscopic model. In particular, Aimsun is desired to execute traffic simulation obeying the parameters reported in Table 3.1.

In order to reproduce the same jam density ρ_m, in Aimsun the parameters affecting the length of the vehicles and the minimum vehicles interdistance need to be regulated. Therefore, the selected jam density $\rho_m = 133$ veh/km is obtained by setting, for instance, the vehicle length equal to 4 meters and the minimum interdistance equal to 3.5 meters.

The other key parameter in Aimsun that influences the maximum flow $\varphi_{\max}$, and consequently the back propagation speed of the congestion w, is the reaction time. Intuitively, the smaller the reaction time (i.e. more reactive drivers), the higher the maximum flow. In order to reproduce the w reported in Table 3.1, the

Table 3.3 – Aimsun parameters

Parameter	Description	Value	Unit
	reaction time	0.5	s
	vehicle length	4	m
	minimum vehicle interdistance	3.5	m
L	section length	300	m
w	congestion propagation speed	21.6	km/h
ρ_m	jam density	133	veh/km
$v_{\max}$	maximum velocity	50	km/h
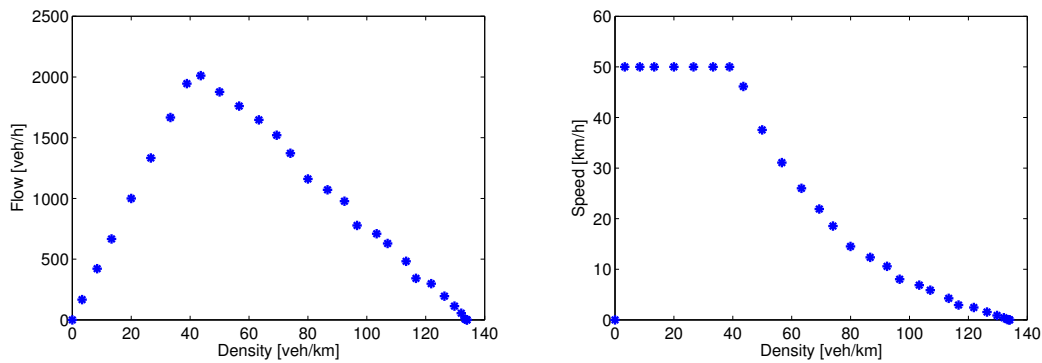
Figure 3.18 – Underlying macroscopic fundamental diagram in Aimsun.

reaction time of the vehicles in Aimsun is set to 0.5 seconds, and the minimum inter-vehicle time is set to 1.2 seconds.

A simple simulation in Aimsun was set up to verify that the underlying macroscopic fundamental diagram is comparable to the one specified in Table 3.1. Such calibration-oriented simulation in Aimsun aims at exciting the system in all the operation points described by the fundamental diagram. In particular, the simulation reproduces free-flow traffic conditions, fully-jammed traffic conditions, and back-propagation of the congestion. As shown in Figure 3.18 and in Table 3.3, the underlying fundamental diagram in Aimsun, with the chosen microscopic parameters, results to be comparable to the fundamental diagram used for the proposed macroscopic model.

3.9.2 State Variables Evolution

After the illustrated calibration process, a fair comparison of the VLM and the microscopic simulator requires the knowledge of the state variables evolution
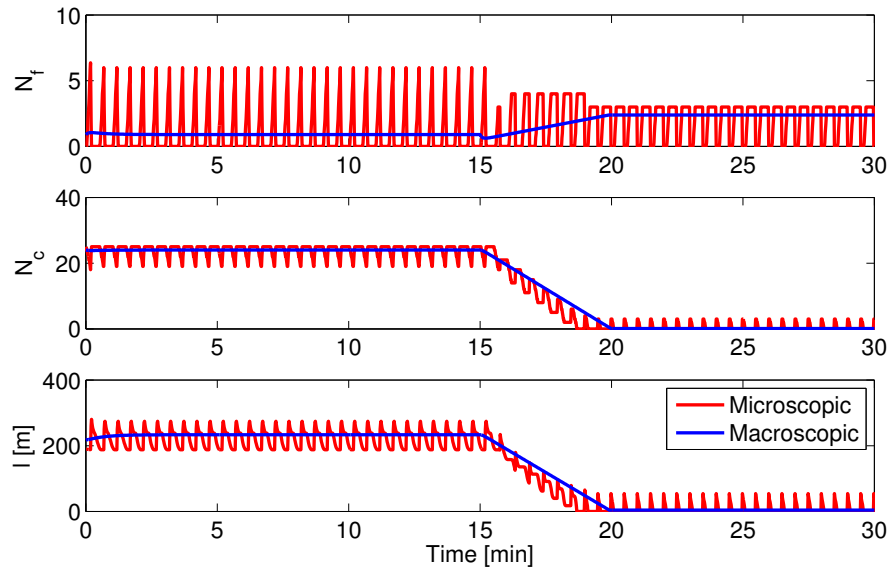
Figure 3.19 – State evolution comparison between the VLM and Aimsun.

of both systems. The macroscopic state variables of the VLM (ρ_f, ρ_c, l) are not directly accessible in Aimsun, therefore a method needs to be devised to get information from Aimsun about the length of the congestion, and about the densities in the free and the congested cell.

An algorithm to detect the length of the congested cell in the road section simulated in Aimsun has been proposed (see Appendix A). The microscopic information required by the algorithm is the position, speed and acceleration of the vehicles in the section. When a vehicle in the microscopic simulator has a negative acceleration and a speed lower than the speed limit, it is flagged as a candidate last-of-the-queue vehicle. The gap between the flagged vehicle and the last verified last-of-the-queue vehicle is checked to be smaller than the nominal gap. The nominal gap is defined as the safety interdistance that the vehicles have to keep, and it is a function of the maximum speed limit and the drivers' reaction time. A vehicle entering the congestion starts to decelerate and keeps a distance from the preceding vehicle lower than the nominal one. Among the flagged vehicles, the most upstream one is marked as the front of the congestion. Once the length of the congested cell is calculated, the number of vehicles downstream and upstream from the congestion front is derived.

An experiment was conducted both numerically with the VLM and in Aimsun to verify that the two models show a similar state evolution given certain initial conditions, as well as a similar response to a variation of the boundary flows. The results are shown in Figure 3.19 and Figure 3.20. In Aimsun the periodic nature of the traffic lights has an impact on the alternating behavior of the state
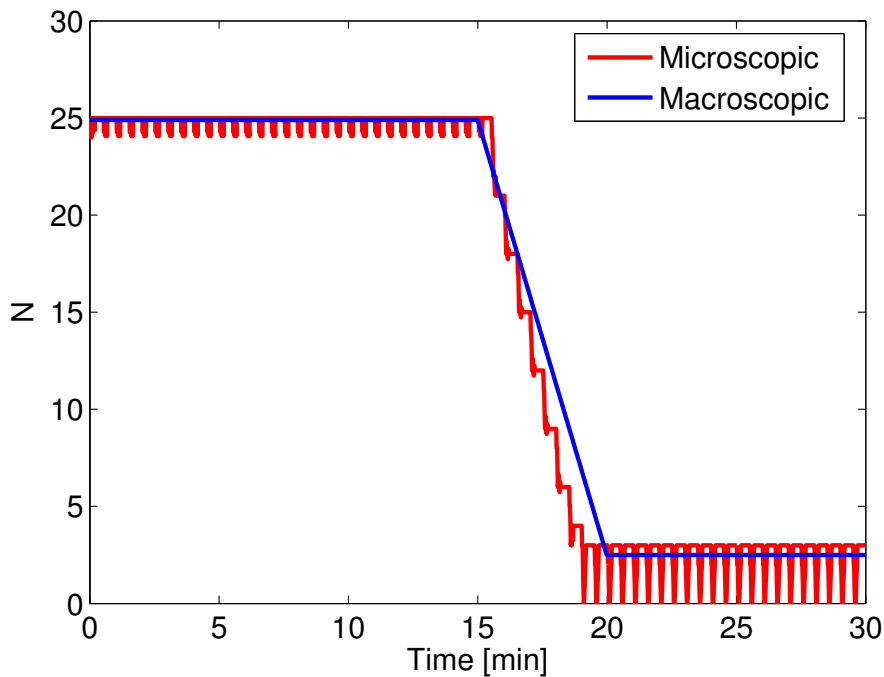
Figure 3.20 – Number of vehicles evolution comparison between the VLM and Aimsun.

evolution. On the contrary, that effect is averaged in the VLM proposed in this work. Nevertheless, the macroscopic model proves to be reliable in representing the average behavior of the true system, which here is assumed to be Aimsun. In particular, in the first half of the simulation the boundary flows are set to be equal and both models reach the equilibrium associated with the initial conditions. At $t = 15$ minutes, the upstream traffic light is set to have a smaller split ratio than the one downstream, therefore the section starts to empty, the number of vehicles in the congested cell decreases, the number of vehicles in the free cell increases, and the phenomenon is well depicted by both models. The total number of vehicles evolution is also closely comparable between the two models.

3.9.3 Traffic Performance Metrics

The traffic performance metrics have been defined and adapted to the proposed macroscopic model. For a meaningful validation and comparison between the macroscopic and the microscopic performance, the metrics need to be adapted also to the microscopic framework. The analysis and the comparison of the performance is carried out at steady-state over a traffic light cycle.

The ITT is calculated as the average travel time of the vehicles in the section
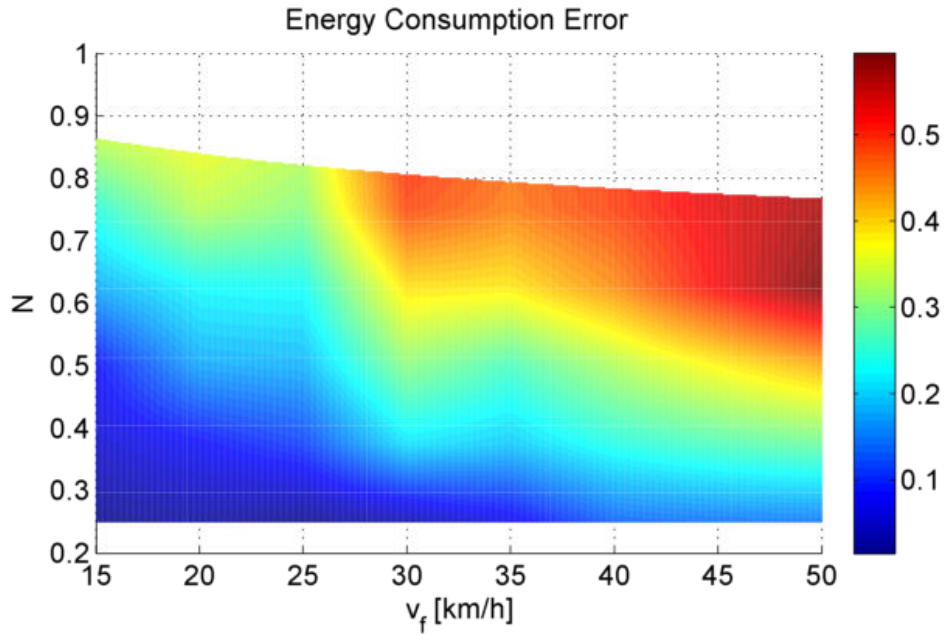
Figure 3.21 – Difference between the microscopic evaluation of the energy consumption and the macroscopic consumption model. The error is normalized with respect to the maximum value of the microscopic energy consumption.

at steady-state. In particular, only the vehicles that complete the trip in the section contribute to the average ITT.

The TTS is calculated using the microscopic time information of each vehicle traveling in the section. Therefore the calculation is carried out by simply summing the time spent by each vehicle in the section during the time horizon T. Thus, if during the simulation time T a total number N of vehicles passes through the section, the TTS in Aimsun can be computed as follows:

$$\text{TTS} = \sum_{i=1}^{N} \text{TTS}_i \tag{3.85}$$

where TTS_i is the time spent in the section by vehicle i. Note that at steady-state the TTS does not vary over time, and it will not be considered in the following comparison.

The TTD is calculated by taking into account the distance covered by each vehicle in the section, also considering the vehicles that do not complete the trip within the cycle time.

Finally, in the microscopic simulation, the calculation of the energy consumption is carried out without the simplifications adopted at macroscopic level. Information about acceleration and speed of each vehicle is directly accessible, and
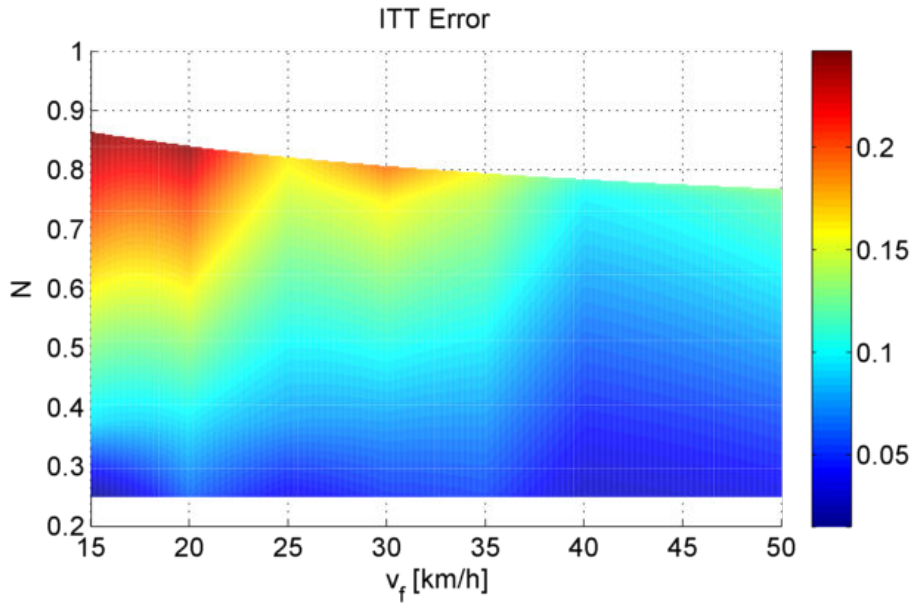
Figure 3.22 – Difference between the microscopic and the macroscopic evaluation of the average travel time. The error is normalized with respect to the maximum value of the macroscopic ITT.

the energy consumption can be calculated with a standard integration over time of the instantaneous power demand. The analysis is conducted in the case of equal boundary flows, therefore at steady-state over a traffic light cycle. So the energy consumption can be calculated as:

$$\sum_{i=1}^{N} \int_{t}^{t+T_{\text{cycle}}} P_i \, d\tau = \sum_{i=1}^{N} \int_{t}^{t+T_{\text{cycle}}} b_1 u_i v_i + b_2 u_i^2 \, d\tau \tag{3.86}$$

where v_i is available for each vehicle at each time step, and u_i is given by:

$$u_i = \frac{1}{h_1}(a + h_2 v_i^2 + h_3 v_i + h_0) \tag{3.87}$$

assuming that $\dot{v} = a$. If the microscopic control input u (i.e. torque) is negative, the expression for the power demand is modified by taking into account only the electric losses. In other words, braking regenerative effects are neglected in this analysis.

In Figure 3.21, the difference between the microscopic energy consumption over a traffic light cycle calculated in Aimsun and the macroscopic energy consumption calculated with the model presented in this work is shown. The error
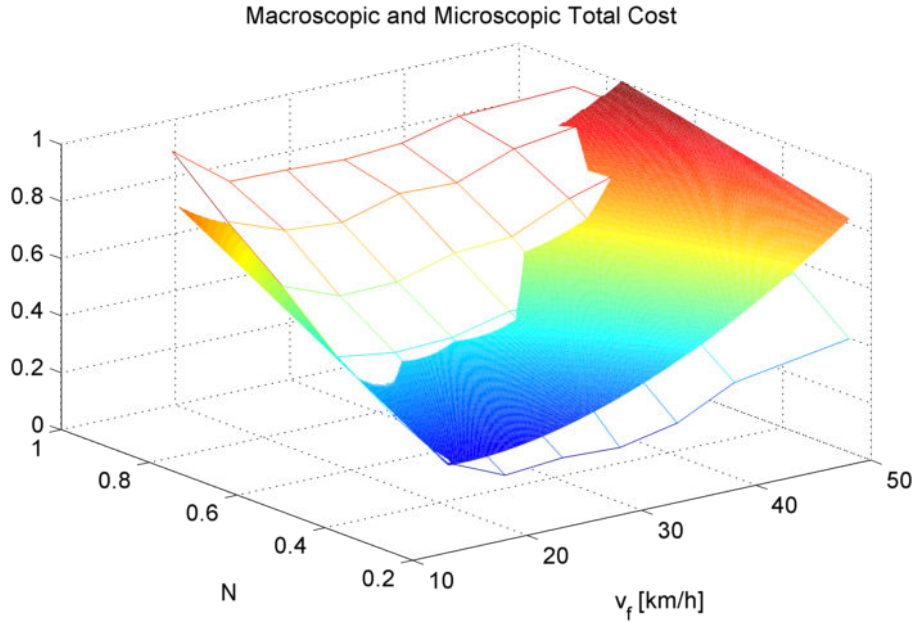
Figure 3.23 – Microscopic and macroscopic evaluation of the overall cost function. The two costs are normalized with respect to their respective maximum value. The surface with fewer data points corresponds to the microscopic cost function calculated in Aimsun.
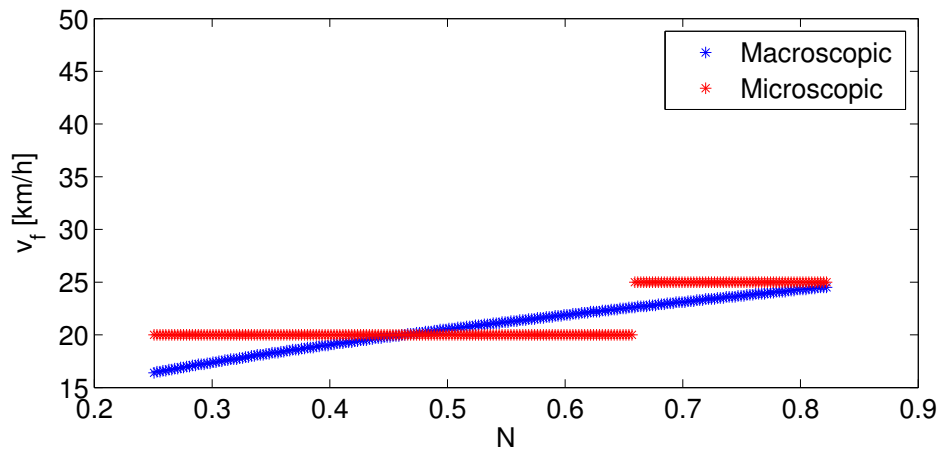
Figure 3.24 – Optimal speed limits as a function of the number of vehicles in the section for both the macroscopic and microscopic case.

is normalized with respect to the maximum value of the microscopic energy consumption, which is assumed to be the true reference. From a quantitative point of view, the macroscopic energy consumption model systematically underestimates the true consumption. The largest error is for high values of the speed limit and high number of vehicles in the section, since the macroscopic energy consumption model neglects the temporal accelerations, as well as all the stops and departures of the vehicles queuing in the congested cell. On the contrary, this phenomenon is well represented by the microscopic simulator and consequently the energy consumption is high due to the higher number of accelerations in the queue. Furthermore, note that the reaction time parameter in Aimsun might induce a slower depletion of the queue as compared to the macroscopic model (e.g. slower drivers' reaction to a green traffic light), causing additional accelerations. However, from a qualitative point of view, both energy consumption models show a decreasing behavior towards low speed limits and low number of vehicles.

As for the average travel time of the vehicles in the section, in Figure 3.22, the macroscopic model yields a closer approximation of the microscopic travel time. The error is at most 20% for low speed limits and high number of vehicles, but in general the macroscopic computation of the average travel time only slightly overestimates the true travel time. Qualitatively, the two travel time functions show the same decreasing behavior towards high speeds and low number of vehicles.

In order to compare the overall cost function defined in Problem 2 for both macroscopic and microscopic metrics, its evaluation is reported in Figure 3.23. Evidently, the two cost functions exhibit similar convexity properties, and the minima are expected to be closely located, as shown in Fig 3.24.

3.10 Conclusions

In this chapter a new version of the Variable Length Model, adapted to the urban framework and regulation via variable speed limits, has been employed to simulate traffic flow evolution. Macroscopic traffic performance metrics have been defined to assess the behavior of the system at steady-state, and it has been shown that there exists an optimal velocity v_f^* that minimizes the total objective function, resulting in a trade-off between energy consumption reduction and penalization of ITT and TTD.

The steady-state analysis of the Urban Variable Length Model has been extended with a thorough presentation of the existence and stability properties of the equilibrium points. Controllability of the nonlinear system has been discussed, stability of the reduced-state model for the equal boundary flows case has been studied, and an LQ feedback controller was designed on the linearized system. The controller was tested in simulation initially in a scenario with equal boundary

flows to assess its capability of driving the system to the desired optimal equilibrium. Then a control algorithm was proposed to respond to a varying upstream demand. The feedback controller was able to track the varying reference states, also improving the overall performance as compared to the standard city speed limit of 50 km/h and the feedforward control action $v_f = v_f^*$.

Future developments could take into account the split ratio $\bar{\alpha}$ as an additional degree of freedom to reach desired operation points at steady-state. The macroscopic energy consumption model could be improved by taking into account also temporal accelerations besides spatial ones. Moreover, it is important to look at the effects of concatenation of successive sections on the selection of the optimal speed limit, also in presence of fluctuations in the inflow. The strategy should be robust to variations in the upstream demand, by limiting the excessive inflow via variable speed limits and a feedback control action would be desirable in order to increase the responsiveness of the system.

Chapter 4

Arterial Control via Signal Offsets and Variable Speed Limits

4.1 Introduction

Benefits of traffic light coordination on traffic relief is undeniable. Well coordinated traffic lights can reduce travel times, delays, and unnecessary stops. As a consequence, they improve mobility and access, reduce driver frustration, and energy and fuel consumption. Beneficial effects may be observed also in reduced rerouting through nearby neighborhoods, fewer accidents, improved emergency service, and pollution.

Many traffic-signals optimization algorithms aim to reduce the total length of the queues in the monitored network area, and consequently reduce delays. Though delay reduction and minimization of stops are considered as important performance targets, maximization of progression bands (i.e. the green interval that allows uninterrupted traffic flow along the entire arterial [9]) is still considered essential by many practitioners. For this reason, some algorithms (e.g. TRANSYT-7F) also incorporate progression measures.

The size of the progression band enabled by a sequence of signalized intersections is known as the bandwidth. Maximizing the bandwidth of a signalized arterial corresponds to maximizing the time during which vehicles can drive the entire length of the arterial without stopping. Bandwidth-based signal timings are generally preferred because they meet driver expectations [126].

The first mathematical formulation of the bandwidth maximization problem was given by Morgan and Little in [96]. The nature of the problem was combinatorial and it addressed a simplified two-stage version, thus neglecting more complex phases. An extension of this first work was published by Little in [86], where the problem was formulated for the first time as a mixed-integer linear pro-

gram (MILP).

This pioneering work evolved into the MAXBAND software [87], which offered as main features the possibility to choose cycle times and select offsets to maximize bandwidth in the two directions of travel, as well as the possibility to deal with triangular networks (i.e. a three-artery triangular loop) and more complex turning phases at the intersections. MAXBAND gave rise to several research efforts and extensions, first in order to solve triangular networks (MAXBAND-86) [22], and then to allow different bandwidths for each segment of a single arterial (MULTIBAND) [47] or a network of arterials (MULTIBAND-96) [122, 48]. Recent research has combined link-based and arterial-based techniques [139], as well as introduced network partitioning algorithms in order to deal with larger networks [126]. The assumption of under-saturated traffic (i.e. all queues at the traffic lights are dissipated within the cycle time) has been relaxed in [82, 131].

All of the mentioned works and software packages for bandwidth maximization are based on the original MILP formulation of [86]. However results provided in [56] show that the arterial bandwidth maximization problem can also be cast as a linear program (LP) without the need for integer variables. This result is based on the observation that the integer unknowns are closely related to the inter-signal travel times, and can therefore be computed a priori. This idea is captured in the use of "relative offsets", measured with respect to a moving coordinate frame, instead of absolute offsets.

In the original formulation of the arterial bandwidth maximization by Little [86] and the MAXBAND software package [87], the speed in the segments of the two-way arterial was allowed to vary as an additional decision variable of the MILP to further improve the progression bands. However both in the software implementation and testing of MAXBAND, the potential benefits induced by the variable speed limits (VSL) on actual traffic performance were never assessed. Only recently microscopic traffic simulators are used to assess the benefits of bandwidth maximization on traffic performance. In [9] the maximization of bandwidth is achieved with both lights and speeds control and the performance is evaluated in terms of delay and travel time for small arterials with three intersections. The impact of the VSL on the energy consumption and other performance metrics was not considered.

A general and often misleading assumption made by drivers is that an increase in speed will lead to a proportionate decrease in travel time. However, travel time is more dependent on congestion and roadway design and geometry factors than on the posted speed limits. [8] has pointed out that at traffic density levels where a flow can be maintained, it is theoretically possible that lower speed limits could actually bring about a reduction in overall travel time. Reduced speed limits are likely to have their greatest safety impact at low to medium levels of traffic density where traffic is periodically able to travel at or near the speed limit. We will also

show in this paper that a lower average speed limit may translate into a similar or lower average travel time, while drastically reducing the environmental impact.

In this work, the two-way arterial bandwidth maximization problem is addressed with a particular focus on the benefits induced by the variable speed limits, and on reducing energy consumption. The present mathematical formulation, inspired by the idea in [56], allows to solve the one-way bandwidth maximization problem as an LP, even with segment speeds as decision variables. However, as we will see, the two-way problem with internal offsets constraints presents difficulties that make necessary the formulation of the problem as an MILP. The first contribution of the paper lies in the addition of terms representing traffic energy consumption and network travel time to the objective function of the two-way arterial bandwidth maximization. The variable speed limits, as additional control action, allow to reach higher theoretical bandwidths but might induce driving discomfort and higher energy consumption if the variability of the speeds between the segments is too high. Furthermore, optimal solutions with low speed limits and high travel time are to be avoided, in trade-off with the energy consumption. The second contribution of the paper is given by the extensive evaluation of the benefits of bandwidth maximization via a microscopic traffic simulator. Bandwidth is a theoretical quantity and a correlation with known traffic performance metrics needs to be established in order to justify its use. The combined control of offsets and speed limits is shown to have a large impact on energy consumption without affecting the travel time. Lastly, a simulation analysis of the traffic performance at different levels of traffic demands has been conducted, testing both under-saturated traffic conditions with the existence of a green wave, and saturated conditions. The goals of this analysis are to identify the best operation conditions of the presented approach, to assess the performance degradation with traffic load, and, most importantly, to propose a demand-dependent optimization. Different strategies were compared to the presented one in order to assess its performance.

In the following we will first describe the problem and the used notation. Then we will provide the mathematical formulation of the optimization problem. Finally, we will define the simulation setup, and we will show the conducted experiments and the obtained results.

4.2 Problem Setup

A two-way arterial with n signalized intersections is considered. The two opposing directions of travel are referred to as inbound and outbound. Intersections are located at $x_1 < x_2 < \ldots < x_n$, with the subscript index increasing in the outbound direction. All quantities related to the inbound direction are denoted with an overbar. The travel speeds in the $n-1$ segments are assumed to be equal to the
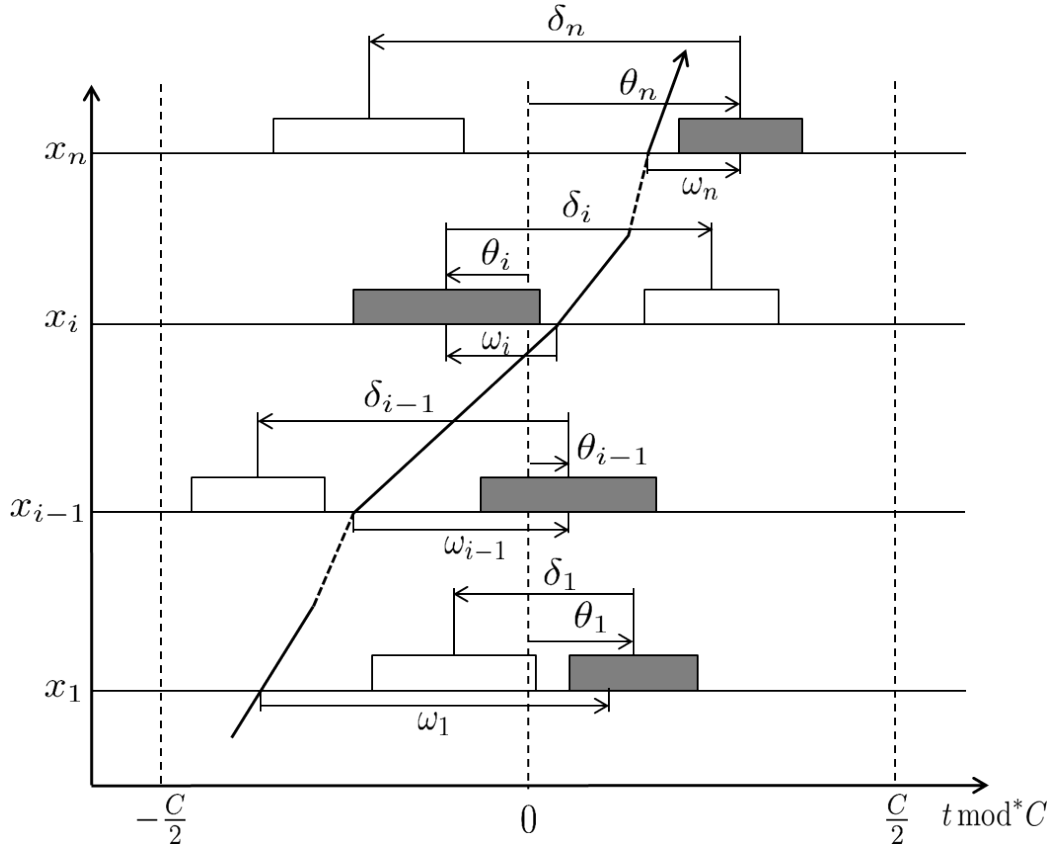
Figure 4.1 – Problem notation. Green windows of the outbound direction of travel are shaded. Green windows in the inbound direction are in white. The travel speed trajectory and the basic notation is indicated only for the outbound direction for clarity.

imposed speed limits, and denoted as v_i and $\bar{v}_i$.

The outbound and inbound travel times on segment i are,

$$t_i = \frac{x_{i+1} - x_i}{v_i} > 0, \quad i \in \{1, \dots, n-1\} \tag{4.1}$$

$$\bar{t}_i = \frac{\bar{x}_i - \bar{x}_{i+1}}{\bar{v}_i} < 0, \quad i \in \{1, \dots, n-1\} \tag{4.2}$$

with the segment length being $L_i = x_{i+1} - x_i$.

The n signals are to be coordinated with a common cycle time C, which is assumed throughout this paper to be given and fixed. All signals are also on a fixed schedule and they release vehicles in pulses that travel without diffusing. Denote with g_i and $\bar{g}_i$ the green times at intersection i in the outbound and inbound direction respectively.

The mapping of time from the real domain onto the interval $[-C/2, C/2]$ is performed with a non-standard modulo operator which will be denoted mod^* [56]. $t \, \text{mod}^* C$ returns the distance from t to the nearest integer multiple of C, with negative sign if the integer is to the right of t and positive sign if it is to the left of t. For example, $7 \, \text{mod}^* 5 = 2$, and $8 \, \text{mod}^* 5 = -2$.

The absolute offsets θ_i ($\bar{\theta}_i$) are defined as the displacement of the center of the green window of the outbound (inbound) direction at intersection i with respect to a fixed coordinate system (see Figure 4.1). The absolute offsets are in $[-C/2, C/2]$. The relative displacement of the centers of the inbound and outbound green windows is defined as,

$$\delta_i = (\bar{\theta}_i - \theta_i) \, \text{mod}^* C \tag{4.3}$$

In addition to the absolute offsets, the relative offsets ω_i and $\bar{\omega}_i$ are defined. These are measured with respect to the outbound and inbound moving coordinate frames which travel at speeds v_i and $\bar{v}_i$ respectively. The outbound relative offset ω_i is defined as the time between the passage of the outbound moving coordinate frame and the center of the nearest outbound green window. A corresponding definition applies to the inbound relative offset. The relative offsets are also in $[-C/2, C/2]$. Note that the moving frame does not stop at the red signals.

The conversion between absolute and relative offsets may be derived as follows:

$$(\omega_{i-1} - \theta_{i-1} + \theta_i - \omega_i - t_{i-1}) \, \text{mod}^* C = 0 \tag{4.4}$$

Therefore the following recursive formula for relative offsets applies:

$$\omega_i = (\omega_{i-1} - \theta_{i-1} + \theta_i - t_{i-1}) \, \text{mod}^* C \tag{4.5}$$

which eventually yields:

$$\omega_i = \left(\omega_1 - \theta_1 + \theta_i - \sum_{k=1}^{i-1} t_k \right) \text{mod}^* C \tag{4.6}$$

The inverse formula allows to determine the absolute offsets from the relative offsets:

$$\theta_i = \left(\theta_1 - \omega_1 + \omega_i + \sum_{k=1}^{i-1} t_k \right) \text{mod}^* C \tag{4.7}$$

These formulas apply with overbars for the inbound direction. Because the map between relative and absolute offsets is invertible, we are free to formulate the bandwidth maximization problem in terms of either set of unknowns.

Bandwidth is a theoretical quantity defined as the size of the time window in which vehicles can travel the length of the arterial without stopping. The outbound bandwidth is denoted with b, and the inbound bandwidth is denoted with $\bar{b}$.

4.3 Problem Formulation

The objective of this work is to solve the two-way bandwidth maximization problem, using both offset and VSL control. The degrees of freedom of the optimization will be the relative offsets ω_i and $\bar{\omega}_i$, and the travel times t_i and $\bar{t}_i$.

The two-way problem has been formulated in [56] as a continuous linear program, without use of integer variables, exploiting the a priori information about the speeds in each segment of the arterial network. Only the offsets were used as decision variables. This work extends the previous result by introducing the speeds in the different segments of the network as additional decision variables. It will be shown that a higher bandwidth is achieved thanks to VSL control. However, the objective of the current analysis is also to avoid impractical solutions, as well as to evaluate the actual benefits of the maximization of the theoretical bandwidth on traffic performance. In particular, the optimization will account for traffic energy consumption, travel time and driver comfort.

In order to express both b and $\bar{b}$ in terms of the relative offsets, the green windows are translated along the outbound and inbound coordinate frames to $x = x_1$. This operation induces a mapping from δ_i to δ_i^0 with $i \in \{1, \ldots, n\}$. The mapping is given by (see [56] for details):

$$\delta_i^0 = \left(\delta_i + \sum_{k=1}^{i-1} (t_k - \bar{t}_k) \right) \bmod{}^* C \tag{4.8}$$

with $\delta_i^0 \in [-C/2, C/2]$. The equality constraint that fixes the internal offset is given by:

$$\omega_i - \bar{\omega}_i = \delta_1^0 - \delta_i^0 \tag{4.9}$$

In vector notation:

$$\bar{\omega} = \omega - \delta \tag{4.10}$$

with $\omega \triangleq (\omega_1, \ldots, \omega_n)$ and $\delta \triangleq (\delta_1^0, \delta_1^0 - \delta_2^0, \ldots, \delta_1^0 - \delta_n^0)$.

4.3.1 Directional Interference Constraints

The progression band, in the case of fixed green times and no platoon dispersion, is equivalent to the intersection of all of the green intervals, measured with respect to the moving coordinate frame. Hence, as was demonstrated in [56], the bandwidth is the size of the intersection of the following set of intervals:

$$\{[\omega_i - g_i/2, \omega_i + g_i/2] : \ i \in \{1, \ldots, n\}\}$$

This leads to a simple expression for the outbound bandwidth:

$$b(\omega_1, \ldots, \omega_n) = \max(0, \min_{i,j \in \{1,\ldots,n\}} (\omega_i - \omega_j + g_{i,j})) \tag{4.11}$$

where $g_{i,j} \triangleq (g_i + g_j)/2$. Equation (4.11) is the solution to the following linear program:

$$
\begin{aligned}
\max \quad & b \\
\text{s.t.} \quad & b \leq g_{i,j} + \omega_i - \omega_j \\
& b \geq 0
\end{aligned}
$$

Similarly, the inbound bandwidth can be found with:

$$
\begin{aligned}
\max \quad & \bar{b} \\
\text{s.t.} \quad & \bar{b} \leq \bar{g}_{i,j} + \bar{\omega}_i - \bar{\omega}_j \\
& \bar{b} \geq 0
\end{aligned}
$$

By combining the two, and imposing the constraint (4.10), the constraints can be written as:

$$
\begin{aligned}
b &\leq g_{i,j} + \omega_i - \omega_j, & \forall i \neq j \in \{1, \ldots, n\} & \quad (4.12) \\
\bar{b} &\leq \bar{g}_{i,j} + \omega_i - \omega_j + \delta_i^0 - \delta_j^0, & \forall i \neq j \in \{1, \ldots, n\} & \quad (4.13)
\end{aligned}
$$

and in matrix form:

$$
b\mathbf{1} \leq \Omega \cdot \omega + \frac{1}{2}|\Omega| \cdot \mathbf{g} \tag{4.14}
$$

$$
\bar{b}\mathbf{1} \leq \Omega \cdot \omega + \Delta \cdot \delta^0 + \frac{1}{2}|\Omega| \cdot \bar{\mathbf{g}} \tag{4.15}
$$

where $\Omega, \Delta \in \mathbb{R}^{n(n-1) \times n}$. The upper and lower bounds for the bandwidths are:

$$
b \leq g^*, \quad b \geq 0 \tag{4.16}
$$

$$
\bar{b} \leq \bar{g}^*, \quad \bar{b} \geq 0 \tag{4.17}
$$

where $g^* = \min(g_i)$ and $\bar{g}^* = \min(\bar{g}_i)$. We have therefore a total of $[2n(n-1)+4]$ constraints for the bandwidths.

4.3.2 Travel Time Constraints

The travel times in the two directions t_i and $\bar{t}_i$ are now decision variables of the optimization problems. The maximum and minimum speed limits are assumed to be the same in both directions, and therefore the bounds of the travel times will depend on the length of the segments. These constraints can be written in vector form as follows:

$$
\mathbf{t}_{\min} \leq \mathbf{t} \leq \mathbf{t}_{\max} \tag{4.18}
$$

$$
-\mathbf{t}_{\max} \leq \bar{\mathbf{t}} \leq -\mathbf{t}_{\min} \tag{4.19}
$$

where the vector of travel times is $\mathbf{t} = (t_1, \ldots, t_{n-1})$, and the bounds on the travel times are:

$$t_{i,\min} = \frac{x_{i+1} - x_i}{v_{\max}}, \quad t_{i,\max} = \frac{x_{i+1} - x_i}{v_{\min}} \tag{4.20}$$

Analogous equations apply to the inbound direction. This defines $4(n-1)$ constraints.

4.3.3 Internal Offset Constraints

In this framework, the displaced internal offsets δ_i^0 are not known a priori, but depend on decision variables t_i and $\bar{t}_i$ through (4.8). The difficulty is represented by the modulo operator, which has to be accounted for in the optimization.

Constraints with modulo operator break the standard continuous form of the problem, which now becomes an integer programming problem. Constraint (4.8) can be rewritten as:

$$\delta_i + \sum_{k=1}^{i-1} (t_k - \bar{t}_k) = \alpha_i C + \delta_i^0 \tag{4.21}$$

where $\alpha_i \in \mathbb{N}$, with $i \in \{2, \ldots, n\}$, is a new integer decision variable. Note that the δ_i are given, $\delta_1^0 = \delta_1$ and therefore $\alpha_1 = 0$. The constraints will be constructed as follows:

$$\delta_1^0 = \delta_1$$
$$\delta_2^0 = \delta_2 + t_1 - \bar{t}_1 - \alpha_2 C$$
$$\delta_3^0 = \delta_3 + t_1 - \bar{t}_1 + t_2 - \bar{t}_2 - \alpha_3 C$$
$$\vdots$$

In matrix form, bringing the unknowns on the left-hand side, the n constraints on δ^0 are as follows:

$$\delta^0 - \Psi \cdot \mathbf{t} + \Psi \cdot \bar{\mathbf{t}} + \alpha \cdot C = \delta \tag{4.22}$$

where the matrix $\Psi \in \mathbb{R}^{n \times (n-1)}$, and the vector of integer variables is $\alpha = [0, \alpha_2, \ldots, \alpha_n]^T$.

4.3.4 Optimization Problem

As already mentioned, the objective is to maximize bandwidth in the two directions (i.e. sum of the bandwidths). The problem will be solved with respect to the outbound relative offsets and the transformed internal offsets (i.e. offset control), the travel times (i.e. variable speed limits), and the integer variables that

keep count of the number of cycles. Therefore the number of unknowns of the optimization problem is $5n - 1$:

$$\mathbf{x} = \big[b, \bar{b}, \omega_1, \ldots, \omega_n, \delta_1^0, \ldots, \delta_n^0, t_1, \ldots, t_{n-1}, \\ \bar{t}_1, \ldots, \bar{t}_{n-1}, \alpha_2, \ldots, \alpha_n \big]^T \tag{4.23}$$

Besides the maximization of the bandwidth, it is also of interest to minimize the variance of the speed advisory, as well as the theoretical travel time. The former may be thought of as a control variance term, or as a comfort term because the drivers would be less willing to follow a highly variable speed advisory. This term also serves to reduce vehicle accelerations that increase energy consumption. The second term drives the optimization away from trivial solutions with impractically low velocities. These additional terms may be written as a function of $\mathbf{x}$.

Smoothness Term

The speed difference between adjacent segments induced by the VSL control can be seen as a proxy for the acceleration at the intersection. Acceleration has major impact on the energy consumption. Therefore, by discouraging large variations in speed between segments, the energy consumption associated with the VSL is minimized. The quantity to be minimized for the outbound direction is:

$$\left\lVert \frac{L_i}{t_i} - \frac{L_{i+1}}{t_{i+1}} \right\rVert_1, \quad i \in \{1, \ldots, n-2\} \tag{4.24}$$

The same expression applies for the inbound direction, with $\bar{t}_i$ and $\bar{t}_{i+1}$. In order to avoid the introduction of nonlinear terms in the objective function, we will approximate (4.24) with a linear function corresponding to its numerator. Therefore the smoothness term of the objective function can be rewritten as:

$$\lVert L_i t_{i+1} - L_{i+1} t_i \rVert_1, \quad i \in \{1, \ldots, n-2\} \tag{4.25}$$

which can be expressed in matrix form with:

$$\lVert \mathcal{L}^* \cdot \mathbf{t} \rVert_1 \tag{4.26}$$

where $\mathcal{L}^* \in \mathbb{R}^{(n-2) \times (n-1)}$ is a matrix of this form:

$$\mathcal{L}^* = \begin{bmatrix} -L_2 & L_1 & 0 & \ldots & 0 & 0 \\ \vdots & & & & & \vdots \\ 0 & \ldots & -L_{i+1} & L_i & 0 & \ldots \\ \vdots & & & & & \vdots \\ 0 & 0 & \ldots & 0 & -L_{n-1} & L_{n-2} \end{bmatrix}$$

Analogously for the inbound direction. This simplification does not affect the convexity of the problem and in particular does not modify the minimum of the smoothness term, which will still be reached when the speeds are equal. The approximation will change the shape of the function away from the minimum, but its convexity will still drive the optimization towards the desired point. In this way, the decision variables t and $\bar{t}$ do not appear at the denominator and the linearity of the smoothness term is preserved.

Travel Time Term

In order to minimize the theoretical travel time in the network induced by the speed limits, the L_1-norm of t is also to be minimized. Therefore the travel time term for the outbound direction in vector form is:

$$||\mathbf{t}||_1 \tag{4.27}$$

Analogously for the inbound direction.

Final Formulation

The problem can be finally formulated as a nonlinear integer program as follows:

$$
\begin{cases}
\max_{\mathbf{x}} & b + \bar{b} - \lambda_1 \left(||\mathcal{L}^* \mathbf{t}||_1 + ||\mathcal{L}^* \bar{\mathbf{t}}||_1 \right) - \lambda_2 \left(||\mathbf{t}||_1 + ||\bar{\mathbf{t}}||_1 \right) \\
\text{s.t.} & b\mathbf{1} \leq \Omega \cdot \omega + \dfrac{1}{2}|\Omega| \cdot \mathbf{g} \\
& \bar{b}\mathbf{1} \leq \Omega \cdot \omega + \Delta \cdot \delta^{\mathbf{0}} + \dfrac{1}{2}|\Omega| \cdot \bar{\mathbf{g}} \\
& b \leq g^* \\
& b \geq 0 \\
& \bar{b} \leq \bar{g}^* \\
& \bar{b} \geq 0 \\
& \mathbf{t}_{\min} \leq \mathbf{t} \leq \mathbf{t}_{\max} \\
& -\mathbf{t}_{\max} \leq \bar{\mathbf{t}} \leq -\mathbf{t}_{\min} \\
& \delta^{\mathbf{0}} - \Psi \cdot \mathbf{t} + \Psi \cdot \bar{\mathbf{t}} + \alpha \cdot C = \delta
\end{cases}
\tag{4.28}
$$

The objective function can be linearized by introducing slack variables that behave as maximum bounds for the L_1-norms [16]. Four such variables $\gamma \in \mathbb{R}^{(n-2)}$, $\bar{\gamma} \in \mathbb{R}^{(n-2)}$, $\tau \in \mathbb{R}^{(n-1)}$ and $\bar{\tau} \in \mathbb{R}^{(n-1)}$ are introduced such that:

$$
\begin{aligned}
|\mathcal{L}^* \cdot \mathbf{t}| \leq \gamma \qquad &\text{and} \qquad |\mathbf{t}| \leq \tau \\
|\mathcal{L}^* \cdot \bar{\mathbf{t}}| \leq \bar{\gamma} \qquad &\text{and} \qquad |\bar{\mathbf{t}}| \leq \bar{\tau}
\end{aligned}
$$

Thus, the vector of the unknowns is extended:

$$\mathbf{z} = [\mathbf{x}, \gamma, \bar{\gamma}, \tau, \bar{\tau}]^T \tag{4.29}$$

and new constraints appear in the optimization problem.

Therefore the problem can be finally formulated as a mixed-integer linear program with $(9n - 7)$ unknowns and $(4n^2 + 11n - 11)$ constraints:

$$
\begin{cases}
\max_{\mathbf{z}} \quad b + \bar{b} - \lambda_1 \left(\mathbf{1}^T \gamma + \mathbf{1}^T \bar{\gamma} \right) - \lambda_2 \left(\mathbf{1}^T \tau + \mathbf{1}^T \bar{\tau} \right) \\[2mm]
\text{s.t.} \quad b\mathbf{1} \leq \Omega \cdot \omega + \frac{1}{2} |\Omega| \cdot \mathbf{g} \\[2mm]
\qquad \bar{b}\mathbf{1} \leq \Omega \cdot \omega + \Delta \cdot \delta^{\mathbf{0}} + \frac{1}{2} |\Omega| \cdot \bar{\mathbf{g}} \\[2mm]
\qquad b \leq g^* \\
\qquad b \geq 0 \\
\qquad \bar{b} \leq \bar{g}^* \\
\qquad \bar{b} \geq 0 \\
\qquad \mathbf{t}_{\min} \leq \mathbf{t} \leq \mathbf{t}_{\max} \\
\qquad -\mathbf{t}_{\max} \leq \bar{\mathbf{t}} \leq -\mathbf{t}_{\min} \\
\qquad \delta^{\mathbf{0}} - T \cdot \mathbf{t} + T \cdot \bar{\mathbf{t}} + \alpha \cdot C = \delta \\
\qquad \mathcal{L}^* \cdot \mathbf{t} - \gamma \leq 0 \\
\qquad -\mathcal{L}^* \cdot \mathbf{t} - \gamma \leq 0 \\
\qquad \mathcal{L}^* \cdot \bar{\mathbf{t}} - \bar{\gamma} \leq 0 \\
\qquad -\mathcal{L}^* \cdot \bar{\mathbf{t}} - \bar{\gamma} \leq 0 \\
\qquad \mathbf{t} - \tau \leq 0 \\
\qquad -\mathbf{t} - \tau \leq 0 \\
\qquad \bar{\mathbf{t}} - \bar{\tau} \leq 0 \\
\qquad -\bar{\mathbf{t}} - \bar{\tau} \leq 0
\end{cases}
\tag{4.30}
$$

Note that in the current formulation the norms $||\mathcal{L}^*\mathbf{t}||$ and $||\mathcal{L}^*\bar{\mathbf{t}}||$ are symmetric, thus a reduction in consecutive speeds is penalized as heavily as an increase in speed. The formulation can be generalized by defining an asymmetric norm, so that positive values (i.e. coasting down to a lower speed) are weighted differently from negative values.

This is achieved by introducing a weight $\beta \in [0, 1]$ on the constraints contain-

ing the slack variables γ and $\bar{\gamma}$ in problem (4.30), as follows:

$$\begin{aligned}
\beta \cdot \mathcal{L}^* \cdot \mathbf{t} - \gamma &\leq 0 \\
-\mathcal{L}^* \cdot \mathbf{t} - \gamma &\leq 0 \\
\mathcal{L}^* \cdot \bar{\mathbf{t}} - \bar{\gamma} &\leq 0 \\
-\beta \cdot \mathcal{L}^* \cdot \bar{\mathbf{t}} - \bar{\gamma} &\leq 0
\end{aligned} \tag{4.31}$$

The weight β regulates the relative detriment of positive and negative changes in speed. In particular, $\beta < 1$ means that decelerations are less penalized than accelerations. In the following, the case with $\beta = 1$ is treated.

4.4 Simulation Setup

The goal of the simulation campaign is to assess the performance of our optimization and the impact of VSL. Specifically, the proposed approach, by means of both offset and variable speed limits control, is expected to achieve a higher bandwidth than the offset-based optimization in [56]. Furthermore, the benefits analysis will not be focused only on comparing the levels of total bandwidth achieved. Real traffic performance metrics, such as energy consumption, travel time, idling time at the traffic lights and number of stops, will be analyzed. The objective is to prove that the simple optimization problem hereby formulated will give significant improvements in terms of real traffic performance.

4.4.1 Numerical Implementation

The two-way bandwidth optimization problem (4.30) has been implemented in MATLAB, using the native solver `intlinprog` for MILPs. For the sake of comparison, the problem was always solved along with the one formulated in [56] in order to directly observe the differences between the two formulations and the benefits introduced by VSL in terms of theoretical bandwidth. The two optimization problems are designed in such a way that the theoretical bandwidth is always at least the size of the shortest green time in the network. In other words, if the result of the optimization yields:

$$b + \bar{b} < \min\{g^*, \bar{g}^*\}$$

then the direction of travel with the higher bandwidth is set to have a progression band equal to its shortest green time. In this way we ensure that the highest possible theoretical bandwidth is always achieved.

The computation time is negligible: 0.3 seconds for the problem here presented, 0.15 seconds for the problem presented in [56], for an arterial network

with 10 intersections. It has also been observed that the MILP here presented scales better with the increasing number of intersections, whereas the simpler offsets-based optimization runs more slowly when n increases. For instance, for $n = 20$, the MILP optimization converges in about 0.4 seconds, while the LP converges in about 0.9 seconds. This can be explained by the generally larger space of optimal solutions available when combining offset and VSL control. In other words, as n increases, the offset-only optimization search for the solution in a smaller and smaller space, therefore taking longer to converge. On the contrary, the combined optimization converges faster to one possible optimal solution because the search space is larger. Based on this, it is also possible to conclude that the integer variables in the optimization problem under analysis do not affect significantly the convergence time.

The simulations were run with a laptop equipped with an Intel(R) Core(TM) i7-2760QM at 2.40GHz and 8GB of RAM.

4.4.2 Microscopic Traffic Simulator

Aimsun was adopted as microscopic simulator for the tests. The traffic demand used in the traffic simulation was required to be feasible, in the sense that the green times were sufficient to dissipate the queues in each cycle. A conservative upper bound for the feasible demand is given by:

$$D \leq D_{\max} = \frac{g^*}{C} \varphi_m(v_{\min}) \quad \text{[veh/h]} \tag{4.32}$$

where g^* is the minimum of the green times in the signalized corridor, and $\varphi_m(v_{\min})$ is the demand/supply saturation function for the imposed minimum speed limit, as discussed in Chapter 3 and analogously to equation (3.13). This definition of feasible demand is applied to each direction of travel.

A communication protocol between Aimsun and MATLAB was set up in order to retrieve from the microscopic simulator information about the vehicles in the network, at each simulation step. Namely the vehicles send information about their position, current speed and acceleration. These data are used to compute traffic performance metrics. Each one of the performance metrics was obtained per segment and per vehicle completing the trip on the segment. Vehicles that at the end of the simulation time horizon remained in the network, do not fully contribute to the overall performance. After computing the performance per segment and per vehicle, the average performance per segment was obtained. In the following analysis, only the network-wide performance is reported, that is the sum over the two directions of travel of the mean performance in each segment. The performance metrics used in this work are defined as follows:

Travel Time

The time that a vehicle spends in the network.

Idling Time

The time during which a vehicle has zero speed.

Number of Stops

The number of idling periods of a vehicle in the network.

Energy Consumption

The energy is defined as the integration over time (i.e. the time the vehicle is in the segment) of the power demand.

$$E = \int_0^{T_f} P \, \mathrm{d}t = \int_0^{T_f} b_1 uv \, \mathrm{d}t \tag{4.33}$$

The torque u is derived from the longitudinal model of the vehicle [105]:

$$\dot{x} = v$$
$$\dot{v} = h_1 u - h_2 v^2 - h_3 v - h_0$$

where u is a function of the speed and the acceleration of the vehicle. The constants b_i and h_i were identified in [37]. Note that such energy consumption model can be also adapted to electric vehicles by adding a term proportional to the square of the torque, representing the electrical losses in the armature of the motor.

4.5 Experiments

4.5.1 Bandwidth Degradation

The first experiment aims at showing the degradation of the theoretical bandwidth with the increasing number of signalized intersections on the arterial. Several network parameters have been varied randomly in order to test different sets of green times, segment lengths, and internal offsets. The range of the parameters is shown in Table 4.1.

In order to extensively explore the space of varying parameters, for each number of intersections n, the other parameters (i.e. green split ratio, segment's length,
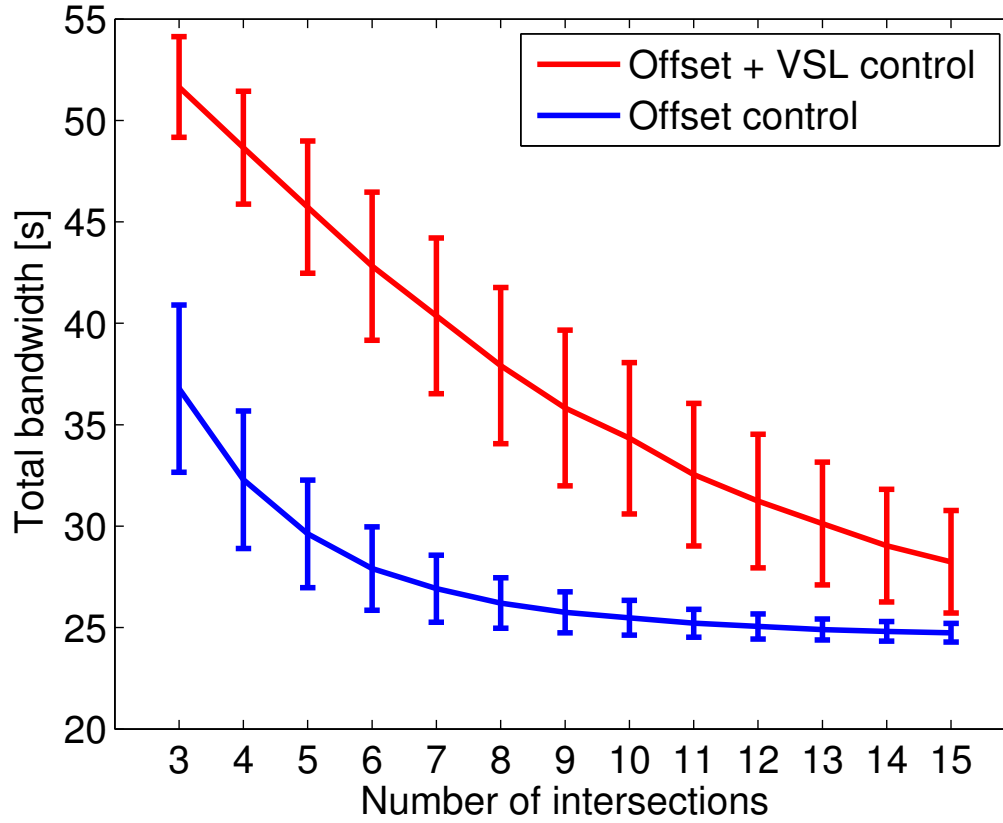
Figure 4.2 – Bandwidth degradation with increasing number of intersections. In blue the offset control strategy in [56].

Table 4.1 – Network parameters range for stochastic simulation

n	$[3, \ldots, 15]$	number of intersections (per direction)
C	60	cycle time [s]
g	$[0.4, 0.6]$	green signal split ratio
L	$[225, 375]$	segment lengths [m]
δ	$[-C/2, C/2]$	internal offset [s]
$[v_{\min}, v_{\max}]$	$[15, 50]$	speed limits [km/h]

and internal offset) were allowed to vary randomly within the specified ranges. A total of 10,000 simulations per each value of n were run (i.e. 130,000 total different configurations). Furthermore, for each randomly generated configuration, both problem (4.30) and the two-way bandwidth maximization presented in [56] were solved. The comparison of the theoretical bandwidth achieved by the two optimizations is shown in Figure 4.2.

In the graph, the solid lines represent the average bandwidth varying with the number of intersections. The vertical error bars at each value of n represent the standard deviation of the bandwidth calculated over the random set of parameters. As n increases the bandwidth decreases for both types of control action. However control of both offsets and VSL results to be significantly more effective, especially for a lower number of intersections. Note that for each n, the bandwidth achieved using the proposed approach is always greater than or equal to that obtained using only offset control.

The weights used in the optimization are $\lambda_1 = \lambda_2 = 0.5$. Interestingly, note that the red line would move depending on the selection of weights λ_1 and λ_2. Specifically, when $\lambda_2 >> 0$, the red line would coincide with the blue one, meaning that the presented optimization is forced to select the maximum speeds. When the two weights are set to zero, the red line would move up at its maximum, meaning that the VSL would be fully employed by the optimization to maximize only the total bandwidth.

4.5.2 Microscopic Simulation

For the microscopic simulations a single random network configuration was selected. The network parameters used in Aimsun are summarized in Table 4.2.

Table 4.2 – Network parameters for microscopic simulation

n	6	number of intersections
g	$[33, 30, 25, 28, 31, 26]$	outbound green times [s]
$\bar{g}$	$[33, 27, 35, 27, 33, 26]$	inbound green times [s]
L	$[268.1, 238.7, 311.4, 327.5, 307]$	length of the segments [m]
δ	$[25, -21, -21, -19, -22, -3]$	internal offsets [s]
D	500	traffic demand [veh/h]

For the choice of macroscopic network parameters (i.e. jam density, congestion speed, etc.), the arterial capacity is $Q = 1850$ veh/h, and the maximum

feasible demand is $D_{\text{max}} = 536$ veh/h. Therefore, the simulations were conducted using a traffic demand close to the limit of existence of a green wave.

Given these network parameters, the two bandwidth optimization problems were solved numerically, in order to obtain the control parameters (i.e. offsets and speed limits) to be tested in the microscopic simulator.

Bandwidth and Traffic Performance

For the assessment of the results of the combined optimization of offsets and speed limits, the space of the weights λ_1 and λ_2 of the multi-objective function has been spanned. The results are reported in Figure 4.3 and Figure 4.4.

In Figure 4.3 it is evident how the theoretical bandwidth is monotonically decreasing in the direction of the increasing λ_1 and λ_2. Higher weights on the smoothness term and/or the travel time term in the optimization would achieve smoother and/or higher overall speed limits profiles between adjacent segments. Therefore, for high values of λ_2 the optimization converges towards the blue area of the bandwidth plot, which is equivalent to the bandwidth achieved by the offset-only optimization, with speed limits equal to the maximum in the entire network. The benefits of the VSL for bandwidth maximization are evident for lower values of the weights λ_1 and λ_2. In particular, by setting the weights equal to zero, the maximum bandwidth value is achieved, and the full potential of the VSL is exploited. The plot of the smoothness term of the objective function (lower values correspond to higher smoothness) shows how it is monotonically decreasing in the direction of increasing λ_1, as expected. On the contrary the travel time term improves (i.e. higher speed limits are selected) monotonically in the direction of increasing λ_2. Note that the abrupt variations in the contour plot of the total bandwidth can be easily explained with the presence of integer variables in the problem.

The traffic performance metrics, computed from the microscopic simulation data, are reported in Figure 4.4. It is of interest to observe how the theoretical bandwidth is correlated with actual traffic performance. Energy consumption is low in the area of maximum bandwidth, since higher bandwidth reduces also the idling time and the number of stops. However, energy is optimized for low values of λ_2, showing the positive impact of lower speed limits. If λ_2 is increased in order to aim at lower travel time, an increase of λ_1 is required for the energy consumption to stay at its minimum. Therefore, lower and/or smoother speed limits are to be preferred for optimal energy consumption. Interestingly also travel time is minimized in the area of higher bandwidth, even though the average total speed limit is lower than the maximum. This is an interesting demonstration of the fact that higher speed limits do not always correspond to lower travel times. For high λ_1 and small λ_2 the travel time increases because the optimization forces
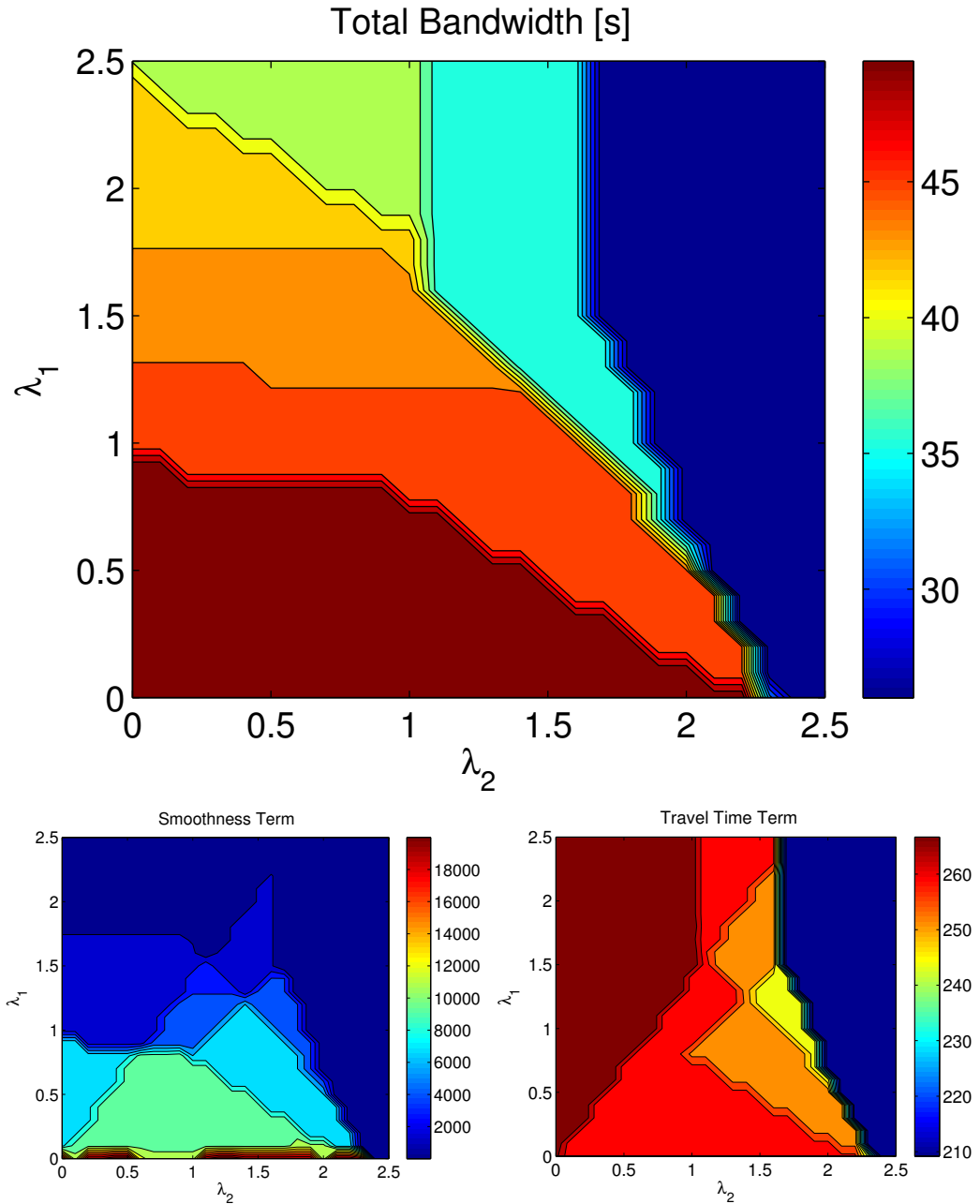
Figure 4.3 – Contour plots of the numerical results. For the theoretical bandwidth, higher values (towards red) are better. For the smoothness term and the travel time term of the objective function, lower values (towards blue) are better.
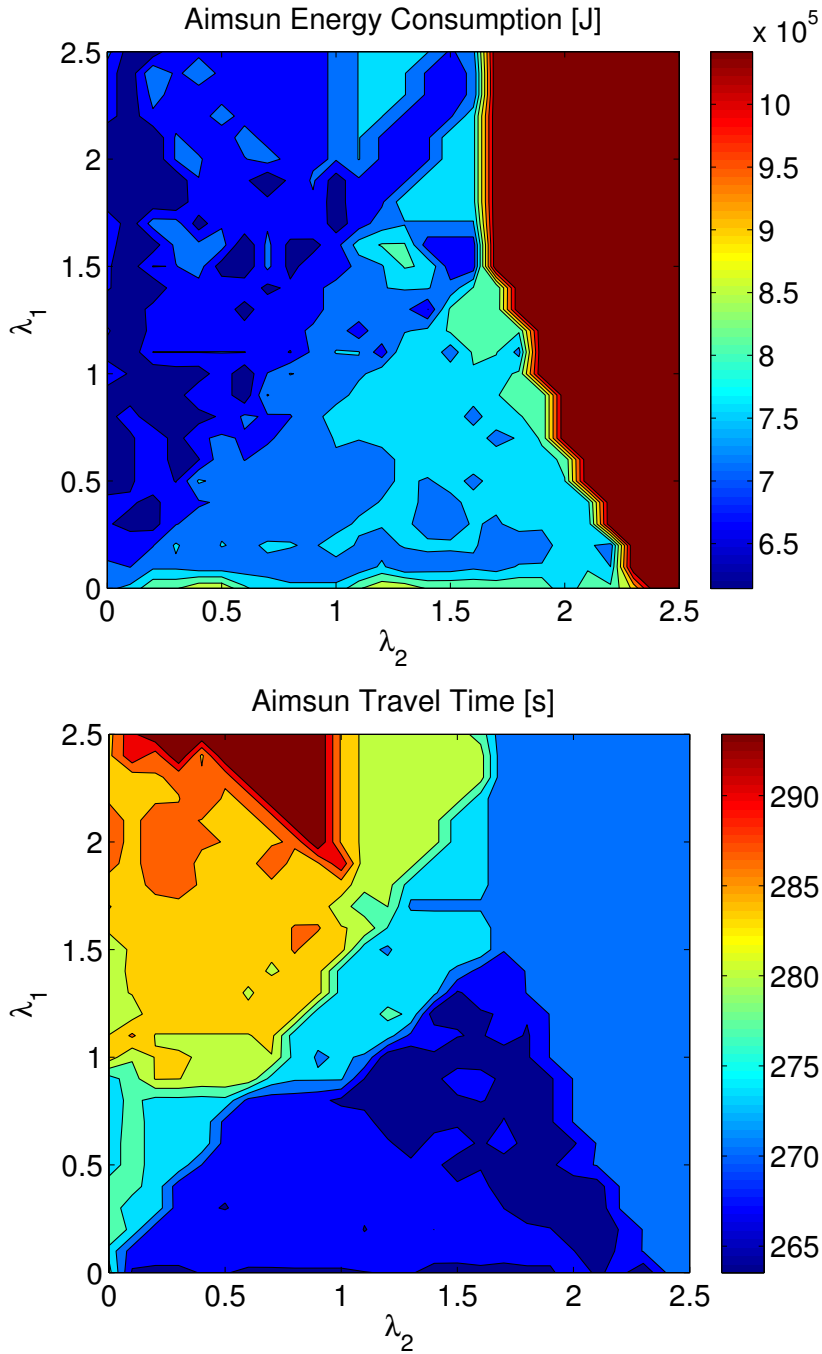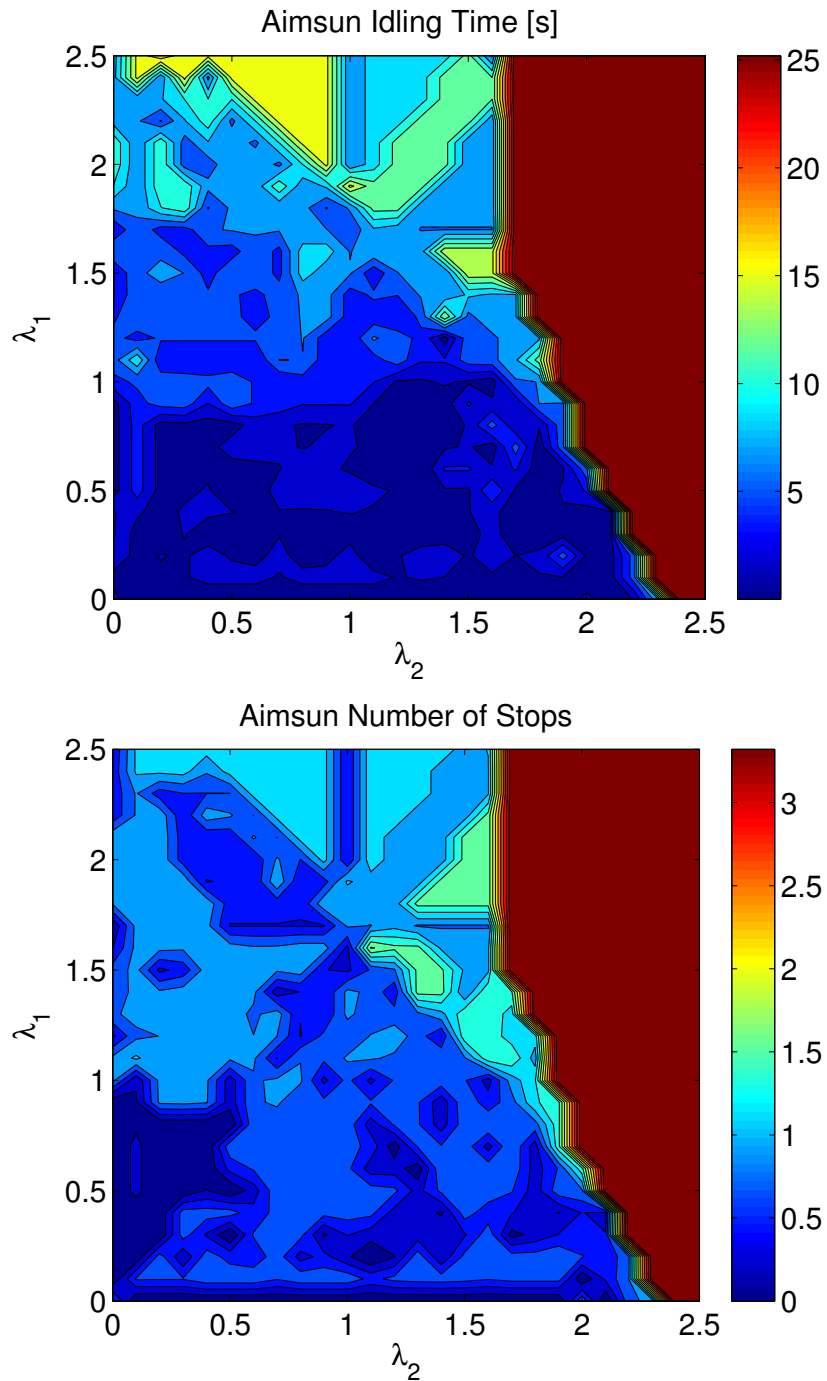
Figure 4.4 – Contour plots of the Aimsun results. The performance metrics reported here (i.e. energy consumption, travel time, idling time, and number of stops) are optimized for lower values (towards blue).

the speed limits to be as close as possible, without giving priority to high speeds. Idling time and number of stops appear to be the most correlated metrics to bandwidth, and they show overall similar behavior in the λ_1-λ_2 plane in Figure 4.3 and Figure 4.4. More specifically, the correlation coefficient between bandwidth and idling time is $R_{\mathrm{bi}} = 0.95$, and the correlation coefficient between bandwidth and number of stops is $R_{\mathrm{bs}} = 0.94$. Also note that where the bandwidth is minimum, all the performance metrics worsen significantly.

When facing a multi-objective optimization it is always challenging to make the right choice of the weighting factors. A Pareto efficiency analysis has been conducted on the problem in order to assist the designer in making decisions within the set of points belonging to the Pareto front. The Pareto frontier is defined as the set of points that cannot be said to be strictly worse than any other belonging to the set. All the points on the frontier are equivalently Pareto-efficient. In the case under analysis, the terms of the objective function are three and the Pareto frontier is a surface in a three-dimensional space. In order to find the set of the Pareto-efficient points, a standard non-dominated sorting algorithm was used. The adopted methodology is described as follows. The entire set of solutions obtained from the optimization problem (4.30) for the three terms of the objective function and for different weights combinations (as shown in Figure 4.3) is searched for non-dominated solutions. This gives the Pareto frontier of the optimization problem. The same procedure is run for the set of Aimsun performance metrics. In other words, a Pareto front is found also for the results obtained in Aimsun for energy consumption, travel time, idling time and number of stops. The two Pareto fronts are then mapped onto the λ_1-λ_2 plane and only the intersection of the two Pareto-efficient sets is considered. The idea is to reduce the set of weight options to the ones that are Pareto efficient both for the theoretical optimization problem and for the actual traffic performance obtained in the microscopic simulator. Within this reduced set, we have chosen the weights that achieve the lowest energy consumption, and obtained $\lambda_1 = \lambda_2 = 0.4$.

In order to evaluate the performance of the presented optimization, which in the following will be indicated as "Offset+VSL", a comparative study was conducted with preexisting strategies and a reference. The reference used hereafter is a non-optimized case, where the random choice of offsets still respects the internal offset constraint (4.3). A comparison will be made also with the offset optimization strategy in [56]. Finally, the MAXBAND algorithm will be compared to the proposed strategy. The presented optimization problem can be seen as a generalization of the MAXBAND algorithm in [86, 87] with the segment speeds allowed to vary in $[v_{\min}, v_{\max}]$. In MAXBAND, the formulation for the outbound/inbound arterial problem corresponds to the particular case of $\lambda_1 = \lambda_2 = 0$ in the presented framework.

The comparative results for both theoretical bandwidth and Aimsun perfor-

Table 4.3 – Numerical and Aimsun results comparison

	Numerical	AIMSUN			
	Theoretical Bandwidth	Travel Time	Idling Time	Stops	Energy
Non-optimized	N/A	367.9 s	102.8 s	6.7	1.3E6 J
Offset	26 s	270.3 s	26.9 s	3.5	1.09E6 J
MAXBAND	51 s	278 s	2.3 s	0.7	7.48E5 J
Offset+VSL	51 s	268.3 s	1.9 s	0.8	7.03E5 J

mance metrics are reported in Table 4.3. Besides the significant difference in terms of bandwidth achieved thanks to the introduction of VSL as a decision variable, important improvements are achieved also in terms of traffic performance. The presented strategy yields a reduction of the overall network travel time of 1% with respect to the offset optimization, although the average speed limit is lower. The idling time and the number of stops at the intersections are almost completely eliminated. The overall energy consumption is reduced by 35.5%. With respect to MAXBAND, the proposed strategy is able to reduce the travel time by 3.5%, and the energy consumption by 6%. Much larger improvement is evidently achieved with respect to the non-optimized case: travel time is reduced by 27% and energy consumption is reduced by 46%.

Note that for the considered level of demand (i.e. demand is feasible and equal to 500 veh/h) and for the choice of weights in the objective function (i.e. $\lambda_1 = \lambda_2 = 0.4$), the improvement of the presented strategy with respect to MAXBAND is not very large. In the following, the analysis of the performance at different levels of traffic demand will lead to a demand-based optimization and the benefits

Table 4.4 – Control variables of the optimization problems

	Offsets [s]	Speed Limits [km/h]
Non-optimized	$\theta = [-16, -20, -16, -4, -11, 25]$ $\bar{\theta} = [9, 19, 23, -23, 27, 22]$	$v = [50, 50, 50, 50, 50]$ $\bar{v} = [50, 50, 50, 50, 50]$
Offset	$\theta = [0, 27, 10, -15, 25, -17]$ $\bar{\theta} = [25, 6, -11, 26, 3, -20]$	$v = [50, 50, 50, 50, 50]$ $\bar{v} = [50, 50, 50, 50, 50]$
MAXBAND	$\theta = [0, -29, 18, -12, 28, -13]$ $\bar{\theta} = [25, 10, -3, 29, 6, -16]$	$v = [40, 17, 35, 33, 50]$ $\bar{v} = [50, 50, 50, 50, 50]$
Offset+VSL	$\theta = [0, 21, -4, -24, 12, -26]$ $\bar{\theta} = [25, 0, -25, 17, -10, -29]$	$v = [50, 26, 29, 34, 43]$ $\bar{v} = [44, 44, 50, 50, 50]$

of the Offset+VSL strategy will further increase.

In Table 4.4 the output of the three optimization problems is reported. The strategy here presented, as well as MAXBAND, shows some variability in the speed advisory due to the VSL control, which may cause some drivers to ignore the speed limit.

Price of Noncompliance with the Speed Advisory

An additional simulation in Aimsun was conducted in order to assess the "price of noncompliance" with the speed advisory. The set of offsets outputted by the optimization for the combined control was implemented, but the vehicles were allowed to drive freely up to the maximum speed limit (i.e. 50 km/h).

Table 4.5 – Aimsun traffic performance in the case of noncompliance with the speed advisory

	AIMSUN			
	Travel Time	Idling Time	Stops	Energy
Offset+VSL	260.9 s	21.1 s	3	1.05E6 J
MAXBAND	274.3 s	33.6 s	2.7	1.07E6 J

From Table 4.5, it is evident how the noncompliance with the speed advisory is very costly in terms of energy consumption, idling time and number of stops, yielding only a slight reduction of the overall travel time.

Variation of Traffic Demand

As previously mentioned, the experiments were conducted at a feasible level of demand, which guarantees the existence of a progression band. However, different levels of traffic demand are very likely to arise in reality and it is important to study the effects on traffic performance. Simulations were run in order to assess the sensitivity of the traffic performance to a demand up to the limit of feasibility. Infeasible demands were also tested in order to evaluate the impact of heavy traffic on the network optimized by the arterial bandwidth maximization algorithm.

The variation of energy consumption, travel time, idling time, and number of stops, as a function of traffic demand, is reported in Figure 4.5. The demand is expressed as a percentage of the arterial capacity. Up to the feasible demand, the queues at each intersection are dissipated within the cycle time, as previously
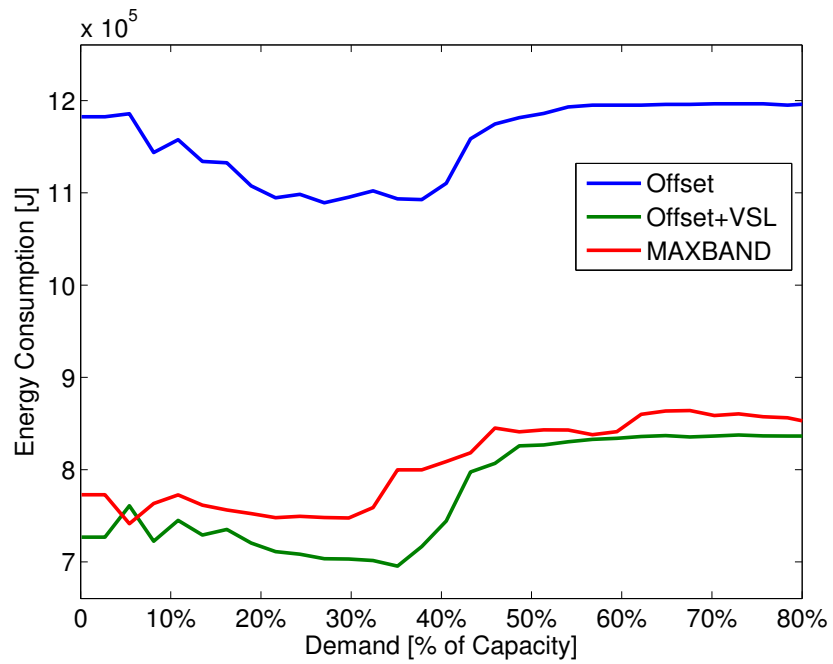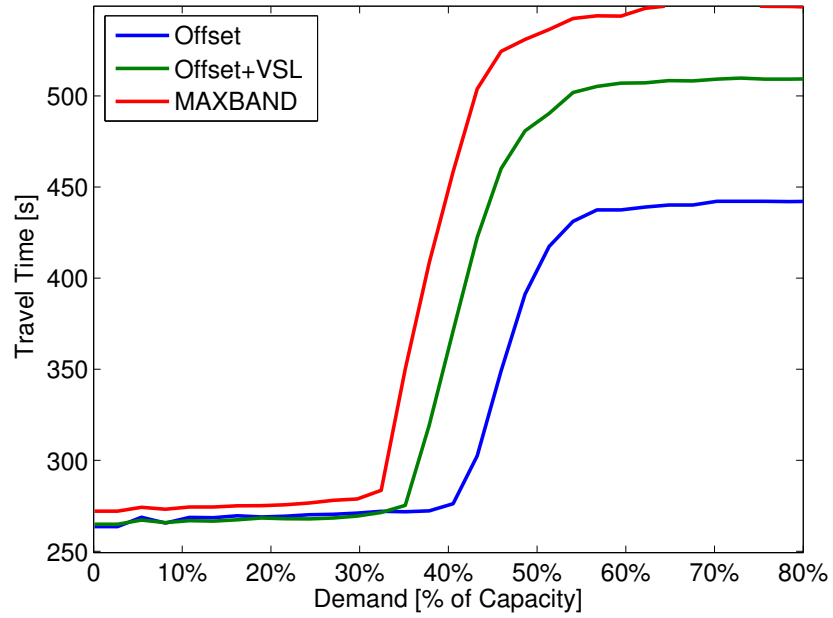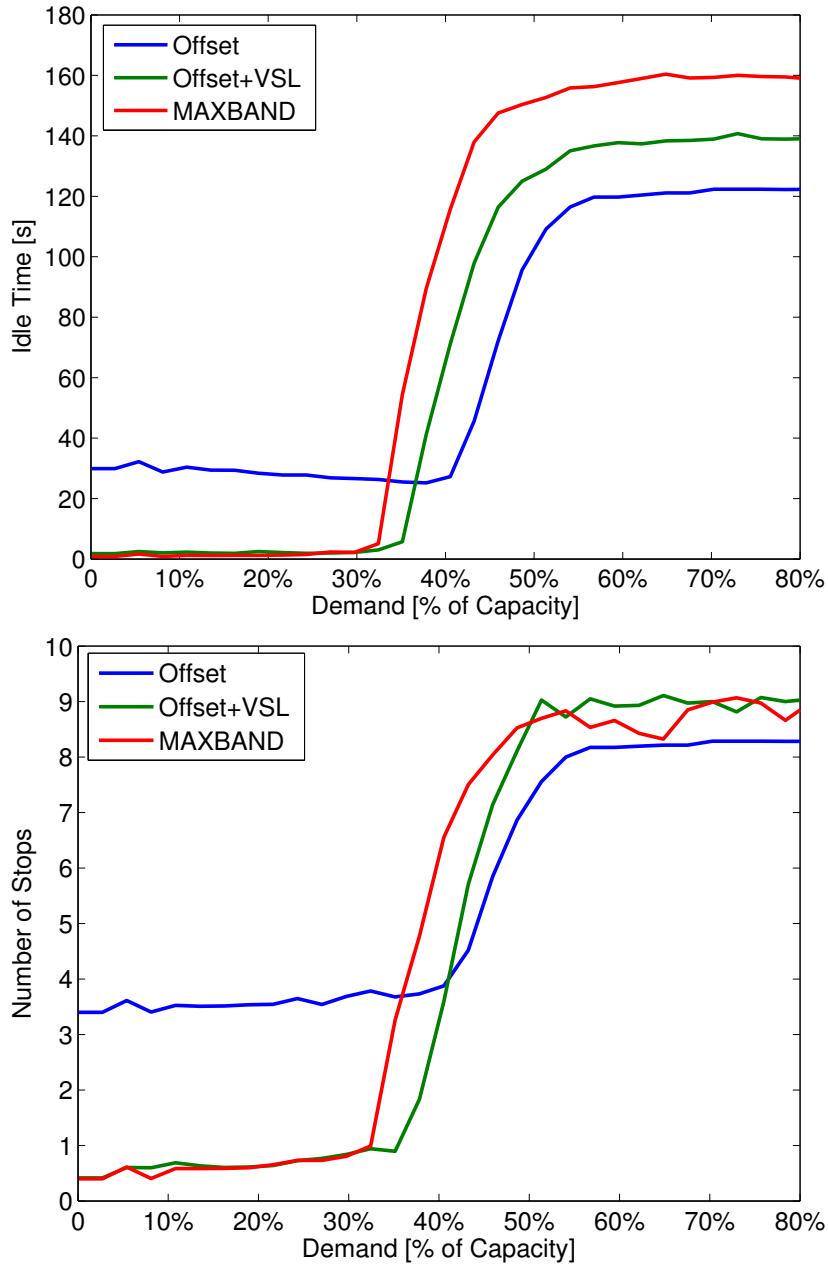
Figure 4.5 – Variation of the traffic performance metrics as a function of the traffic demand.

mentioned. For higher demands, queues begin to form at the bottleneck intersection, which corresponds to the traffic light with the smallest outflow. This critical value of demand can be exactly computed, by knowing the traffic light green split ratio and the imposed speed limit in the segment given by the optimization, as follows:

$$D_{\text{crit}} = \min \left\{ \min \left\{ \frac{g_i}{C} \varphi_m(v_i) \right\}, \min \left\{ \frac{\bar{g}_i}{C} \varphi_m(\bar{v}_i) \right\} \right\} \tag{4.34}$$

for $i = 1, \ldots, n$. This critical demand corresponds in Figure 4.5 to the point at which the performance metrics begin to degrade (i.e. between 30% and 40% of the road capacity).

Interestingly, up to the critical demand, the travel time for the strategy here presented is absolutely comparable to the one achieved with offset optimization, even though the VSL control induces a lower average speed limit. This can be explained by looking at the number of stops and the idling time, which are drastically reduced by the VSL. In other words, the presented approach allows to convert the time wasted idling at a red traffic light into a slower approach to the traffic light, without affecting the travel time. The proposed optimization presents also an improvement with respect to the MAXBAND algorithm (i.e. $\lambda_1 = \lambda_2 = 0$), reducing the travel time by 3% for demands up to the critical one. It should be noted also that the offset-only optimization, with the uncontrolled maximum speed limit, achieves the best performance in terms of travel time for demands beyond the critical one.

As for the energy consumption, the proposed strategy, is consistently better than the offset optimization, yielding an average reduction of about 33% at any level of demand. An average reduction of about 5% is also achieved with respect to MAXBAND. It is interesting to note that the average network energy consumption is lower for demands approaching the critical one. Longer platoons of non-stopping vehicles allow for a better use of the infrastructure and to improve the average traffic performance.

In terms of idling time and number of stops, MAXBAND and the proposed strategy are comparable and allow to almost eliminate stops and idling in the network. However, when the traffic demand grows beyond the critical value, the offset optimization and the higher speed limits allow for better performance because the vehicles are able to leave the queues faster.

Therefore, it is possible to conclude that for under-saturated traffic conditions and feasible demands, the proposed optimization of offsets and variable speed limits is able to drastically reduce the traffic energy consumption without affecting the travel time. A more fluid driving experience is also provided by almost completely eliminating stops at red lights.

Demand-Based Optimization

This important result suggests the possibility of a demand-based optimization. An analysis of the Pareto optimum at different levels of traffic demand should indicate different optimal operation conditions and, consequently, different weights λ_1 and λ_2 to be used in the optimization. Experiments were conducted for $D = \{250, 500, 750, 1000\}$ veh/h, corresponding to $\{14\%, 27\%, 41\%, 54\%\}$ of road capacity. The performance at each level of demand was studied as in Figure 4.4, and the mapping of the Pareto front on the λ_1-λ_2 plane was obtained. Intuitively, as the traffic conditions become saturated and the original hypothesis of feasible demand does not hold anymore, the Pareto optimum leaves the region of the λ_1-λ_2 plane corresponding to the maximum theoretical bandwidth. At saturated traffic conditions (as shown in Figure 4.5), the travel time is minimized for high-average speed limits (i.e. $\lambda_2 >> 0$ and $\lambda_1 >> 0$), whereas the energy consumption is minimized for low-average and smooth speed limits (i.e. $\lambda_2 \simeq 0$ and $\lambda_1 >> 0$). The demand-based optimization can be summarized as follows. The choice of $\lambda_1 = \lambda_2 = 0.4$ is Pareto efficient up to saturation, which arises in this scenario at a traffic demand equal to about 50% of road capacity. At saturation, therefore for a demand beyond 50% of road capacity, the previous selection of weights is no longer Pareto efficient. A new set of Pareto-efficient weights that minimize energy consumption was chosen, and we obtained $\lambda_1 = 1.6$ and $\lambda_2 = 1.4$. The speed limits yielded by the optimization with such set of weights are: $v = [43, 34, 34, 34, 34]$ km/h and $\bar{v} = [50, 50, 50, 50, 50]$ km/h.

The traffic performance obtained for the levels of demand $D = 500$ veh/h (i.e. under-saturated) and $D = 1000$ veh/h (i.e. saturated), normalized with respect to the non-optimized case previously described, is reported in Figure 4.6. At under-saturated conditions, as already summarized in Table 4.3, the set of weights $\lambda_1 = \lambda_2 = 0.4$ is Pareto efficient and outperforms all the competitors. At saturated conditions, the previously used set of weights is no longer Pareto-efficient, and the new set of weights $\lambda_1 = 1.6$ and $\lambda_2 = 1.4$ allows to achieve better performance. In particular, the demand-based optimization improves all four performance metrics with respect to the previous optimization with the original set of weights. Also, the improvement with respect to MAXBAND is larger than in under-saturated conditions: energy consumption is reduced by 5%, the number of stops is reduced by 22%, the idling time is reduced by 14%, and the travel time is reduced by 11%. Evidently, the advantages with respect to the non-optimized case are much larger. The interesting competing strategy in the case of saturated traffic conditions is represented by the offset-only optimization, due to the trade-off between travel time and energy consumption. As one may notice, the idling time and the number of stops are approximately equivalent in the two strategies, while significant differences are observed in the travel time and the energy consumption. Namely, the
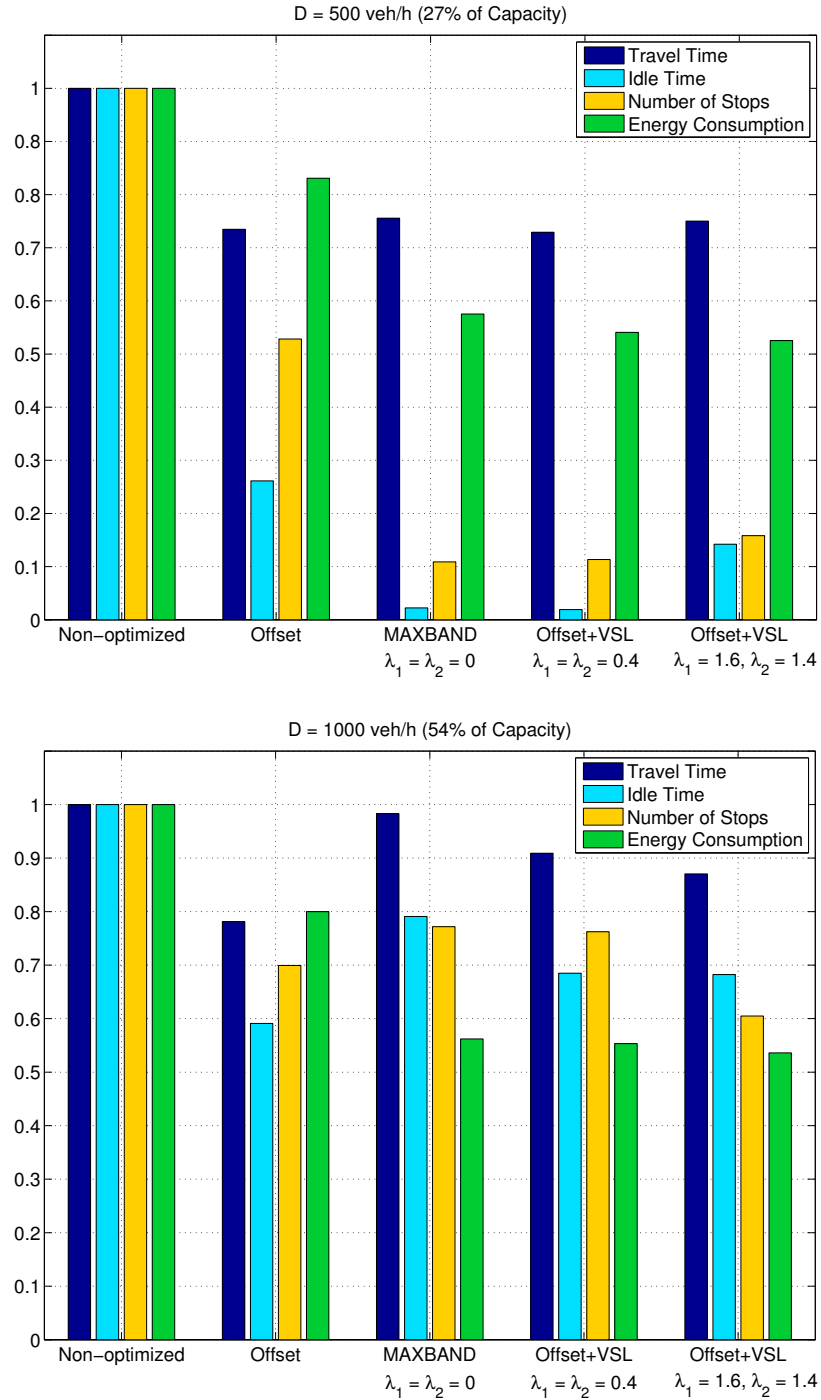
Figure 4.6 – Performance comparison of the demand-based optimization.

demand-based Offset+VSL strategy reduces energy consumption by 33%, while increasing the travel time by 10%. The traffic manager could opt for a different Pareto-efficient combination of weights if willing to reduce the travel time at the expenses of energy consumption.

4.6 Conclusions

This chapter has outlined a solution of the arterial bandwidth maximization by using both offset control and variable speed limits, and by taking into account the effects on energy consumption and network travel time. An extensive evaluation of the proposed solution has been carried out in a microscopic traffic simulator in order to assess the correlation between the theoretical bandwidth and the standard traffic performance metrics. It has been found that higher bandwidth corresponds mainly to lower idling time, number of stops, and energy consumption. The correlation with travel time is weaker and it depends on the applied speed-limits control. The weights used in the objective function allow to find a trade-off between energy consumption and travel time. Finally an analysis of the Pareto front allowed to choose an efficient combination of weights that resulted in drastic energy consumption reduction. It has also been shown that noncompliance with the advised speed limits leads to a significant performance degradation. Finally, an analysis of traffic performance at different levels of demand, including infeasible demands, was conducted. It has been shown that the proposed approach outperforms other existing strategies, and in particular, for under-saturated traffic conditions, achieves reduction of energy consumption without affecting the travel time.

Future research will include investigations into more complex networks with cross streets and additional inflows within the arterial, which might open interesting analyses of the benefits of the variable speed limits on the traffic performance.

Chapter 5

Conclusions

In this dissertation we have addressed the problem of the energy-aware traffic management in urban traffic networks. A set of solutions has been proposed that cover different applications, methodologies, and implementation costs.

The vehicle-oriented control, with the energy-aware speed profile advised directly to each driver, seems to have a reasonable implementation cost and provides some advantages also with a low technology penetration rate. The costs involve mainly the connectivity between the traffic lights and the vehicles (i.e. Wi-Fi antennas and communication setup). As for the vehicle onboard equipment, a smartphone could be enough to process the information and visualize the speed advisory.

The infrastructure control requires mainly the installation of adjustable road side panel to remotely change the speed limit in the road sections. This could be quite costly and more invasive, as compared to the vehicle control strategy. As for the computational costs, all the information coming from the traffic lights and the flows sensors would be processed in a central unit. Therefore, there would not be any vehicle onboard calculation.

The main results and contributions of the study presented in this dissertation may be summarized as follows.

5.1 Review of the Contributions

Given a sequence of signalized intersections, there exists an energy optimal speed profile that a vehicle can follow while avoiding to stop at the traffic lights. The proposed vehicle control is able to identify the best no-stop driving profile, among all the possible no-stop trajectories. Validated simulations have proved that the best driving profile is more energy-efficient than the other available no-stop trajectories by up to 25%. The proposed strategy is fast and flexible enough

---

to be employed online, and the best driving trajectory can be calculated in real time on a receding time horizon. Extensive experimental studies in a microscopic traffic simulator have shown that the proposed control strategy can be applied independently to each vehicle in a traffic flow. The presence of the surrounding vehicles, perturbing the optimal driving profiles, challenges the proposed strategy and forces it to constantly re-adapt to the changing traffic situation. An analysis of the impact of the technology penetration rate on the traffic energy consumption has shown promising results. On a typical signalized corridor, if the totality of the vehicles were equipped with the proposed strategy, the energy consumption would be reduced by almost 30%. A more moderate improvement of 10% could be achieved with about 40% technology penetration rate. Note that, the proposed algorithm, besides ensuring drastic reduction of the energy consumption, was also able to reduce the average travel time, proving that energy consumption and travel time are not always orthogonal.

The consideration of saturated traffic conditions makes inevitable stopping and queuing at the traffic lights. The analysis of an isolated road section with boundary flows regulated by traffic lights has shown that there exists an optimal speed limit for the considered section. The optimality depends on different cost functions, namely traffic energy consumption is to be minimized without sacrificing much the travel time and the efficient utilization of the infrastructure. The proposed macroscopic model and performance metrics, used to describe the traffic evolution and behavior inside the road section, have proved that for the system in equilibrium there exists an efficient speed limit for each level of vehicle occupancy. The optimal speed limit could ensure a performance improvement of up to 25% with respect to the standard city speed limits. A controller has been designed and applied both for the system in equilibrium and for the case of unequal boundary flown. The control action, which gives an insight into the drivers' response to the variable speed limits, facilitates the convergence to the optimal operation conditions. A validation analysis in a microscopic traffic simulator has proved the reliability of the macroscopic modeling approach for control purposes.

The infrastructure control has been then moved to a larger scale. A combination of variable speed limits on road-side panels and traffic lights coordination via offset control has been applied to an urban arterial with multiple signalized intersections. The main novelty lies in direct energy consumption consideration in the infrastructure control, with the objective of bandwidth maximization. Numerically, the optimization problem has been formulated in a simple and descriptive way, and the simulations have proved that wider vehicles progression bands can be achieved by combining the control of the speed limits and the signals offsets. A microscopic traffic simulator has been used to assess the correlation between

bandwidth and the canonical traffic performance metrics. In particular, experiments have shown that the proposed optimization achieves significant improvements with respect to the existing bandwidth maximization approaches. Once again, the proposed strategy was able to drastically reduce the traffic energy consumption, as well as the travel time, by completely eliminating unnecessary stops and idling at the traffic lights. Finally, an analysis of the performance of the proposed approach has been carried out also at saturated traffic conditions. In such conditions, the notion of signals coordination for bandwidth maximization loses significance. However, the multi-objective optimization can be adapted to different levels of traffic congestion, and microscopic simulations have proved that the proposed strategy still outperforms existing algorithms.

5.2 Extensions and Future Works

The first contribution of this work, involving the vehicle control and the individual speed advisory, has been developed under the assumption of one vehicle in the road network. This abstraction allowed to formulate and solve the problem in a simpler way. Experiments have then proved that the proposed solution remains valid when this assumption is not satisfied, namely the algorithm is able to find the optimal speed profile in real time for each vehicle even in presence of disturbance coming from the traffic. However, the optimal speed advisory is independently provided to each vehicle, only reacting to the arising perturbation. A possible extension of this work is the coordination of the speed advisory, in order to detect the formation of platoons and use the green phases in a more cooperative way for platoon allocation. Another possible extension is represented by the speed advisory in the presence of queues at the traffic lights. This extension could involve the estimation of the queue-depletion time, possibly by means of a macroscopic traffic model.

As for the single section control via variable speed limits, a natural extension would be to consider concatenation effects and sequences of saturated links. In the case of multiple connected sections and different speed limits for each road link, the assumption of equal boundary flows would not hold anymore. Some experiments in this work have proved that it is still possible to track an optimal density equilibrium. However, a centralized or distributed optimization would provide interesting insight into the real optimal operation conditions for saturated traffic. In particular, such coordinated optimization could suggest whether it is best to have a homogeneous congestion in all the sections or to set gradually higher speed limits in the downstream direction to facilitate congestion relief.

Lastly, the arterial control via variable speed limits and offsets synchronization has been mathematically formulated without any dependence on the traffic

demand. The assumption of feasible demand was made for the existence of a green wave. However, experiments in the case of saturated traffic conditions have proved that the proposed strategy, with a suitable choice of the weighting factors in the multi-objective optimization, is still able to provide interesting benefits. If such level of abstraction in the problem formulation with independence from the traffic demand is desirable, a possible extension of this work could be to consider cross streets for the arterial and additional incident inflows or outflows. This would probably lead to consider a variable bandwidth through the arterial, and the control should respond accordingly.

Appendices

Appendix A

Aimsun/MATLAB Interface

The microscopic traffic simulator Aimsun offers the possibility to customize the network model, and to control the traffic behavior via a set of interfacing tools.

The Application Programming Interface (API) is a collection of functions that extend the functions of Aimsun environment, and allow to include intelligent transportation systems in the simulation. These include, among others, non-standard adaptive traffic control, advanced traffic management, vehicle guidance, etc.

For the experiments included in this dissertation, an API designed by the NeCS team, at Inria Rhône-Alpes, was adopted. The API description that follows is partly taken from Aimsun documentation, and is completed by the particular features introduced for the experiments contained in this dissertation.

Aimsun Environment
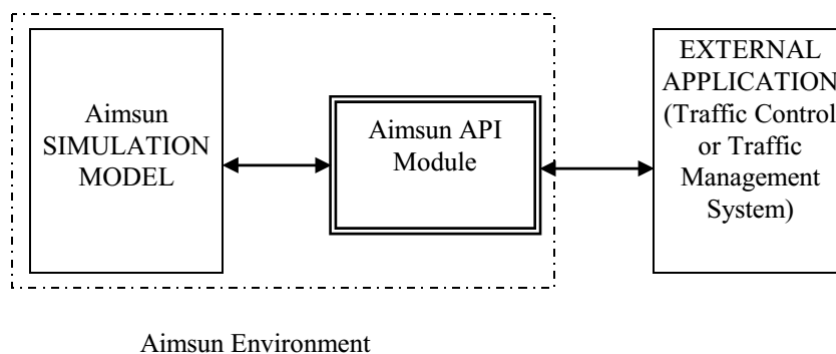
Figure A.1 – Aimsun API module.

The Aimsun API module is functionally located between the Aimsun simulation model and the external application defined by the user (i.e. MATLAB in this dissertation). There are two types of communication processes, as shown in Figure A.1: on one side there is a communication process between the Aimsun and

the Aimsun API module, and on the other side between the Aimsun API module and the external application. The communication process between Aimsun API module and the Aimsun simulation model is provided by the Aimsun environment, but the communication between the Aimsun API module and the external application has to be implemented by the user.

Aimsun-side Interface

The Aimsun API module has six high level functions defined in order to guarantee the communication between the Aimsun API module and the Aimsun simulation model:

- *AAPILoad* is called once when the module is loaded by Aimsun. It is used to create the TCP/IP global socket, to open the connection, and configure the TCP/IP client.
- *AAPIInit* is called once, when Aimsun loads the scenario. It sends to the external application the configuration information, and receives the operation mode of the API.
- *AAPIManage* is called at the beginning of every simulation step. It receives the control action from the external application, and applies it. Information exchange with the external application occurs only at aggregated detection time intervals.
- *AAPIPostManage* is called at the end of every simulation step. At every aggregated detection time intervals, it sends the state information to the external application.
- *AAPIFinish* is called once when Aimsun ends the simulation. It sends the finish message to the external application.
- *AAPIUnLoad* is called once when the module is unloaded by Aimsun. It closes the connection with the external application, and deletes the TCP/IP client.

The Aimsun-side communication process is illustrated in Figure A.2.

The control action occurs in the core of the simulation, that is the AAPI-Manage function. Within this high-level communication function, several control functions can be implemented to manage the traffic in the simulation. For the experiments conducted in this dissertation, the following functions have been implemented:

- *Traffic lights offset control.* Once the external application computes the optimal offsets for the traffic lights in the Aimsun model, this function initializes the traffic lights with the desired offsets. The offsets are set once at the beginning of the simulation, and are not meant to vary throughout the simulation. In the scope of the dissertation, variable offsets and, therefore, variable green splits are not considered. However the function could be
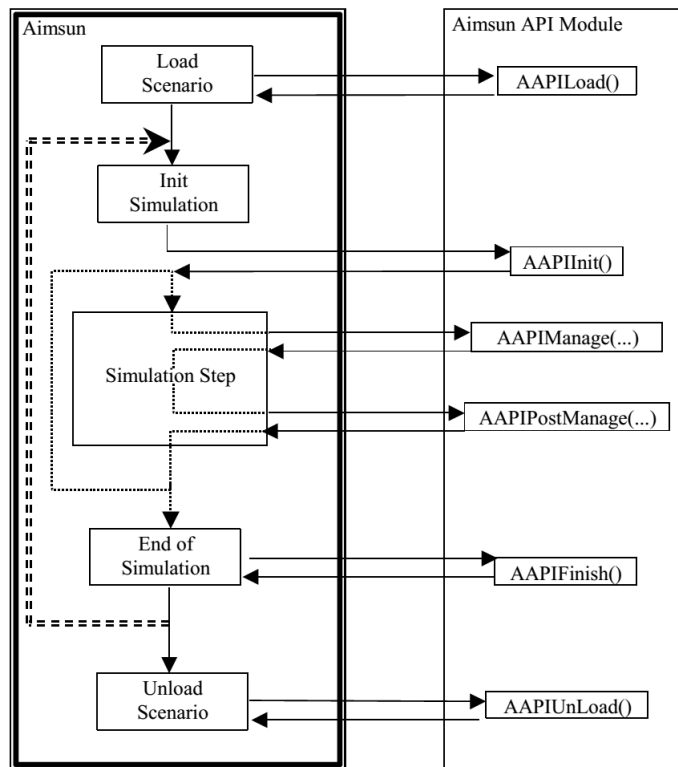
Figure A.2 – Communication process between Aimsun and the API module.

easily extended to the variable offsets framework.

- *Vehicles speed control*. This function allows to set dynamically, at every simulation step, the maximum speed of the vehicles in the Aimsun simulation. The function applies the speed control to each vehicle independently. The maximum speed for each vehicle is transmitted to Aimsun by the external application.

- *Variable speed limits control*. This function sets the speed limits in each section of the Aimsun model. The speed limits can be set either once at the beginning of the simulation, or dynamically in order to test traffic-responsive strategies.

Other user-defined functions serve the purpose of setting up the communication itself. A configuration packet is defined, containing information about the topology of the modeled network, such as the number of sections, the number of traffic lights, etc. The configuration packet is sent once during the AAPIInit. Then, the data packet to be sent to the external application at each simulation step is defined. The data packet, in our framework, contains the identification number of all the vehicles currently in the network, the identification number of the

AIMSUN   **MATLAB**
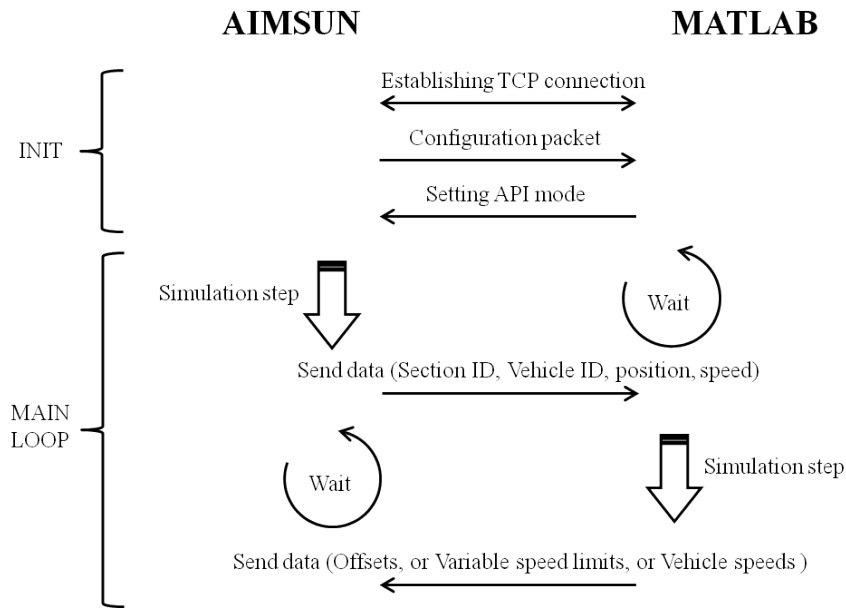
Figure A.3 – Description of the API communication protocol.

section in the network where each vehicle currently is, and the vehicles position, current speed, and previous speed. Also, functions to send and receive the data are defined, and such functions are blocking in the sense that the simulation is held until the transmission is complete.

MATLAB-side Interface

The MATLAB-side of the interface consists of scripts and functions, dual with respect to the Aimsun-side functions, that set up the communication, and use the real-time data coming from Aimsun to devise a control action.

The communication setup requires a TCP/IP address (i.e. localhost) and a port used for the data transmission, an initialization function that reads the configuration packet sent by Aimsun and transmits back the API operation mode (i.e. the control function to be executed in Aimsun), transmission functions to send and receive the data buffer, and synchronization functions to ensure that Aimsun and MATLAB run simultaneously. A summary of the interface and the communication protocol between Aimsun and MATLAB is provided in Figure A.3.

Once the communication is initialized, and the two platforms are synchronized, MATLAB processes the information coming in real-time from Aimsun during its simulation step. The objective in MATLAB is to provide a control action to be applied in Aimsun in real-time, in the form of traffic lights offsets, or maximum speed for each vehicle, or variable speed limits in each section. In or-

der to design and provide a controller, the microscopic data received from Aimsun must be treated to extrapolate additional information. In particular, macroscopic information can be obtained, which is useful both for validation of the proposed macroscopic models, and for the design of a controller. In the following, we will briefly describe the MATLAB data processing algorithms implemented for the experiments contained in this dissertation:

- *Number of vehicles in the section*. Knowing the position of each vehicle currently in the network, it is straightforward to compute the number of vehicles in each section.

- *Vehicle density in the section*. From the number of vehicles in the section, the density is computed.

- *Average speed in the section*. The current speed of each vehicle is provided by Aimsun, and from that the instantaneous average is calculated.

- *Length of the congested area within a section*. From a macroscopic perspective, the system is said to be in congestion when the average density grows past the critical density, and the speed decreases below the nominal free flow speed (see Chapter 3 for more details). Congestion in the microscopic simulator, analogously to the macroscopic case, arises whenever the vehicles decelerate below the maximum allowed speed. In practice, when a vehicle in the microscopic simulator has a negative acceleration and a speed lower than the speed limit, it is flagged as a candidate last-of-the-queue vehicle. Then the position of the flagged vehicles is checked in order to verify whether there is any inconsistent gap between the flagged vehicles and the last verified last-of-the-queue vehicle; it might happen that a vehicle has to slow down much upstream from the beginning of the actual queue. A compatible gap is defined as the safety interdistance that the vehicles have to keep, and it is a function of the maximum speed limit and the drivers' reaction time. A vehicle entering the congestion starts to decelerate and keeps a distance from the preceding vehicle lower than the nominal one. If the distance of the flagged vehicles from the preceding vehicles is bigger than the nominal one, they are unflagged, meaning that they had to decelerate because of other obstacles and they are not in the theoretical congestion. Among the remaining flagged vehicles, the most upstream one is marked as the last of the queue.

Extended Summary in French

Introduction

Le Coût du Trafic

L'Agence Internationale de l'Énergie IEA affirme que les tendances actuelles de la consommation et de l'approvisionnement d'énergie ne sont pas viables économiquement, écologiquement et socialement. Sans une action décisive, les émissions de CO_2 liées à l'énergie vont plus que doubler d'ici 2050, et l'augmentation de la demande de pétrole accroîtra les inquiétudes sur la sécurité des approvisionnements. Le IEA estime également que plus de 50% de la consommation de pétrole dans le monde est pour le transport, et les trois quarts de l'énergie utilisée dans le secteur du transport est consommée sur les routes. Par conséquent, il est crucial que les gouvernements du monde entier abordent le problème de la gestion de la consommation de carburant des véhicules [124].

La croissance de l'activité de transport soulève des inquiétudes pour sa durabilité environnementale. Selon les données de l'Agence Européenne pour l'Environnement [125], les transports ont représenté près d'un quart (23,8%) du total des émissions de gaz à effet de serre et un peu plus d'un quart (27,9%) des émissions totales de CO_2 dans le EU-27 en 2006. Aucun autre secteur montre un taux d'émissions de gaz à effet de serre aussi élevé que le secteur du transport.

L'élimination de la congestion urbaine est ni un objectif abordable, ni réalisable dans les zones urbaines économiquement dynamiques. Néanmoins, beaucoup peut être fait pour réduire son occurrence et son impact sur les usagers de la route. L'approche traditionnelle de l'expansion continue de l'infrastructure existante pour augmenter la capacité, malgré utile, est trop coûteuse, en plus d'être écologiquement intrusive. La plupart des villes ont pris ou envisagent de prendre des mesures pour résoudre ces problèmes en vue d'atteindre leurs objectifs à court et à long terme, qui comprennent l'évolution de la répartition modale du transport en faveur des transports publics, la réduction des émissions, la diminution d'accidents sur la route, etc.

Par conséquent, la motivation pour les ingénieurs et les chercheurs à aborder

le problème d'une meilleure gestion du trafic est très forte. Un large scénario de stratégies peut être adopté pour remédier à ces problèmes, et dans les dernières années, nous avons été témoins de différentes techniques et de nouvelles technologies. La littérature scientifique sur les stratégies de la gestion éco-responsable du trafic et de la congestion peut être divisée en deux grandes catégories : le contrôle du véhicule et le contrôle de l'infrastructure.

Dans ce qui suit, un bref aperçu des technologies existantes dans le domaine de la gestion du trafic sera présenté.

Éco-Management du Véhicule

L'adoption d'un style de conduite éco-responsable est l'objectif de "l'éco-conduite". Le comportement au volant peut avoir un grand impact sur les émissions, comme a été démontré par plusieurs études [133]. Typiquement quelques directives heuristiques sont généralement connus, tels que prévoir les flux de trafic, éviter les freinages, changer de rapport de vitesse plus tôt, couper le moteur lors des arrêts de courte durée. En outre, des outils et des systèmes qui aident le conducteur (ou le remplacent) dans l'exécution de l'éco-conduite ont également émergé. Une classification possible des systèmes d'éco-conduite existants est [117] comme suit :

1. Le systèmes *pré-trajet*, en plus de donner des conseils génériques sur l'éco-conduite, sont intégrés dans les systèmes de navigation. Pour tous les points d'origine et de destination donnés, et pour les fenêtres temporelles définies pour départ ou arrivée, le système calcule le temps de départ et la route optimale, basée sur les caractéristiques de la voiture et du conducteur, de manière à minimiser l'impact environnemental du voyage. Les dispositifs de conseil pré-trajet à bord du véhicule comprennent l'équipement, internet, les services de téléphonie, les appareils mobiles et la radio. Ces dispositifs de communication peuvent également être consultés par un utilisateur potentiel de la route pour prendre des décisions sur le moment auquel commencer le voyage, le choix des moyens de transport, le choix de l'itinéraire, etc.

2. Les systèmes *en-route* font partie de la catégorie plus large des ADAS et sont en outre classés en systèmes d'*évaluation en-ligne*, qui fournissent des conseils de rétroaction sur la base des performance actuelles, systèmes de *conseil en-ligne*, qui donnent un conseil prédictif basé sur les événements à venir, et "*predictive cruise control*", où la conduite automatique est effectuée. Le conseil en-route est accompli grâce aux services radio, messages variables au bord de la route et l'équipement à bord du véhicule, qui aident et informent les conducteurs de manière à prendre des

décisions de conduite appropriées. Bien que les services de radio fonctionnent depuis nombreuses années, le concept de la technologie dans les véhicules, les véhicules intelligents et la notion de ADAS sont relativement nouveaux et d'un grand intérêt pour la communauté scientifique et les entreprises. Comme interface principale, la majorité des systèmes utilisent des affichages visuels, tandis que des alertes sonores et pédale de gaz haptique sont appliquées en seulement quelques solutions. Les conseils en-route peuvent être fournis sous la forme d'un message d'information uniquement ou comme une recommandation de route explicite. Selon différentes enquêtes [130], la majorité des conducteurs semblent préférer le seul message d'information moins intrusive et être en mesure de prendre leurs propres décisions. Cependant ce type de conseils présente plusieurs inconvénients. La traduction de l'information dans une décision de routage appropriée nécessite une bonne connaissance du réseau de trafic et une réponse très rapide du conducteur. La diffusion de l'information est limitée par la capacité des moyens employés. La vraie limite est imposée de toute façon par la quantité d'informations que les conducteurs sont en mesure de traiter assez rapidement pour prendre une décision. Enfin l'influence sur les conditions de circulation n'est pas assurée car la décision est laissée aux conducteurs, et la conformité joue un rôle majeur. D'autre part, bien que capable d'influencer les conditions de circulation, les recommandations explicites de route sont limitées par l'obligation de ne pas suggérer des itinéraires désavantageux aux conducteurs.

3. Les systèmes *post-trajet* tentent d'accroître la motivation du conducteur pour l'éco-conduite en affichant des résultats encourageants, et des résumés et des statistiques qui peuvent être comparés à ceux d'autres conducteurs.

La plupart des approches sont basées sur des règles heuristiques ou bonnes pratiques qui sont associées à une conduite efficace en termes d'énergie. En outre, seulement quelques-uns sont prédictives, tandis que le reste est uniquement basé sur les informations de conduite actuelle, généralement extraites à partir des données de réseau du véhicule.

Cependant, plusieurs concepts émergent qui tentent de mettre en œuvre l'éco-conduite dans un cadre plus rigoureux. Dans ces concepts, l'éco-conduite est considérée comme un problème de contrôle optimal où les commandes minimisent la consommation d'énergie pour un trajet donné. Dans ce qui suit, une brève revue de la littérature sur le problème de l'éco-gestion du véhicule est présentée. La catégorisation sera basée sur le niveau de communication des différentes approches. En particulier, nous distinguons entre les stratégies isolées, qui n'utilisent pas les informations reçues de l'environnement, et les stratégies qui

utilisent les réseaux de communication de la route afin de fusionner différents éléments d'information provenant des agents du trafic à proximité.

Contrôle Isolé

Des travaux sur le contrôle optimal de l'énergie se retrouvent dans plusieurs domaines d'application. Des systèmes pré-trajet et post-trajet ont été proposées pour EVs [34, 35, 36, 37, 105], où les solutions analytiques et numériques du problème de contrôle optimal d'énergie visent à trouver le couple moteur et/ou la force de freinage. Des métriques pour l'évaluation du profil de conduite réelle par rapport à la solution optimale théorique sont fournies au conducteur pour une éducation à l'éco-conduite. Des travaux similaires ont été effectués pour HEVs où une solution analytique du problème de l'éco-conduite a été proposée [43, 71] pour trouver le rapport de vitesse optimal, la politique de commutation entre le moteur à combustion interne et le moteur électrique, la quantité de carburant injectée, ou la vitesse du moteur et le couple. En outre, des stratégies d'optimisation en-ligne sans connaissance préalable de l'horizon de conduite ont été présentées [115]. Quant aux ICEs, les solutions d'éco-conduite impliquent l'optimisation de la trajectoire [93], et/ou l'optimisation de la sélection du rapport de vitesse [55], afin de réduire la consommation de carburant.

D'autres travaux représentent des systèmes en-route d'éco-conduite. Il y a eu des cas de ADAS visuel avec l'objectif de minimiser la consommation de carburant et les émissions en fournissant des suggestions sur les profils de vitesse [11]. Aussi, il est possible de trouver dans la littérature quelques tentatives pour fournir une éco-gestion en-ligne des HEVs, avec une action transparente au conducteur qui minimise la consommation de carburant [97, 72].

Tous les travaux mentionnés ci-dessus traitent le problème de l'éco-conduite dans la perspective du véhicule, sans exploiter les informations provenant d'autres agents du réseau de trafic (par exemple d'autres véhicules, feux de circulation, etc.). Avec la montée des technologies de la communication, l'intérêt pour "la communication coopérative" est en croissance. Ceci peut être utilisé pour avertir les conducteurs des dangers à venir, de formuler des recommandations pour éviter le trafic, ou pour suggérer un profil optimal de conduite.

Contrôle Coordonné

Le concept d'utiliser la communication sans fil dans les véhicules a fasciné les chercheurs depuis la fin des années 80. Au cours de ces dernières années, il y a eu un intérêt croissant pour la recherche et le développement dans le domaine des réseaux de communication de route pour un contrôle coordonné du véhicule .

Les communications V2I et V2V promettent des améliorations révolutionnaires dans les transports, une meilleure efficacité énergétique, réduction des collisions, et la sécurité des occupants des véhicules ainsi que des piétons et des cyclistes.

Dans la communication V2I, l'infrastructure joue un rôle de coordination en rassemblant de l'information globale ou locale sur la circulation et les conditions routières, et ensuite en proposant certains comportements à des groupes de véhicules. Il est bien connu que environ la moitié de la consommation de carburant dans le trafic urbain est causée par démarrages et arrêts, par conséquent, le rôle des feux de circulation est crucial. Bien que les feux de circulation sont très importants pour la régulation du débit aux intersections, en particulier aux heures de pointe, ils provoquent une augmentation de la consommation d'énergie d'environ 10-20% sur les principales artères par rapport au cas d'une route idéale, sans intersections. La situation devient encore pire si on considère également le trafic additionnel aux intersections, qui a une priorité inférieure et est plus susceptible de s'arrêter aux feux de circulation. Par conséquent, la présence de feux de circulation dans la zone urbaine peut amener à une consommation 20-40% plus élevée [14]. La recherche dans cette sous-catégorie de la communication a montré comment la communication V2I peut réduire la consommation de carburant et les émissions à une intersection signalisée. En d'autres termes, il est possible de suivre un profil de vitesse et d'accélération optimal pour éviter l'arrêt aux feux de circulation et réduire la consommation d'énergie. L'application GLOSA offre l'avantage d'une information exacte et opportune sur les temps et la localisation des feux de signalisation. Elle fournit des conseils de vitesse aux conducteurs, pour les guider avec une vitesse plus constante et avec moins de temps d'arrêt à travers les feux de signalisation. Une réduction de 7% de la consommation moyenne de carburant et jusqu'à 89% du temps d'arrêt moyen a été prouvé dans des études préliminaires [69]. Lorsque le scénario implique un feu de circulation unique, l'objectif est d'optimiser les profils de vitesse et d'accélération pour l'approche à l'intersection afin de réduire la consommation d'énergie [78, 80, 107]. Cependant, il a été démontré qu'un GLOSA impliquant multiples intersections signalisées donne une meilleure performance, à la fois en termes de consommation d'énergie et de temps de parcours [119].

Une autre application de la communication V2I est représentée par le ARC dans lequel la communication entre les véhicules et l'infrastructure est bidirectionnelle, et est utilisée pour recueillir des informations sur la longueur des files d'attente aux feux de circulation. Lorsque la file d'attente grandit à un certain seuil, un avis routage est diffusé aux véhicules afin de trouver des routes alternatives et plus rapides [142].

La communication V2V, plus difficile à réaliser en raison de sa structure décentralisée, vise à organiser l'interaction entre les véhicules, et à établir des col-

laborations entre eux. L'information est échangée, et les décisions sont prises sur une base "locale". Dans le concept V2V, lorsque deux ou plusieurs véhicules ou des stations au bord de route sont à portée de communication radio, ils se connectent automatiquement et établissent un réseau ad-hoc permettant le partage des données de position, vitesse et direction. La recherche sur les avantages de l'utilisation de la communication V2V a soulevé plusieurs applications intéressantes pour améliorer la performance de la circulation [73, 77, 76, 67].

Éco-Management de l'Infrastructure

Dan le domaine du contrôle du trafic, on trouve souvent des termes techniques indiquant les composants de l'architecture du réseau de trafic. Une *intersection* se compose d'un certain nombre d'approches et de la zone de croisement. Une *approche* peut avoir une ou plusieurs voies, mais a une file d'attente unique et indépendante. Les approches sont utilisées par les flux de trafic, qui sont généralement mesurés en véhicules par heure. Le *flux de saturation* est le débit moyen traversant la ligne d'arrêt d'une approche lorsque le flux correspondant a droit de passage, la demande en amont (ou la file d'attente) est suffisamment grande, et le tronçon de route en aval n'est pas bloqué par les files d'attente. Deux flux compatibles peuvent traverser en toute sécurité l'intersection simultanément, sinon ils sont appelés antagonistes.

Lorsque on utilise les feux de circulation comme entrées de commande pour le problème de contrôle de la circulation, les ingénieurs du trafic ont la possibilité d'agir sur quatre variables qui décrivent pleinement les modes de fonctionnement des feux [103] :

- *Temps de cycle* : une répétition de la série de base des combinaisons des signaux à un carrefour ; des cycles plus longs augmentent généralement la capacité d'intersection car le proportion des temps perdus devient en conséquence plus petit ; d'autre part, l'allongement des temps de cycle peut augmenter les retards des véhicules aux intersections en raison de plus longues attentes lors de la phase rouge.
- *Stage* ou *phase* : une partie du cycle du signal, au cours de laquelle un ensemble de flux a le droit de passage ; il peut avoir un impact majeur sur la capacité d'intersection et l'efficacité.
- *Split* : durée relative du vert de chaque phase qui doit être optimisée en fonction de la demande.
- *Offset* : décalage entre les cycles d'intersections successives qui peut donner lieu à une "onde verte".

Le stratégies de réglage des feux de circulation peuvent être soit de type *temps fixe* soit *sensibles au trafic*. Les stratégies temps fixe (également appelées pré-programmées) utilisent des données historiques de trafic, et donnent un réglage

du signal de trafic selon le moment de la journée. Le problème d'optimisation est résolu hors ligne. D'autre part, les méthodes sensibles au trafic (aussi appelées en temps réel) utilisent des données en temps réel pour définir les plans des feux pour la mise en œuvre immédiate sur un horizon temporel court.

Une autre stratégie de contrôle du trafic par l'infrastructure est représenté par les panneaux à messages variables. Les panneaux affichant des conseils de vitesse ont été proposé dans les années 80 en tant que service d'aide à la conduite, et sont devenus de plus en plus populaires pour leur impact sur la consommation d'énergie et la réduction du temps d'arrêt. Un des inconvénients de ce type d'assistance à la conduite est le taux de conformité aux conseils. Toutefois, les informations sur la vitesse en milieu urbain peuvent compter sur l'aversion innée des conducteurs de s'arrêter aux feux de signalisation, ce qui peut assurer un niveau élevé de conformité.

L'idée clé est plutôt simple : une certaine vitesse est suggéré aux conducteurs afin de trouver un feu vert à la prochaine intersection signalisée. La façon la plus simple de le faire est de placer un panneau, affichant des chiffres contrôlés électroniquement, sur le côté de la route à une centaine de mètres après le feu de circulation précédent. Le panneau est relié au feu à venir et, à partir de la connaissance de combien de secondes manquent au prochain vert, une vitesse appropriée est calculée et affichée. Le conducteur qui se conforme est récompensé avec un feu vert ; les non-conformistes vont très probablement trouver un rouge. Cette stratégie est très efficace, comme l'expérience avec un tel système a montré à Düsseldorf, en Allemagne, où pratiquement tous les conducteurs respectent la vitesse affichée [14]. De toute évidence, les vitesse affichées augmentent avec le temps, jusqu'à une vitesse maximale. À ce stade, le panneau est réinitialisé avec un conseil de vitesse relatif à la phase verte suivante. Düsseldorf, en Allemagne, a été probablement l'un des pionniers de cette stratégie, qui remonte à il y a plus de 30 ans.

Une brève revue littéraire des stratégies de gestion du trafic sera présentée. Il existe des enquêtes très complètes et exhaustives sur les stratégies de contrôle de la circulation routière [103, 100]. Dans ce qui suit, la classification sera faite en fonction du niveau et de la complexité de communication et d'information que les différentes utilisent. En particulier, nous ferons la distinction entre les stratégies isolées de gestion, qui utilisent seulement l'information locale, et les stratégies coordonnées, ce qui utilisent l'information provenant du réseau afin de concevoir une mesure de contrôle centralisée ou distribuée.

Contrôle Isolé

Les stratégies isolées à temps fixe ne sont applicables et efficaces que en conditions de faible saturation du trafic. Dans cette classe les stratégies basées sur les

stages déterminent les *splits* optimaux et les temps de cycle de façon à minimiser le retard total (le temps perdu en raison de la congestion) ou à maximiser la capacité de l'intersection. Les stratégies basées sur les *phases* ne déterminent pas seulement les *splits* optimaux et les temps de cycle, mais aussi la séquence optimale des phases, qui peut être un élément important pour les intersections complexes.

En revanche, le stratégies isolées sensibles au trafic utilisent des mesures en temps réel fournies par les capteurs inductifs, qui sont généralement situés à quelques mètres en amont de la ligne d'arrêt aux intersections. Une des stratégies les plus simples dans cette classe est la méthode de véhicule-intervalle qui est applicable aux intersections à deux *phases*. Une durée minimale de vert est assignée aux deux *phases*. Si aucun véhicule ne passe les détecteurs au cours du vert, la stratégie procède à la *phase* suivante. Si un véhicule est détecté, un intervalle critique est créé, au cours duquel chaque véhicule détecté correspond à un prolongement du vert qui permet au véhicule de traverser l'intersection. Si aucun véhicule n'est détecté pendant l'intervalle critique, la stratégie passe à la phase suivante, sinon, un nouvel intervalle critique est créé, et ainsi de suite, jusqu'à une valeur maximale de vert pré-spécifiée.

Des études sur l'allocation de pelotons aux intersections signalisées en ajustant la durée du vert ont également été menées dans [23], et, dernièrement, ont trouvé la mise en œuvre pratique dans quelques cas [99]. Pour intersections complexes isolées avec des approches multiples, une optimisation des paramètres de priorité de passage a été présentée dans [27]. Une solution intéressante de la gestion des intersections isolées est représentée par les méthodes d'auto-organisation pour le contrôle des feux de circulation [51, 52, 74]. Ces méthodes sont totalement décentralisées, pas de communication entre les feux de circulation est nécessaire, et les feux de circulation sont affectés par leurs voisins indirectement, en utilisant des véhicules et des pelotons comme information.

Contrôle Coordonné

En présence d'une séquence d'intersections signalisées sur une artère urbaine, la coordination des feux de circulation est très importante et la notion de *offset* entre en jeu. Si l'artère est correctement coordonnée et les signaux décalés dans le temps, les feux de circulation peuvent donner lieu à un "onde verte", de sorte que trouver un feu vert à une intersection assure trouver un vert aussi à celles en aval. Cela est vrai dans des conditions de "free flow" ; si une congestion survient et perturbe le système, cette coordination devient inefficace et les files d'attente se propagent en arrière. D'autres mesures sont donc nécessaires afin d'atténuer la congestion.

MAXBAND [86, 87] considère une artère à deux directions avec n feux (in-

tersections), et précise les *offsets* afin de maximiser le nombre de véhicules qui peuvent voyager au long de l'artère en suivant une vitesse conseillée sans s'arrêter aux feux, dans les deux directions de voyage.

TRANSYT [111] est probablement le plus célèbre algorithme "offline" de contrôle des feux de signalisation et est basé sur un modèle de trafic qui est utilisé pour estimer l'évolution dans le temps de la taille des files d'attente. La fonction objectif à minimiser est la somme des files d'attente moyennes.

Le principal inconvénient des stratégies à temps fixe est que leurs paramètres sont basés sur des données historiques plutôt que des données en temps réel. La circulation routière et les exigences ne sont pas constantes dans le même jour, et peuvent varier dans le long terme ou occasionnellement en raison d'événements spéciaux. Les mouvements tournants peuvent aussi varier et affecter les demandes. En outre, les mouvements tournants peuvent varier en réponse aux paramètres des signaux optimisés, puisque les conducteurs peuvent essayer d'optimiser leur temps de parcours individuel. Vieillissement des réglages optimisés peut également conduire à une forte inefficacité. SCOOT [63], développé en Angleterre, est probablement aujourd'hui le plus célèbre et adopté mesure de contrôle sensible aux changements des conditions de trafic. SCATS [89] a été élaboré presque en même temps en Australie. Après ces premiers, et pourtant largement employées, stratégies dynamiques de gestion de la congestion, un certain nombre d'algorithmes plus rigoureux basés sur des modèles ont été développés : OPAC [46], RHODES [118], PRODYN [61], Cronos [15], UTOPIA [92].

Les stratégies susmentionnées représentent des solutions industrielles qui ont trouvé large diffusion pratique. Cependant, leur architecture hiérarchique et stratifiée complexe, ainsi que l'absence de références scientifiques détaillées, rend difficile de comprendre pleinement leurs principes de fonctionnement, et de les comparer à d'autres stratégies. Au contraire, les stratégies de contrôle décrites ci-après sont bien documentées dans la littérature. TUC [32] est basé sur l'approche de modélisation *store-and-forward* [49], et il se compose de quatre modules de commande distinctes pour les *splits*, les *temps de cycle*, les *offsets* et les priorités pour les transports publics.

Une approche distribuée récente qui a largement inspiré les chercheurs est l'algorithme "max-pressure", défini pour les réseaux arbitraires d'intersections signalisées [135, 134, 138], et inspiré par la planification de la transmission de paquets dans les réseaux sans fil. Les calculs de la stratégie "max-pressure" sont locaux : l'évaluation à chaque intersection à tout moment exige des connaissances que des files d'attente aux routes adjacentes à ce moment.

Contributions Principales de la Thèse

Les contributions de ce travail à la gestion éco-responsable du trafic se situent à la fois dans la gestion côté véhicule et dans la gestion côté infrastructure, et peuvent être résumées comme suit.

Tout d'abord, une solution pour le contôle coordonné des véhicules a été proposée, dans laquelle la communication avec l'infrastructure est exploitée pour réduire la consommation d'énergie du véhicule. En particulier, les plans des feux de circulation sont supposés être communiqués au véhicule et connus, et une vitesse optimale de conduite est suggérée au véhicule à travers une séquence de carrefours à feux sans arrêt, tout en suivant une trajectoire à énergie minimale. Par rapport à la littérature existante, la solution proposée aborde le problème de la consommation d'énergie en la considérant explicitement dans l'optimisation, prend en compte multiples feux de circulation dans un grand axe urbain, et présente un modèle de consommation énergétique qui représente également les accélérations causées par les conseils de vitesse variables. L'algorithme proposé, appliqué indépendamment à chaque véhicule, a été testé dans un simulateur de trafic microscopique afin d'évaluer l'impact sur les performances du trafic. L'analyse a montré que la consommation d'énergie et le nombre d'arrêts peuvent être considérablement réduits sans affecter le temps de parcours.

D'autre part, une solution pour la gestion isolée de l'infrastructure a été proposée. Un nouveau modèle macroscopique de trafic urbain a été introduit pour décrire l'évolution de la circulation, et les limites de vitesse variables ont été utilisées comme actionnement pour améliorer les performances de la circulation. Un modèle de la consommation d'énergie macroscopique a été adaptée au modèle de circulation mis en place. L'analyse a été effectuée sous des conditions de trafic saturé, avec des plans des feux donnés et fixes. L'optimisation vise à réduire la consommation d'énergie en compromis avec le temps de parcours moyen des véhicules dans le tronçon de route considéré. Des expériences ont démontré qu'il existe une limite de vitesse optimale qui améliore les performances du trafic en réduisant la longueur de la file d'attente au feu de signalisation, et en redistribuant la densité de véhicules de façon plus efficace.

Enfin, une solution pour la gestion coordonnée de l'infrastructure a été proposée. La coordination des feux de circulation sur les artères a été prouvée pour être efficace en termes de réduction des retards. Notre analyse a démontré qu'un problème d'optimisation peut être défini pour prendre en compte également les aspects énergétiques. En particulier l'action de contrôle est exercée à la fois sur la coordination des feux de circulation et sur les limites de vitesse variables dans chaque section de la route de la topologie considérée. Des expériences approfondies dans un simulateur de trafic microscopique ont montré qu'il existe une corrélation entre la progression du trafic et des mesures de performance de la
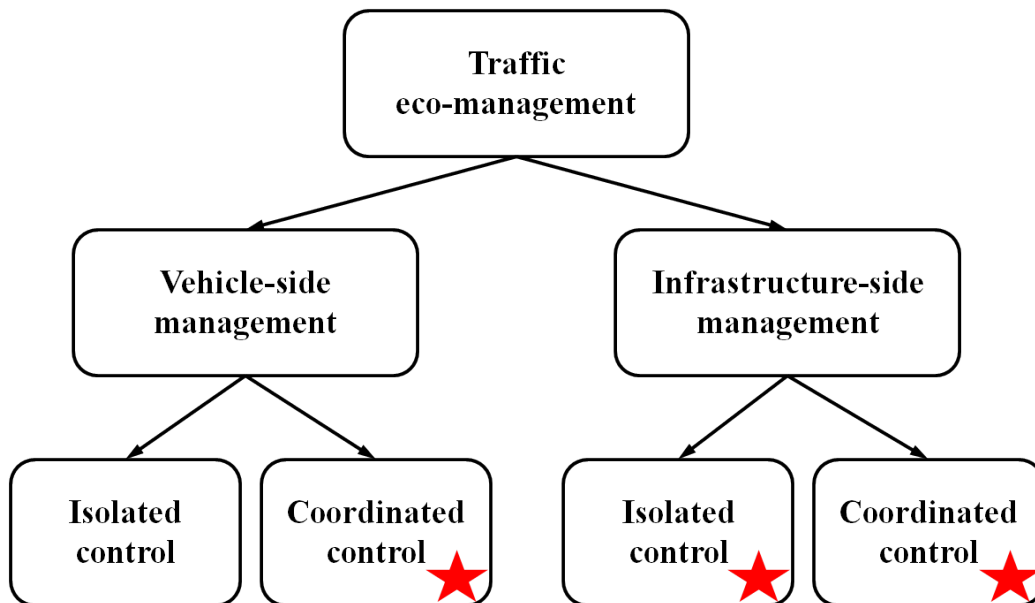
Figure 1 – Classification des stratégies de gestion du trafic. Les étoiles rouges indiquent où les contributions de cette thèse se situent par rapport à la littérature scientifique existante.

circulation, comme la consommation d'énergie et le temps de parcours. La stratégie de contrôle proposée est capable d'atteindre une réduction significative de la consommation d'énergie, presque complètement éliminer le nombre d'arrêts et le temps à l'arrêt, sans affecter le temps de parcours.

Trajectoire Optimale du Véhicule dans une Artère Urbaine Signalisée

Formulation du Problème

Ce travail a pour objectif la minimisation de l'énergie consommée par les véhicules dans un réseau de trafic pour aller d'une origine à une destination, en présence d'intersections signalisées dans l'horizon de conduite. Il est clair que ce problème n'est pas banale car le temps de parcours, et les profils d'accélération et de vitesse d'un véhicule, sont affectés par d'autres agents du réseau de trafic, dont les actions et les priorités peuvent entrer en conflit avec les contraintes de temps des véhicules.

L'analyse est effectuée pour un réseau de trafic urbain simplifié avec des véhicules en "free flow", sans contraintes provenant d'autres utilisateurs de l'infra-

structure. Cependant, nous allons montrer que l'algorithme peut être utilisé également dans des scénarios plus réalistes où la présence de plusieurs véhicules nécessite que le conseil de vitesse soit mis à jour dynamiquement.

On assume que la communication I2V donne aux véhicules une connaissance complète des plans des n feux de signalisation dans l'horizon de conduite.

D'un point de vue mathématique, un problème d'optimisation sous contrainte peut être formalisé. La consommation d'énergie au cours du déplacement doit être minimisée, sous contrainte du modèle dynamique du véhicule, et des temps d'arrivée aux intersections au cours d'une phase verte.

Modèle du Véhicule

Les véhicules équipés de moteurs électriques seront pris en compte dans ce travail. Le modèle dynamique longitudinale du véhicule peut être généralement écrit :

$$m\frac{\mathrm{d}v}{\mathrm{d}t} = F_t - F_{\text{aero}} - F_{\text{friction}} - F_{\text{slope}} \tag{1}$$

où F_t est la force de traction sur les roues, F_{aero} la force aérodynamique, F_{friction} la force de résistance au roulement, F_{slope} la force de gravité, v la vitesse du véhicule, et m sa masse.

Dans ce qui suit, nous supposons qu'il n'y a pas de pertes dans la transmission, pas de glissement au niveau des roues, et que la pente de la route ne varie pas dans l'espace. En particulier, la pente de la route peut être approximée par une valeur moyenne. La somme des frottements aérodynamiques et de roulement peut être approximée comme un polynôme de deuxième ordre en fonction de la vitesse v [34, 36].

Sous ces hypothèses le modèle du véhicule peut être simplifiée comme suit :

$$\begin{cases} \dot{x} = v \\ \dot{v} = h_1 u - h_2 v^2 - h_3 v - h_0 \end{cases} \tag{2}$$

avec

$$h_1 = \frac{R_t}{mr}, \quad h_2 = \frac{a_2}{m}, \quad h_3 = \frac{a_1}{m}, \quad h_0 = \frac{a_0}{m} + g\sin(\alpha) \tag{3}$$

Par conséquent, la demande de puissance peut être exprimée comme suit :

$$P = b_1 u v^2 + b_2 u \tag{4}$$

où

$$b_1 = \frac{R_t}{r}, \quad b_2 = \frac{R_a}{\kappa^2} \tag{5}$$

Plan des Feux de Signalisation

Dans cette étude, les feux de circulation ne sont pas actionnés, donc le temps de cycle, temps de phase et de décalage sont déterministes et donnés. Il est possible de formuler mathématiquement l'évolution de l'état des feux de circulation comme suit :

$$s_i(\tau) = \begin{cases} 1, & kT < \tau - \theta_i \leqslant kT + T_{\text{gr}} \\ 0, & kT + T_{\text{gr}} < \tau - \theta_i \leqslant (k+1)T \end{cases} \tag{6}$$

où s_i est l'état de l'i-ième feu, $k \in \mathbb{Z}$ est le nombre de cycles, T est le temps de cycle, T_{gr} est la durée de la phase verte, et $\theta_i \in [0, T)$ est le décalage du feu à l'intersection i, pour $i \in \{1, \ldots, n\}$.

Problème de Contrôle Optimal

Enfin, le problème d'optimisation peut être énoncé comme suit :

$$\begin{cases} \min_u & J = \int\limits_{t_0}^{t_f} b_1 uv + b_2 u^2 \, \mathrm{d}t \\ \text{s.t.} & \dot{x} = v \\ & \dot{v} = h_1 u - h_2 v^2 - h_3 v - h_0 \\ & x(t_0) = d_0, \quad x(t_f) = D \\ & x(t_i) = d_i \wedge s_i(t_i) = 1 \\ & v(t_0) = v_0, \quad v(t_f) = v_f \\ & v_{\min} \leq v \leq v_{\max} \\ & u_{\min} \leq u \leq u_{\max} \end{cases} \tag{7}$$

où (t_0, D_0) sont les coordonnées du véhicule à l'origine de l'horizon de conduite, (t_f, D) sont les coordonnées de la destination de l'horizon de conduite, t_i est le temps de passage à la i-ième intersection, d_i est la position de l'i-ième intersection, pour $i \in \{1, \ldots, n\}$, v_0 et v_f sont les vitesses initiale et finale.

Une solution à un problème simple, sans feux de circulation et avec un modèle du véhicule simplifié, a été trouvée analytiquement dans [105]. Dans le cas sous analyse, les feux de circulation introduisent une complexité supplémentaire au problème, exprimée mathématiquement par la contrainte :

$$x(t_i) = d_i \wedge s_i(t_i) = 1 \tag{8}$$

L'équation (8) impose une exigence de ne pas s'arrêter à l'intersection signalisée, en précisant que le véhicule doit être à l'intersection d_i a l'instant t_i, lorsque

le feu s_i est vert. Cette contrainte représente des ensembles disjoints en raison de la présence de plusieurs phases vertes disponibles à chaque intersection, et peut affecter la convexité du problème. En d'autres termes la contrainte (8) définit un ensemble non-convexe, et la fonction objective non linéaire, en raison de cette discontinuité dans les contraintes, assume minima locaux multiples. Par conséquent, la solution à ce problème de contrôle optimal doit être recherchée d'une manière sous-optimale, par l'utilisation d'algorithmes qui simplifient l'enveloppe de contrôle, récupèrent la convexité des contraintes fixées et résolvent l'optimisation en conseillant au conducteur la vitesse à suivre.

Algorithme d'Optimisation

Le problème initial de la commande optimale (7) sera désormais divisé en sous-problèmes pour la simplification de la contrainte (8) et la formulation d'un problème d'optimisation convexe. L'idée est d'identifier la meilleure phase verte à chaque intersection, pour finalement optimiser sur une trajectoire unique de l'origine à la destination.

La méthodologie peut être décrite comme suit :

1. Algorithme d'"élagage" pour identifier l'ensemble des intervalles faisables de phases verts à chaque intersection. La notion de faisabilité se réfère à des intervalles de temps qui permettent de ne pas s'arrêter et de conduire dans le respect des limites de vitesse ($v \in [v_{\min}, v_{\max}]$). L'algorithme d'élagage permettra de réduire l'espace de recherche de la meilleure trajectoire dans l'horizon de conduite.

2. Construction d'un graphe orienté acyclique pondérée dans la région de faisabilité, rapprochant le coût de l'énergie de toutes les trajectoires possibles dans l'horizon de conduite. L'algorithme de Dijkstra [38] est ensuite exécuté sur le graphe d'approximation afin d'identifier la meilleure trajectoire, ou bien la plus efficace en termes d'énergie. Avec le choix d'une trajectoire unique dans l'horizon de conduite, le problème d'optimisation deviendra convexe.

3. Solution d'un problème d'optimisation convexe simple pour obtenir les temps de passage optimaux à chaque intersection à travers les phases vertes sélectionnées.

Algorithme d'Élagage

L'algorithme d'élagage de vitesse réduit l'espace de recherche des phases vertes disponibles en identifiant que ceux qui permettent d'atteindre la destination au temps fixé sans arrêt, et en conformité avec les limites de vitesse imposées.
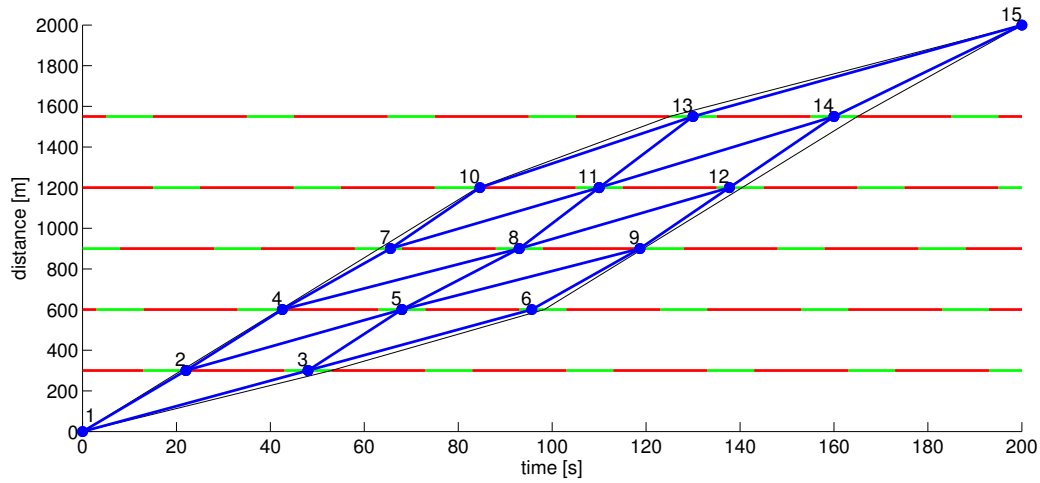
Figure 2 – Graph of the possible trajectories within the feasibility region, with one node per green phase (nodes = 15, edges = 22). The labels indicate the ID of the node.

La sortie de l'algorithme est $\{t_{i,\min}, t_{i,\max}\}$, $\forall i \in \{1, \ldots, n\}$, qui représentent respectivement le temps d'arrivée minimal et maximal possible à la i-ième intersection.

Trajectoire Optimale

Après l'exécution de l'algorithme d'élagage, l'ensemble des phases vertes possibles est considérablement réduit. Cependant, beaucoup de trajectoires possibles de l'origine à la destination sont toujours présentes, et la contrainte (8) définit encore un ensemble disjoint, en raison de la présence de plusieurs phases vertes disponibles à chaque intersection.

L'idée est de rapprocher, au moyen d'un graphe orienté acyclique pondéré, le coût énergétique de toutes les trajectoires possibles dans la région de faisabilité, comme le montre la Figure 2. L'approximation consiste à placer les nœuds du graphe en correspondance de certains temps de passage dans les phases vertes acceptables. Le nombre de nœuds par phase verte possible dépend de la finesse de l'approximation. Dans le cas d'un nœud par phase verte, le nœud sera placé au milieu de l'intervalle vert possible. Dans le cas de trois nœuds par phase verte, les nœuds seront placés au milieu et aux deux extrémités de l'intervalle vert possible. Dans le cas d'une approximation plus fine, les nœuds seront également espacés, en gardant toujours un nœud au milieu et deux nœuds aux deux extrémités de l'intervalle vert possible.

Par conséquent, soit $\mathcal{G} = (N, M)$ un tel graphe, où N est l'ensemble des

nœuds p_i, pour $i = 1, \ldots, |N|$, représentant les temps de passage à chaque phase verte possible, et M est l'ensemble des trajets possibles (ou arcs) reliant les nœuds du graphe. Définissons également une fonction de pondération $w : M \rightarrow W$, qui associe chaque arc du graphe avec un poids. Dans cette application, le poids W est le coût énergétique pour voyager le long de la trajectoire, et il peut être considéré comme la somme de deux contributions :

$$W = E_{\text{total}} = E_{\text{link}} + E_{\text{jump}} \tag{9}$$

L'énergie consommée par le véhicule sur un arc est due à un déplacement à vitesse constante, qui est achevé en ΔT secondes, sans aucune accélération et avenc une demande de puissance invariable dans le temps :

$$E_{\text{link}} = \Delta T \left(b_1 \bar{u}\bar{v} + b_2 \bar{u}^2 \right) \tag{10}$$

où $\bar{v} = \frac{d_i - d_{i-1}}{\Delta T}$ est la vitesse constante sur l'arc, et $\bar{u} = \frac{1}{h_1} \left(h_2 \bar{v}^2 + h_3 \bar{v} + h_0 \right)$ est dérivé de (2). Le temps de parcours sur un arc est défini comme $\Delta T = \tau_{p_j} - \tau_{p_i}$, pour chaque arc $(p_i, p_j) \in M$, et $p_i, p_j \in N$, étant τ le temps de passage associé au nœud.

L'énergie associée au changement de vitesse à un nœud entre les deux arcs, se définit comme :

$$E_{\text{jump}} = \int_0^{t_{\text{jump}}} b_1 u(t)v(t) + b_2 u(t)^2 \, \mathrm{d}t \tag{11}$$

où $u(t) = \frac{1}{h_1} \left(\dot{v}(t) + h_2 v(t)^2 + h_3 v(t) + h_0 \right)$ de (2), et $v(t)$ est la vitesse variante dans le temps dans chaque transitoire linéairement modélisée comme $v(t) = \bar{v}_{\text{in}} \pm a \cdot t$, avec a étant une accélération constante fixe, et $\bar{v}_{\text{in}}$ la vitesse constante sur l'arc entrant au nœud. Le changement de vitesse est supposé être effectué en $t_{\text{jump}} = \frac{|\bar{v}_{\text{out}} - \bar{v}_{\text{in}}|}{a}$, avec $\bar{v}_{\text{out}}$ étant la vitesse constante sur l'arc sortant du nœud. Notez que le freinage par récupération est pas considéré dans cette analyse, donc E_{jump} est borné inférieurement par 0.

Le principal défi de cette approximation est représenté par l'assignation des poids sur les arcs. Chaque nœud du graphe avec deux ou plusieurs arcs entrants est critique car $\bar{v}_{\text{in}}$ n'est pas unique, et cela génère contributions E_{jump} multiples et ambiguës pour l'arc sortant. Par conséquent, les nœuds critiques doivent être "découplés" afin d'avoir une affectation de poids correcte.

L'analyse conduite sur le graphe dual permet de résoudre cette criticité. Finalement, l'algorithme de Dijkstra peut être exécuté sur le graphe dual afin d'obtenir la trajectoire la plus efficace en termes d'énergie de l'origine à destination. L'algorithme de Dijkstra restitue les nœuds optimales à traverser.

Problème d'Optimisation Simplifié

Une fois que l'algorithme de Dijkstra a fourni la trajectoire la plus efficace sur le graphe d'approximation, le problème peut être enfin formulé comme une optimisation convexe. Les ensembles disjoints donnés par la contrainte (8) sont résolus, et un seul intervalle de temps par intersection représente désormais le domaine de l'optimisation.

Définissons d'abord un vecteur de variables d'optimisation (temps d'arrivée aux intersections), étant n le nombre d'intersections :

$$\mathbf{x} = [t_1, t_2, \ldots, t_n]^T \in \mathbb{R}^n \tag{12}$$

Puis un vecteur des temps de parcours pour chaque segment est défini :

$$\mathbf{t} = \mathbf{t}(\mathbf{x}) = [t_1 - t_0, t_2 - t_1, \ldots, t_n - t_{n-1}, t_f - t_n]^T \tag{13}$$

Connaissant la position des feux de circulation, nous définissons alors le vecteur des vitesses constantes dans chaque segment :

$$\mathbf{v} = \mathbf{v}(\mathbf{x}) = [v_1, v_2, \ldots, v_n, v_{n+1}]^T$$
$$= \left[\frac{d_1 - d_0}{t_1 - t_0}, \frac{d_2 - d_1}{t_2 - t_1}, \ldots, \frac{d_n - d_{n-1}}{t_n - t_{n-1}}, \frac{D - d_n}{t_f - t_n} \right]^T \tag{14}$$

où d_i est la position de l'i-ième feu, D est la destination, t_f est le temps final de l'horizon de conduite, $\mathbf{t} \in \mathbb{R}^{n+1}$, $\mathbf{v} \in \mathbb{R}^{n+1}$.

La fonction objectif peut être écrite sous la forme :

$$J(\mathbf{x}) = \mathbf{t}^T \bar{P}(\mathbf{v}) + \sum_{i=0}^{n+1} E_{\text{jump}} \tag{15}$$

où $\bar{P}(\mathbf{V})$ est la puissance requise par le véhicule lors des déplacements à vitesse constante :

$$\bar{P}(\mathbf{v}) = b_1 \bar{u}(\mathbf{v})\mathbf{v} + b_2 \bar{u}(\mathbf{v})^2 \tag{16}$$

avec

$$\bar{u}(\mathbf{v}) = \frac{1}{h_1} \left(h_2 \mathbf{v}^2 + h_3 \mathbf{v} + h_0 \right) \tag{17}$$

Enfin, le problème d'optimisation peut être formulée comme :

$$\begin{cases} \min_{\mathbf{x}} J(\mathbf{x}) \\ \max \left\{ t_i^-, t_{i,\min} \right\} \leq t_i \leq \min \left\{ t_i^+, t_{i,\max} \right\} \end{cases} \tag{18}$$

où t_i^- et t_i^+ sont constantes et représentent les instants aux marges de la phase verte sélectionnée à chaque intersection, et $t_{i,\min}$ et $t_{i,\max}$ sont les temps de passage minimales et maximales faisables donnés par l'algorithme d'élagage.

Expériences

Scénario de Contrôle

Le cas à l'étude présente un scénario avec un seul véhicule dans le réseau de trafic. Cependant, il peut être conceptuellement étendu au cas de plusieurs véhicules en "fre flow", chacun équipé de l'algorithme présenté. Effets de la circulation, tels que les contraintes d'interdistance et de passages de piétons, sont pris en charge par nouvelles exécutions de l'algorithme.

Le véhicule doit traverser $n = 5$ intersections signalisées, le long d'un tronçon de route de $2000\,\mathrm{m}$ sur un horizon temporel total de $200\,\mathrm{s}$. La distance entre les intersections est d'environ $300\,\mathrm{m}$. Le choix du temps et de la distance finale de l'horizon de conduite est fait de telle manière à maintenir une vitesse moyenne globale réaliste d'environ $v = 10\,\mathrm{m/s}$. L'objectif du véhicule est de suivre un profil de vitesse optimale énergétiquement qui permet de trouver tous les feux au vert. On ne fait aucune hypothèse sur l'existence d'une "onde verte". Il est clair que son existence permettrait une solution plus facile, ce qui l'algorithme présenté est en mesure de trouver. Le problème est rendu encore plus complexe et intéressant par la disposition aléatoire des phases vertes, et par conséquent par la présence de plus d'options de trajectoire. La durée de la phase verte est de $10\,\mathrm{s}$, le temps de cycle total est fixé à $30\,\mathrm{s}$.

La vitesse initiale du véhicule est variée tout au long des simulations pour évaluer son impact sur la consommation d'énergie et sur la trajectoire optimale. Les feux de circulation, la vitesse finale et l'horizon sont fixés pour la cohérence des résultats. L'objectif des simulations effectuées est de prouver l'importance d'une méthodologie qui permet de parvenir à une solution sous-optimale rapide appropriée pour l'assistance en ligne à l'éco-conduite.

Validation de la Trajectoire Optimale

La première partie des résultats de simulation présentés vise à valider l'algorithme d'élagage et l'identification de la trajectoire optimale au moyen du graphe d'approximation et l'algorithme de Dijkstra. La Programmation Dynamique (DP), utilisée par la suite comme une référence, fournit la solution optimale au problème, et elle a été utilisée pour calculer le coût énergétique de toutes les trajectoires possibles dans la région faisable.

Dans la Figure 3 la consommation d'énergie de chaque trajectoire calculée via DP est comparée avec l'approximation de la consommation d'énergie calculée par la stratégie proposée (évaluation numérique de la fonction objectif du problème (18). Les résultats pour les deux choix différents de vitesse initiale sont reportés après normalisation par rapport au coût maximal calculé avec la DP dans chaque configuration. La trajectoire de coût minimal, pour chaque cas, est en vert. L'ap-
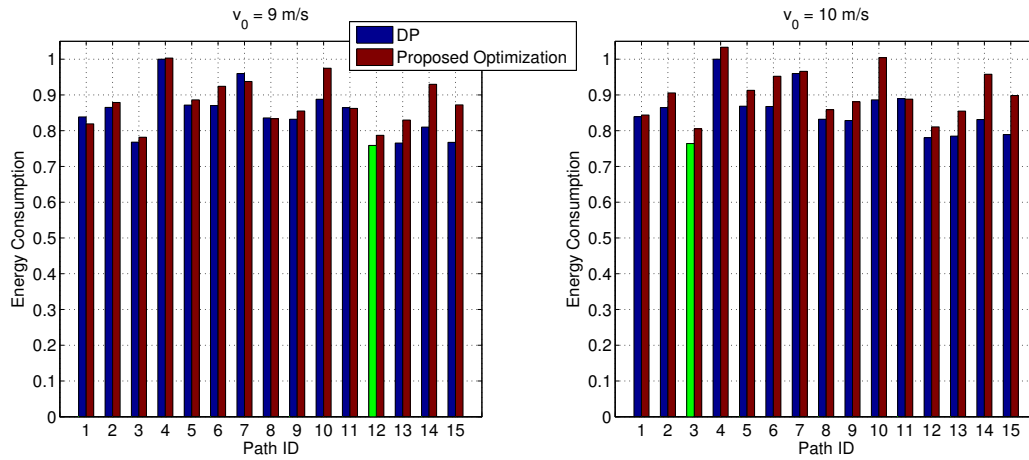
Figure 3 – Comparaison entre la DP et la stratégie proposée pour le calcul de la consommation d'énergie sur toutes les trajectoires possibles. Deux cas avec différentes vitesses initiales sont reportés. En vert la trajectoire la plus efficace en termes d'énergie.

Tableau 1 – Identification de la trajectoire optimale (Graphe vs. DP)

v_0 [m/s] Graphe	5	6	7	8	9	10	11	12	13	14
1 nœud/phase verte	15	15	15	15	3	3	3	3	3	3
3 nœuds/phase verte	12	12	12	12	12	3	3	3	3	3
DP (trajectoire optimale)	12	12	12	12	12	3	3	3	3	3

proximation des coûts énergétiques obtenue avec la stratégie proposée est très proche du vrai coût énergétique calculé avec la DP.

La consommation d'énergie varie en fonction du choix de la trajectoire ; dans le pire des cas, le choix d'une trajectoire plutôt que la solution optimale, peut être jusqu'à 25% plus coûteux en termes d'énergie.

Comme résumé dans le Tableau 1, le graphe avec trois nœuds par phase verte se rapproche mieux au vrai coût énergétique, tandis que le graphe plus petit échoue dans cinq cas.

Temps de Passage Optimaux

Enfin, une fois que l'algorithme de Dijkstra fournit les phases vertes optimales, les temps de passage optimaux à chaque intersection sont calculés, de manière à fournir l'assistance d'éco-conduite en suggérant un profil de vitesse au conduc-
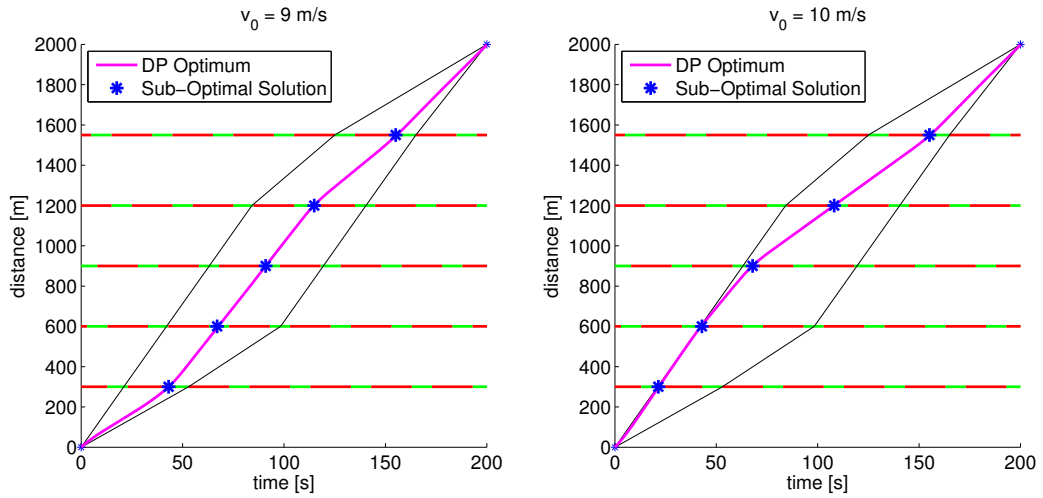
Figure 4 – Temps de passage sous-optimaux comparés avec la solution optimale fournie par la DP, pour deux differentes valeurs de vitesse initiale.

Tableau 2 – Difference temporelle entre les temps de passage optimaux et sous-optimaux aux cinque intersections

	Int. #1	**Int. #2**	**Int. #3**	**Int. #4**	**Int. #5**
$v_0 = 9$ m/s	0.03 s	0.62 s	0.03 s	0.07 s	0.5 s
$v_0 = 10$ m/s	0.22 s	0.36 s	0.05 s	0.08 s	0.4 s
Difference moyenne : 0.23 s					

teur.

Dans la Figure 4, la solution optimale fournie par la DP à travers les phases vertes optimales (chemin 12 pour $v_0 = 9$ m/s et chemin 3 pour $v_0 = 10$ m/s) est comparée à la solution sous-optimale proposée. Dans le Tableau 2, les differences temporelles entre la solution sous-optimale et la solution de la DP dans les cinq intersections sont reportées, pour les deux vitesses initiales choisies.

La DP prend environ 2,5 heures par chemin pour calculer la solution optimale. Afin d'avoir une évaluation du coût de toutes les trajectoires et de trouver celle à énergie minimale, la DP doit être exécutée autant de fois que le nombre de chemins possibles. La méthodologie proposée prend 1,2 secondes (graphe à trois nœuds/phase verte) ou 0,85 secondes (graphe à un nœud/phase verte) pour exécuter toutes les étapes présentées et fournir les temps de passage sous-optimaux à chaque intersection.
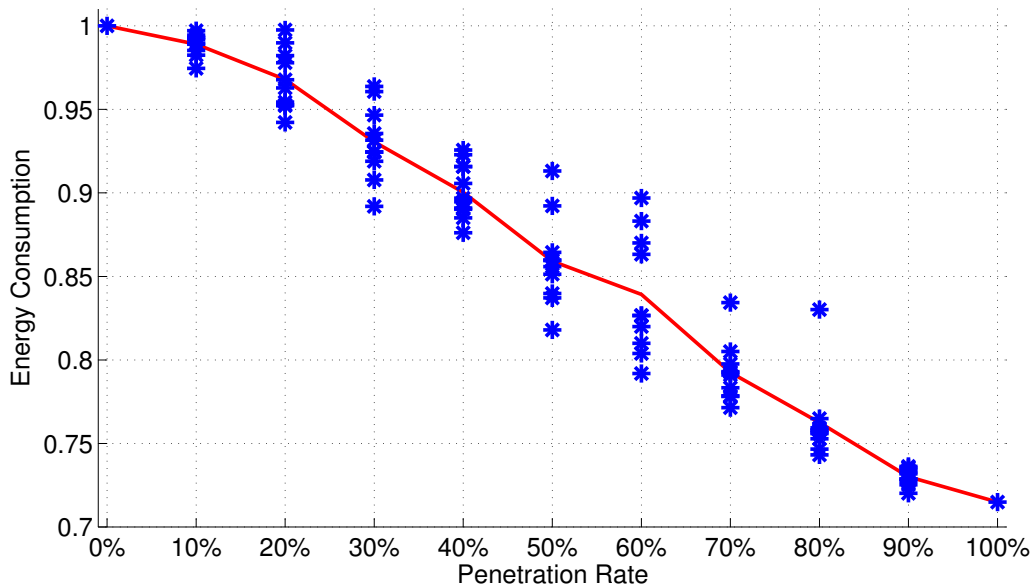
Figure 5 – Variation de la consommation énergétique en fonction du taux de pénétration de la technologie. La ligne rouge décrit la consommation énergétique moyenne.

Simulateur Microscopique de Trafic

Afin de prouver les capacités réelles de la stratégie proposée dans un scénario plus réaliste, le simulateur microscopique de trafic AIMSUN a été utilisé. La topologie de route traitée dans ce travail a été fidèlement reproduite dans AIMSUN, ainsi que les positions des feux de circulation et les plans des feux. Un débit de 400 véhicules par heure entre dans le réseau routier à la vitesse initiale $v_0 = 50$ km/h. Les véhicules ont été équipés avec l'algorithme présenté, et, évidemment, l'hypothèse de véhicules non perturbés dans un tel scénario réaliste est violée. En particulier, chaque véhicule étant équipé de façon indépendante avec l'algorithme et entrant dans le réseau à différents instants, les conseils de vitesse peuvent entrer en conflit avec l'un l'autre.

Dans la Figure 5, la variation de la consommation énergétique en fonction du taux de pénétration de la technologie est affichée. La stratégie proposée a été appliquée à un nombre progressivement croissant de véhicules sur le réseau routier. À taux de pénétration égal à 0%, l'expérience a été menée avec aucun véhicule équipé de l'algorithme, et tous les véhicules ont été autorisés à conduire jusqu'à la limite de vitesse maximale. Pour des taux supérieurs à 0%, un total de 10 simulations par chaque valeur testée a été exécuté. Les véhicules équipés ont été choisis au hasard, et il est possible de constater que l'ordre de "véhicules intelligents"

dans le trafic peut affecter de manière significative la consommation d'énergie. Comme prévu, un taux de pénétration de 100% est très bénéfique en termes de plusieurs indicateurs de performance de la circulation. Une réduction de 28,5% de la consommation d'énergie du trafic a été observée, sans impact négatif sur le temps de parcours moyen. Plus précisément, le temps de parcours moyen est encore plus petit que dans le cas incontrôlé d'environ 4%. Les arrêts et le temps à l'arrêt sont totalement éliminés.

Contrôle d'un Tronçon de Route à l'Aide de Limites de Vitesse Variables

Modèle à Longueur Variable

Malgré sa notoriété et sa simplicité dans la modélisation du trafic routière, le *Cell Transmission Model* (CTM) présente quelques inconvénients critiques dans la représentation réaliste de l'évolution et de la répartition de la densité lorsque la discrétisation n'est pas assez fine (petit nombre de cellules), ou lorsque la congestion se pose.

Une alternative au CTM, en mesure de répondre plus efficacement aux problèmes mentionnés ci-dessus, est représentée par le Modèle à Longueur Variable (VLM), proposé à l'origine dans [20] et encore modifié dans [21]. Un des principaux avantages de ce modèle est la réduction de la dimension de l'espace d'état. En fait, le nombre de cellules par section, indépendamment de sa longueur, se réduit à deux seulement. Une autre caractéristique intéressante est la meilleure représentation de la congestion, qui dans les réseaux urbains est très susceptible de se produire en raison de la présence de feux de circulation, et doit être traitée correctement. Comme le montre la Figure 6, chaque tronçon de route est divisé en seulement deux cellules et modélisé avec seulement trois variables d'état : la densité de la cellule libre ρ_f, la densité de la cellule congestionnée ρ_c, la longueur de la cellule congestionnée l. Considérons un tronçon de route d'une longueur L, alors la longueur de la cellule libre sera $(L-l)$, et la longueur de la cellule congestionnée sera l. La densité de véhicules dans les deux cellules est moyennée, ce qui signifie que le comportement individuel des véhicules n'est pas décrit, comme il est typique pour les modèles macroscopiques.

Le domaine d'existence des densités dans les deux cellules est :

$$
\begin{aligned}
\rho_f &\in [0, \rho_{\mathrm{cr}}(v_f)] \\
\rho_c &\in (\rho_{\mathrm{cr}}(v_f), \rho_m]
\end{aligned}
\tag{19}
$$

où $\rho_{\mathrm{cr}}(v_f)$ est la densité critique par rapport à la vitesse maximale autorisée dans
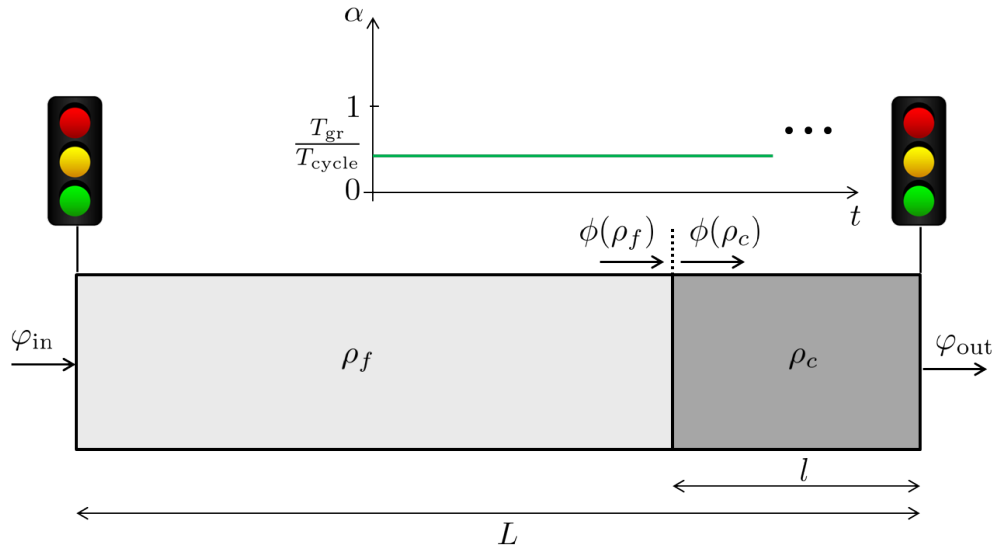
Figure 6 – Modèle à Longueur Variable adapté au milieu urbain.
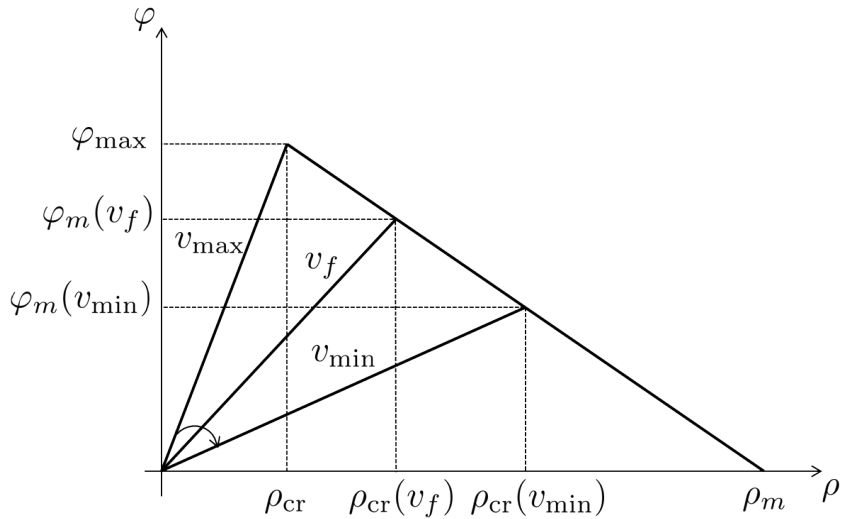
Figure 7 – Diagramme fundamental avec limites de vitesse variables.

la cellule libre,

$$\rho_{\mathrm{cr}}(v_f) = \frac{w\rho_m}{v_f + w} \tag{20}$$

v_f sera utilisée comme l'entrée de contrôle du trafic, et ρ_m est la densité maximale de congestion de la section de route (voir Figure 7).

Une simplification intéressante de ce modèle, afin d'éviter le comportement binaire de la variable discrète qui modélise les feux de signalisation, est obtenue et formellement justifiée par la théorie des perturbations et de la moyenne [70]. Si

on calcule la moyenne de la durée de la phase verte du feu sur le temps de cycle, on peut modéliser les feux avec une variable continue. La formulation du système moyenne, qui sera le modèle de référence dans l'analyse qui suit, est la suivante :

$$
\begin{cases}
\dot{\rho}_f = [\bar{\varphi}_{\text{in}} - \rho_f v_f] \, \dfrac{1}{L-l} \\[2mm]
\dot{\rho}_c = [w(\rho_m - \rho_c) - \bar{\varphi}_{\text{out}}] \, \dfrac{1}{l} \\[2mm]
\dot{l} = \dfrac{\rho_f v_f - w(\rho_m - \rho_c)}{\rho_c - \rho_f}
\end{cases}
\tag{21}
$$

Le comportement discret du système, induit par les feux de signalisation, est ainsi éliminé. Le feu de circulation est modélisée comme une vanne ouverte, comme montré dans la Figure 6, et les véhicules entrant ou sortant de la section peuvent être considérés comme un flux continu restreint. Comme conséquence naturelle de ce rapprochement, les oscillations des files d'attente au feu de circulation et les notions de temps de cycle et de décalage pour les feux de circulation ne sont pas représentées par le modèle moyenné.

Analyse des Propriétés du Modèle

Dans le cas d'inégalité des flux limites, le système converge naturellement vers un état pleinement libre ou un état totalement congestionné. Ces cas représentent une criticité du modèle et de l'analyse de l'éco-conduite. Si la section est entièrement encombrée l'autorité de contrôle est considérablement réduite et presque complètement perdue. Les véhicules ne pourraient pas suivre l'entrée de commande v_f, et la limite de vitesse conseillée aurait un impact uniquement sur la sortie (la vitesse à laquelle les véhicules sont autorisés à quitter la section). Une section entièrement libre, au contraire, a contrôlabilité complète et représente tout simplement un cas particulier de l'analyse pour flux limites égaux. Par conséquent, l'existence d'un niveau de congestion d'équilibre dans les limites de la section représente un contexte intéressant aux fins de l'éco-conduite.

Flux Limites Égaux

Prenons une section de route et supposons que les feux de circulation aux deux extrémités sont également temporisés, que la demande est suffisante en amont et la réserve suffisante en aval, et que la limite de vitesse v_f est le même en amont et en aval. Donc, les flux limites ne sont déterminés que par la valeur maximale de la fonction demande/réserve :

$$
\bar{\varphi}_{\text{in}}(v_f) = \bar{\varphi}_{\text{out}}(v_f) = \varphi_m(v_f) = \bar{\alpha} \frac{w\rho_m}{v_f + w} v_f
\tag{22}
$$

Ainsi, le système peut être réécrit sous la forme :

$$
\begin{cases}
\dot{\rho}_f = \left[\bar{\alpha}\dfrac{w\rho_m}{v_f + w}v_f - \rho_f v_f \right] \dfrac{1}{L - l} \\[3mm]
\dot{\rho}_c = \left[w(\rho_m - \rho_c) - \bar{\alpha}\dfrac{w\rho_m}{v_f + w}v_f \right] \dfrac{1}{l} \\[3mm]
\dot{l} = \dfrac{\rho_f v_f - w(\rho_m - \rho_c)}{\rho_c - \rho_f}
\end{cases}
\tag{23}
$$

Étant donné un ensemble de conditions initiales $(\rho_f^0, \rho_c^0, l^0)$, le système (23) converge vers l'équilibre :

$$
\begin{aligned}
\rho_f^* &= \bar{\alpha}\frac{w\rho_m}{v_f + w} \\[3mm]
\rho_c^* &= \rho_m - \bar{\alpha}\frac{v_f \rho_m}{v_f + w} \\[3mm]
l^* &= \frac{N_0(v_f + w) - \bar{\alpha}\rho_m w L}{\rho_m(v_f + w)(1 - \bar{\alpha})}
\end{aligned}
\tag{24}
$$

où N_0, le nombre initial et invariant dans le temps de véhicules, est donné par :

$$
N_0 = N = \rho_f^0(L - l^0) + \rho_c^0 l^0
\tag{25}
$$

Il est intéressant de noter que la définition bien connue de la stabilité d'un point d'équilibre ne tient pas pour le système (23). En particulier, pour chaque choix de conditions initiales et de la vitesse dans la cellule libre, le système évolue et converge naturellement vers un point d'équilibre différent. À partir de conditions initiales arbitraires sera impossible de parvenir à un équilibre $(\rho_f^*, \rho_c^*, l^*)$ associé à des conditions initiales différentes tout en conservant également la vitesse v_f qui lui est associée. En d'autres termes, étant donné un certain état initial du trafic et une limite de vitesse optimale v_f^*, il est possible de suivre seulement l'équilibre (24) tout en conservant la vitesse optimale.

Cette dépendance des conditions initiales, ce qui affecte la définition canonique de la stabilité de l'équilibre, peut être surmontée en observant que N_0 apparaît uniquement dans l'expression de l^*. La longueur de la congestion peut être exprimée en fonction des deux densités ρ_f et ρ_c comme suit :

$$
l = \frac{N - \rho_f L}{\rho_c - \rho_f}
\tag{26}
$$

et une transformation de l'état de l à N permettra au système (21) d'être écrit de façon équivalente comme un système à deux états, étant le nombre de véhicules

invariants dans le temps :

$$\begin{cases} \dot{\rho}_f = \left[\bar{\alpha} \dfrac{w\rho_m}{v_f + w} v_f - \rho_f v_f \right] \dfrac{\rho_c - \rho_f}{\rho_c L - N} \\[4mm] \dot{\rho}_c = \left[w(\rho_m - \rho_c) - \bar{\alpha} \dfrac{w\rho_m}{v_f + w} v_f \right] \dfrac{\rho_c - \rho_f}{N - \rho_f L} \end{cases} \tag{27}$$

avec $N(t) = N_0$ pour tous les $t > 0$, qui maintenant peut être considéré comme un paramètre de système.

Le paramètre N possède un domaine bien défini de l'existence, dans le but de veiller à ce que la longueur de la cellule encombrée l à l'équilibre ne dépasse pas les limites de la section ($0 < l < L$). Par conséquent, en imposant $l^* \in (0, L)$, il résulte de (24) que :

$$\rho_m L \frac{\bar{\alpha} w}{v_f + w} < N < \rho_m L \left[(1 - \bar{\alpha}) + \frac{\bar{\alpha} w}{v_f + w} \right] \tag{28}$$

qui peut également être écrit comme :

$$\rho_f^* L < N < \rho_c^* L \tag{29}$$

Puis, une condition doit être respectée aussi par les conditions initiales pour les densités dans les deux cellules :

$$\rho_f^0 L < N < \rho_c^0 L \tag{30}$$

Après cette simplification, un théorème pour la stabilité du système (27) peut être donné :

Théorème 1. *Le point d'équilibre (ρ_f^*, ρ_c^*) est asymptotiquement stable si et seulement si :*

— *N satisfait (29) ;*

— *les conditions initiales (ρ_f^0, ρ_c^0) satisfont (30).*

Flux Limites Inégaux

Dans le cas de flux limites inégaux, l'hypothèse sur l'invariance temporelle du nombre de véhicules dans la section n'est pas vérifiée, et le système (27) ne suffit pas à décrire la dynamique de l'état. En outre, la notion de convergence vers les trois états d'équilibre perd sa signification car le déséquilibre des flux limites conduira finalement le système à converger vers un état entièrement encombré ou entièrement libre.

L'analyse précédente sur la stabilité des points d'équilibre ne peut pas être appliqué directement dans ce cas, en raison de l'absence d'expressions analytiques décrivant l'équilibre $(\rho_f^*, \rho_c^*, l^*)$. Cependant, même si une expression analytique de la valeur de convergence de l ne peut pas être trouvée, les densités préservent un équilibre bien défini affecté par le nombre variant de véhicules :

$$
\begin{aligned}
\rho_f^* &= \bar{\alpha}_1 \frac{w\rho_m}{v_f + w} \\
\rho_c^* &= \rho_m - \bar{\alpha}_2 \frac{v_f \rho_m}{v_f + w}
\end{aligned}
\tag{31}
$$

où $\bar{\alpha}_1$ et $\bar{\alpha}_2$ sont les variables qui modélisent les feux de circulation en alont et en aval, respectivement.

Métriques de Performance du Trafic

Les indicateurs de performance du trafic seront écrits dans ce qui suit pour le régime permanent, en les évaluant sur le temps de cycle des feux de circulation T_{cycle}.

Le temps de parcours instantané (ITT) peut être défini comme le temps de parcours qui se produirait si les conditions de circulation restaient inchangées au cours de la période de temps en cours d'analyse. Dans le cas des flux limites égaux, l'ITT peut être écrit en fonction de l'entrée de côntrole v_f, comme suit :

$$
\text{ITT}(v_f) = \frac{N(v_f + w)}{\bar{\alpha} \rho_m v_f w}
\tag{32}
$$

La distance totale parcorue (TTD) est une mesure de l'efficacité de l'infrastructure en termes de taux d'occupation et de vitesse de déplacement. Dans le cas de flux limites égaux, le TTD est calculé à l'équilibre et sur un cycle de feu de circulation. Par conséquent, il peut être écrit comme une fonction de l'entrée de commande de la manière suivante :

$$
\text{TTD}(v_f) = v_f \bar{\alpha} \frac{w\rho_m}{v_f + w} L \cdot T_{\text{cycle}}
\tag{33}
$$

Une autre mesure importante, généralement pas considérée au niveau macroscopique, est la consommation d'énergie des véhicules. La demande de puissance pour un moteur électrique est donnée par :

$$
P = b_1 uv + b_2 u^2 = f(v, \dot{v})
\tag{34}
$$

où b_1 et b_2 sont paramètres du moteur. Au niveau macroscopique, la consommation d'énergie est influencée par le nombre de véhicules se déplaçant dans la section

de route en cours d'analyse. Le coût énergétique pour le modèle VLM peut être formulé comme suit :

$$E = E_f + E_c + E_{f \to c} + E_{c \to f} \tag{35}$$

où la consommation d'énergie dans la cellule libre est :

$$E_f = \int\limits_0^T P_f \cdot \rho_f \cdot (L - l) \, \mathrm{d}t \tag{36}$$

avec P_f étant calculée comme dans (34) utilisant v_f comme vitesse. La consommation d'énergie dans la cellule congestionnée est :

$$E_c = \int\limits_0^T P_c \cdot \rho_c \cdot l \, \mathrm{d}t \tag{37}$$

avec P_c étant calculée comme dans (34) utilisant v_c comme vitesse. La consommation d'énergie causée par le changement de vitesse entre la cellule libre et la cellule congestionnée est :

$$E_{f \to c} = \int\limits_0^{\frac{|v_c - v_f|}{a}} P \, \mathrm{d}t \cdot \int\limits_0^T w(\rho_m - \rho_c) \, \mathrm{d}t \tag{38}$$

où la première intégrale calcule la consommation d'énergie d'un seul véhicule faisant la transition entre la cellule libre et la cellule encombrée. L'horizon temporel de l'intégrale est tout simplement le temps nécessaire pour achever la transition, compte tenu de la différence de vitesse $|v_c - v_f|$ et l'accélération a. La seconde intégrale calcule le nombre de véhicules qui font vraiment la transition de la cellule libre à la encombrée sur l'horizon de temps T. De manière analogue, la consommation d'énergie due à la variation de vitesse entre la cellule congestionné et la cellule virtuelle libre après le feu de circulation en aval est :

$$E_{c \to f} = \int\limits_0^{\frac{|v_f - v_c|}{a}} P \, \mathrm{d}t \cdot \int\limits_0^T \bar{\varphi}_{\text{out}} \, \mathrm{d}t \tag{39}$$
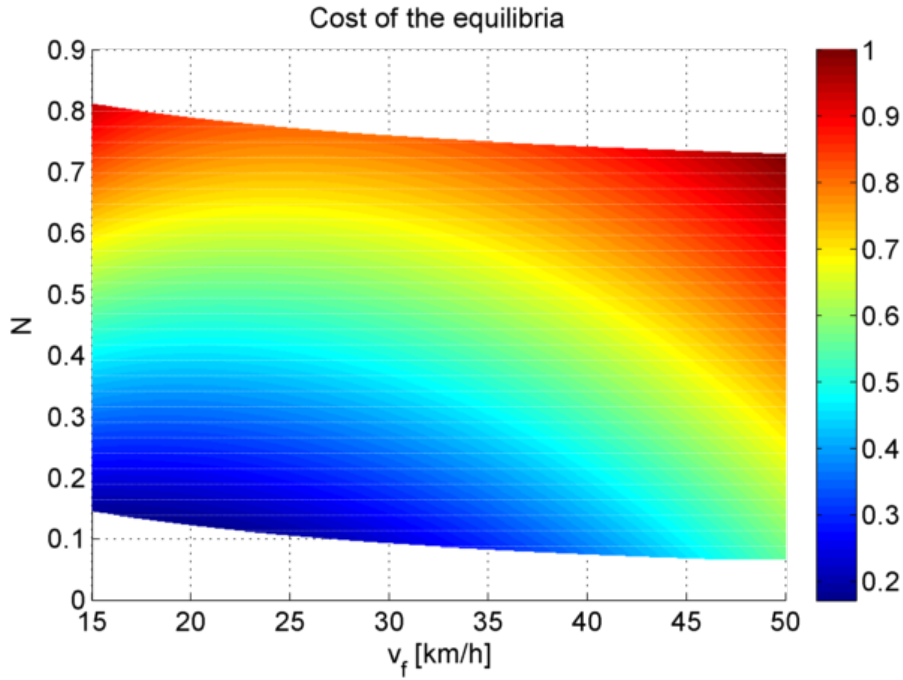
Figure 8 – Coût normalisé de tous les points d'équilibre possibles en fonction de l'entrée de commande v_f et du nombre de véhicules normalisé N.

Limite de Vitesse Optimale

Si les flux limites de la section sont égaux, le problème d'optimisation est plus intéressant en raison de la présence de nombreux équilibres possibles, donnés par l'équation (24). La variation de la limite de vitesse dans la cellule libre amenera le système à atteindre un équilibre différent sans modifier le nombre de véhicules, donc conforme à l'hypothèse de flux limites égaux. Ceci correspond à une redistribution des véhicules à l'intérieur de la section, en modifiant la longueur de la congestion l.

Le problème d'optimisation peut être formulé comme suit :

Problème 1. *Étant donné le système* (21)*, conditions initiales acceptables* $(\rho_f^0, \rho_c^0, l^0)$*, et $\bar{\alpha}$ constant pour les feux de circulation, trouver la limite de vitesse optimale*

$$v_f^* = \operatorname*{argmin}_{v_f} \{\sigma_1 E + \sigma_2 ITT - \sigma_3 TTD\}$$
$$v_{min} \leq v_f \leq v_{max}$$
$$l_{min} \leq l \leq l_{max}$$

La fonction de coût dans le Problème 1 a été évaluée à l'équilibre pour chaque combinaison possible de la limite de vitesse et du nombre de véhicules dans la

section. La faisabilité des points d'équilibre est assurée par les conditions (29) et (30) sur le nombre de véhicules et sur les conditions initiales. Une carte complète des coûts des équilibres est donnée dans la Figure 8, qui donne un aperçu de la cherté en termes de performance de la circulation des conditions de circulation possibles.

Système de Contrôle

Le système de contrôle a été conçu pour le cas de flux limites égaux. Puisque le système est asymptotiquement stable, un dispositif de contrôle ne sert pas des fins de stabilisation, mais, en l'absence de perturbations extérieures, il peut accélérer la convergence du système au point d'équilibre optimal calculé. L'action de contrôle peut être considérée comme la réponse des conducteurs conformes à l'avis de la vitesse optimale.

Compte tenu du système linéarisé à partir du système (27), un régulateur linéaire quadratique (LQR) est conçu pour suivre l'équilibre optimale $(x^*, u^*) = (\rho_f^*, \rho_c^*, v_f^*)$. La loi de commande est de la forme :

$$u = u^* - K(x - x^*) \tag{40}$$

où $\tilde{u} = -K\hat{x} = -K(x - x^*)$.

Pour le choix des matrices de pondération Q et R du LQR, une caractéristique spécifique des valeurs propres du système linéaire a été utilisée. La partie réelle des valeurs propres du système linéarisé devient plus ou moins négative selon les conditions initiales et le choix du paramètre N. En particulier, grosso modo, si N est élevé, le mode associé à ρ_f est plus stable que celui de ρ_c, et vice-versa. Par conséquent, dans la conception des matrices de pondération Q et R, une sorte d'approche *gain scheduling* a été mise en place, afin de pondérer plus le mode moins stable :

$$Q = \begin{bmatrix} 2000(1 - \frac{N}{\rho_m L}) & 0 \\ 0 & 2000\frac{N}{\rho_m L} \end{bmatrix} \tag{41}$$
$$R = 0.00005$$

Expériences

Le scénario de la simulation présente un tronçon de route d'une longueur L avec deux feux de circulation aux deux extrémités réglementant l'entrée et la sortie. Les feux de circulation sont modélisés par la variable continue $\bar{\alpha}$. La section est divisée en deux cellules selon la dynamique du modèle, et un diagramme fondamental macroscopique est défini par les paramètres w, ρ_m et l'entrée de commande v_f. Deux séries de simulations, avec le contrôleur appliquée au système
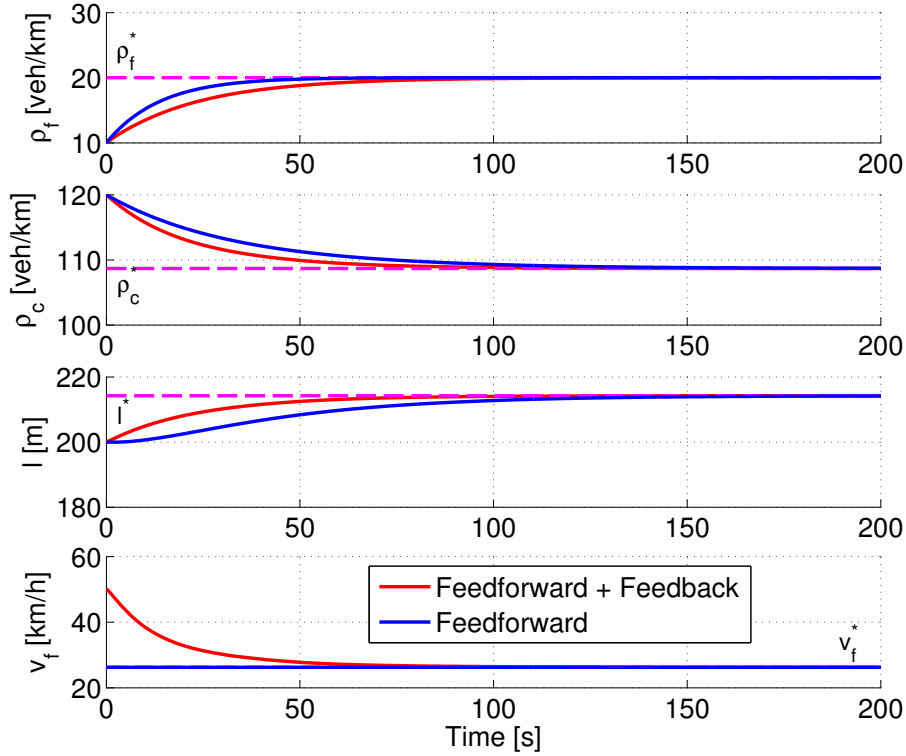
Figure 9 – Flux Limites Égaux - Dinamique du système nonlinéaire et entrée de contrôle avec et sans la rétroaction du LQ.

général (21), visent à montrer l'efficacité de la commande de rétroaction à la fois dans le cas de flux limites égaux et dans le cas de la variation de la demande en amont.

Flux Limites Égaux

La première simulation est menée avec les feux de circulation aux deux extrémités de la section également temporisés. En vertu de cette hypothèses, le modèle (27) est valide. La vitesse optimale v_f^* est calculée sur la base des conditions initiales, correspondant à un nombre initial de véhicules $N_0 = N = 25$. Le contrôleur est capable d'amener plus vite le système à l'équilibre optimal $(\rho_f^*, \rho_c^*, l^*, v_f^*)$, comme indiqué dans la Figure 9.

Figure 10 – Flux Limites Inégaux - La stratégie de contrôle proposée (en rouge) est comparée au simple contrôleur *feedforward* $v_f = v_f^*$ (en bleu), et au cas standard avec la limite de vitesse maximale $v_f = 50\,$km/h (en noir).

Flux Limites Inégaux

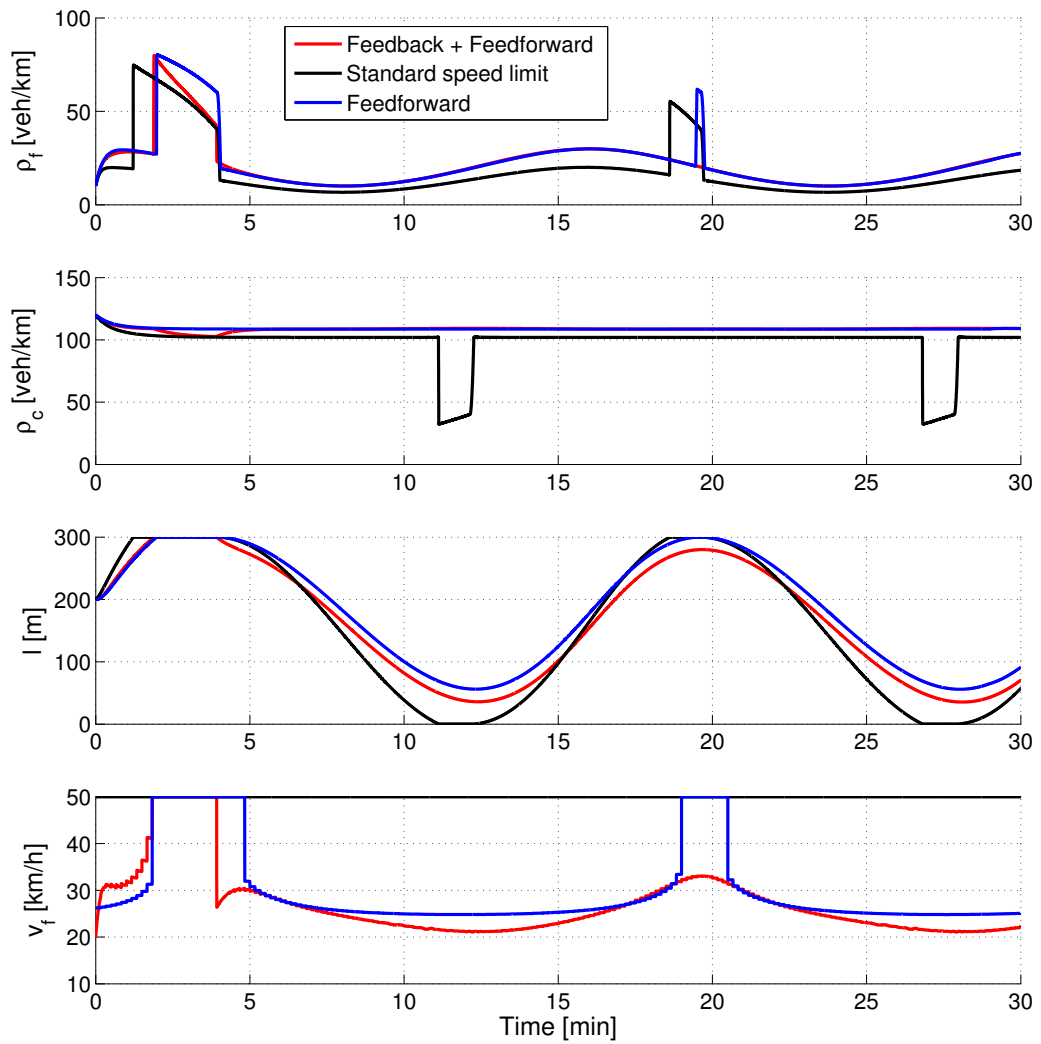Dans le cas d'une demande variable, l'hypothèse sur l'invariance du nombre de véhicules n'est pas valide, et le système (27) ne suffit plus pour décrire la dynamique de l'état. Le déséquilibre des flux limites conduira finalement le système à converger vers une section entièrement encombrée ou entièrement libre. Le contrôleur LQ sera encore testé sur le système (21).

L'analyse précédente sur l'optimalité des points d'équilibre possibles et stables ne peut pas être appliquée directement dans ce cas, en raison de l'absence d'expressions analytiques décrivant parfaitement l'équilibre $(\rho_f^*, \rho_c^*, l^*)$. Cependant, bien que rien ne peut être dit à propos de la valeur de convergence de l^*, les densités préservent un équilibre bien défini, comme indiqué dans (31), et peuvent donc être utilisées pour la rétroaction.

Comme le montre la Figure 10, cette stratégie de contrôle est bénéfique dans le cas de la variation de la demande en amont et l'action de rétroaction est en mesure de fournir l'amélioration des performances par rapport au simple contrôleur *feedforward* $v_f = v_f^*$, et au cas standard avec la limite de vitesse maximale $v_f = 50$ km/h. Tout au long de la simulation, il est évident que le contrôleur à rétroaction est en mesure de soulager l'encombrement beaucoup plus efficacement que les deux autres politiques de limitation de vitesse, en particulier à $t \simeq 20$ minutes la saturation est complètement évitée. La stratégie de contrôle proposée atteint une amélioration globale du coût de 14% par rapport à la limite de vitesse standard, et une amélioration de 6% par rapport à la commande *feedforward*.

Contrôle d'une Artère Urbaine Signalisée à l'Aide de Limites de Vitesse Variables et Offsets

Formulation du Problème

Notation du Problème

Un artère à deux directions avec n intersections signalisées est considérée. Les deux directions opposées de voyage seront nommées entrante et sortante. Les intersections sont situées à $x_1 < x_2 < \ldots < x_n$, avec l'indice qui augmente dans le sens sortant. Toutes les quantités liées à la direction entrante sont indiquée avec une barre supérieure. Les vitesses de déplacement dans les $n-1$ segments sont supposées être égales aux limites de vitesse imposées, et égales à v_i et $\bar{v}_i$.
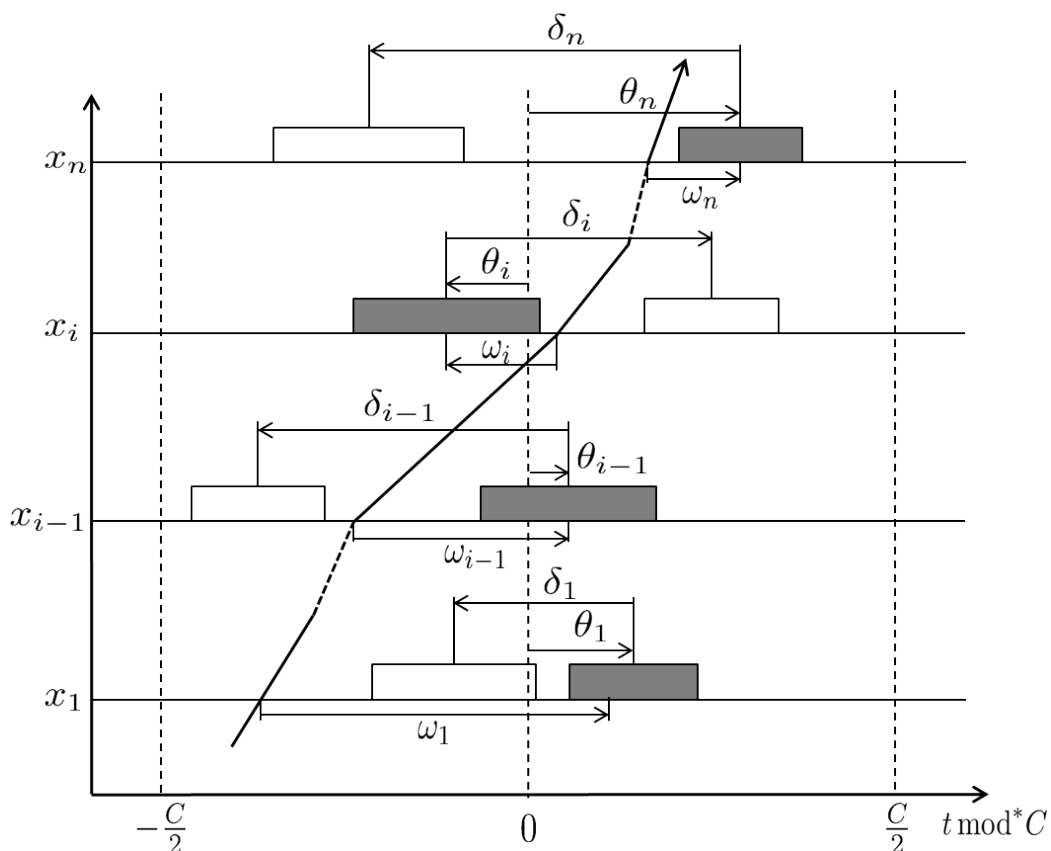
Figure 11 – Les phases vertes de la direction de voyage sortante sont en gris. Les phases vertes dans le sens entrant sont en blanc. La trajectoire de vitesse et la notation de base sont indiquées uniquement pour la direction sortante pour plus de clarté.

Les temps de parcours entrants et sortants sur le segment i sont :

$$t_i = \frac{x_{i+1} - x_i}{v_i} > 0, \quad i \in \{1, \ldots, n-1\} \tag{42}$$

$$\bar{t}_i = \frac{\bar{x}_i - \bar{x}_{i+1}}{\bar{v}_i} < 0, \quad i \in \{1, \ldots, n-1\} \tag{43}$$

étant la longueur du segment $L_i = x_{i+1} - x_i$.

Les n signaux doivent être coordonnés avec un temps de cycle commun C, qui est assumé fixe dans ce travail. On définit avec g_i et $\bar{g}_i$ les temps verts à une intersection i dans la direction sortante et entrante, respectivement.

Le mappage du domaine réel de temps sur l'intervalle $[-C/2, C/2]$ est réalisé avec un opérateur modulo non-standard qui sera indiqué mod* [56].

Les *offsets* absolus θ_i ($\bar{\theta}_i$) sont définis comme la distance du centre de la fenêtre

vert de la direction sortante (entrante) à l'intersection i par rapport à un système de coordonnées fixe (voir la Figure 11). Les offsets absolus sont en $[-C/2, C/2]$. Le déplacement relatif des centres des fenêtres vertes entrantes et sortantes est défini comme,

$$\delta_i = (\bar{\theta}_i - \theta_i) \, \text{mod}^* C \tag{44}$$

En plus des offsets absolus, les ofsets relatifs ω_i et $\bar{\omega}_i$ sont définis. Ceux-ci sont mesurés par rapport à un système de coordonnées mobile qui se déplace à vitesse $v_i(\bar{v}_i)$. L'offset relatif sortant ω_i est défini comme le temps entre le passage du système de coordonnées mobile et le centre de la fenêtre verte sortante le plus proche. Une définition correspondante s'applique pour l'offset relatif entrant. Les offsets relatifs sont également en $[-C/2, C/2]$. Notez que le système de coordonnées mobile ne s'arrête pas aux signaux rouges.

La conversion entre les décalages absolus et relatifs peut être calculée comme suit :

$$(\omega_{i-1} - \theta_{i-1} + \theta_i - \omega_i - t_{i-1}) \, \text{mod}^* C = 0 \tag{45}$$

Par conséquent, la formule récursive suivante pour les offsets relatifs s'applique :

$$\omega_i = (\omega_{i-1} - \theta_{i-1} + \theta_i - t_{i-1}) \, \text{mod}^* C \tag{46}$$

ce qui donne finalement :

$$\omega_i = \left(\omega_1 - \theta_1 + \theta_i - \sum_{k=1}^{i-1} t_k \right) \text{mod}^* C \tag{47}$$

La formule inverse permet de déterminer les décalages absolus à partir des décalages relatifs :

$$\theta_i = \left(\theta_1 - \omega_1 + \omega_i + \sum_{k=1}^{i-1} t_k \right) \text{mod}^* C \tag{48}$$

Ces formules sont applicables aussi pour la direction entrante. Puisque la relation entre les décalages relatifs et absolus est inversible, nous sommes libres de formuler le problème de maximisation de la bande passante soit en fonction de l'un des deux ensembles de variables.

La bande passante est une quantité théorique définie comme la taille de l'intervalle de temps dans lequel les véhicules peuvent parcourir la longueur de la artère sans arrêt. La bande passante sortante est notée avec b, et la bande passante entrante est notée avec $\bar{b}$.

Problème d'Optimisation

L'objectif de ce travail est de résoudre le problème de maximisation de la bande passante dans les deux sens de voyage, en utilisant à la fois les offsets et le limites de vitesse variables. Les degrés de liberté de l'optimisation seront les offsets relatifs ω_i et $\bar{\omega}_i$, et les temps de parcours t_i et $\bar{t}_i$.

Le problème pour les deux sens de voyage a été formulée dans [56] comme un programme linéaire continu, sans utilisation de variables entières, en exploitant l'information a priori sur les vitesses dans chaque segment du réseau. Seulement les offsets ont été utilisés en tant que variables de décision. Ce travail étend le résultat précédent en introduisant les vitesses dans les différents segments du réseau en tant que variables de décision supplémentaires. Il sera montré qu'une bande passante plus élevée est obtenue grâce à un contrôle des vitesses. Cependant, l'objectif de la présente analyse est également d'éviter des solutions peu pratiques, ainsi que d'évaluer les avantages réels de la maximisation de la bande passante sur les performances du trafic. En particulier, l'optimisation prendra en compte aussi le consommation d'énergie du trafic, le temps de parcours et le confort du conducteur.

Afin d'exprimer à la fois b et $\bar{b}$ en fonction des offsets relatifs, les fenêtres vertes sont décalées sur le système de coordonnées mobile vers $x = x_1$. Cette opération induit une transformation de δ_i à δ_i^0 avec $i \in \{1, \ldots, n\}$. La transformation est donnée par (voir [56] pour plus de détails) :

$$\delta_i^0 = \left(\delta_i + \sum_{k=1}^{i-1} (t_k - \bar{t}_k) \right) \mathrm{mod}^* C \tag{49}$$

avec $\delta_i^0 \in [-C/2, C/2]$. La contrainte d'égalité qui fixe le décalage interne est donnée par :

$$\omega_i - \bar{\omega}_i = \delta_1^0 - \delta_i^0 \tag{50}$$

Comme déjà mentionné, l'objectif est de maximiser la bande passante dans les deux sens. Le problème sera résolu par rapport aux offsets sortants relatifs et les offsets internes transformés, les temps de parcours, et les variables entières qui maintiennent le compte du nombre de cycles. Par conséquent, le nombre d'inconnues du problème d'optimisation est $5n - 1$:

$$\mathbf{x} = \big[b, \bar{b}, \omega_1, \ldots, \omega_n, \delta_1^0, \ldots, \delta_n^0, t_1, \ldots, t_{n-1},$$
$$\bar{t}_1, \ldots, \bar{t}_{n-1}, \alpha_2, \ldots, \alpha_n \big]^T \tag{51}$$

En plus de l'optimisation de la bande passante, il est également intéressant de minimiser la variance du conseil de vitesse, ainsi que le temps de parcours. Le premier terme peut être considéré comme un terme de variance de commande,

ou comme un terme de confort puisque les conducteurs seraient moins disposés à suivre un conseil de vitesse très variable. Ce terme sert également à réduire les accélérations des véhicules qui accroissent la consommation d'énergie. Le second terme favorise l'optimisation loin de solutions triviales avec très faibles vitesses. Ces conditions supplémentaires peuvent être exprimées en fonction de $\mathbf{x}$.

La différence de vitesse entre les segments adjacents induite par l'optimisation peut être considérée comme un indicateur de l'accélération à l'intersection. L'accélération a un impact majeur sur la consommation d'énergie. Par conséquent, en décourageant les grandes variations de vitesse entre les segments, la consommation d'énergie associée est réduite. La quantité à être réduite pour le sens sortant est :

$$\left\| \frac{L_i}{t_i} - \frac{L_{i+1}}{t_{i+1}} \right\|_1, \quad i \in \{1, \ldots, n-2\} \tag{52}$$

La même expression vaut pour le sens entrant, avec $\bar{t}_i$ et $\bar{t}_{i+1}$. Afin d'éviter l'introduction de termes non linéaires dans la fonction objectif, nous allons approcher (52) avec une fonction linéaire correspondante à son numérateur. Par conséquent le terme de lissage de la fonction objectif peut être réécrit comme :

$$\left\| L_i t_{i+1} - L_{i+1} t_i \right\|_1, \quad i \in \{1, \ldots, n-2\} \tag{53}$$

ce qui peut être exprimé sous forme de matrice avec :

$$\left\| \mathcal{L}^* \cdot \mathbf{t} \right\|_1 \tag{54}$$

Le problème peut être formulé sous la forme finalement d'un programme entier non linéaire comme suit :

$$
\begin{cases}
\max_{\mathbf{x}} \quad b + \bar{b} - \lambda_1 \left(\left\| \mathcal{L}^* \mathbf{t} \right\|_1 + \left\| \mathcal{L}^* \bar{\mathbf{t}} \right\|_1 \right) - \lambda_2 \left(\left\| \mathbf{t} \right\|_1 + \left\| \bar{\mathbf{t}} \right\|_1 \right) \\
\text{s.t.} \quad b\mathbf{1} \leq \Omega \cdot \omega + \frac{1}{2} |\Omega| \cdot \mathbf{g} \\
\quad \bar{b}\mathbf{1} \leq \Omega \cdot \omega + \Delta \cdot \delta^{\mathbf{0}} + \frac{1}{2} |\Omega| \cdot \bar{\mathbf{g}} \\
\quad b \leq g^* \\
\quad b \geq 0 \\
\quad \bar{b} \leq \bar{g}^* \\
\quad \bar{b} \geq 0 \\
\quad \mathbf{t}_{\min} \leq \mathbf{t} \leq \mathbf{t}_{\max} \\
\quad -\mathbf{t}_{\max} \leq \bar{\mathbf{t}} \leq -\mathbf{t}_{\min} \\
\quad \delta^{\mathbf{0}} - \Psi \cdot \mathbf{t} + \Psi \cdot \bar{\mathbf{t}} + \alpha \cdot C = \delta
\end{cases}
\tag{55}
$$

La fonction objectif peut être linéarisée par l'introduction de variables *slack* qui se comportent comme des limites maximales pour les normes L_1 [16]. Par

conséquent, le problème peut être finalement formulé en tant que programme linéaire entier mixte avec $(9n - 7)$ inconnues et $(4n^2 + 11n - 11)$ contraintes :

$$
\begin{cases}
\max_{\mathbf{z}} \quad b + \bar{b} - \lambda_1 \left(\mathbf{1}^T \gamma + \mathbf{1}^T \bar{\gamma} \right) - \lambda_2 \left(\mathbf{1}^T \tau + \mathbf{1}^T \bar{\tau} \right) \\
\text{s.t.} \quad b\mathbf{1} \le \Omega \cdot \omega + \frac{1}{2}|\Omega| \cdot \mathbf{g} \\
\qquad \bar{b}\mathbf{1} \le \Omega \cdot \omega + \Delta \cdot \delta^{\mathbf{0}} + \frac{1}{2}|\Omega| \cdot \bar{\mathbf{g}} \\
\qquad b \le g^* \\
\qquad b \ge 0 \\
\qquad \bar{b} \le \bar{g}^* \\
\qquad \bar{b} \ge 0 \\
\qquad \mathbf{t}_{\min} \le \mathbf{t} \le \mathbf{t}_{\max} \\
\qquad -\mathbf{t}_{\max} \le \bar{\mathbf{t}} \le -\mathbf{t}_{\min} \\
\qquad \delta^{\mathbf{0}} - T \cdot \mathbf{t} + T \cdot \bar{\mathbf{t}} + \alpha \cdot C = \delta \\
\qquad \mathcal{L}^* \cdot \mathbf{t} - \gamma \le 0 \\
\qquad -\mathcal{L}^* \cdot \mathbf{t} - \gamma \le 0 \\
\qquad \mathcal{L}^* \cdot \bar{\mathbf{t}} - \bar{\gamma} \le 0 \\
\qquad -\mathcal{L}^* \cdot \bar{\mathbf{t}} - \bar{\gamma} \le 0 \\
\qquad \mathbf{t} - \tau \le 0 \\
\qquad -\mathbf{t} - \tau \le 0 \\
\qquad \bar{\mathbf{t}} - \bar{\tau} \le 0 \\
\qquad -\bar{\mathbf{t}} - \bar{\tau} \le 0
\end{cases}
\tag{56}
$$

Expériences

Dégradation de la Bande Passante

La première expérience vise à montrer la dégradation de la bande passante théorique avec le nombre croissant de carrefours à feux sur l'artère. Plusieurs paramètres du réseau ont été variés au hasard afin de tester différents ensembles de temps du vert, de longueurs des segments, et d'offsets internes.

Afin d'explorer largement l'espace des paramètres, pour chaque nombre d'intersections n, les autres paramètres (durée du vert, longueur des segment, et décalage interne) ont été varies de façon aléatoire. Un total de 10.000 simulations par chaque valeur de n ont été exécutées. En outre, pour chaque configuration générée de façon aléatoire, à la fois le problème (56) et le problème présenté dans [56] ont été résolus. La comparaison de la bande passante théorique atteinte par les deux
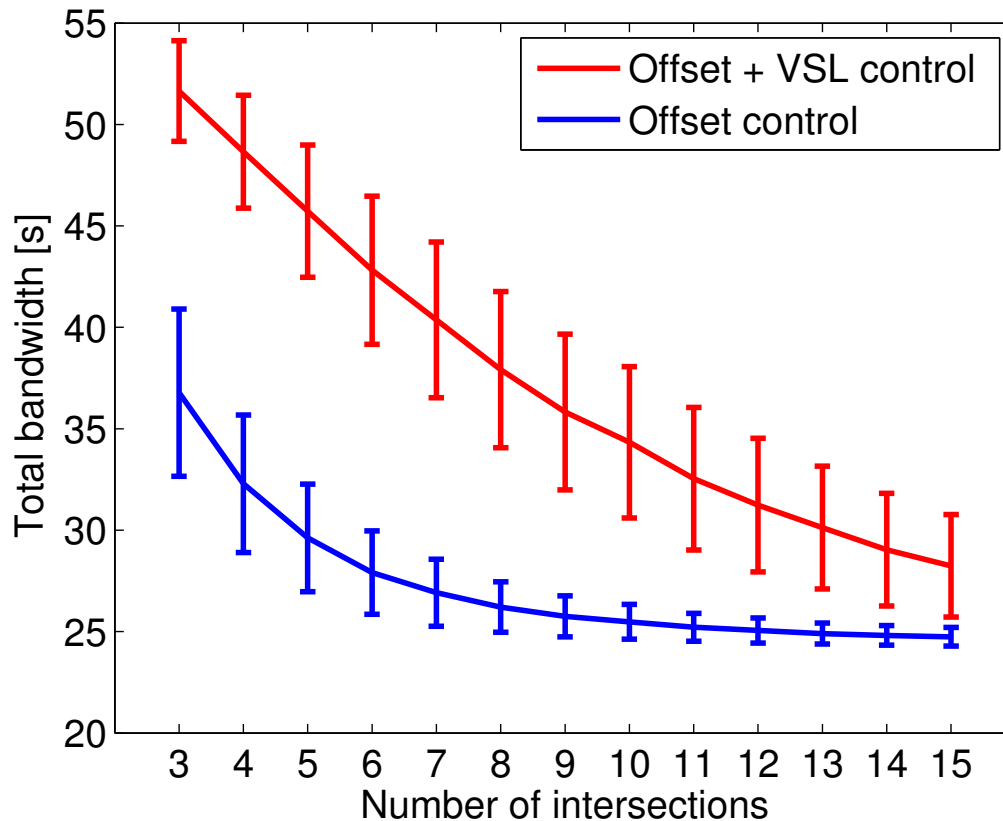
Figure 12 – Dégradation de la bande passante avec le nombre croissant de carrefours à feux. En bleu la stratégie de contrôle d'offsets proposée dans [56].

optimisations est représentée dans la Figure 12. Comme n augmente la bande passante diminue pour tous les deux systèmes de contrôle. Cependant le contrôle ici proposé est plus efficace et atteint une bande passante plus élevée, en particulier pour un nombre inférieur d'intersections.

Simulation Microscopique

Pour les simulations microscopiques une configuration de réseau aléatoire a été sélectionné. Les paramètres de réseau utilisés dans Aimsun sont résumés dans le Tableau 3.

Compte tenu de ces paramètres de réseau, les deux problèmes d'optimisation de bande passante ont été résolus numériquement, afin d'obtenir les paramètres de contrôle à tester dans le simulateur microscopique.

En Figure 13 il est évident comment la bande passante théorique est monotone décroissante dans la direction de l'incrément de λ_1 et λ_2. Poids plus élevés sur
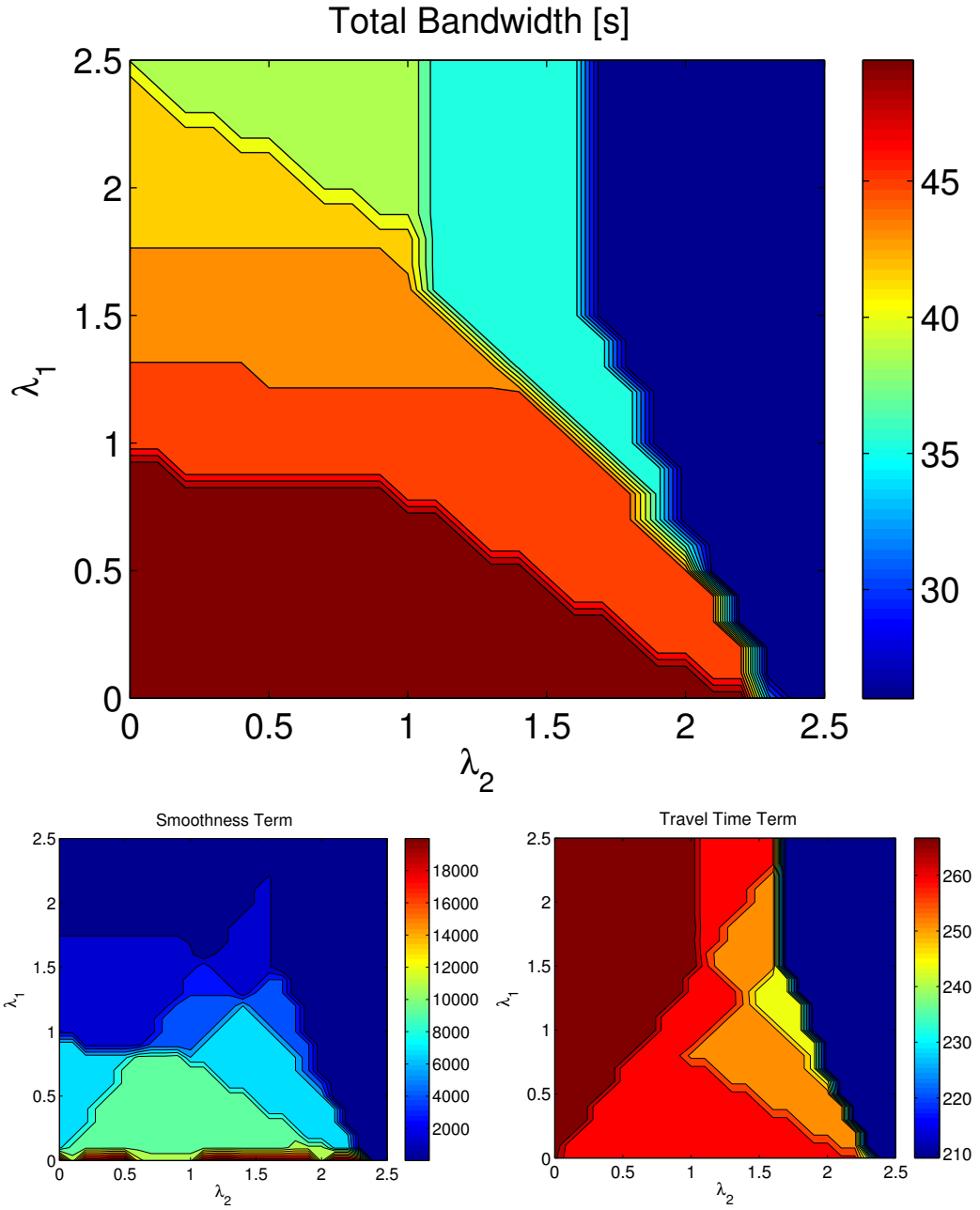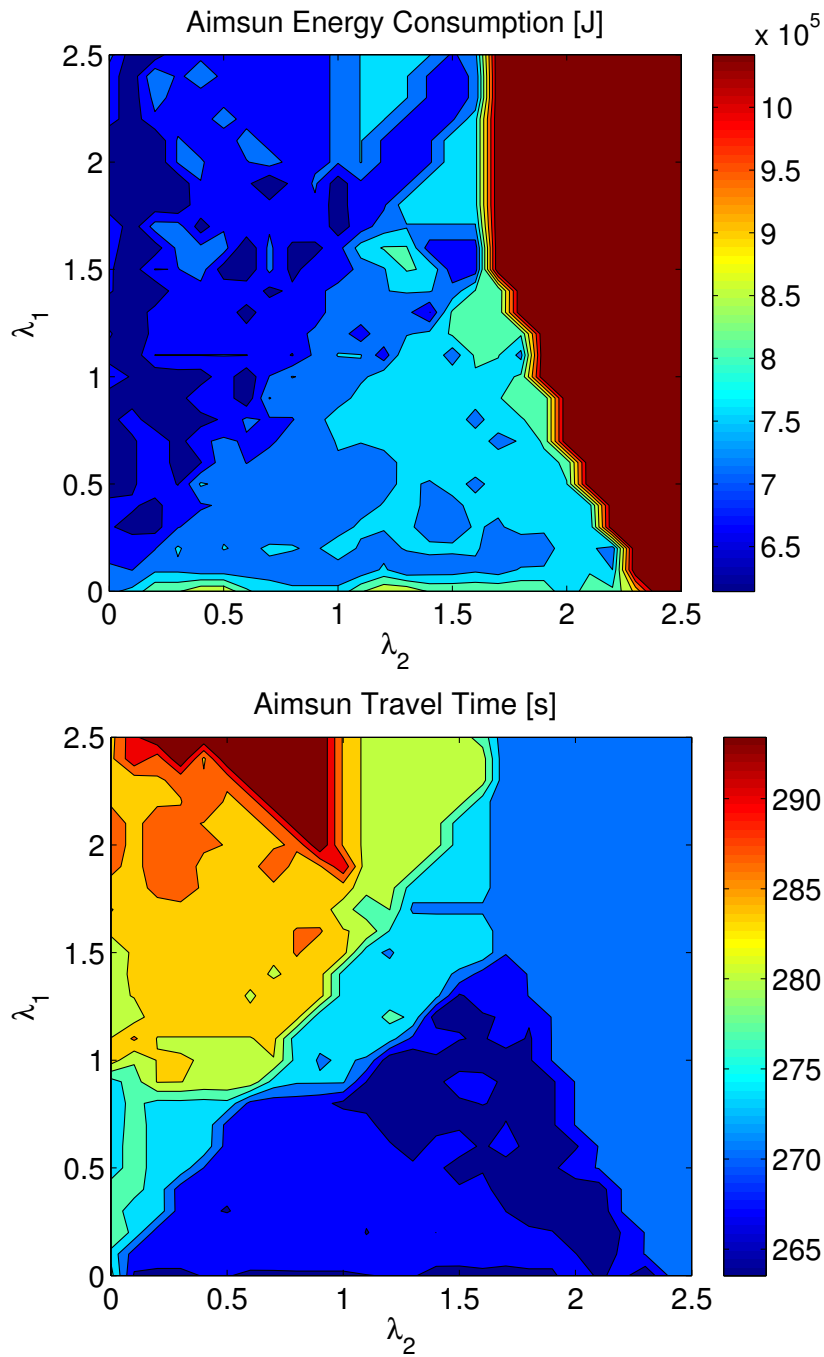
Figure 13 – Pour la bande passante théorique, des valeurs plus élevées (vers le rouge) sont meilleures. Pour le terme de lissage des vitesses et le terme du temps de parcours de la fonction objectif, des valeurs plus basses (vers le bleu) sont meilleures.
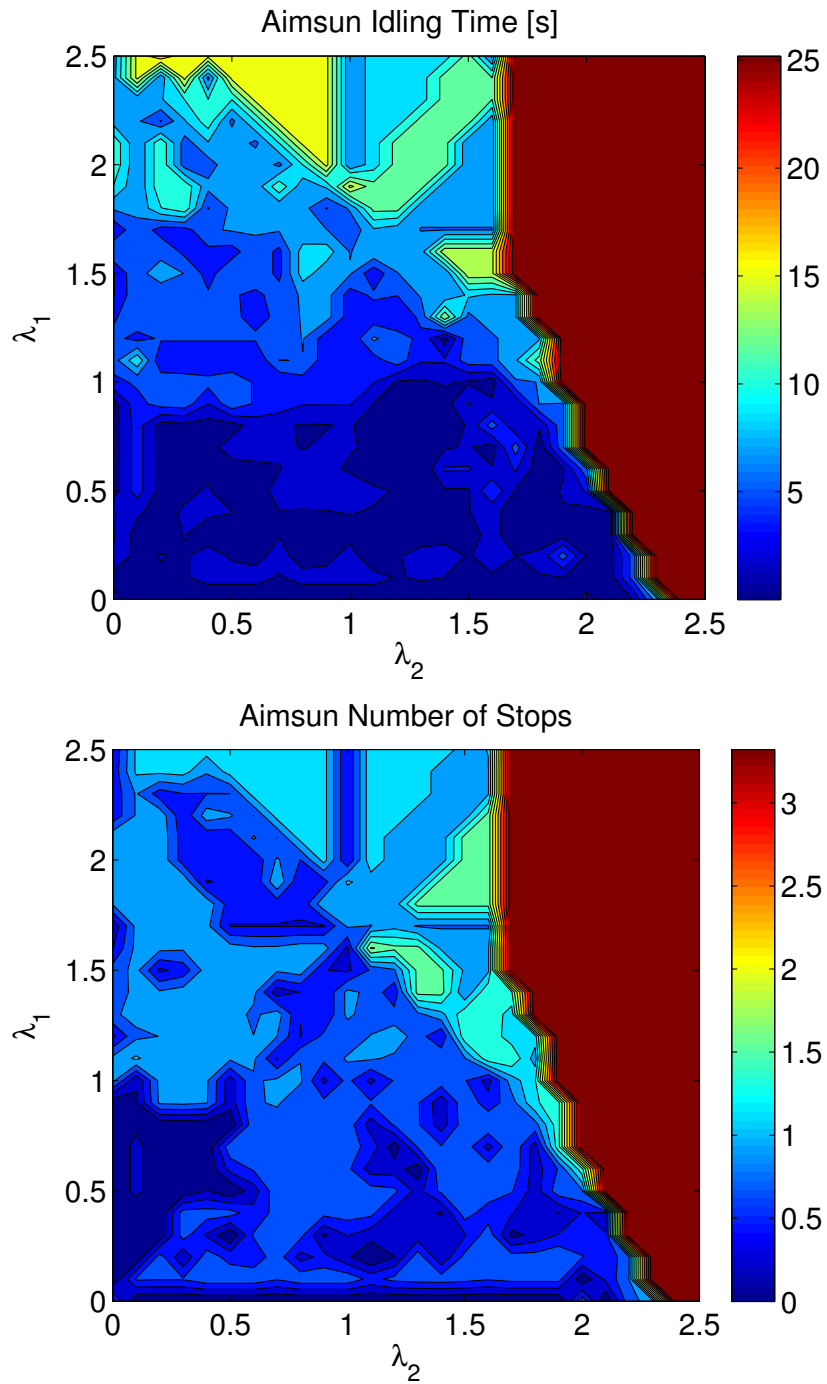
Figure 14 – Les indicateurs de performance présentés ici sont optimisés pour les valeurs plus basses (vers le bleu).

Tableau 3 – Paramètres de réseau utilisés dans la simulation microscopique

n	6	nombre d'intersections
g	$[33, 30, 25, 28, 31, 26]$	phase vertes dans le sens sortant [s]
$\bar{g}$	$[33, 27, 35, 27, 33, 26]$	phase vertes dans le sens entrant [s]
L	$[268.1, 238.7, 311.4, 327.5, 307]$	longueur des segments [m]
δ	$[25, -21, -21, -19, -22, -3]$	offsets internes [s]
D	500	demande de trafic [veh/h]

le terme de lissage et/ou du temps de parcours dans l'optimisation permettraient d'atteindre des profils de vitesse plus lisses et/ou plus élevés entre les segments adjacents. Les avantages des vitesses variables pour la maximisation de la bande passante sont évidents pour des valeurs basses des poids λ_1 et λ_2. En particulier, en définissant les poids égaux à zéro, la valeur maximale de la bande passante est atteinte, et le plein potentiel des vitesses variables est exploité.

Les indicateurs de performance du trafic, calculés à partir des données de simulation microscopique, sont rapportés dans la Figure 14. Il est intéressant d'observer comment la bande passante théorique est en corrélation avec la performance réelle du trafic. La consommation d'énergie est faible dans la zone de bande passante maximale, puisqu'une bande passante supérieure réduit également le temps à l'arrêt et le nombre d'arrêts. Cependant, l'énergie est optimisée en général pour les faibles valeurs de λ_2, montrant l'impact positif des basses limites de vitesse.

En présence d'une optimisation multi-objectif, il est toujours difficile de faire le bon choix des facteurs de pondération. Une analyse de l'efficacité de Pareto a été menée sur le problème afin d'aider le concepteur à prendre des décisions au sein de l'ensemble des points appartenant au front de Pareto.

Afin d'évaluer la performance de l'optimisation présentée, qui par la suite sera indiqué comme "Offset+VSL", une étude comparative a été menée avec des stratégies préexistantes et une référence. La référence utilisée ci-après est un cas non optimisé, où le choix aléatoire des offsets respecte encore la contrainte de décalage interne (44). Une comparaison sera faite aussi avec la stratégie d'optimisation d'offsets dans [56]. Enfin, l'algorithme de MAXBAND sera comparé à la stratégie proposée. Le problème d'optimisation présenté peut être considéré comme une généralisation de l'algorithme de MAXBAND dans [86, 87] avec les vitesses des segments autorisées à varier dans $[v_{min}, v_{max}]$. Dans MAXBAND, la formulation du problème correspond au cas particulier de $\lambda_1 = \lambda_2 = 0$ dans l'analyse présentée.

Les résultats comparatifs pour la bande passante théorique et les indicateurs de

Tableau 4 – Comparaison des résultats numériques et Aimsun

	Numérique	AIMSUN			
	Bande Passante Théorique	Temps de Parcours	Temps d'Arrêt	Arrêts	Énergie
Non-optimisé	N/A	367.9 s	102.8 s	6.7	1.3E6 J
Offset	26 s	270.3 s	26.9 s	3.5	1.09E6 J
MAXBAND	51 s	278 s	2.3 s	0.7	7.48E5 J
Offset+VSL	51 s	268.3 s	1.9 s	0.8	7.03E5 J

performance en Aimsun sont présentés dans le Tableau 4. Outre la différence significative en termes de bande passante atteinte grâce à l'introduction des vitesses variables comme variable de décision, des améliorations importantes sont atteintes aussi en termes de performances du trafic. La stratégie présentée donne une réduction du temps de parcours de 1% par rapport à l'optimisation des offsets, bien que la limite de vitesse moyenne est plus faible. Le temps d'arrêt et le nombre d'arrêts aux intersections sont presque complètement éliminés. La consommation globale d'énergie est réduite de 35,5%. En ce qui concerne MAXBAND, la stratégie proposée est en mesure de réduire le temps de parcours de 3,5%, et la consommation d'énergie de 6%. Une amélioration plus élevée est évidemment atteinte par rapport au cas non-optimisé : le temps de parcours est réduit de 27% et la consommation d'énergie est réduite de 46%.

La stratégie proposée peut être adaptée aussi à différents niveaux de demande de trafic et on peut démontrer que le problème d'optimisation permet d'améliorer les performance du trafic même en conditions de saturation en absence d'une "onde verte".

Conclusions

Les principaux résultats et les contributions de l'étude présentée dans cette thèse peuvent être résumés comme suit.

Compte tenu d'une séquence d'intersections signalisées, il existe un profil de vitesse optimale en énergie qu'un véhicule peut suivre tout en évitant de s'arrêter aux feux de circulation. Le contrôle du véhicule proposé est en mesure d'identifier le meilleur profil de conduite sans arrêt, parmi toutes les trajectoires possibles. Des simulations validées ont prouvé que le meilleur profil de conduite est plus efficace énergétiquement jusqu'à 25% par rapport aux autres possibles. La stratégie pro-

posée est rapide et suffisamment flexible pour être utilisé en ligne, et la meilleure trajectoire de conduite peut être calculé en temps réel. Études expérimentales approfondies dans un simulateur de trafic microscopique ont montré que la stratégie de contrôle proposée peut être appliquée indépendamment à chaque véhicule d'un flux de trafic. La présence de véhicules perturbant les profils de conduite optimaux force à se ré-adapter constamment à la situation du trafic. Une analyse de l'impact du taux de pénétration de la technologie sur la consommation d'énergie de la circulation a montré des résultats prometteurs. Dans une artère signalisée typique, si la totalité des véhicules sont équipés de la stratégie proposée, la consommation d'énergie serait réduite d'environ 30%. Notez que, l'algorithme proposé, en plus d'assurer la réduction drastique de la consommation d'énergie, a également été en mesure de réduire le temps de parcours moyen, ce qui prouve que la consommation d'énergie et le temps de parcours ne sont pas toujours orthogonaux.

La prise en compte des conditions de circulation saturées rend les arrêts et les files d'attente aux feux de circulation inévitables. L'analyse d'une section de route isolée avec des flux limites réglementée par des feux de circulation a montré qu'il existe une limite de vitesse optimale pour la section considérée. L'optimalité dépend de fonctions de coût différentes. La consommation d'énergie de la circulation doit être minimisée sans pour autant sacrifier le temps de parcours et l'utilisation efficace de l'infrastructure. Les modèles et les indicateurs de performance macroscopiques proposées, utilisés pour décrire l'évolution du trafic et le comportement à l'intérieur de la section de route, ont prouvé que pour le système en équilibre il existe une limite de vitesse efficace pour chaque niveau d'occupation. La limite de vitesse optimale pourrait assurer une amélioration de la performance de jusqu'à 25% par rapport aux limites de vitesse standard de la ville. Une analyse de validation dans un simulateur de trafic microscopique a prouvé la fiabilité de la méthode de modélisation macroscopique à des fins de contrôle.

Le contrôle de l'infrastructure a été enfin etudié à plus grande échelle. Une combinaison de limites de vitesse variables et de coordination des feux de circulation a été appliquée à une artère urbaine avec multiples intersections signalisées. La principale nouveauté réside dans l'analyse de la consommation d'énergie dans le contrôle de l'infrastructure, avec l'objectif de maximisation de la bande passante. Numériquement, le problème d'optimisation a été formulé d'une manière simple et descriptive, et des simulations ont montré que des bandes de progression des véhicules plus larges peuvent être obtenues en combinant le contrôle des vitesses et des offsets. Un simulateur de trafic microscopique a été utilisé pour évaluer la corrélation entre la bande passante et les indicateurs de performance de la circulation. En particulier, des expériences ont montré que l'optimisation proposée apporte des améliorations significatives par rapport aux approches existantes.

Une fois de plus, la stratégie proposée a été en mesure de réduire considérablement la consommation d'énergie de la circulation, ainsi que le temps de parcours, en éliminant complètement les arrêts inutiles et le temps d'arrêt aux feux de circulation. Enfin, une analyse de la performance de l'approche proposée a été réalisée également dans des conditions de circulation saturées. Dans ces conditions, la notion de coordination des signaux pour la maximisation de la bande passante perd sa signification. Cependant, l'optimisation multi-objectif peut être adaptée à différents niveaux de congestion de la circulation, et les simulations microscopiques ont prouvé que la stratégie proposée surpasse encore les algorithmes existants.

Bibliography

[1] *2020 Climate & Energy Package*, *European Commission Climate Action*, URL: http://ec.europa.eu/clima/policies/strategies/2020/index_en.htm.

[2] K. Aboudolas, M. Papageorgiou, and E. Kosmatopoulos, "Control and Optimization Methods for Traffic Signal Control in Large-scale Congested Urban Road Networks," *IEEE American Control Conference*, pp. 3132–3138, 2007.

[3] K. Aboudolas, M. Papageorgiou, and E. Kosmatopoulos, "Store-And-Forward Based Methods for the Signal Control Problem in Large-Scale Congested Urban Road Networks," *Transportation Research Part C*, vol. 17, pp. 163–174, 2009.

[4] K. Aboudolas, M. Papageorgiou, A. Kouvelas, and E. Kosmatopoulos, "A Rolling-Horizon Quadratic-Programming Approach to the Signal Control Problem in Large-Scale Congested Urban Road Networks," *Transportation Research Part C*, vol. 18, no. 5, pp. 680–694, 2010.

[5] D. Aeyels, "Stabilization of a Class of Nonlinear Systems by a Smooth Feedback Control," *Systems & Control Letters*, vol. 5, no. 5, pp. 289–294, 1985.

[6] R. B. Allsop, "SIGSET: A Computer Program for Calculating Traffic Capacity of Signal-Controlled Road Junctions," *Traffic Engineering and Control*, vol. 12, no. 2, 1971.

[7] R. E. Allsop, "SIGCAP: A Computer Program for Assessing the Traffic Capacity of Signal-Controlled Road Junctions," *Traffic Engineering and Control*, vol. 17, no. 819, 1976.

[8] J. Archer, N. Fotheringham, M. Symmons, and B. Corben, *The Impact of Lowering Speed Limits in Urban/Metropolitan Areas*, Monash University Accident Research Center, Australia, 2008.

[9] T. Arsava, Y. Xie, N. Gartner, and J. Mwakalonge, "Arterial Traffic Signal Coordination Utilizing Vehicular Traffic Origin-Destination Information," *IEEE 17th International Conference on Intelligent Transportation Systems*, pp. 2132–2137, 2014.

[10] B. Asadi and A. Vahidi, "Predictive Cruise Control: Utilizing Upcoming Traffic Signal Information for Improving Fuel Economy and Reducing Trip Time," *IEEE Transactions on Control Systems Technology*, vol. 19, no. 3, pp. 707–714, 2011.

[11] J. Barbé and G. Boy, "On-Board System Design to Optimise Energy Management," *European Annual Conference on Human Decision-Making and Manual Control*, 2006.

[12] A. Barisone, D. Giglio, R. Minciardi, and R. Poggi, "A Macroscopic Traffic Model for Real-Time Optimization of Signalized Urban Areas," *IEEE 41st Conference on Decision and Control*, pp. 900–903, 2002.

[13] J. Barnes and V. Paruchuri, "Optimal Phase Ordering of Traffic Signals to Reduce Stopped Delay," *IEEE 26th International Conference on Advanced Information Networking and Applications*, pp. 113–119, 2012.

[14] A. Bell, "If You Always Caught the Green Light," *ECOS*, vol. 40, pp. 10–13, 1984.

[15] F. Boillot, J. M. Blosseville, J. B. Lesort, V. Motyka, M. Papageorgiou, and S. Sellam, "Optimal Signal Control of Urban Traffic Networks," *Road Traffic Monitoring*, 1992.

[16] S. Boyd and L. Vandenberghe, *Convex Optimization*, Cambridge University Press, 2004.

[17] E. Brockfeld, R. Barlovic, A. Schadschneider, and M. Schreckenberg, "Optimizing Traffic Lights in a Cellular Automaton Model for City Traffic," *Physical Review E*, vol. 64, no. 5, 2001.

[18] *C2C-CC Project*, URL: https://www.car-2-car.org/index.php?id=5.

[19] E. Camponogara, H. F. Scherer, and L. V. Moura, "Distributed Optimization for Predictive Control with Input and State Constraints: Preliminary Theory and Application to Urban Traffic Control," *IEEE International Conference on Systems, Man, and Cybernetics*, pp. 3726–3732, 2009.

[20] C. Canudas de Wit, "Best-Effort Highway Traffic Congestion Control via Variable Speed Limits," *IEEE 50th Conference on Decision and Control and European Control Conference*, pp. 5959–5964, 2011.

[21] C. Canudas de Wit and A. Ferrara, *A New Variable-Length Cell Model for Traffic Systems*, Internal, 2014.

[22] E. Chang, S. Cohen, C. Liu, N. Chaudhary, and C. Messer, "MAXBAND-86: Program for Optimizing Left-Turn Phase Sequence in Multiarterial Closed Networks," *Transportation Research Record*, no. 1181, pp. 61–67, 1988.

[23] N. A. Chaudhary, M. M. Abbas, H. Charara, and R. Parker, *Platoon Identification and Accommodation System for Isolated Traffic Signals on Arterials*, Texas Transportation Institute, 2003.

[24] Y. Chen, D. Zhang, and K. Li, "Enhanced Eco-Driving System Based on V2X Communication," *IEEE 15th Conference on Intelligent Transportation Systems*, pp. 200–205, 2012.

[25] D. Cheng and Y. Guo, "Stabilization of Nonlinear Systems via the Center Manifold Approach," *Systems and Control Letters*, vol. 57, no. 6, pp. 511–518, 2008.

[26] *COMeSafety2 Project*, URL: http://www.ecomove-project.eu/links/comesafety/.

[27] A. Cutolo, C. D'Apice, and R. Manzo, "Traffic Optimization at Junctions to Improve Vehicular Flows," *ISRN Applied Mathematics*, vol. 2011, 2011.

[28] C. F. Daganzo, "The Cell Transmission Model: A Dynamic Representation of Highway Traffic Consistent with the Hydrodynamic Theory," *Transportation Research Part B*, vol. 28, no. 4, pp. 269–287, 1994.

[29] C. F. Daganzo, "The Cell Transmission Model, Part II: Network Traffic," *Transportation Research Part B*, vol. 298, no. 2, pp. 79–93, 1995.

[30] G. De Nunzio, C. Canudas De Wit, P. Moulin, and D. Di Domenico, "Eco-Driving in Urban Traffic Networks Using Traffic Signal Information," *IEEE 52nd Conference on Decision and Control*, pp. 892–898, 2013.

[31] B. De Schutter and B. De Moor, "Optimal Traffic Light Control for a Single Intersection," *European Journal of Control*, vol. 4, no. 3, pp. 260–276, 1998.

[32] C. Diakaki, "Integrated Control of Traffic Flow in Corridor Networks," PhD thesis, Technical University of Crete, 1999.

[33] C. Diakaki, M. Papageorgiou, and K. Aboudolas, "A Multivariable Regulator Approach to Traffic-Responsive Network-Wide Signal Control," *Control Engineering Practice*, vol. 10, no. 2, pp. 183–195, 2002.

[34] W. Dib, A. Chasse, P. Moulin, A. Sciarretta, and G. Corde, "Optimal Energy Management for an Electric Vehicle in Eco-Driving Applications," *Control Engineering Practice*, vol. 29, pp. 299–307, 2014.

[35] W. Dib, L. Serrao, and A. Sciarretta, "Optimal Control to Minimize Trip Time and Energy Consumption in Electric Vehicles," *IEEE Vehicle Power and Propulsion Conference*, pp. 1–8, 2011.

[36] W. Dib, A. Chasse, D. Di Domenico, P. Moulin, and A. Sciarretta, "Evaluation of the Energy Efficiency of a Fleet of Electric Vehicle for Eco-Driving Application," *Oil & Gas Science and Technology – Rev. IFP Energies nouvelles*, vol. 67, no. 4, pp. 589–599, 2012.

[37] W. Dib, A. Chasse, A. Sciarretta, and P. Moulin, "Optimal Energy Management Compliant with Online Requirements for an Electric Vehicle in Eco-Driving Applications," *IFAC Workshop on Engine and Powertrain Control, Simulation and Modeling*, pp. 334–340, 2012.

[38] E. W. Dijkstra, "A Note on Two Problems in Connection with Graphs," *Numerische Mathematik*, vol. 1, no. 1, pp. 269–271, 1959.

[39] V. Dinopoulou, C. Diakaki, and M. Papageorgiou, "Applications of the Urban Traffic Control Strategy TUC," *European Journal of Operational Research*, vol. 175, no. 3, pp. 1652–1665, 2006.

[40] M. Dotoli, M. P. Fanti, and C. Meloni, "A Signal Timing Plan Formulation for Urban Traffic Control," *Control Engineering Practice*, vol. 14, no. 11, pp. 1297–1311, 2006.

[41] *Drive C2X Project*, URL: http://drive-c2x.eu/project.

[42] D. Eckhoff, T. Gansen, M. Robert, D. Thum, O. Klages, and C. Sommer, "Simulative Performance Evaluation of the simTD Self Organizing Traffic Information System," *The 10th IFIP Annual Mediterranean Ad Hoc Networking Workshop*, pp. 79–86, 2011.

[43] C. Fontaine, S. Delprat, and T. M. Guerra, "Toward Analytical Solution of Optimal Control Problems for HEV Energy Management," *IEEE Vehicle Power and Propulsion Conference*, pp. 1–6, 2010.

[44] T. Galpin, Y. L. Han, and P. G. Voulgaris, "Fuel Minimization of a Moving Vehicle in Suburban Traffic," *WSEAS Transactions on Systems and Control*, vol. 9, pp. 672–686, 2014.

[45] T. Galpin and P. Voulgaris, "Fuel Minimization of a Moving Vehicle in Suburban Traffic," PhD thesis, University of Illinois-Urbana Champaign, 2013.

[46] N. Gartner, "OPAC: A Demand Responsive Strategy for Traffic Signal Control," *Transportation Research Record*, vol. 906, pp. 75–81, 1983.

[47] N. Gartner, S. Assmann, F. Lasaga, and D. Hou, "A Multi-Band Approach to Arterial Signal Optimization Traffic," *Transportation Research Part B: Methodological*, vol. 25B, no. 1, pp. 55–74, 1991.

[48] N. Gartner and C. Stamatiadis, "Arterial-Based Control of Traffic Flow in Urban Grid Networks," *Mathematical and Computer Modelling*, vol. 35, no. 5-6, pp. 657–671, 2002.

[49] D. C. Gazis and R. B. Potts, "The Oversaturated Intersection," *2nd International Symposium on the Theory of Traffic Flow*, pp. 221–237, 1963.

[50] N. Geroliminis, J. Haddad, and M. Ramezani, "Optimal Perimeter Control for Two Urban Regions With Macroscopic Fundamental Diagrams: A Model Predictive Approach," *IEEE Transactions on Intelligent Transportation Systems*, vol. 14, no. 1, pp. 348–359, 2013.

[51] C. Gershenson, "Self-Organizing Traffic Lights," *Complex Systems*, vol. 16, no. 1, pp. 29–53, 2005.

[52] C. Gershenson and D. A. Rosenblueth, "Self-Organizing Traffic Lights at Multiple-Street Intersections," *Complexity*, vol. 17, no. 4, pp. 23–39, 2012.

[53] C. Godsil and G. Royle, *Algebraic Graph Theory*, Springer, 2001.

[54] A. Goel and P. Kumar, "Characterisation of Nanoparticle Emissions and Exposure at Traffic Intersections through Fast–Response Mobile and Sequential Measurements," *Atmospheric Environment*, vol. 107, pp. 374–390, 2015.

[55] M. Goharimanesh, A. Akbari, and A. Akbarzadeh Tootoonchi, "More Efficiency in Fuel Consumption Using Gearbox Optimization Based on Taguchi Method," *Journal of Industrial Engineering International*, vol. 10, 2014.

[56] G. Gomes, "Bandwidth Maximization Using Vehicle Arrival Functions," *IEEE Transactions on Intelligent Transportation Systems*, vol. 16, no. 4, pp. 1977–1988, 2015.

[57] B. D. Greenshields, J. R. Bibbins, W. S. Channing, and H. H. Miller, "A Study of Traffic Capacity," *Highway Research Board*, pp. 448–477, 1935.

[58] J. Haddad, B. De Schutter, D. Mahalel, I. Ioslovich, and P.-O. Gutman, "Optimal Steady-State Control for Isolated Traffic Intersections," *IEEE Transactions on Automatic Control*, vol. 55, no. 11, pp. 2612–2617, 2010.

[59]   F. Harary and R. Z. Norman, "Some Properties of Line Digraphs," *Rendiconti del Circolo Matematico di Palermo*, vol. 9, no. 2, pp. 161–168, 1960.

[60]   H. Hartenstein and K. P. Laberteaux, "A Tutorial Survey on Vehicular Ad Hoc Networks," *IEEE Communications Magazine*, vol. 46, no. 6, pp. 164–171, 2008.

[61]   J. Henry, J. Farges, and J. Tuffal, "The PRODYN Real-Time Traffic Algorithm," *4th IFAC-IFIC-IFORS Conference on Control in Transportation Systems*, pp. 305–310, 1984.

[62]   S. P. Hoogendoorn and P. H. L. Bovy, "State-Of-The-Art of Vehicular Traffic Flow Modelling," *Journal of Systems and Control Engineering*, vol. 215, no. 4, pp. 283–303, 2001.

[63]   P. B. Hunt, D. I. Robertson, R. D. Bretherton, and R. I. Winton, *SCOOT - A Traffic Responsive Method of Co-Ordinating Signals*, TRRL Laboratory Report 1014, 1981.

[64]   G. Improta and G. E. Cantarella, "Control System Design for an Individual Signalized Junction," *Transportation Research Part B*, vol. 18, no. 2, pp. 147–167, 1984.

[65]   I. Ioslovich, P.-O. Gutman, D. Mahalel, and J. Haddad, "Design of Optimal Traffic Flow Control at Intersection with Regard for Queue Length Constraints," *Automation and Remote Control*, vol. 72, no. 9, pp. 1833–1840, 2011.

[66]   *iTetris Project*, URL: http://www.ict-itetris.eu/.

[67]   M. A. S. Kamal, M. Mukai, J. Murata, and T. Kawabe, "Model Predictive Control of Vehicles on Urban Roads for Improved Fuel Economy," *IEEE Transactions on Control Systems Technology*, vol. 21, no. 3, pp. 831–841, 2013.

[68]   I. Kaparias, K. Zavitsas, and M. G. H. Bell, *State-Of-The-Art of Urban Traffic Management Policies and Technologies*, CONDUITS, Coordination Of Network Descriptors for Urban Intelligent Transport Systems, Imperial College London, 2010.

[69]   K. Katsaros, R. Kernchen, M. Dianati, and D. Rieck, "Performance Study of a Green Light Optimized Speed Advisory (GLOSA) Application Using an Integrated Cooperative ITS Simulation Platform," *7th International Wireless Communications and Mobile Computing Conference*, pp. 918–923, 2011.

[70]   H. K. Khalil, *Nonlinear Systems*, 3rd, Prentice Hall, 2002.

[71] N. Kim, S. Cha, and H. Peng, "Optimal Control of Hybrid Electric Vehicles Based on Pontryagin's Minimum Principle," *IEEE Transactions on Control Systems Technology*, vol. 19, no. 5, pp. 1279–1287, 2011.

[72] T. S. Kim, C. Manzie, and R. Sharma, "Two-Stage Optimal Control of a Parallel Hybrid Vehicle with Traffic Preview," *18th IFAC World Congress*, pp. 2115–2120, 2011.

[73] E. Koukoumidis, M. Martonosi, and L.-S. Peh, "Leveraging Smartphone Cameras for Collaborative Road Advisories," *IEEE Transactions on mobile computing*, vol. 11, no. 5, pp. 707–723, 2012.

[74] S. Lämmer and D. Helbing, "Self-Control of Traffic Lights and Vehicle Flows in Urban Road Networks," *Journal of Statistical Mechanics: Theory and Experiment*, vol. 2008, 2008.

[75] S. Lämmer and D. Helbing, "Self-Stabilizing Decentralized Signal Control of Realistic, Saturated Network Traffic," 2010.

[76] D. Lang, T. Stanger, and L. del Re, "Fuel Efficient Quasi Optimal Adaptive Cruise Control by Control Identification," *IEEE International Conference on Control Applications*, pp. 229–234, 2013.

[77] D. Lang, T. Stanger, and L. del Re, "Opportunities on Fuel Economy Utilizing V2V Based Drive Systems," *SAE International*, 2013.

[78] A. Lawitzky, D. Wollherr, and M. Buss, "Energy Optimal Control to Approach Traffic Lights," *IEEE/RSJ International Conference on Intelligent Robots and Systems*, pp. 4382–4387, 2013.

[79] R. J. LeVeque, *Numerical Methods for Conservation Laws*, 2nd, Birkhäuser Verlag, 1992.

[80] M. Li, K. Boriboonsomsin, G. Wu, W.-B. Zhang, and M. Barth, "Traffic Energy and Emission Reductions at Signalized Intersections: A Study of the Benefits of Advanced Driver Information," *International Journal of ITS Research*, vol. 7, no. 1, pp. 49–58, 2009.

[81] M. J. Lighthill and G. B. Whitham, "On Kinematic Waves. II. A Theory of Traffic Flow on Long Crowded Roads," *Proceedings of the Royal Society A: Mathematical, Physical and Engineering Sciences*, vol. 229, no. 1178, pp. 317–345, 1955.

[82] L. Lin, L. Tung, and H. Ku, "Synchronized Signal Control Model for Maximizing Progression along an Arterial," *Journal of Transportation Engineering*, vol. 136, no. 8, pp. 727–735, 2010.

[83] S. Lin, B. De Schutter, Y. Xi, and H. Hellendoorn, "Efficient Network-Wide Model-Based Predictive Control for Urban Traffic Networks," *Transportation Research Part C*, vol. 24, pp. 122–140, 2012.

[84] S. Lin, B. De Schutter, Y. Xi, and J. Hellendoorn, "A Simplified Macroscopic Urban Traffic Network Model for Model-Based Predictive Control," *IFAC 12th Symposium on Control in Transportation Systems*, pp. 286–291, 2009.

[85] S. Lin, B. De Schutter, S. K. Zegeye, H. Hellendoorn, and Y. Xi, "Integrated Urban Traffic Control for the Reduction of Travel Delays and Emissions," *IEEE Transactions on Intelligent Transportation Systems*, vol. 14, no. 4, pp. 1609–1619, 2013.

[86] J. Little, "The Synchronization of Traffic Signals by Mixed-Integer Linear Programming," *Operations Research*, vol. 14, no. 4, pp. 568–594, 1966.

[87] J. Little, M. Kelson, and N. Gartner, "MAXBAND. A Versatile Program for Setting Signals on Arteries and Triangular Networks," *Transportation Research Record: Journal of the Transportation Research Board*, vol. 795, 1981.

[88] H. Liu, K. N. Balke, and W.-H. Lin, "A Reverse Causal-Effect Modeling Approach for Signal Control of an Oversaturated Intersection," *Transportation Research Part C*, vol. 16, no. 6, pp. 742–754, 2008.

[89] P. R. Lowrie, "The Sydney Coordinated Adaptive Traffic System (SCATS) - Principles, Methodology, Algorithms," *International Conference on Road Traffic Signaling*, 1982.

[90] G. Mahler and A. Vahidi, "Reducing Idling at Red Lights Based on Probabilistic Prediction of Traffic Signal Timings," *IEEE American Control Conference*, pp. 6557–6562, 2012.

[91] S. Mandava, K. Boriboonsomsin, and M. Barth, "Arterial Velocity Planning Based on Traffic Signal Information under Light Traffic Conditions," *IEEE 12th Conference on Intelligent Transportation Systems*, pp. 1–6, 2009.

[92] V. Mauro and C. Di Taranto, "UTOPIA," *IFAC Control, Computers, Communications in Transportations*, 1989.

[93] F. Mensing, R. Trigui, and E. Bideaux, "Vehicle Trajectory Optimization for Application in ECO-Driving," *IEEE Vehicle Power and Propulsion Conference*, pp. 1–6, 2011.

[94] A. J. Miller, "A Computer Control System for Traffic Networks," *2nd International Symposium on the Theory of Traffic Flow*, pp. 200–220, 1963.

[95] M. Miyatake, M. Kuriyama, and Y. Takeda, "Theoretical Study on Eco-Driving Technique for an Electric Vehicle Considering Traffic Signals," *IEEE 9th Conference on Power Electronics and Drive Systems*, pp. 733–738, 2011.

[96] J. Morgan and J. Little, "Synchronizing Traffic Signals for Maximal Bandwidth," *Operations Research*, vol. 12, no. 6, pp. 896–912, 1964.

[97] C. Musardo, G. Rizzoni, Y. Guezennec, and B. Staccia, "A-ECMS: An Adaptive Algorithm for Hybrid Electric Vehicle Energy Management," *European Journal of Control*, vol. 11, no. 4-5, pp. 509–524, 2005.

[98] D. Niu and J. Sun, "Eco-driving Versus Green Wave Speed Guidance for Signalized Highway Traffic: A Multi-vehicle Driving Simulator Study," *Procedia - Social and Behavioral Sciences*, vol. 96, pp. 1079–1090, 2013.

[99] *No More Traffic Jams in the Port of Hamburg: HPA and NXP Unveil Intelligent Traffic Light*, URL: http://www.nxp.com/news/press-releases/2015/06/no-more-traffic-jams-in-the-port-of-hamburg-hpa-and-nxp-unveil-intelligent-traffic-light.html.

[100] C. Osorio and M. Bierlaire, "A Multiple Model Approach for Traffic Signal Optimization in the City of Lausanne," *8th Swiss Transport Research Conference*, 2008.

[101] E. Ozatay, U. Ozguner, D. Filev, and J. Michelini, "Analytical and Numerical Solutions for Energy Minimization of Road Vehicles with the Existence of Multiple Traffic Lights," *IEEE 52nd Conference on Decision and Control*, pp. 7137–7142, 2013.

[102] M. Papageorgiou, "Some Remarks on Macroscopic Traffic Flow Modelling," *Transportation Research Part A*, vol. 32, no. 5, pp. 323–329, 1998.

[103] M. Papageorgiou, C. Diakaki, V. Dinopoulou, A. Kotsialos, and Y. Wang, "Review of Road Traffic Control Strategies," *Proceedings of the IEEE*, vol. 91, no. 12, pp. 2043–2067, 2003.

[104] M. Papageorgiou, A. Kouvelas, E. Kosmatopoulos, V. Dinopoulou, and E. Smaragdis, "Application of the Signal Control Strategy TUC in Three Traffic Networks: Comparative Evaluation Results," *International Conference on Information and Communication Technologies*, pp. 714–720, 2006.

[105] N. Petit and A. Sciarretta, "Optimal Drive of Electric Vehicles Using an Inversion-Based Trajectory Generation Approach," *IFAC 18th World Congress*, pp. 14519–14526, 2011.

[106] D. Quinn, *A Review of Queue Management Strategies*, *DRIVE II PRIMAV-ERA*, HETS, 1992.

[107] H. Rakha and R. K. Kamalanathsharma, "Eco-Driving at Signalized Intersections Using V2I Communication," *IEEE 14th Conference on Intelligent Transportation Systems*, pp. 341–346, 2011.

[108] *Reclaiming City Streets for People: Chaos or Quality of Life*, European Commission.

[109] P. I. Richards, "Shock Waves on the Highway," *Operations research*, vol. 4, no. 1, pp. 42–51, 1956.

[110] D. I. Robertson, *Research on the TRANSYT and SCOOT Methods of Signal Coordination*, *ITE Journal*, pp. 36–40, 1986.

[111] D. I. Robertson, *TRANSYT: A Traffic Network Study Tool*, Road Research Laboratory Report, 1969.

[112] P. Sanketh Kumar, S. Subbarao, and K. A. Jolapara, "I2V and V2V Communication Based VANET to Optimize Fuel Consumption at Traffic Signals," *IEEE 13th Conference on Intelligent Transportation Systems*, pp. 1251–1255, 2010.

[113] F. Saust, J. M. Wille, and M. Maurer, "Energy-Optimized Driving with an Autonomous Vehicle in Urban Environments," *IEEE 75th Vehicular Technology Conference*, pp. 1–5, 2012.

[114] P. Schuricht, O. Michler, and B. Bäker, "Efficiency-Increasing Driver Assistance at Signalized Intersections Using Predictive Traffic State Estimation," *IEEE 14th Conference on Intelligent Transportation Systems*, pp. 347–352, 2011.

[115] A. Sciarretta, M. Back, and L. Guzzella, "Optimal Control of Parallel Hybrid Electric Vehicles," *IEEE Transactions on Control Systems Technology*, vol. 12, no. 3, pp. 352–363, 2004.

[116] *SCOOT Adaptive Traffic Control System*, URL: http://www.scoot-utc.com/.

[117] P. Seewald, J. Josten, A. Zlocki, and L. Eckstein, "User Acceptance Evaluation Approach of Energy Efficient Driver Assistance Systems," *9th ITS European Congress*, 2013.

[118] S. Sen and K. L. Head, "Controlled Optimization of Phases at an Intersection," *Transportation Science*, vol. 31, no. 1, pp. 5–17, 1997.

[119] M. Seredynski, W. Mazurczyk, and D. Khadraoui, "Multi-Segment Green Light Optimal Speed Advisory," *IEEE 27th International Symposium on Parallel and Distributed Processing Workshops & PhD Forum*, pp. 459–465, 2013.

[120] F. A. de Souza, V. B. Peccin, and E. Camponogara, "Distributed Model Predictive Control Applied to Urban Traffic Networks: Implementation, Experimentation, and Analysis," *IEEE Conference on Automation Science and Engineering*, pp. 399–405, 2010.

[121] *SPEEDD Project*, URL: http://speedd-project.eu.

[122] C. Stamatiadis and N. Gartner, "MULTIBAND-96: A Program for Variable-Bandwidth Progression Optimization of Multiarterial Traffic Networks," *Transportation Research Record*, vol. 1554, pp. 9–17, 1996.

[123] O. Sundström and L. Guzzella, "A Generic Dynamic Programming Matlab Function," *IEEE Control Applications & Intelligent Control*, pp. 1625–1630, 2009.

[124] *Technology Roadmap. Fuel Economy of Road Vehicles*, International Energy Agency, 2012.

[125] H. Thompson, R. Paulen, M. Reniers, C. Sonntag, and S. Engell, *Analysis of the State-of-the-Art and Future Challenges in Cyber-physical Systems of Systems*, EU CPSoS Project, 2015.

[126] Z. Tian and T. Urbanik, "System Partition Technique to Improve Signal Coordination and Traffic Progression," *Journal of Transportation Engineering*, vol. 133, no. 2, pp. 119–128, 2007.

[127] R. S. Trayford, B. W. Doughty, and J. W. van der Touw, "Fuel Economy Investigation of Dynamic Advisory Speeds from an Experiment in Arterial Traffic," *Transportation Research Part A*, vol. 18, no. 5-6, pp. 415–419, 1984.

[128] R. S. Trayford, B. W. Doughty, and M. J. Wooldridge, "Fuel Saving and Other Benefits of Dynamic Advisory Speeds on a Multi-Lane Arterial Road," *Transportation Research Part A*, vol. 18, no. 5-6, pp. 421–429, 1984.

[129] M. Treiber and A. Kesting, *Traffic Flow Dynamics*, Springer, 2013.

[130] S. Trommer and A. Höltl, "Perceived Usefulness of Eco-Driving Assistance Systems in Europe," *IET Intelligent Transport Systems*, vol. 6, no. 2, pp. 145–152, 2012.

[131] H. Tsay and L. Lin, "New Algorithm for Solving the Maximum Progression Bandwidth," *Transportation Research Record*, vol. 1194, pp. 15–30, 1988.

[132] V. Turri, B. Besselink, J. Mårtensson, and K. H. Johansson, "Fuel-Efficient Heavy-Duty Vehicle Platooning by Look-Ahead Control," *IEEE 53rd Conference on Decision and Control*, pp. 654–660, 2014.

[133] J. Van Mierlo, G. Maggetto, E. van de Burgwal, and R. Gense, "Driving Style and Traffic Measures-Influence on Vehicle Emissions and Fuel Consumption," *Proceedings of the Institution of Mechanical Engineers, Part D: Journal of Automobile Engineering*, vol. 218, no. 1, pp. 43–50, 2004.

[134] P. Varaiya, "Max Pressure Control of a Network of Signalized Intersections," *Transportation Research Part C*, vol. 36, pp. 177–195, 2013.

[135] P. Varaiya, "The Max-Pressure Controller for Arbitrary Networks of Signalized Intersections," *Advances in Dynamic Network Modeling in Complex Transportation Systems*, chap. 2, pp. 27–66, Springer, 2013.

[136] *Vehicle Safety Communications – Applications (VSC-A) Final Report*, U.S. Department of Transportation, National Highway Traffic Safety Administration, 2011.

[137] R. A. Vincent and C. P. Young, "Self-Optimizing Traffic Signal Control Using Microprocessors : The TRRL "MOVA" Strategy for Isolated Intersections," *International Conference on Road Traffic Control*, pp. 102–105, 1986.

[138] T. Wongpiromsarn, T. Uthaicharoenpong, Y. Wang, E. Frazzoli, and D. Wang, "Distributed Traffic Signal Control for Maximum Network Throughput," *IEEE 15th Conference on Intelligent Transportation Systems*, pp. 588–595, 2012.

[139] W. Xianyu, H. Peifeng, and Y. Zhenzhou, "Link-Based Signalized Arterial Progression Optimization with Practical Travel Speed," *Journal of Applied Mathematics*, vol. 2013, 2013.

[140] F. Yan, M. Dridi, and A. E. Moudni, "A Scheduling Approach for Autonomous Vehicle Sequencing Problem at Multi-Intersections," *International Journal of Operations Research*, vol. 8, no. 1, pp. 57–68, 2011.

[141] C. Zhang, "Predictive Energy Management in Connected Vehicles: Utilizing Route Information Preview for Energy Saving," PhD thesis, Clemson University, 2010.

[142] C. Zinoviou, K. Katsaros, R. Kernchen, and M. Dianati, "Performance Evaluation of an Adaptive Route Change Application Using an Integrated Cooperative ITS Simulation Platform," *8th International Wireless Communications and Mobile Computing Conference*, pp. 377–382, 2012.